NASA CR-135029

A 200 WATT TRAVELING WAVE TUBE FOR THE COMMUNICATIONS TECHNOLOGY SATELLITE

by

C. L. Jones

LITTON INDUSTRIES

Electron Tube Division

Prepared For

NATIONAL AERONAUTICS AND SPACE ADMINISTRATION

NASA Lewis Research Center

Contract NAS3-15830

1. Report No. NASA CR 135029	2. Government Accession No.	3. Recipient's Catalog No.
4. Title and Subtitle A 200 WATT TRAVELING WAVE TUBE FOR THE COMMUNICATIONS TECHNOLOGY SATELLITE		5. Report Date November, 1976
		6. Performing Organization Code
7. Author(s) C. L. Jones		8. Performing Organization Report No.
		10. Work Unit No.
9. Performing Organization Name and Address Litton Industries Electron Tube Division 960 Industrial Road San Carlos, CA 94070		11. Contract or Grant No. NAS 3-15830
		13. Type of Report and Period Covered Contractor Final Report
12. Sponsoring Agency Name and Address National Aeronautics and Space Administration Washington, DC 20546		14. Sponsoring Agency Code

15. Supplementary Notes

Project Manager, G. J. Chomos, Spacecraft Technology Division
NASA-Lewis Research Center
21000 Brookpark Road
Cleveland, OH 44135

16. Abstract

This final report presents the results of the design, development, and test of experimental and production units of a PPM focused traveling wave tube (L-5394) that produces 225 watts of cw rf power over 85 MHz centered at 12.080 GHz. The tube uses a coupled cavity rf circuit with a velocity taper for greater than 26 percent basic efficiency. Overall efficiency of 50 percent is achieved by the incorporation of a multistage depressed collector designed at NASA Lewis Research Center. This collector is cooled by direct radiation to deep space. The tube was designed to be used for broadcasting power transmission from a satellite.

The efforts discussed in this report were performed during a two phase program that extended from April 1972 thru January 1976. The first phase of the program included the analytical and experimental program to study design techniques, to utilize these techniques to optimize the performance (efficiency) of the tubes, and to then assemble a limited quantity of tubes for competitive evaluation. The second phase of the program included design improvement of operational and functional characteristics through additional testing, qualification of the units for space application, and the production of flight configuration units. A total of thirty-two tubes were produced during the Phase II program. Presently, one tube is in orbit and operational via the Communications Technology Satellite (CTS), one is in life test at LeRC, and one is designated flight unit backup. The remaining tubes are being utilized in various experimental test projects.

17. Key Words (Suggested by Author(s)) Traveling Wave Tube Coupled Cavity Slow Wave Circuit Velocity Resynchronization Multistage Depressed Collector Satellite Communications Transmission	18. Distribution Statement Unclassified - Unlimited

19. Security Classif. (of this report)	20. Security Classif. (of this page)	21. No. of Pages	22. Price*
Unclassified	Unclassified	230	

* For sale by the National Technical Information Service, Springfield, Virginia 22161

NASA-C-168 (Rev. 10-75)

FOREWORD

The work and efforts described herein were performed by Litton Industries, Electron Tube Division, under a two-phase NASA Contract, NAS3-15830. The first phase of the program was directed toward analytical definition, design and assembly of prototype tubes to be used for competitive evaluation. The second phase included design improvement, space qualification, and delivery of production units.

During the program there were three principal investigators (Litton Program Managers): Dr. Otto Sauseng, initially during part of Phase I; Mr. B. D. McNary during the remainder of Phase I and part of Phase II; and Mr. C. Lawrence Jones during the remainder of the program. Others providing significant contribution to the program included Dr. G. E. Pokorny, Dr. J. R. M. Vaughan, Messrs. L. R. Bergera, N. Cazacu, R. S. Cerko, B. J. Hamak, J. Heidenreich, R. L. Holm, R. Lewis, P. G. Marquis, and R. VanIderstine..

Mr. G. J. Chomos, Spacecraft Technology Division, NASA Lewis Research Center (LeRC), was Project Manager.

The author and Litton ETD wish to acknowledge Dr. H. G. Kosmahl, Mr. A. N. Curren, Dr. D. J. Connolly, Dr. R. Forman, and Mr. G. Richard Sharp of LeRC for technical assistance provided during the program, and Mr. J. Bozanic of Service & Consulting Associates, Cupertino, CA, for assistance in preparation of this final report.

ABSTRACT

This final report presents the results of the design, development, and test of experimental and production units of a PPM focused traveling wave tube (L-5394) that produces 225 watts of cw rf power over 85 MHz centered at 12.080 GHz. The tube uses a coupled cavity rf circuit with a velocity taper for greater than 26 percent basic efficiency. Overall efficiency of 50 percent is achieved by the incorporation of multistage depressed collector designed at NASA Lewis Research Center. This collector is cooled by direct radiation to deep space. The tube was designed to be used for broadcasting power transmission from a satellite.

The efforts discussed in this report were performed during a two-phase program that extended from April 1972 through January 1976. The first phase of the program included the analytical and experimental program to study design techniques, to utilize these techniques to optimize the performance (efficiency) of the tubes, and to then assemble a limited quantity of tubes for competitive evaluation. The second phase of the program included design improvement of operational and functional characteristics through additional testing, qualification of the units for space application, and the production of flight configuration units. A total of thirty two tubes was produced during the Phase II program. Presently, one tube is in orbit and operational via the Communications Technology Satellite (CTS), one is in life test at LeRC, and one is designated flight unit backup. The remaining tubes are being utilized in various experimental test projects.

PRECEDING PAGE BLANK NOT FILMED

TABLE OF CONTENTS

TABLE OF CONTENTS (Continued)

LIST OF ILLUSTRATIONS

LIST OF ILLUSTRATIONS (Continued)

LIST OF TABLES

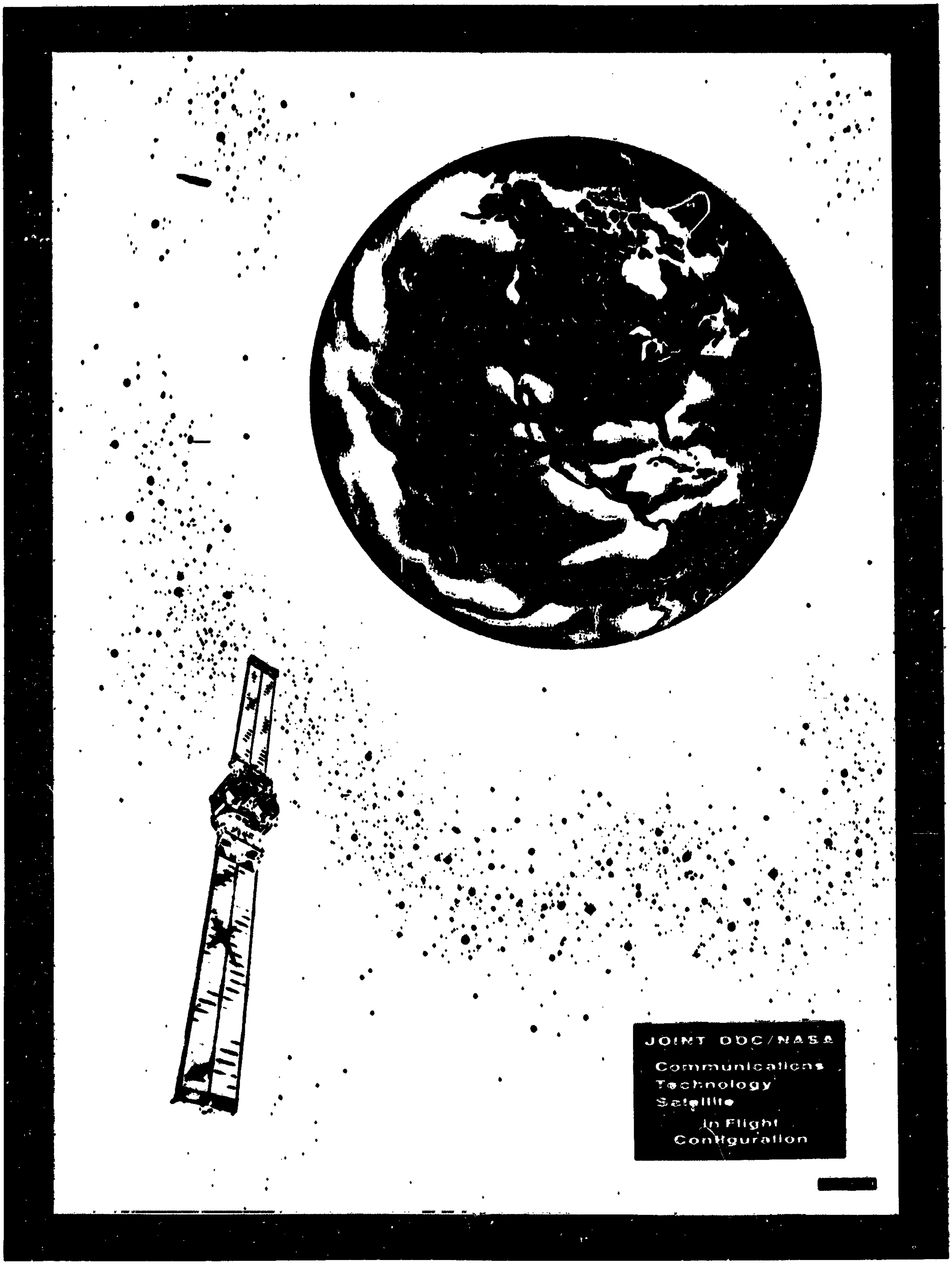
JOINT DOC/NASA
Communications
Technology
Satellite
in Flight
Configuration

1.0 SUMMARY

This final report describes the development of an experimental PPM focused, travelling wave tube (TWT) that produces between 200 and 250 watts of cw rf output power over an 85 MHz frequency band centered at 12.080 GHz. The tube was developed for use in the Communications Technology Satellite (CTS). The tube incorporates a coupled cavity rf circuit with a velocity taper to provide greater than 30 percent basic efficiency. An overall efficiency of 50 percent is achieved through the use of a multiple stage collector with ten depressible elements that is cooled entirely by radiation. To obtain the maximum depressed collector efficiency, a magnetic spent-beam refocusing section is utilized between the output of the rf circuit and the collector. The refocusing section allows reduction of the transverse electron velocities and dilution of the space charge at the entrance to the collector.

The tube was developed during a two phase NASA funded program. For the initial contract phase (Phase I), two firms were awarded identical R&D contracts. This phase included the analytical and experimental efforts necessary to provide assurance that the operational goals were attainable; to study alternative design techniques; to initially optimize the performance of the tubes; and then assemble a limited quantity of tubes for competitive evaluation. At the conclusion of the competitive evaluation, Litton, Electron Tube Division (ETD) was selected as the single contractor for the Phase II contract which included development, qualification and production of flight units.

During Phase I, five traveling wave tubes, Litton Model L5394, were fabricated and tested. The first device incorporated the basic rf circuit design (without the velocity taper), a modulating anode electron gun, periodic permanent magnetic focusing, refocusing solenoid and an undepressed bucket type collector. The tube provided necessary interaction and focusing data used to define the large signal analysis computer program. The remaining four devices had collector aperture openings of 6° and utilized a two step velocity taper and multistage collector for high efficiency. Some difficulty was encountered initially with reflections, instability and oscillations, and Phase I tubes failed to achieve certain specified performance requirements due to the high circuit rf losses and difficulty centering the frequency band. They did, however, meet the specification rf performance requirements at saturation and produced 225 watts cw output power.

One tube (S/N 2006) had a too narrow hot bandwidth and a sharply peaked small signal gain response but, on the positive side, efficiencies of 30 percent without depression and 56 percent overall after depression and 35 db gain were recorded. One tube (S/N 2005) had a properly located and relatively flat power versus frequency response, but low efficiency and marginal gain. The performance of the delivered units did show, however, that the problems or deficiencies could be corrected with additional electrical and mechanical/thermal tests and appropriate design improvements. Based on the results obtained during the competitive evaluation, Litton was awarded the Phase II production contract.

During Phase II, a total of twenty seven additional tubes were fabricated and tested. Prior to the initiation of manufacture of flight model units, the problems or deficiencies revealed during Phase I, and later encountered during Phase II testing, required resolution. These included:

A. Incorrect frequency positioning with the tendency of the power and gain peak to be below the lower band edge (12.038 GHz) and power and gain deficiency at the high frequency end (12.123 GHz).

B. The small signal gain variation across the specified frequency band (12.038 to 12.123 GHz) was about 10 dB, well in excess of the specification requirement.

C. The cathode support sleeve could not tolerate the shock and vibration test requirements.

D. The cathodes were operating at a temperature too high to meet the long life requirements.

E. The electrodes of the multistage collector were supported by U-tabs which were welded between cylinders brazed to the ceramic rods and the vacuum enclosure. These U-tabs failed during vibration tests.

F. The collector, with its relatively large area electrodes had tendencies toward excessive arcing, primarily after long periods of tube shut off.

Due to schedule and monetary restrictions, not all of the possible corrective measures identified were incorporated or implemented in the final flight design units. Those items considered most cost effective and essential to launch or operation were implemented.

The tubes fabricated during Phase II represented numerous unit configurations since various alternatives for subassembly design and fabrication were incorporated. The early fabricated units were assigned to a variety of performance measurements, tests, verifications, and one (S/N 2025) was used for transmitter equipment package qualification testing. Presently, of the flight configuration units manufactured, one tube (S/N 2022) is in orbit and opertional via the Communications Technology Satellite, S/N 2020 is in life test at LeRC, and S/N 2025 is designated prime flight unit backup. Other units are being utilized in various experimental test projects.

The TWT is comprised of five major subassemblies including the (1) electron gun, (2) rf circuit or body, (3) refocusing section, (4) collector, and (5) interface/mechanical items. In order to optimize the tube performance, alternative subassembly configurations and fabrication techniques were analyzed via computer simulation studies during the R&D phase. These analyses were updated and refined during Phase II, and the units fabricated during this phase reflected these updates. The computer analyses of major complexity included the large signal analysis, small signal analysis, rf circuit analysis, and thermal analysis.

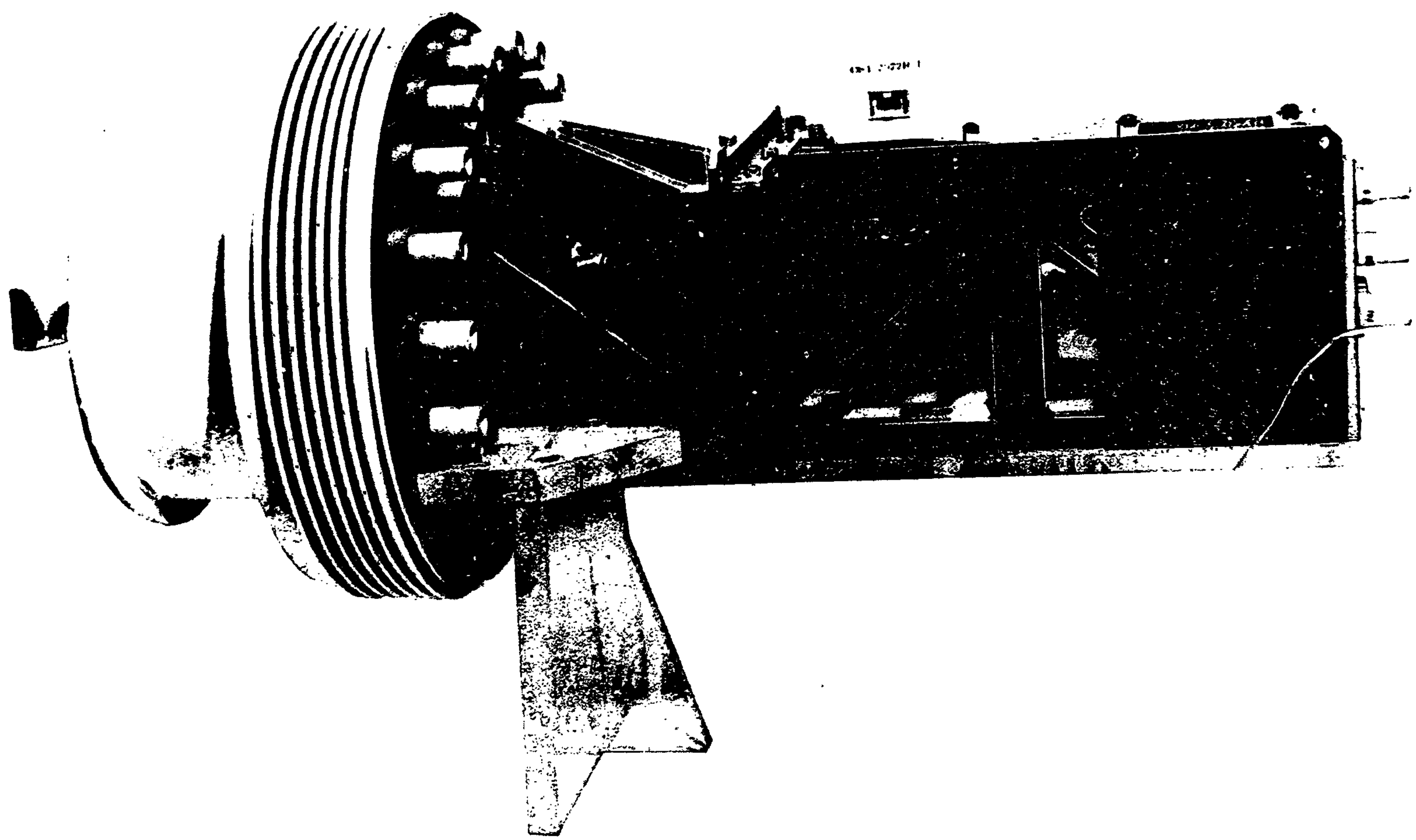

Figure 2-1. TWT, Flight Configuration

2.0 INTRODUCTION

The program described in this report is part of an extensive effort directed by NASA Lewis Research Center to develop satellite communication systems powerful enough to broadcast directly to individual end receivers rather than to ground based distribution systems. These efforts were initiated with detailed studies on several types of power amplifiers for such a system, one of which was an "Analytical Study Program to Develop the Theoretical Design of Traveling Wave Tubes" by NASA Contract NAS3-9719.[1] An outgrowth of this study was a number of development and feasibility evaluation programs which included (1) a high efficiency solenoid focused 12.2 GHz, 4 kW cw coupled cavity traveling wave tube (Contract NAS3-13728),[2] (2) development of a high power 12 GHz. PPM focused traveling wave tube (Contract NAS3-14391)[3], and (3) the Litton Electron Tube Division (ETD) design, development and production of 200 W cw, high efficiency traveling wave tube at 12 GHz (Contract NAS3-15830). All of these above mentioned efforts were in direct support of the Communications Technology Satellite program.

This introductory section provides the reader with some knowledge of the entire NASA program and, in particular, a summary of the Litton effort under Contract NAS3-15830. Through the Litton effort addressed herein, the Model L-5394 TWT shown in figure 2-1 was designed, developed and tested and is currently operating in space aboard the CTS satellite.

2.1 CTS PROGRAM DISCUSSION

The CTS was designed and is currently being utilized by a number of agencies under direction of NASA and the Canadian Department of Communications. The CTS is a high power communications satellite that makes possible the reception of television and two way voice communications using small, low cost ground terminals. Communications links to different parts of Canada and the United States (including Alaska and Hawaii) have been established to support various CTS communications experiments in the areas of education, health and information services. CTS was launched into synchronous orbit by a Delta 2914 launch vehicle in January 1975. An artist's drawing of the CTS in orbit is shown in figure 2-2.

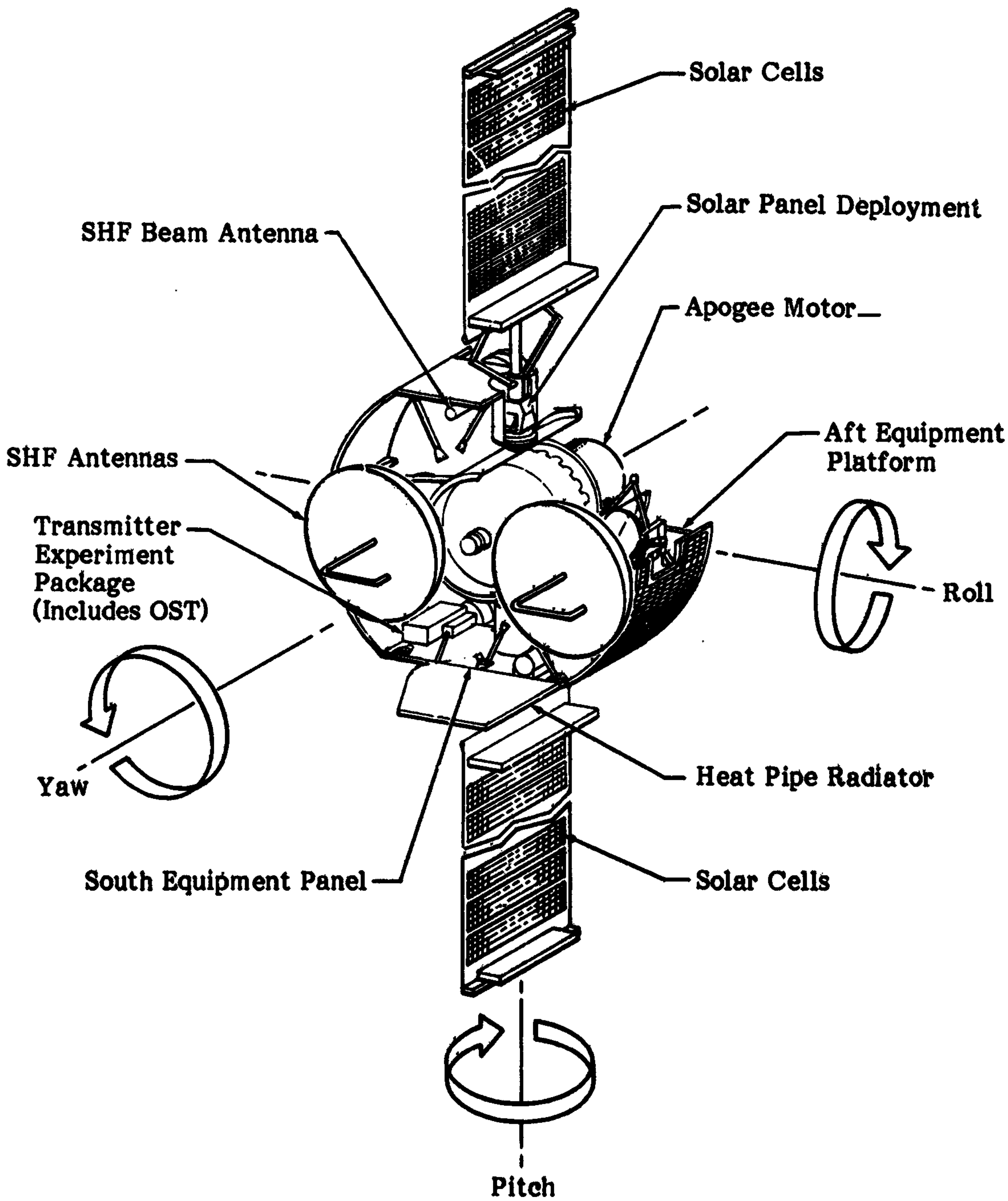

Figure 2-2. CTS in Orbit (Shields Removed)

One of the major responsibilities of the United States in the CTS program was to provide a high power Transmitter Experiment Package (TEP). The TEP is used as the final amplifier in the spacecraft Super High Frequency (SHF) transponder as shown in figure 2-3. The transponder receives signals at 14 GHz, translates, amplifies and transmits these signals at 12 GHz. Two 85 MHz channels are processed through the transponder with one channel amplified to 200 watts through the TEP and the other amplified to 20 watts by a low power traveling wave tube. The 100 mW OST drive power is tapped from one of the 20W Output Tubes. The frequency plan for the CTS is shown in figure 2-4.

The transmitter experiment package (TEP) is made up of two major subassemblies, the Output Stage Tube (OST) and the Power Processor Sub-system (PPS) as shown in figure 2-5. The principal objectives of the TEP development are:

1. To demonstrate in space an amplifier operating with an efficiency greater than 40 percent and a saturated rf output power greater than 180 watts at a frequency of 12 GHz.

2. To demonstrate reliable high efficiency performance for a transmitter experiment package for 2 years in a space environment, and

3. To obtain fundamental data for further advancement in the state-of-the-art of high power microwave amplifier operations in space.

The cross section drawing of the OST (with major subassemblies) is shown in figure 2-6. A photograph of the display model OST cross section with packaging and endplates removed is shown in figure 2-7. The OST is a linear beam traveling wave tube (TWT) amplifier. It achieves a high level of efficient operation by incorporating two unique design features, a velocity taper of the slow-wave structure and a ten element depressed collector (8 potentials different from cathode and body potential). The velocity taper design allows the electron beam to remain in phase at the collector end and the MDC is arranged so the electrons can be collected at or near zero potential. These design features have produced an overall OST efficiency of approximately 50 percent with 200 watts of saturated rf output at 12 GHz.

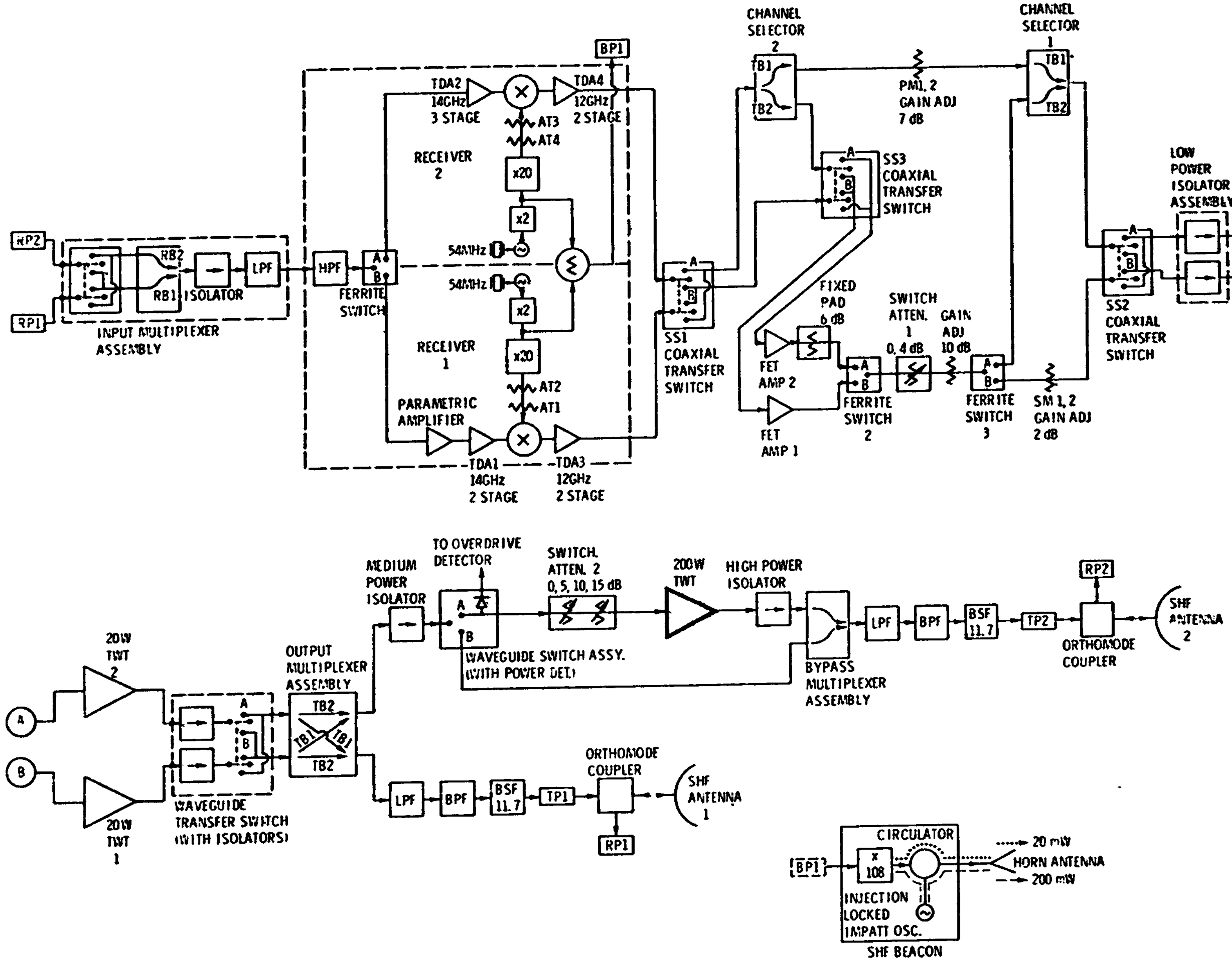

Figure 2-3. CTS SHF System Schematic

ORIGINAL PAGE IS OF POOR QUALITY

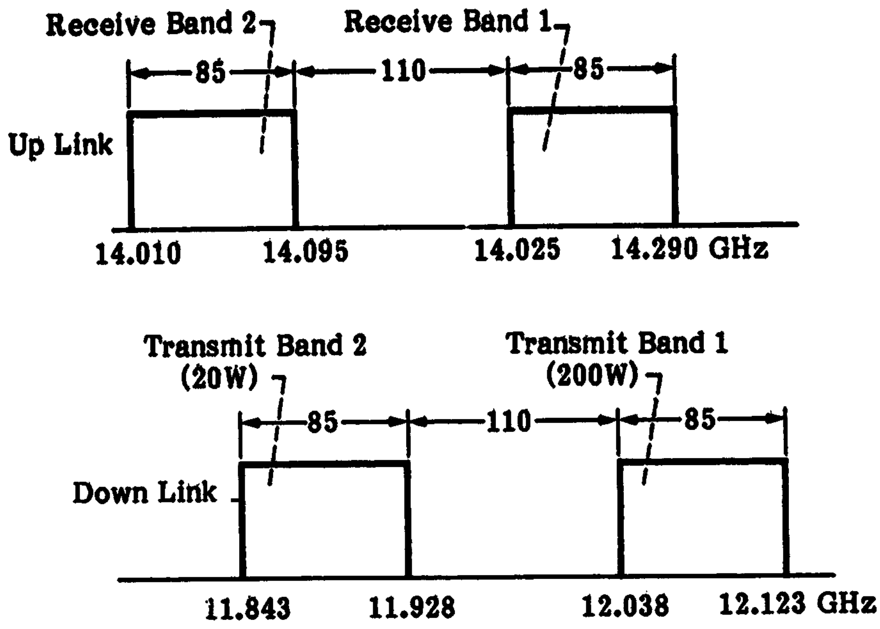

Figure 2-4. CTS Frequency Plan

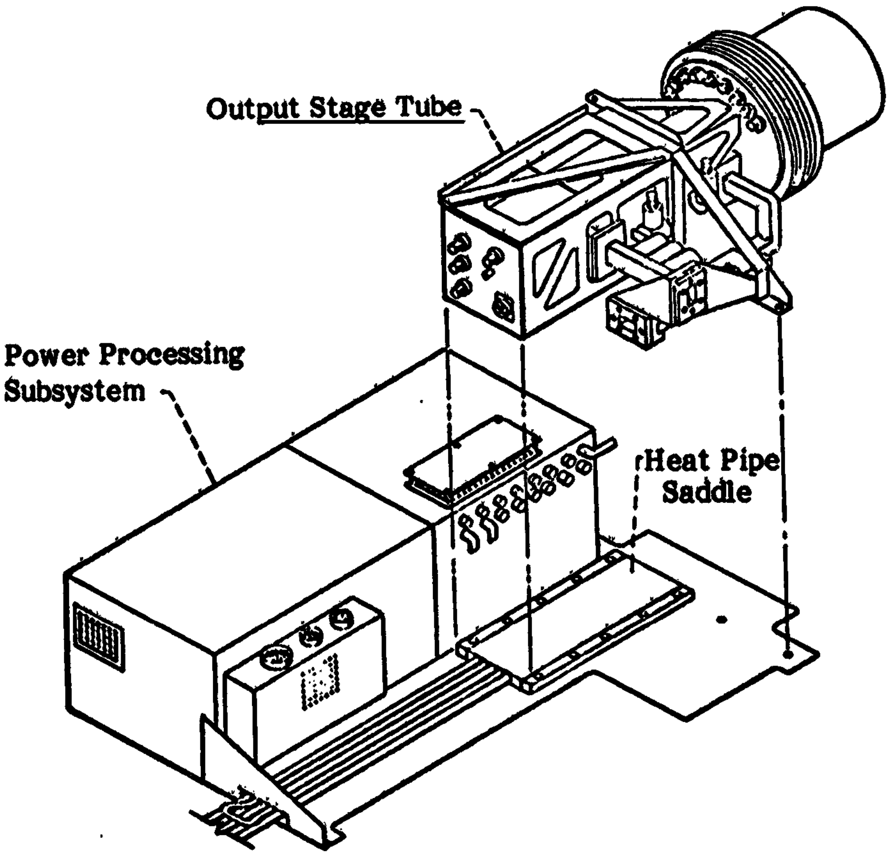

Figure 2-5. TEP Mounting Configuration

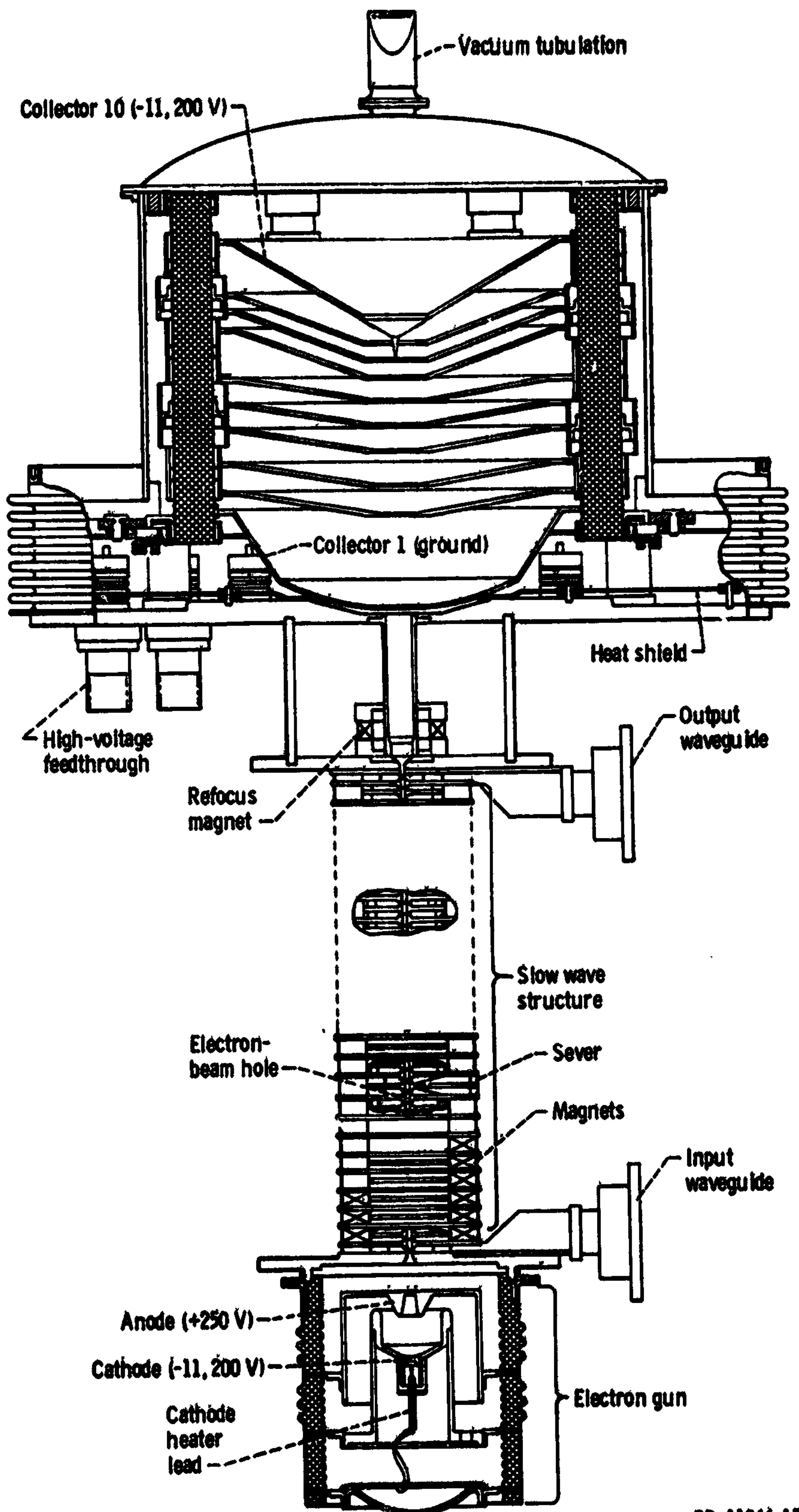

(a) Tube with collector.

Figure 2-6. OST, Cross Section Drawing

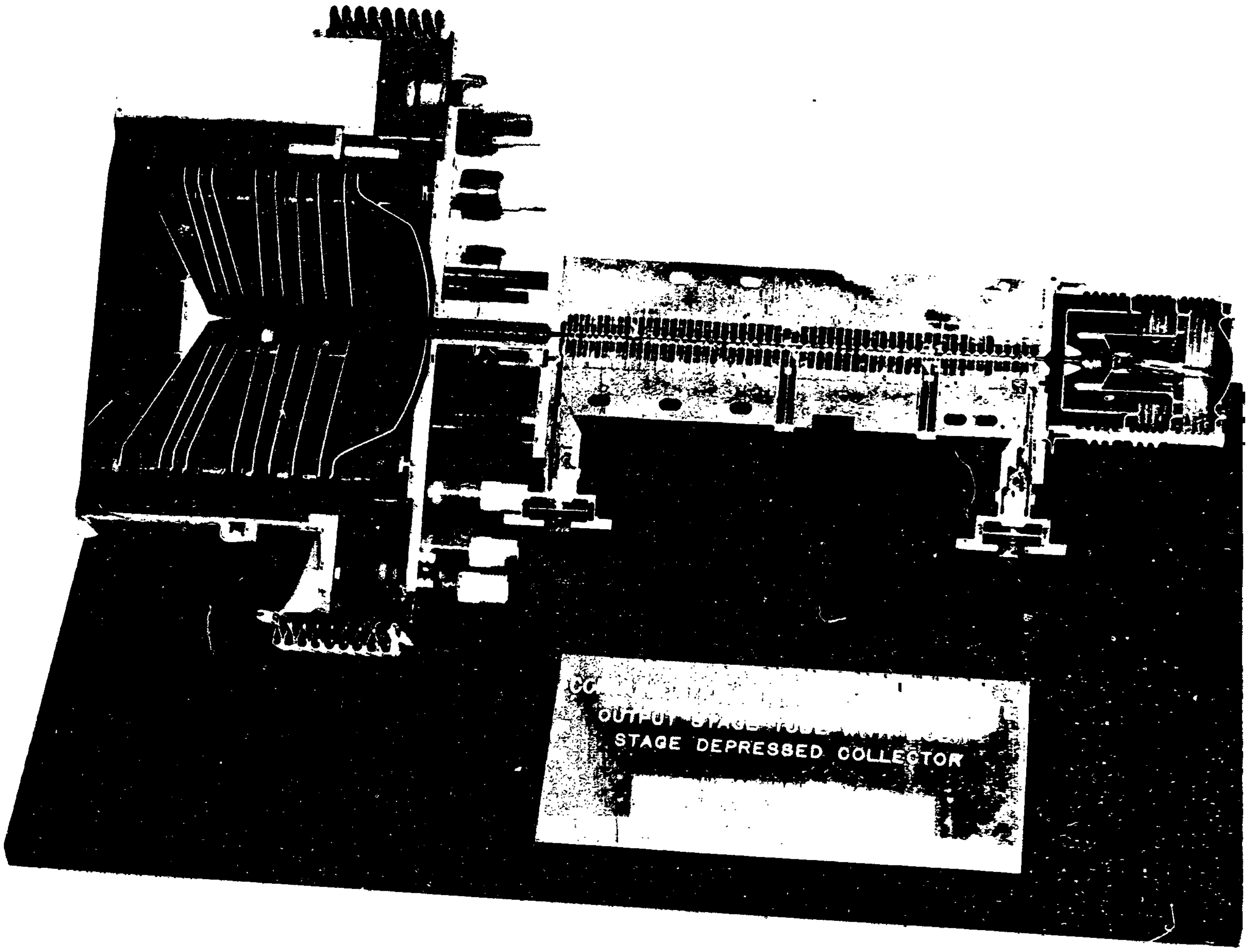

Figure 2-7. OST, Cross Section View

For operation, the OST requires several high voltages. The cathode voltage and current are -11.2 kV at 27 ma. The 10 collector voltages step from the 10th collector element (cathode potential) to the second in 10 percent increments of the cathode voltage. The first collect is tied to ground (body potential). The load on each collector supply varies as a function of rf drive. Two ion pumps on the OST provide telemetry information of internal tube pressure, and require a voltage of 3.2 kV. The cathode heater requires a low voltage supply that operates at cathode potential. An anode is used as an ion trap and requires a positive 250 V potential with respect to the body.

In the complete TEP, the OST is physically mounted onto the PPS with a variable conductance heat pipe system to carry the heat away from the baseplate of the tube to a radiating surface. The TEP is so situated on the spacecraft as to permit the collector cover to radiate directly to space. Four thermistors mounted on the OST are used as temperature sensors. Two diode detectors in the OST output waveguide circuit are used to monitor incident and reflected rf power. The TEP signal conditions all TEP sensors for spacecraft telemetry. Instrumentation has been incorporated into the TEP to permit determination of the OST performance.

The function of the power processor (PPS) is to convert power drawn from the solar array into the forms required by the various system elements. In addition to providing regulated voltages to the output stage tube, the power processor also provides the instrumentation, command, and protection functions for the total system.

2.2 RESEARCH & DEVELOPMENT (PHASE I) CONTRACT DEFINITION

The OST utilized in the CTS was developed under a two-phase NASA contract. The first phase was performed under parallel, identical contracts, by two contractors, (Litton, Electron Tube Division and Hughes Aircraft, Electron Dynamics Division). This research and development phase included the analytical and experimental efforts necessary to provide assurance that the operational goals for the OST were attainable, to study alternative design techniques, to initially optimize the performance characteristics of the tube, and to then assemble a limited quantity of tubes for competitive evaluation. During this phase, contractual requirements and tube performance specification values were as listed in tables 2-1 and 2-2, respectively.

The tubes fabricated during the later period of this R&D phase incorporated the multistage depressed collector designed by LeRC, and also incorporated several other design features that had not previously been used in space applications. These included: (1) an electron gun using a barium impregnated tungsten cathode; (2) a high power coupled cavity rf circuit with a velocity taper for high basic efficiency; (3) a beam refocusing section for high overall efficiency; and (4) radiation cooling of the collector to minimize the thermal load on the satellite system.

During Phase I, three Litton Model L-5394 traveling wave tubes were fabricated and tested. The first device incorporated the basic rf circuit design (without the velocity taper), a modulating anode electron gun, periodic permanent magnetic focusing, refocusing solenoid and an undepressed bucket type collector. The tube provided necessary interaction and focusing data used to define the large signal analysis computer program. The remaining two devices had collector aperature half-angles of 6° and utilized a two step velocity (period) taper and the multistage collector for high efficiency. Some difficulty was encountered initially with reflections, instability and oscillations, and therefore, the initial tubes failed to achieve certain specified performance requirements due to the high circuit rf losses and a mode instability. They did, however, meet the specification rf performance at saturation by producing 225 watts cw output power.

One tube (S/N 2006) had a too narrow hot bandwidth and a sharply peaked small signal gain response but, on the positive side, efficiencies of 30 percent without depression and 56 percent overall after depression and 35 dB gain were recorded. One tube (S/N 2005) had a properly located and relatively flat power versus frequency response, but an inadequate efficiency and marginal gain. The performance of the Phase I delivered units indicated that the problems or deficiencies could be corrected with additional electrical and mechanical/thermal tests and appropriate design improvements. Based on the results obtained during the competitive evaluation of Phase I efforts, Litton was awarded the Phase II production contract.

Table 2-1. Phase I Contractual Requirements/Tasks

TASK NO.	DESCRIPTION
AR	<u>General Task</u> Provide resources necessary to conceive, analyze, optimize, design, fabricate, test, evaluate, and deliver Engineering Test Model OST's, with attendant OST design information. <u>Specific Tasks</u>:
1.	Generate a design for a TWT meeting the design specifications.
2.	Conduct a computer analysis of the design to: (a) Verify analytically that the design will meet the specifications. (b) Disclose by variation of parameters what design modifications will result in an optimized design achieving the highest interaction efficiency within the bounds of the specifications.
3.	Optimize the design of Item 1 based upon the results of (b).
4.	Fabricate one TWT to the optimized design.
5.	Test the TWT per specification and submit the raw data to NASA.
6.	Design and fabricate a multistage depressed collector (MDC), based upon a preliminary field configuration and aperature sizes supplied by LeRC.
7.	Integrate the MDC developed in Task 6 with a TWT into a preliminary OST.
8.	Test the preliminary OST to determine the extent to which the preliminary OST meets the OST specification.
9.	Update the MDC design based upon the results of Task 8 testing.
10.	Fabricate an MDC to the modified MDC design of Task 9, integrate it with the TWT developed Task 8, and test this updated OST. Deliver unit to LeRC.
11.	Generate a design for an ETM OST meeting the specifications.
12.	Fabricate three ETM OST's to the design of Task 11.
13.	Test the ETM OST's to determine that they meet the specifications, and submit test data. Deliver OST to LeRC.
14.	Perform a preliminary OST design study to provide design information for the Transmitter Experiment Package Design. The study shall include documentation of the following: (a) A drawing, showing size and/or location of the OST, input and output waveguides, electrical interconnections for power and instrumentation. (b) Weight of the OST. (c) Method of OST mounting.

Table 2-1. Phase I Contractual Requirements/Tasks (Continued)

TASK NO.	DESCRIPTION
	(d) Thermal interface requirement defining OST mounting, temperature limitations, and thermal losses.
	(e) A drawing showing the mechanical interface between OST and TEP with mechanical interconnections.
	(f) The OST voltages, current, regulation and ripple requirements, method of application and dynamic requirements for startup, method of removal for shutdown and surge current limitations. Collector voltages and computed currents to be based on the TWT design of Task 1.
	(g) Measurements, level of signals, types and location of connectors.
	(h) Electrical input power, voltage, currents, types and location of connectors and/or interconnections.
	(i) Calculated magnetic moment of OST.
	(j) Calculated weight, C.G. and moments of inertia of the OST.
	(k) A power schedule listing OST operational power requirements.
	(l) An estimate of gain vs frequency for output levels -5 dB, -3 dB, and at saturation.
	(m) Definition of a tube parameter which can be used as an indication of overdrive greater than 5 dB.
15.	Fabricate and deliver three Conflat vacuum flanges with rf input and output waveguides, one dynamic mass model of the OST, and one thermal model of the OST.
16.	Select materials used on the OST and suitable for operation in a vacuum (1×10^{-5} Torr). Deliver the list to the NASA Project Manager for evaluation.
17.	Review and provide comments on the CTS Interface Requirements Document.
18.	Design, fabricate and deliver one geometric model of the OST showing the location of electrical connectors and method of attachment to the spacecraft.
19.	Document the results of Phase I in report form, and provide a presentation to NASA Project Manager.

Table 2-2. Phase I TWT Design Specifications

ITEM NO.	PARAMETER	VALUE	TOLERANCE
1.	Frequency, GHz	12.038 to 12.123	N/A
2.	Efficiency, Percent (%)	50	Minimum
3.	Rf Power at saturation, Watts	200	Minimum
4.	Bandwidth, small signal, MHz	85 to 250	N/A
5.	Saturated gain in passband, dB	33	±1
6.	2nd. order phase deviation, Deg./MHz^2	0.2	Maximum
7.	Noise figure, dB	40	Maximum
8.	Beam transmission at saturation, percent (%)	95	Minimum
9.	Power to load (VSWR 1.25), Watts	200	Minimum
10.	Cathode voltage, Volts	16,000	Maximum
11.	Collector region leakage field, percent (%)	0.5	Maximum
12.	Differential gain, any frequency (from constant gain with power output from -70 dBm to 3 dB below saturation), dB	0	±0.5 (max)
13.	2nd and 3rd harmonic content of rf output, dBm	-7	Maximum
14.	Spurious outputs:		
	(a) In a 4 KHz band, 14.0 to 14.3 GHz, dBm	-40	Maximum
	(b) In a 100 MHz band, 10.0 to 18.0 GHz, dBm	-40	Maximum.
15.	Power input without damage/operation effect, dBm	-5	Maximum
16.	Design life, years	2	Minimum
17.	Refocusing technique	Beam coil or PPM	N/A
18	Focusing field	PPM	N/A

2.3 QUALIFICATION AND DELIVERY OF OST FLIGHT HARDWARE (PHASE II)

Utilizing the experimental OST's resulting from Phase I effort as a quantitative basis upon which to proceed, Phase II was concerned with the optimization of design through additional testing and problem resolution, qualification of units to meet CTS spacecraft environmental exposure, and delivery of flight hardware. The specification performance values of the tube for the Phase II units were not altered significantly from the Phase I units. Several specification values were relaxed slightly to compensate for production unit variations. The intent of Phase II effort was to improve the operating characteristics of the tube to the extent possible while performing the contractor activities shown in table 2-3.

During Phase II, a total of twenty seven tubes were fabricated and tested. Prior to the initiation of manufacture of flight model units, the problems or deficiencies revealed during Phase I and later encountered during Phase II testing, required resolution. These included:

A. Incorrect frequency positioning with the tendency of the power and gain peak to be below the lower band edge (12.038 GHz) and power and gain deficiency at the high frequency end (12.123 GHz).

B. The small signal gain variation across the specified frequency band (12.038 to 12.123 GHz) was about 10 dB, well in excess of the specification requirement.

C. The cathode support sleeve could not tolerate the shock and vibration test requirements.

D. The cathodes were operating at a temperature too high to meet the long life requirements.

E. The electrodes of the multistage collector were supported by U-tabs which were welded between cylinders brazed to the ceramic rods and the vacuum enclosure. These U-tabs failed during vibration tests.

F. The collector with its relatively large area electrodes had a strong tendency toward excessive arcing, primarily after long shut off periods of the tube.

Table 2-3. Phase II, Contract Activities

TASK NO.	DESCRIPTION
AR	General Task Utilizing the experimental OST's resulting from the Phase I effort as a quantitative basis upon which to proceed, Phase II includes qualification and delivery of flight hardware. Provide all labor, personnel, and facilities necessary to: fabricate and test the OST's, support PPS and OST compatibility tests, perform limited burn-in testing on two (2) QF OST's, and deliver qualified flight model OST's. Specific Tasks
1.	Support a system compatibility test of the ETM OST, ETM power processing system, driver amplifier, load and AGE. The OST will be operated from zero to saturated rf output power to demonstrate the compatibility of the OST with the supporting system.
2.	Develop acceptance test procedures, provide test facilities, design and fabricate supporting test hardware for the Qualification-Flight OST and provide applicable Test Requirement Documents.
3.	Generate a baseline design document for a QF OST meeting the specifications. The design shall be based upon the ETM OST's developed in Phase I and the results of the system compatibility testing.
4.	Fabricate and test QF OST's to the approved baseline design. Provide rf acceptance test and deliver eight (8) QF OST's to LeRC.
5.	Provide, for each QF OST, a data package containing a complete description of the rf acceptance testing, mechanical inspection and other data per the baseline document.
6..	Provide to NASA the final updated design drawings or as built if construction differs from the baseline design.
7.	Upon completion of rf acceptance testing, subject two (2) QF OST's to one month electrical life tests.
8.	Design and fabricate suitable containers for OST delivery and storage.
9.	Review all of the CRC specifications to determine any discrepancies that may exist between the CRC specifications and the Contract Specifications.
10.	Review and provide comments on the CTS interface requirements document.
11.	Fabricate two rf test systems for production and qualification testing.

3.0 DESIGN APPROACH AND TRADE-OFF CONSIDERATIONS

The basic design approach for the TWT was guided by the requirement for high average output power with reliable operation and long life potential. The coupled cavity circuit was judged to be the only type capable of providing this high power level as a result of its superior thermal properties. A velocity taper was chosen for efficiency enhancement rather than a voltage jump for reasons of reliablity. Brillouin flow beam focusing with low cathode loading was used, consistent with long life design. The values or approach taken in each case was based on the result of the computer analyses, test measurements, and influenced by factors outlined in this section.

3.1 SUMMARY OF SPECIFICATION REQUIREMENTS

Those specifications which most directly effect the choice of design parameters are frequency, power, and efficiency. Frequency and power, taken together, place limits on the mechanical design due to thermal considerations. The choice of alternative circuit and beam parameters for high efficiency, in part conflicted with the selected thermal design. The required performance of the tube represented significant advancements in the state of the art, especially with respect to efficiency enhancement and the thermal design.

Efficiency enhancement was accomplished by velocity resynchronization of the circuit wave and beam wave using a velocity taper near the output of the circuit. The initial tubes were designed to permit experimental evaluation of advanced multistage collector depression schemes for further efficiency enhancement. For this purpose provisions were made to replace the conventional depressed collector by a variety of multistage collectors and include a refocusing section between output coupler and first collector stage. This type of structure can conveniently be combined with an integrated periodic permanent magnet (PPM) focusing configuration, such that portions of the circuit structure (cavity walls and ferrules) are simultaneously used as pole pieces for the focusing configuration. These parts are fabricated from copper since the capability of such a design could better meet the requirements for thermal flow and subsequent radiation cooling.

Since the focusing quality of a PPM tube is generally lower than that of the same size solenoid focused tube, power losses due to beam interception were, therefore, expected to be higher. The power handling capability of such a conventional PPM focused tube was considered marginal for the specified power level. Special advanced thermal design features were incorporated into the tube, including a thick copper cladding of the magnetic focusing system in which the internal pole pieces consist of magnetic ferrules with copper (rather than iron) webs to further improve their thermal conductance. The coupled cavity slow wave structure was selected over a helix type slow wave circuit because its all metal structure provides improved heat transfer and thermal capacity. Temperatures of the circuit remain lower at any given output power and the tendency toward catastrophic failure is minimized. This is especially important above the 200 watt level because it is expected to result in higher tube reliability and longer tube life.

The focusing system incorporated Alnico 8 magnets which exhibit high magnetic performance with exceptional uniformity in characteristics. These magnets were subsequently replaced by similar samarium cobalt magnets. In addition, the initial tubes incorporated several unique features designed to allow use of the tube as a test unit for experimental evaluation of a variety of multistage collector configurations and related design alternatives.

The cold to hot bandwidth ratio of 15:1 was selected to reduce circuit losses, and the band center was placed below a phase shift of 1.2π per cavity in order to raise the interaction impedance. The perveance selected was 62.5 nP, and a collector aperture opening of 6° was utilized in the initial designed units. The primary specification requirements that impacted the initial tube design are shown in table 3-1.

The initial rf circuit design was based on rf cold tests and computer analysis, the development of an electron gun design was based on computer prediction techniques and experimental verification, and the development of the beam focusing design was based on computer prediction and experimental verification through magnetic field measurements.

Table 3-1. Primary Specification Requirements, Phase I

ITEM	PARAMETER	VALUE
1	Frequency	12.038 to 12.123 GHz
2	Efficiency	50 percent, minimum
3	Power Output	200 watts, minimum
4	Bandwidth	85 to 250 MHz
5	Saturated Gain	33 dB, minimum
6	Noise Figure	40 dB, maximum
7	Cathode Voltage	16 kV, maximum
8	Design Life	2 years

The specific value initial design or approach selected for each subassembly was based on the results of the computer analyses, test measurements, and influenced by factors outlined in this section.

3.2 INITIAL ELECTRICAL DESIGN

Five traveling wave tubes were scheduled to be built to verify the analytical design. Only three units were completely assembled, and the parts of the other two were used for subassembly test and design verification. The test results for the three assembled TWT's are shown in table 3-2. The specification values, and the measured (or observed) values are shown to provide a ready comparison of specified versus designed.

The comparison of the specification values with the measured electrical values shows that of the three units, most of the specifications were demonstrated by the initial design, but no single tube provided all of the electrical limits. The results did indicate that the specified limits were probably obtainable. Some of the operational values were based on interpretations of measurement curves and in part are discussed below. Representative graphical presentations of some of the recordings of these initial units in test are also presented in this section.

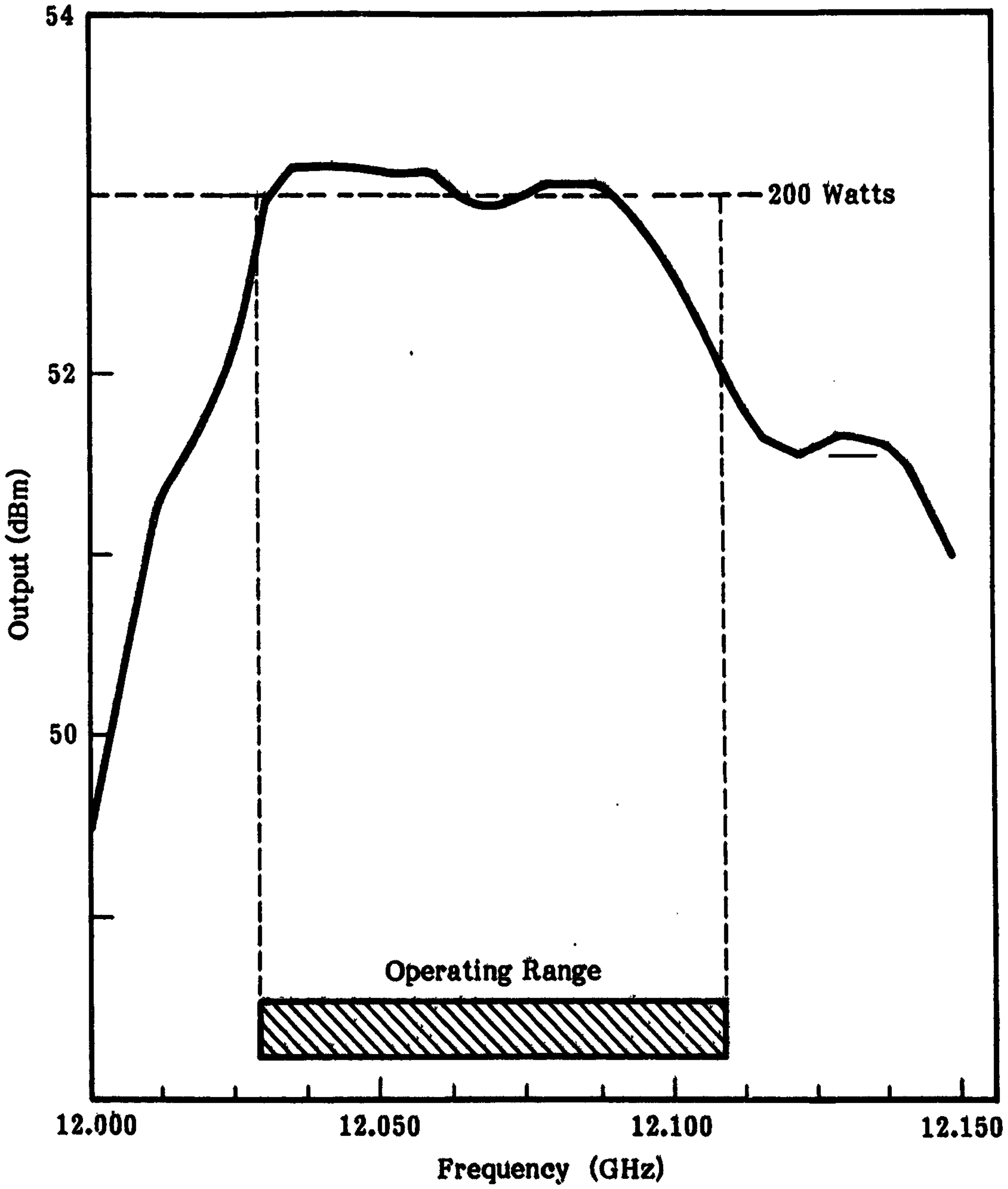

Figure 3-1. Power Output Curve at Saturation (S/N 2006)

Table 3-2. Performance Values, Phase I Units

FUNCTIONAL CHARACTERISTIC	SPEC. VALUE	UNIT NO. 1 S/N 2003	UNIT NO. 2 S/N 2005	UNIT NO. 3 S/N 2006
Interaction Efficiency	30%	28%	26%	33%
Center Frequency, GHz	12.0805	11.960	-	12.065
RF Power Output	200 W	175 W	200 W	200 W
3 dB Band,width, MHz	85-250	210 MHz	200 MHz	150 MHz
Saturated Gain	33 dB	35 dB	35 dB	38.5 dB
PPM Focus	-	Except Refocus	All PPM	All PPM
Noise Figure	40 dB	40 dB	Not Meas.	30 dB
Beam Transmission at Saturation	95%	96%	83%	90%
Maximum Voltage	16 kV	12 kV	11.8 kV	11.3 kV
Shielded Collector	-	yes	yes	yes
Cu Bar to Base	-	yes	yes	yes
2nd & 3rd Harmonic	-7 dBw	-10 dBw	Not Meas.	-10 dBw
Spurious Output	-37 dBw	-50 dBw	Not Meas.	-50 dBw
Weight	12.23 kg (27 lbs.)	15.45 kg (34 lbs.)	12.23 kg (27 lbs.)	15.45 kg (34 lbs.)

Figure 3-1 is a plot of the output power (in dBm) in relationship to frequency (from 12.000 GHz to approximately 12.125 GHz) at saturation. Note that the curve is relatively flat about the center frequency of 12.050 GHz, and that the power level is above or close to the 200 watt level from 12.020 to 12.065 MHz. A slight dip in the output is shown almost at the center frequency, and peak power is reached at approximately 12.035 GHz. At 10 dB below saturation the position of peak power output remains at the same frequency, but the upper band edge falls more rapidly, as expected. This is shown in figure 3-2.

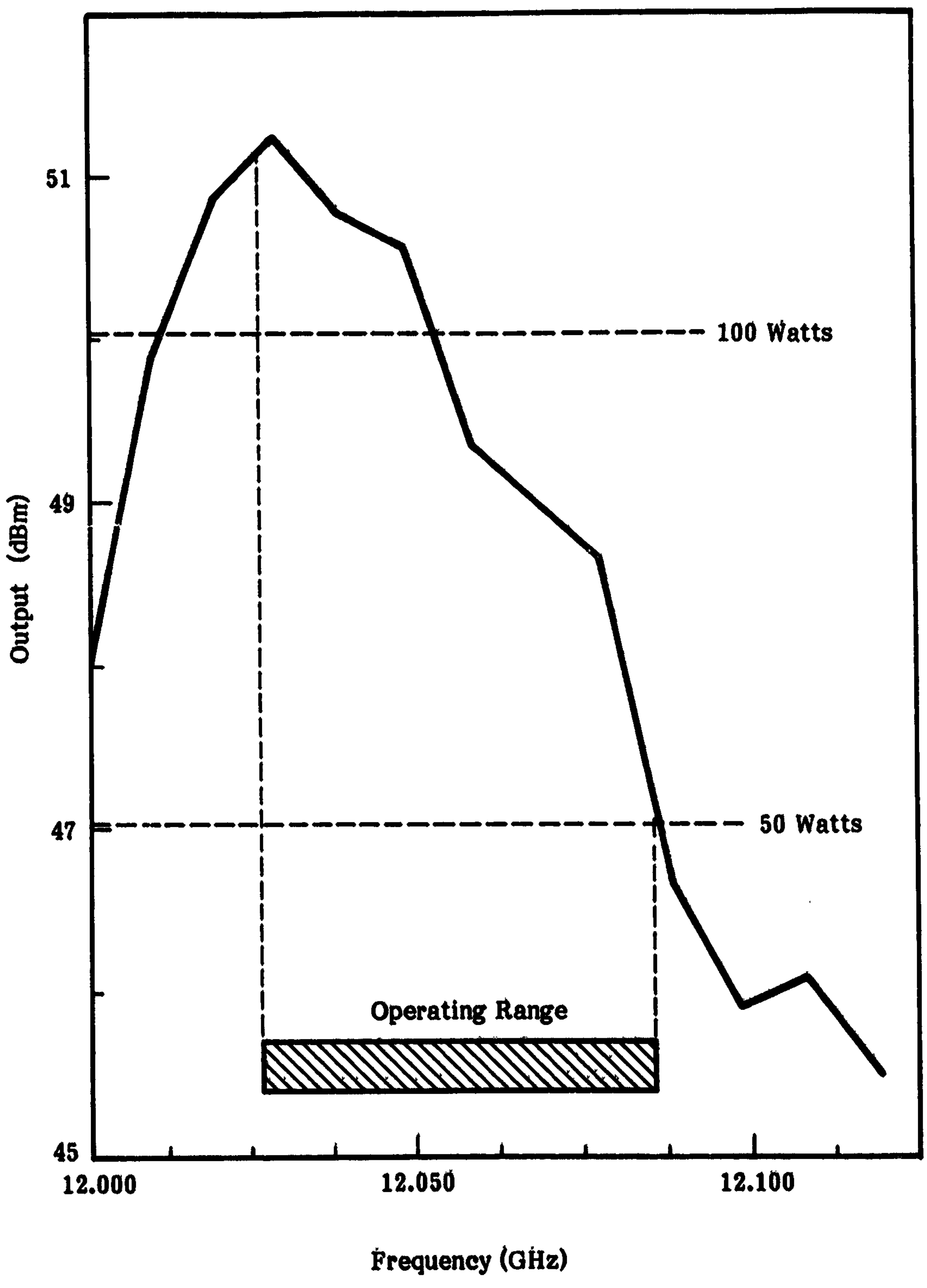

Figure 3-2. Output 10 dB Below Saturation (S/N 2006)

The saturation curves (drive vs. output in dBm) are shown in figure 3-3 for six frequencies, about the center frequency. The frequencies at which the measurements were made are shown on the figure. The relative phase measurements (at varying levels below saturation) are shown in figure 3-4. The incremental slope of the resultant curves can then be used to show the derivative phase vs. frequency relationship ($d\phi/df$). The power output (in watts), versus frequency at different drive power, cathode voltages and current levels is shown in figure 3-5. Figure 3-6 shows the frequency versus output power (dB), with the V_o at 11 kV, and at the five curves below saturation. The relative phase shift (ϕ in degrees) versus frequency at varying V_o is shown in figure 3-7. The results shown yield approximately 25°/500 V. = 0.05°/V. phase shift. A composite of four curves for a Phase I unit at -6 dB and +6 dB, with V_o at 11 Kv and 12 kV are shown in figure 3-8.

3.3 FINAL DESIGN CONFIGURATION

During the second phase of the contract (flight unit qualification and production unit delivery), a total of twenty seven tubes were assembled, fabricated, and/or tested. The final design configuration is representative of approximately the later half of the tubes fabricated. Those include the flight unit, and two flight back-up units. The test results summary for representative final design configuration units is shown in table 3-3. The physical dimensions of the flight unit are shown in figure 3-9 and the measured values are provided in table 3-4. Most of the subassemblies analyzed and developed during the R&D phase (I) were utilized in the final design. The measured power output curve representative of the final design configuration is shown in figure 3-10.

Of the three major subassemblies comprising the OST, the most extensive design effort was completed on the tube body (rf circuit) subassembly. The final tube circuit as shown in figure 3-11, is separated into three gain sections by two internal severs. No other tube stabilization techniques are used, such as loss buttons or distributed loss. For efficiency enhancement, the output section incorporates a two step velocity taper as shown in figure 3-12. A comparison of computed electronic efficiency with and without velocity taper is shown in figure 3-13. The tube is normally operated in "undervoltaged" condition (velocity

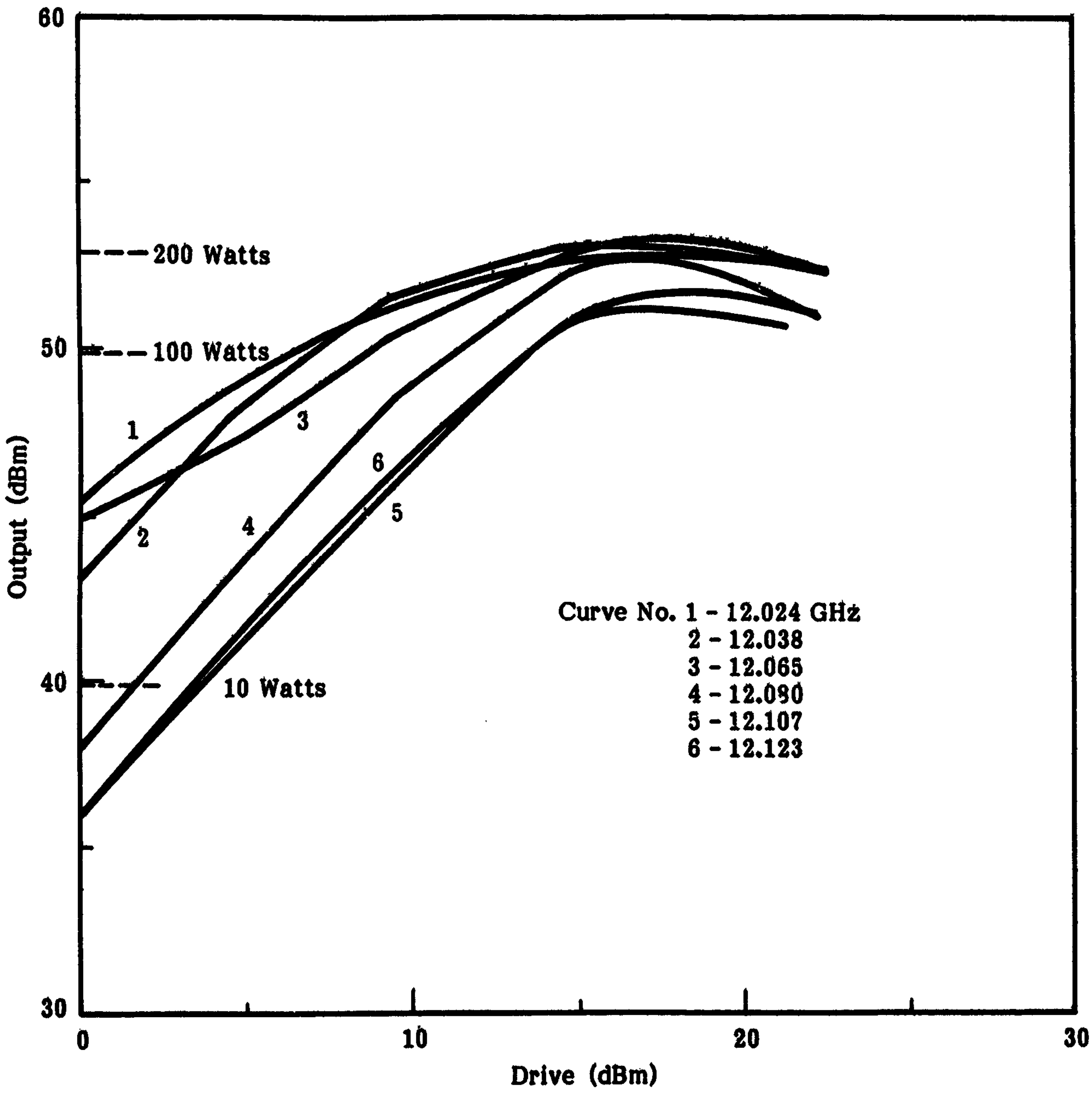

Figure 3-3. Saturation Curves (S/N 2005)

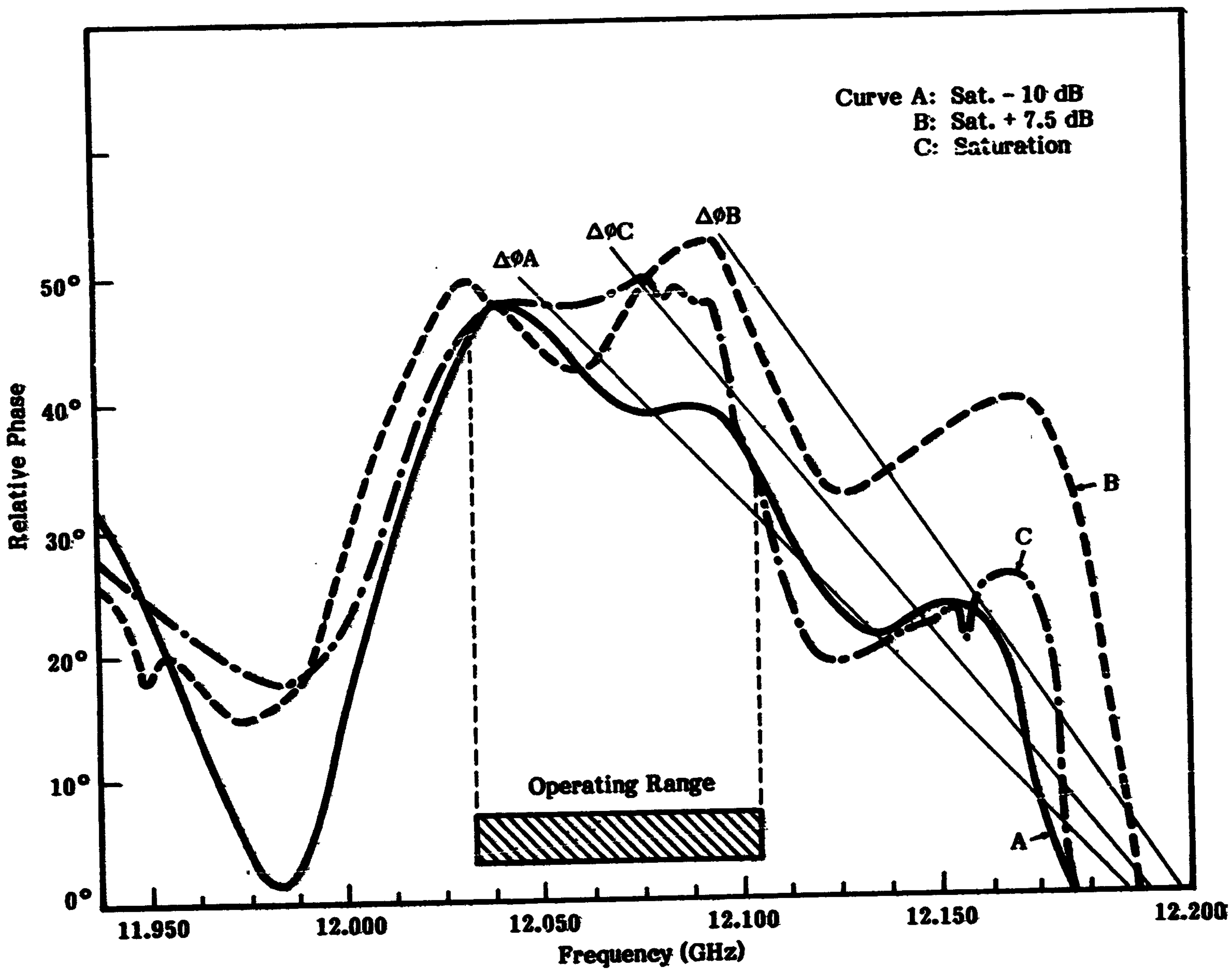

Figure 3-4. Frequency vs. Relative Phase (S/N 2006)

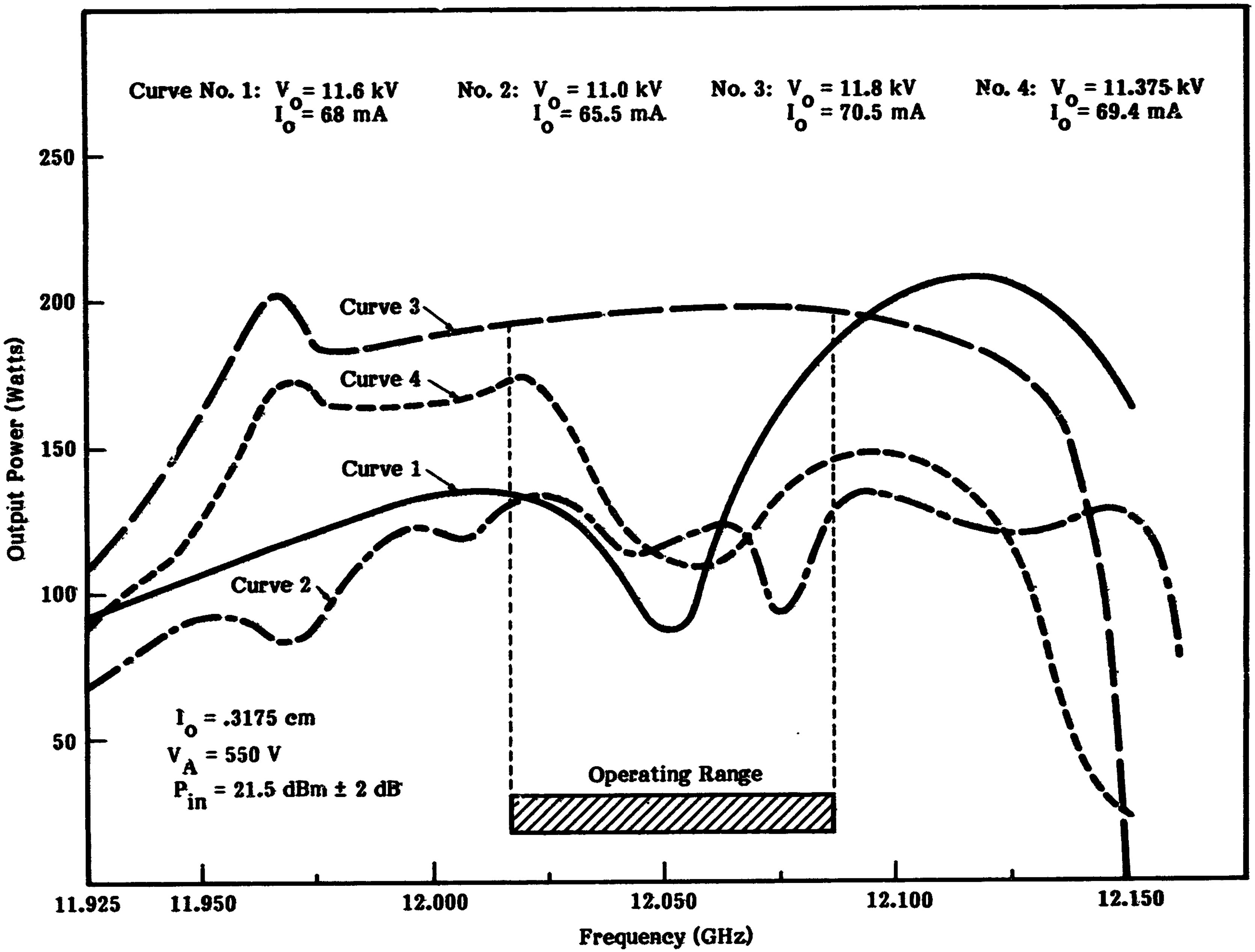

Figure 3-5. Output Power vs. Frequency (S/N 2006)

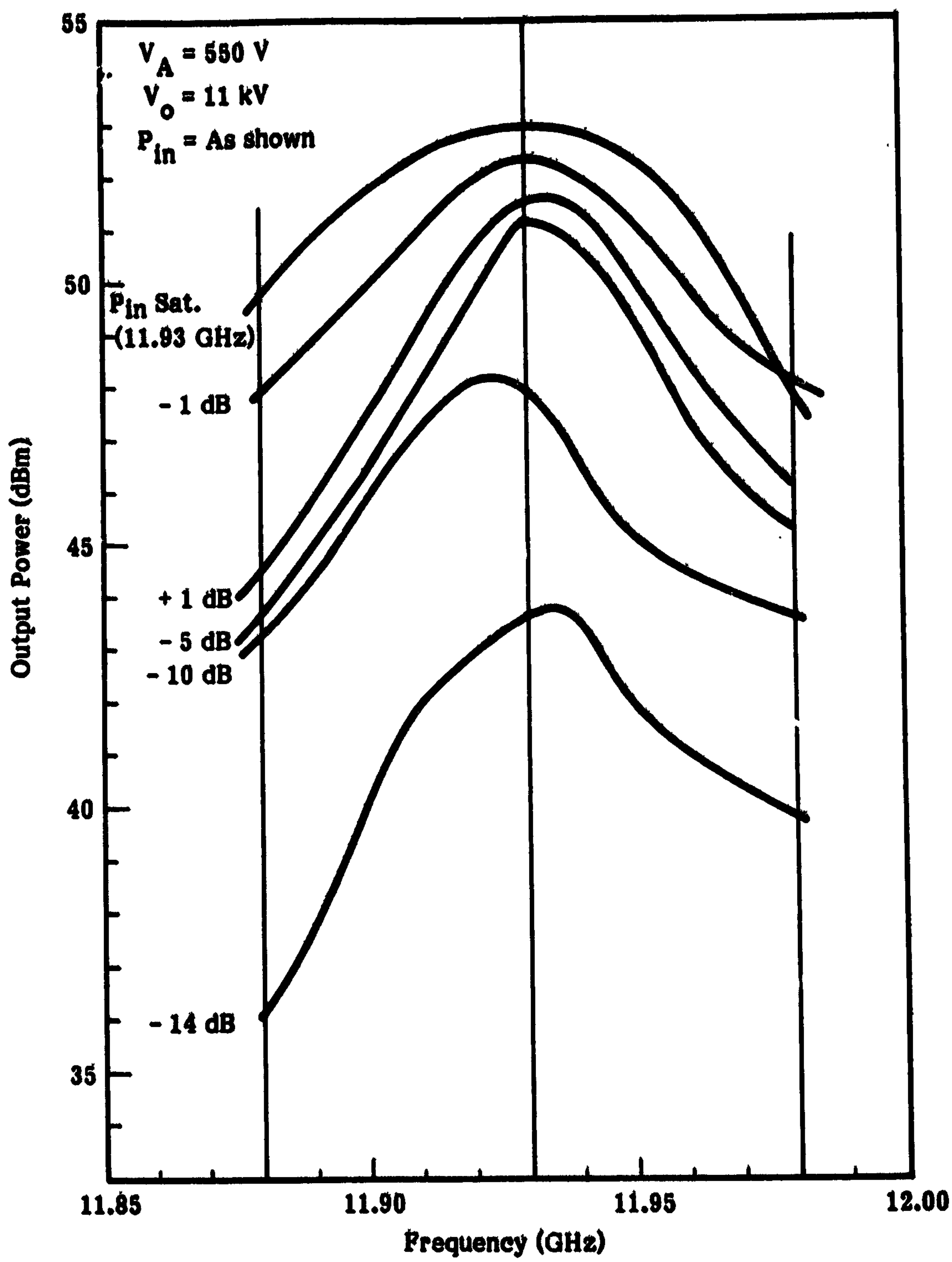

Figure 3-6. Relative Output Power (S/N 2006)

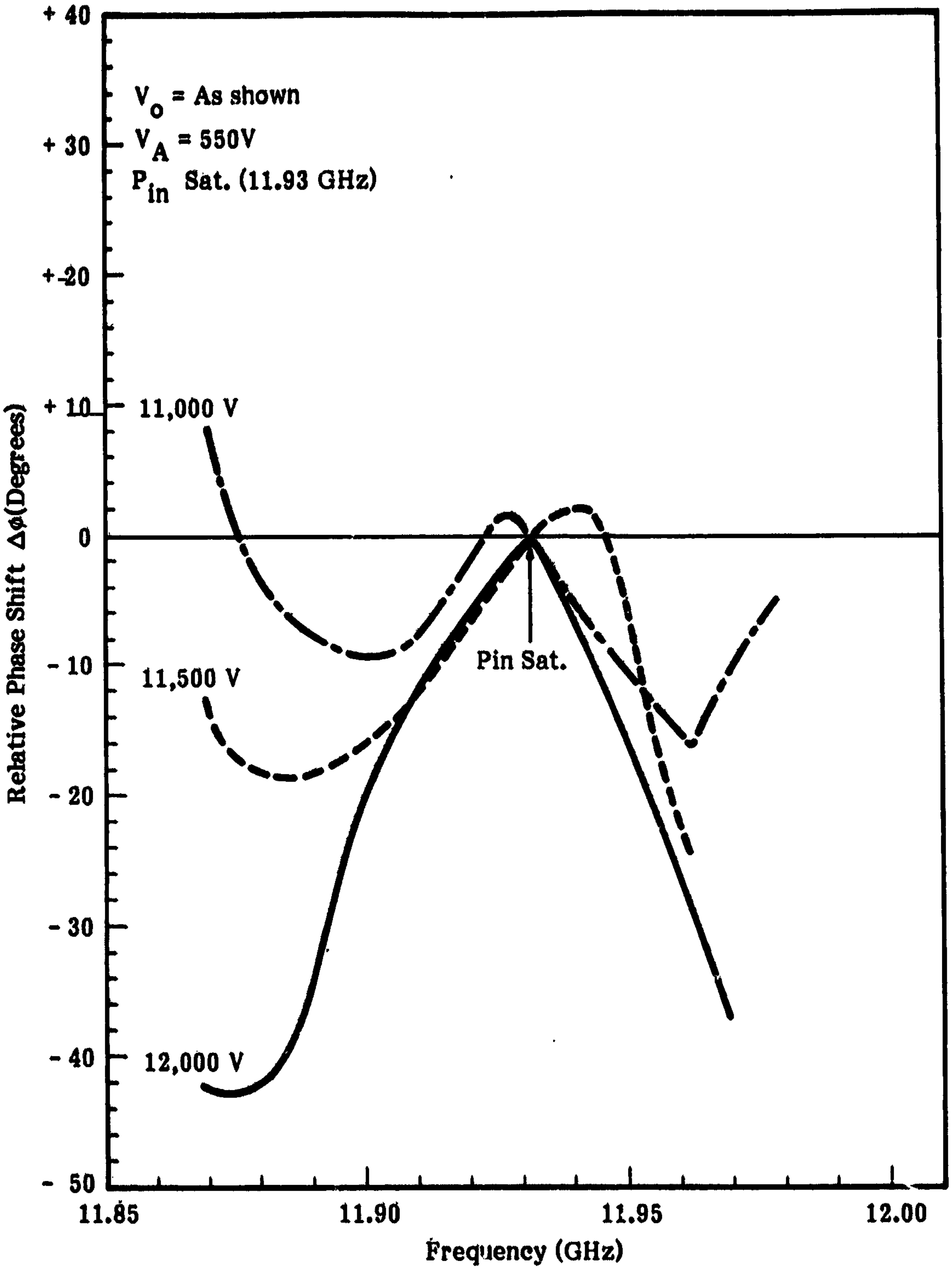

Figure 3-7. Phase Shift vs. Frequency (S/N 2006)

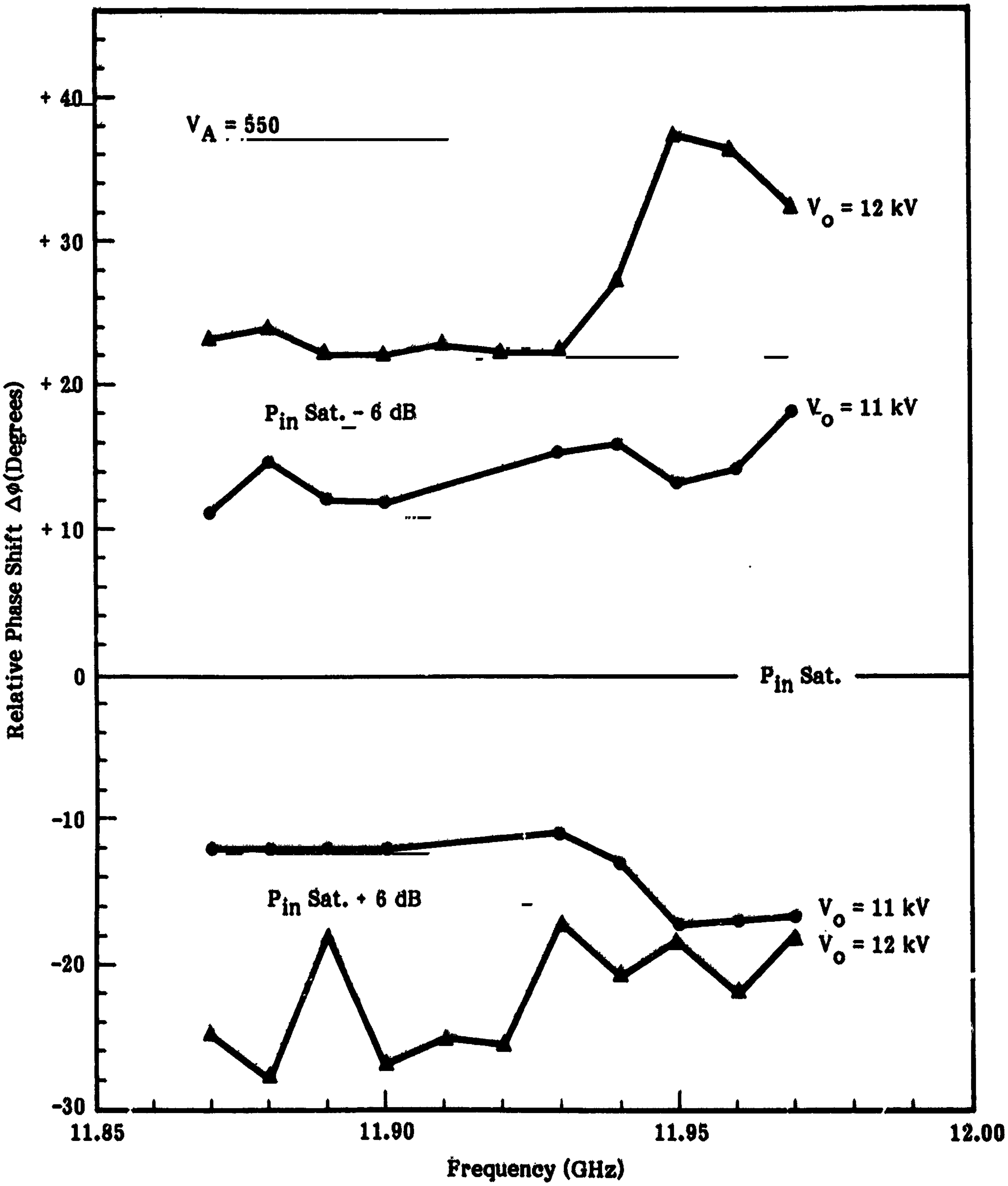

Figure 3-8. Relative Phase Shift vs. Frequency (S/N 2006)

Table 3-3. Performance Summary, Phase II Units

PARAMETER MEASURED	TUBE No. 1 S/N 2022	TUBE No. 2 S/N 2025	TUBE No. 3 S/N 2034
Output Power (w)			
12040 MHz	239	216	255
12080 MHz	227	231	231
12120 MHz	191	210	229
Gain at Saturation (dB)			
12040 MHz	30.8	30.3	31.1
12080 MHz	30.5	30.6	30.6
12120 MHz	30.0	30.3	30.6
Overall Efficieny at Saturation (%)			
12040 MHz	50.6	45.2	53.1
12080 MHz	48.6	47.3	50.8
12120 MHz	44.5	45.9	52.0
Transmission (%DC)	98.1	98.4	99.0
Transmission (% Sat.)	95.5	93.8	96.8
Cathode Voltage, E_k	-11150	-11300	-11400
Anode Voltage, E_a	250	250	300
Cathode Current, I_k	76.0	77.2	78.0

NOTE: No. 1 - CTS Flight Unit (QF-4)
No. 2 - Flight Back-up (QF-3)
No. 3 - Flight Back-up (QF-7)

Note: See Table 3-4 for Dimensions

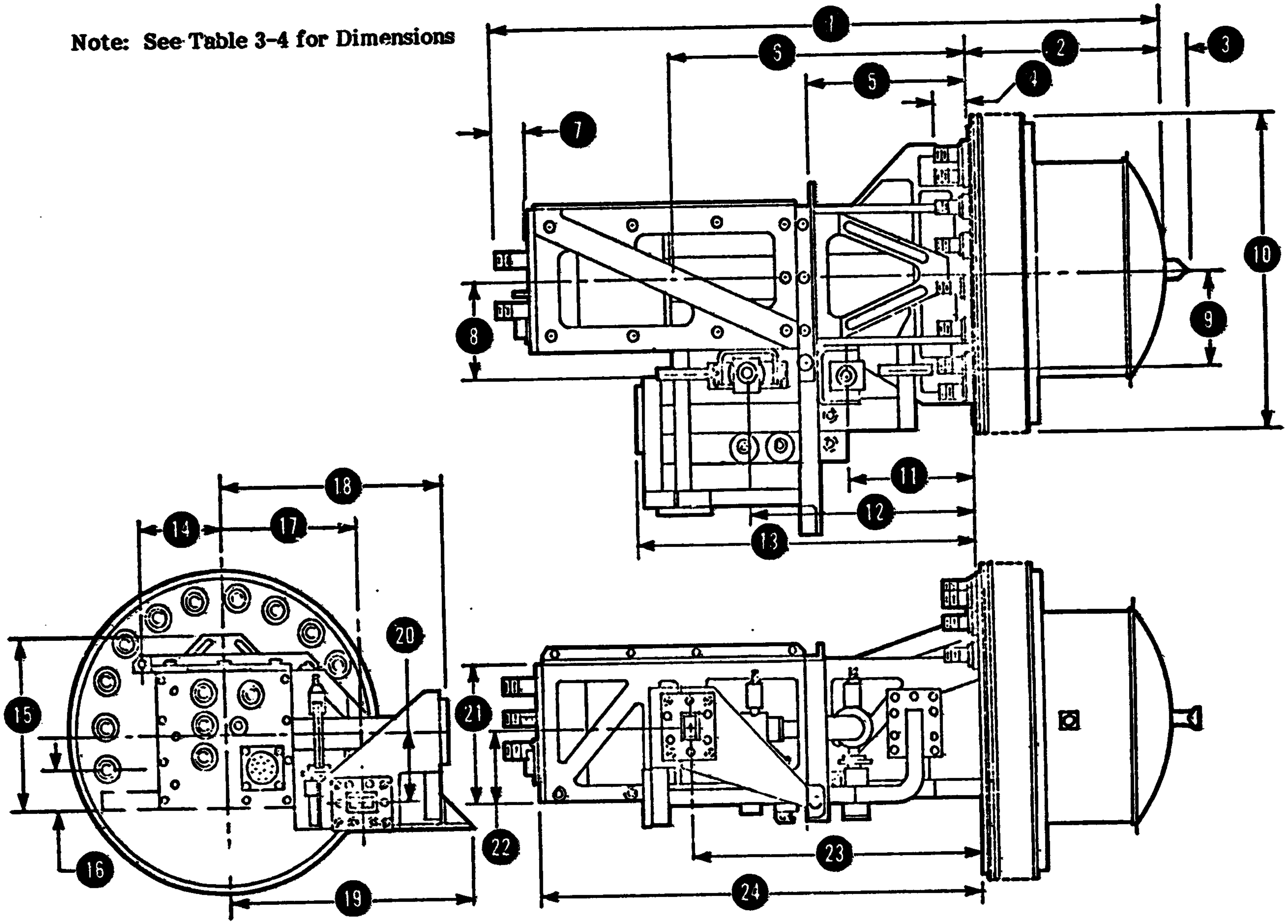

Figure 3-9. Dimensioned Drawing, Production Unit

Table 3-4. OST Flight Unit Physical Dimensions
(Refer to Figure 3-9)

DIMENSION	REQUIRED, INCHES (CM)	ACTUAL, INCHES (CM)
1	20.000 Max. (50.800 Max.)	19.840 (50.394)
2	5.970 ± .060 (15.164 ± .152)	5.940 (15.088)
3	2.500 Max. (6.350 Max.)	1.80 (4.572)
4	1.000 Max. (2.540 Max.)	1.027 (2.609)
5	4.567 ± .030 (11.600 ± .076)	4.505 (11.443)
6	8.790 ± .050 (22.327 ± .076)	8.796 (22.342)
7	1.000 Max. (2.540 Max.)	.840 (2.134)
8	2.750 ± .030 (6.985 ± .076)	2.808 (7.132)
9	2.950 ± .030 (7.493 ± .076)	2.926 (7.432)
10	9.300 ± .060 (23.622 ± .152)	9.243 (23.477)
11	3.700 ± .080 (9.398 ± .203)	3.650 (9.271)
12	6.550 ± .080 (16.637 ± .203)	6.525 (16.574)
13	9.790 ± .030 (24.867 ± .076)	9.780 (24.841)
14	2.610 ± .010 (6.629 ± .025)	2.580 (6.553)
15	5.000 ± .060 (12.700 ± .152)	4.980 (12.649)
16	1.125 ± .030 (2.958 ± .076)	1.130 (2.870)
17	4.000 ± .060 (10.160 ± .152)	4.046 (10.277)
18	6.782 ± .030 (17.226 ± .076)	6.784 (17.231)
19	7.445 ± .030 (18.910 ± .076)	7.458 (18.943)
20	2.025 ± .030 (5.144 ± .076)	2.069 (5.255)
21	4.000 ± .030 (10.160 ± .076)	4.000 (10.160)
22	2.125 ± .030 (5.398 ± .076)	2.096 (5.324)
23	8.350 ± .270 (21.210 ± .686)	8.326 (21.148)
24	13.050 ± .050 (33.147 ± .127)	13.060 (33.172)

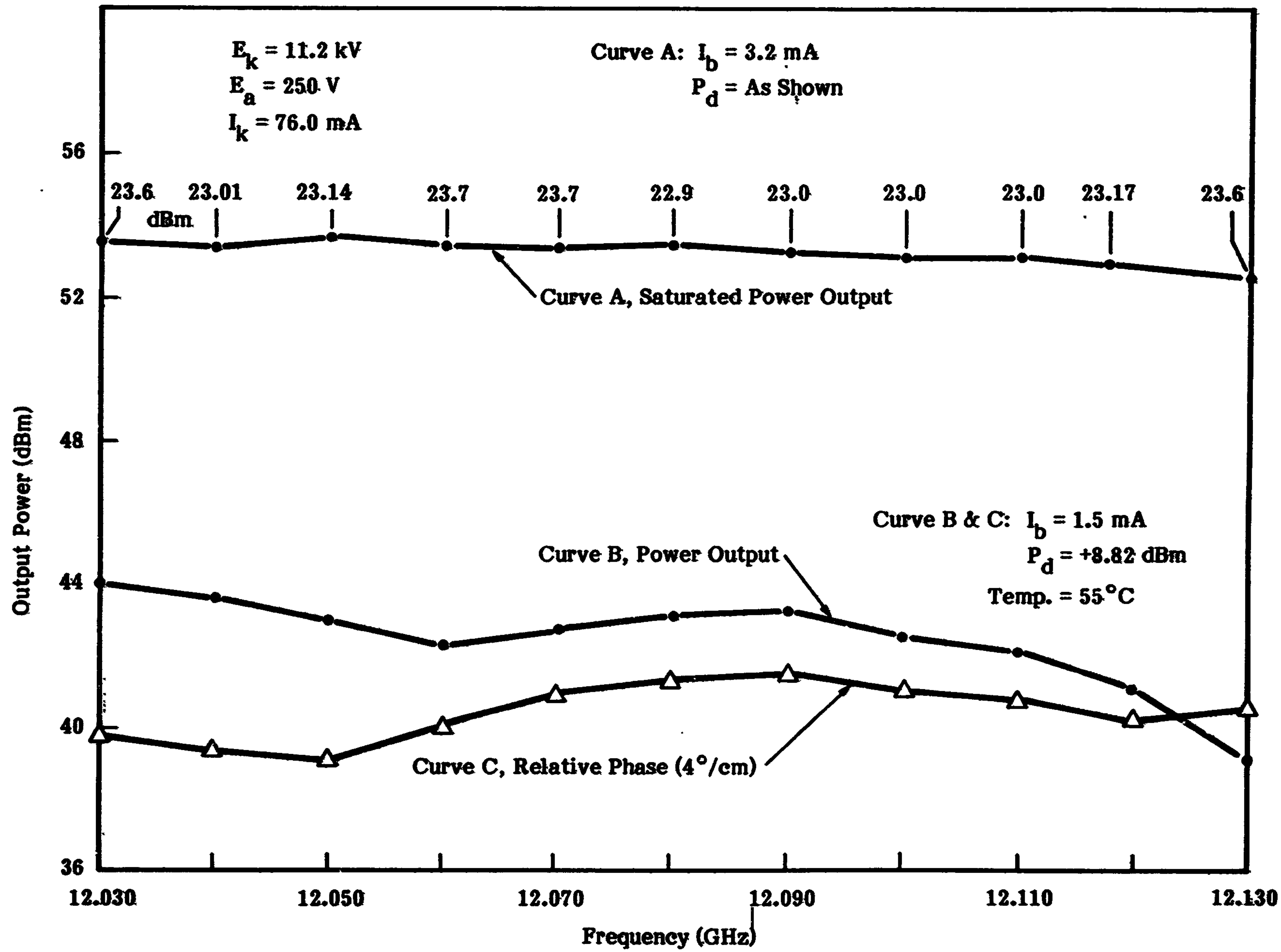

Figure 3-10. Performance Curves (S/N 2022)

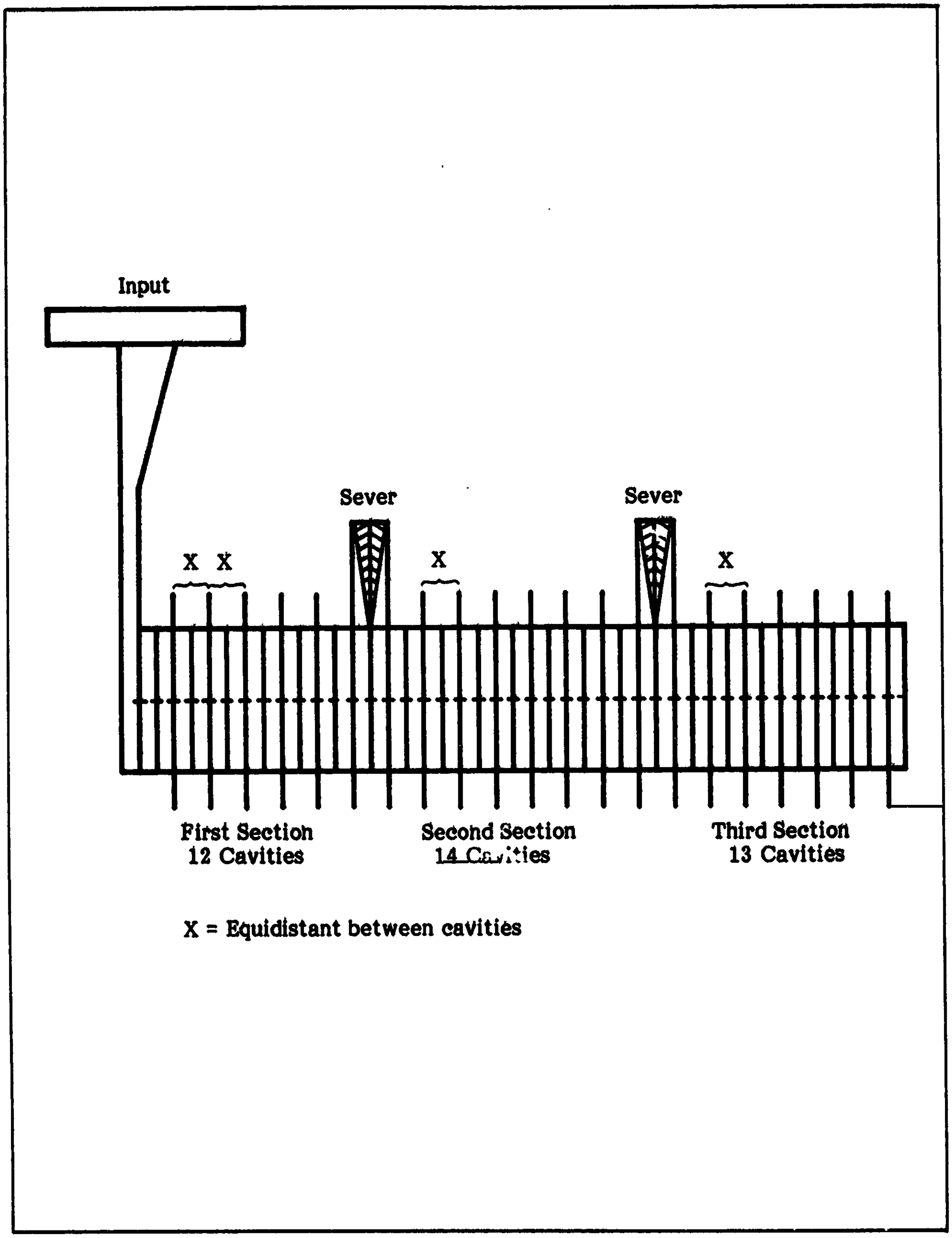

Figure 3-11. Uniform Circuit Cavity Configuration

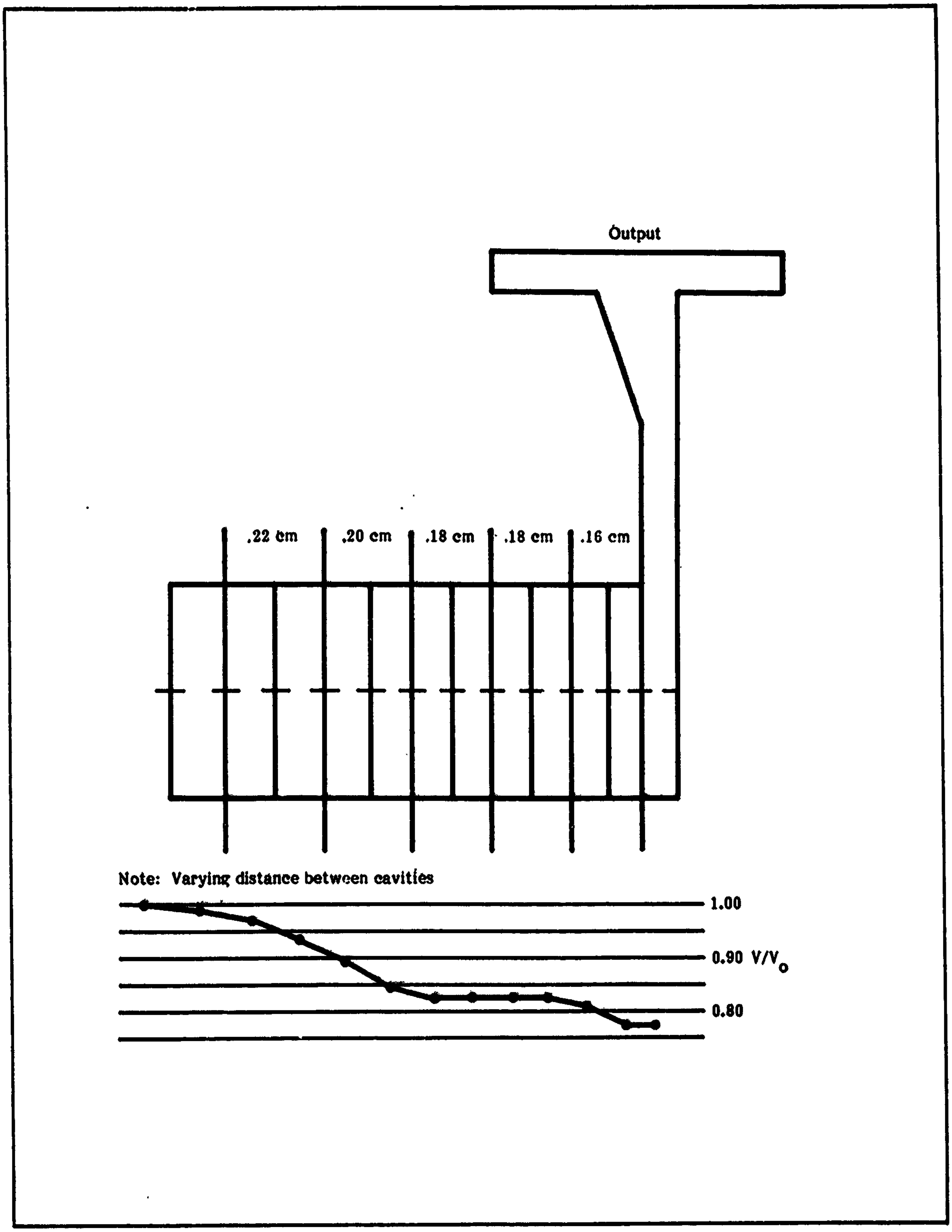

Figure 3-12. Velocity Taper Cavity Configuration

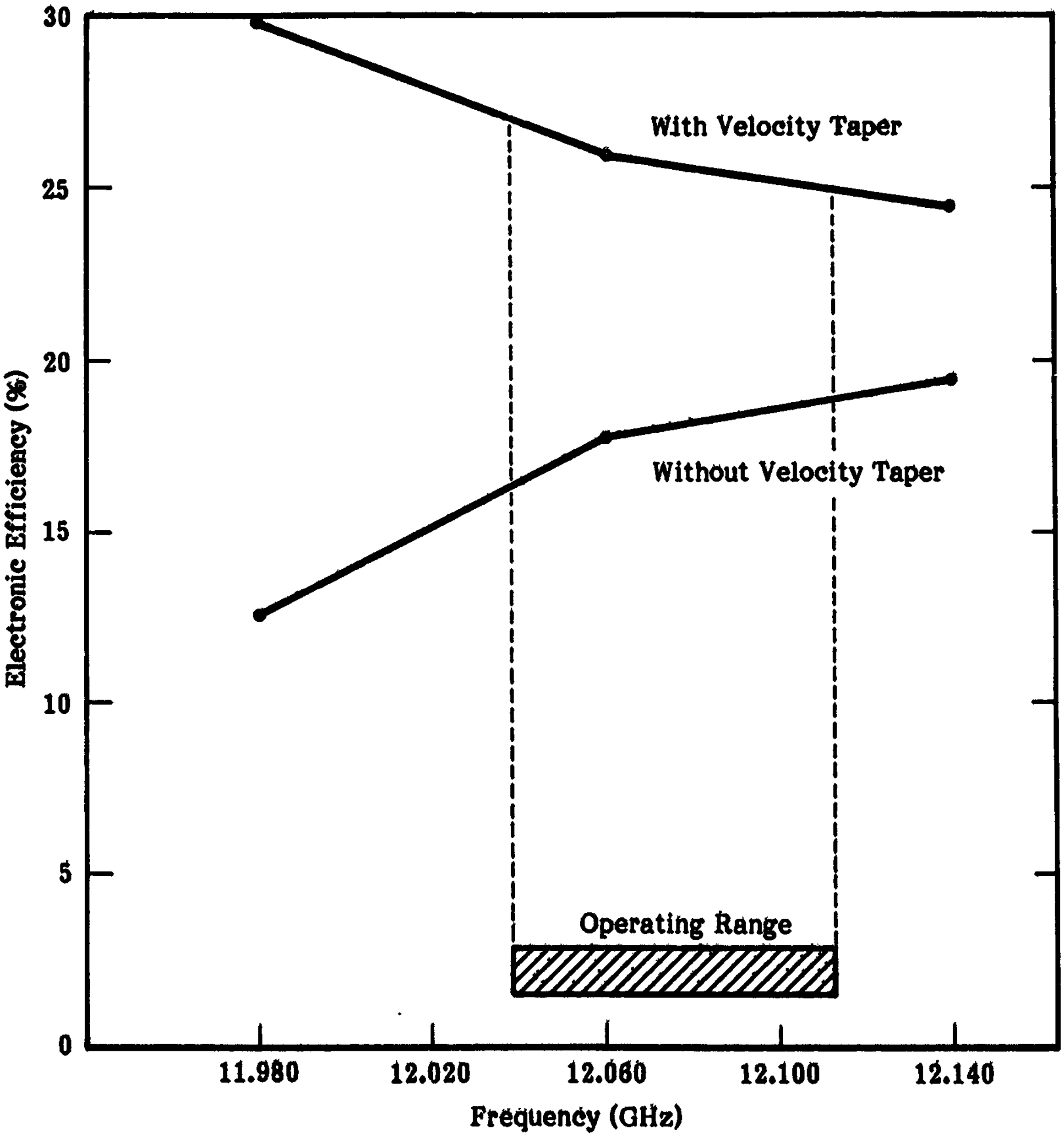

Figure 3-13. Predicted Electronic Efficiency

parameter b = 0) in order to assure good beam bunching for velocity resynchronization.

The length of the output gain section (prior to the velocity taper) is large enough to avoid efficiency degradations due to sever effects. The estimated small signal gain in this section is 23 to 26 dB. The velocity taper was designed with the aid of a large signal computer program using circuit parameters based on the cold test data. The analysis takes the reduction of the interaction impedance in the taper into account, as well as the increase of the losses in the taper. Empirically the interaction impedance K_T in the taper was found to be reduced proportional to the square of the phase-velocity reduction (period reduction). The losses L_T in the taper section tend to increase inversely with impedance. The predicted electronic efficiency was 25 percent at 12.080 GHz, compared to measured values of 25 to 30 percent. Without a velocity taper the electronic efficiency would have been on the order of 15 percent. The rf circuit losses are predicted to cause a reduction of the electronic efficiency to 70 percent of the efficiency obtainable with a lossless circuit.

3.4 TRADE-OFF AND PROBLEM CONSIDERATIONS

Several major trade-off analyses were accomplished during the combined theoretical/experimental and fabrication/qualification effort for the TWT. As design progressed, and units were fabricated and tested, several problems became apparent and corrective action or modification was defined and implemented. Table 3-5 shows the major trade-off studies considered, and their respective outcome or design decision. The design or fabrication problems encountered and the suggested (or implemented) corrective actions are listed in table 3-6. In some cases there is no descriptive explanation for the particular design decision or corrective action implemented, but the final TWT design reflects the alternative or action selected. In some other situations, the design of particular subsystems or parts is described in the following sections of this report.

Table 3-5. Design Trade-off Studies/Alternatives

ITEM	STUDY TITLE	OUTCOME, RESOLUTION OR COMMENT
1.	Efficiency vs. Spec. Parameters	As shown by test results of each TWT.
2.	Efficiency vs. Thermal/Mechanical Design	Selected improved materials for thermal design, optimized radiation from MDC jacket.
3.	Perveance and Bandwidth Ratio	Perveance set at 62 nP, cold to hot bandwidth ratio at 15:1.
4.	Bandwidth vs. Circuit Losses	As shown by test of individual units.
5.	Kidney vs. Thin Slot Coupling	Thin slot coupling utilized.
6.	Voltage Jump vs. Velocity Taper	Velocity taper selected for design.
7.	Optimization of Velocity Taper	Design selection included 2-stage taper.
8.	Gun and Focusing Design	Utilized electrostatic beam analyzer and inhouse gun and cathode fabrication.
9.	Multistage Collector Design	As described in MDC section of this report; 10 element unit designed by LeRC.
10.	Refocusing Definition (Solenoid vs. permanent magnet)	Permanent magnet design selected.
11.	Refocusing Magnet and Pole Piece Design	Design is reflected in current configuration.

Table 3-6. Design Problems and Corrective Actions

ITEM	DESCRIPTION	SUGGESTED ACTION
1.	Sensitivity of the Kidney Slot Circuit	Provide additional design/test effort on the kidney slot circuit.
2.	Low Power	1. Build circuits of varying slot and kidney designs for additional tests. 2. Revise circuit taper. 3. Add cavities to the input section.
3.	Low Gain	
4.	Low Efficiency	
5.	Secondary emission from the collector plates.	Shorten spike, change processing procedures for electrodes.
6.	Refocus magnet optimization	Continue to use solenoid for setup Design new permanent magnet refocus assemblies.
7.	Collector gas accumulation	Operate tube with collector jacket temperature greater than 200°C. Provide longer bakeouts.
8.	Cathode support damage during vibration tests.	Establish a second source vendor as a back-up. Specify tests to identify potential faulty construction.
9.	Damage to collector element supports during vibration test.	Improve design to insure compliance to vibration requirements. Strengthen support geometry.
10.	Tube gassy after bus bar soldering.	Attach bus bars using 56C Eccobond.
11.	Temperature sensitivity of equalizer.	Design Hi Q metal cavity to replace Hi Q dielectric resonator. Change resonator stub material from aluminum to Kovar.

4.0 ANALYTICAL DESIGN

The design of the TWT evolved through a combined theoretical and experimental effort. The analytical design included the utilization of several existing Litton computer simulation models and application of analyses/results of similar programs. This section presents the discussion of the analytical design effort as they applied to the tube definition and subassembly selection.

4.1 REVIEW OF THEORETICAL DESIGN

The theoretical analyses completed on the tube as a complete unit included the large signal analysis, the small signal analysis, and the thermal/mass analysis. Those completed on the subassemblies included the electron gun definition; rf focusing, refocusing, input/output section optimization, and multistage depressed collector design finalization. In part, the discussion of the analytical design is reflected, or in some cases partially redundant to the discussion of the mechanical design of the particular subassembly. Table 4-1 provides a brief summary of the theoretical analyses considered, the type of analysis or technique utilized, and the significant output or result of each. Each of these are additionally discussed below.

4.2 DESIGN EVOLUTION

Initial large signal computer analysis indicated that for high electronic efficiency a low beam voltage would be required. The computer analysis assumed a fixed beam power. and varying interaction impedance (directly proportional to the square root of the voltage). Single and double step velocity taper circuits were investigated during the evaluation. A beam voltage of 11 kV was selected for focusing considerations, since at lower voltages the magnet pole pieces tended to saturate. Using the experience gained from prior narrow band tube studies, the circuit was designed for high interaction impedance at a relatively low value of phase shift per cavity (about 1.20π). The beam tunnel diameter was selected for a radial propagation parameter "a" of 0.85 consistent with high efficiency.

The transmission loss measurement of the rf circuit in the initially fabricated tube yielded a value of 0.11 dB per cavity at a phase shift of 1.20π. In the preceding

PRECEDING PAGE BLANK NOT FILMED

Table 4-1. Theoretical Design Analyses

DESIGN OBJECTIVE OR ASSEMBLY/ SUBASSEMBLY	TYPE OF ANALYSIS OR TECHNIQUE UTILIZED	SIGNIFICANT OUTPUT OR DEFINED RESULTS
Electrical Design	Computer simulation, large signal disc model interaction program, and closed form interaction analysis program.	Coupling slot configuration, circuit and taper dimensions as described herein. Output power, gain and efficiency as shown by test results.
Electron Gun	Simulation model and gun trajectory analysis.	Gun design definition, material selection.
RF and Magnet Circuit	Magnetic simulator and computer simulation model, cold test and data reduction programs.	Magnet spacing, sever locations, tube stabilization methods, bandwidth.
MDC	Previous program model, LeRC design application simulation	MDC configuration, dimensioning, spacing, voltage applications
Thermal	Transient circuit analysis computer program, simulation model	Material selection, mess requirements, power dissipation requirements.

computer design work of the first taper tube, a loss of 0.1 dB per cavity in the standard circuit had been expected. The loss per unit length in the two step phase velocity taper had been assumed to be constant. It became readily apparent that the loss would be a significant element in the design and performance of the tube, particularly since the cavity losses in the tapers were expected to be significantly larger as shown in figures 4-1 and 4-2. Both theoretical and experimental efforts were initiated to reduce the rf dissipation and improve the circuit efficiency.

The first velocity taper tube was built to the original design except that the number of cavities in the first and second tapers was decreased from 12 to 8 and 7 respectively, and the phase velocity reductions in the tapers were 15 and 25 percent, respectively. This was accomplished by proportionately decreasing the cavity height. The transmission loss was approximately 0.12 dB per cavity in the first taper and 0.25 dB per cavity in the second taper (at a phase shift of 1.20π), resulting in significant rf dissipation.

Two approaches to reduce the loss were considered due to the inverse relation of the rf loss with the group velocity. Either the cold bandwidth could be increased or the operating point could be shifted toward the middle of the passband (larger phase shift per cavity). In both cases a reduction in interaction impedance would result, as shown in figures 4-3 and 4-4.

The loss versus bandwidth relationship was investigated through rf cold tests and was found to increase more rapidly with decreasing bandwidth than predicted by theory. If a cold bandwidth of approximately 1280 MHz were used, the loss would probably be reduced to a level below 0.1 dB per cavity. The passband would also be shifted downward in frequency from the result of beam space charge loading and circuit brazing as shown in figure 4-5.

The result of the combined experimental and theoretical design work produced a reduction in the loss by one-third in the standard circuit, to 0.067 dB per cavity at midband, with a decrease of interaction impedance of less than 15 percent as shown in figure 4-6. The loss reduction in the tapers was even larger; at operating midband frequency; the loss per cavity was 0.08 dB and 0.12 dB in the first and second tapers respectively.

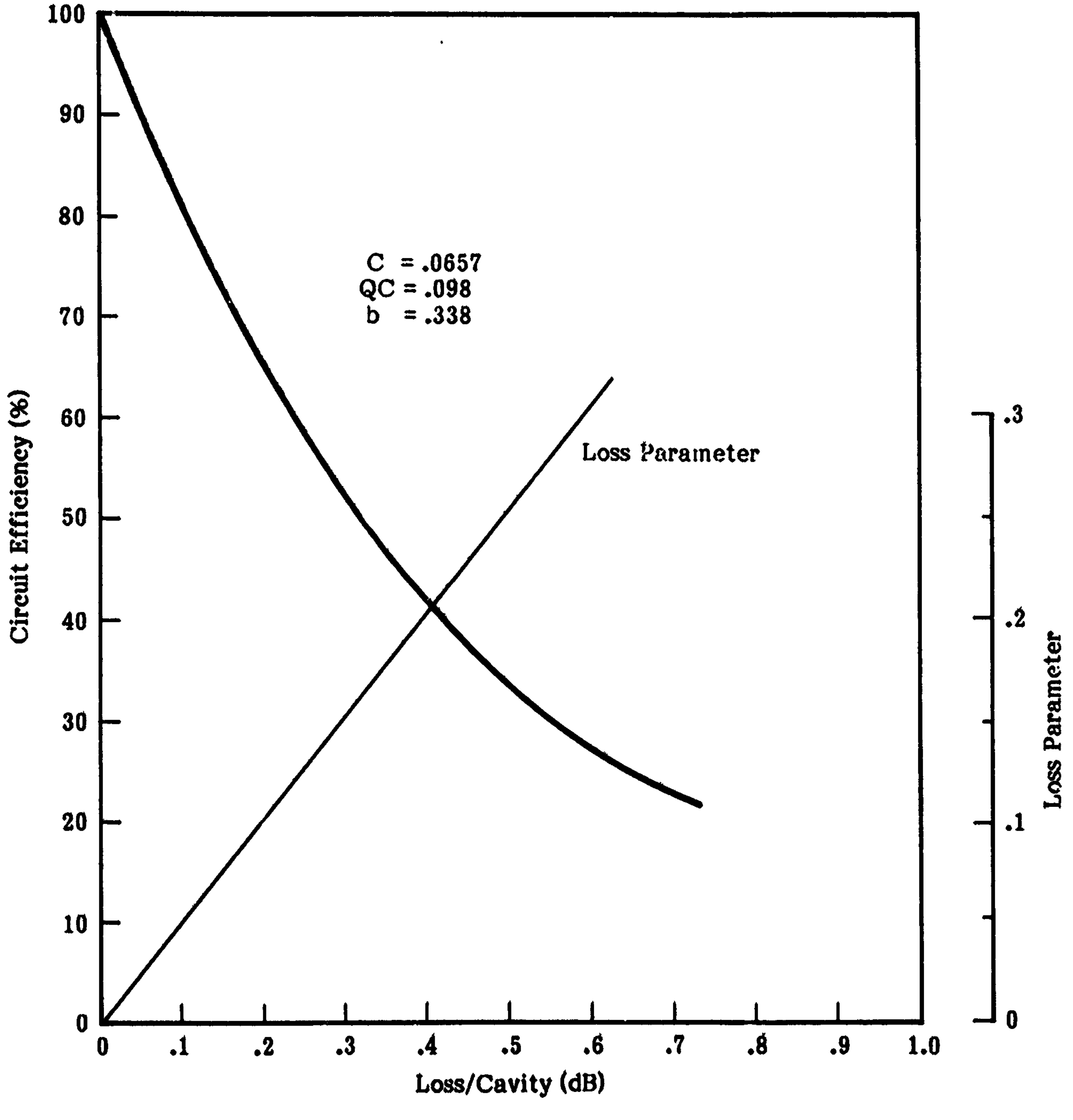

Figure 4-1. Predicted Efficiency Reduction

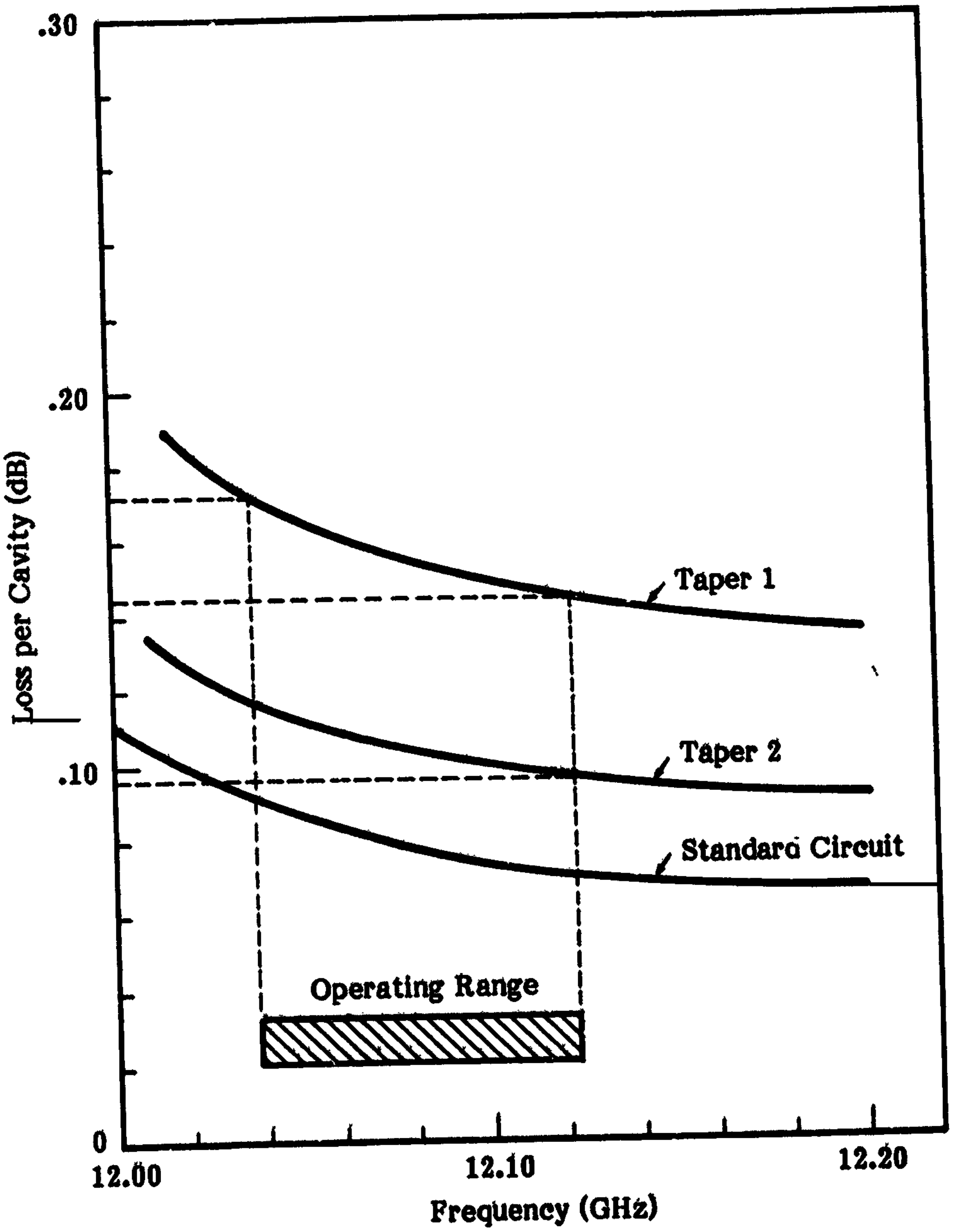

Figure 4-2. Cavity Loss Characteristics

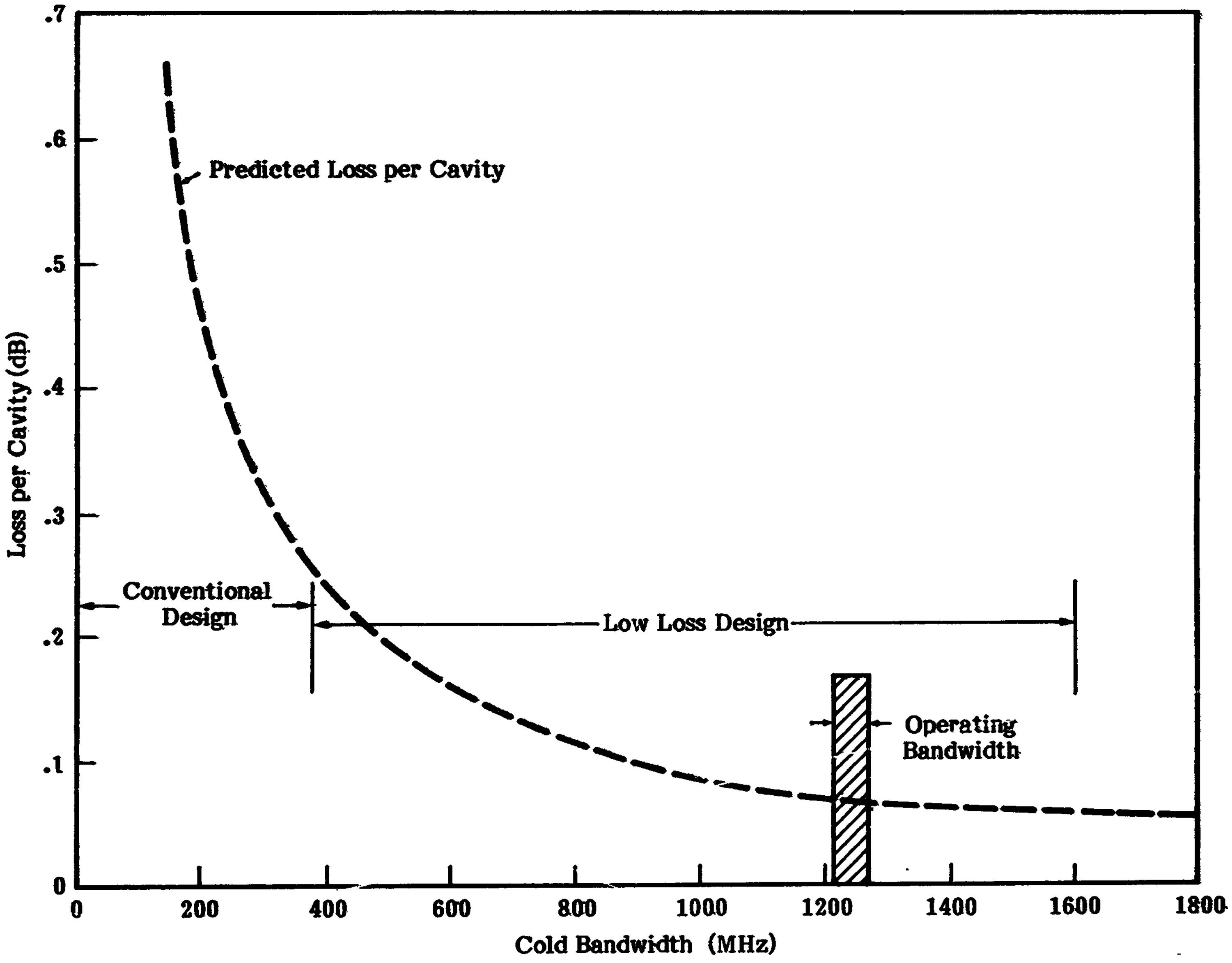

Figure 4-3. Effect of Cold Bandwidth on Circuit Losses

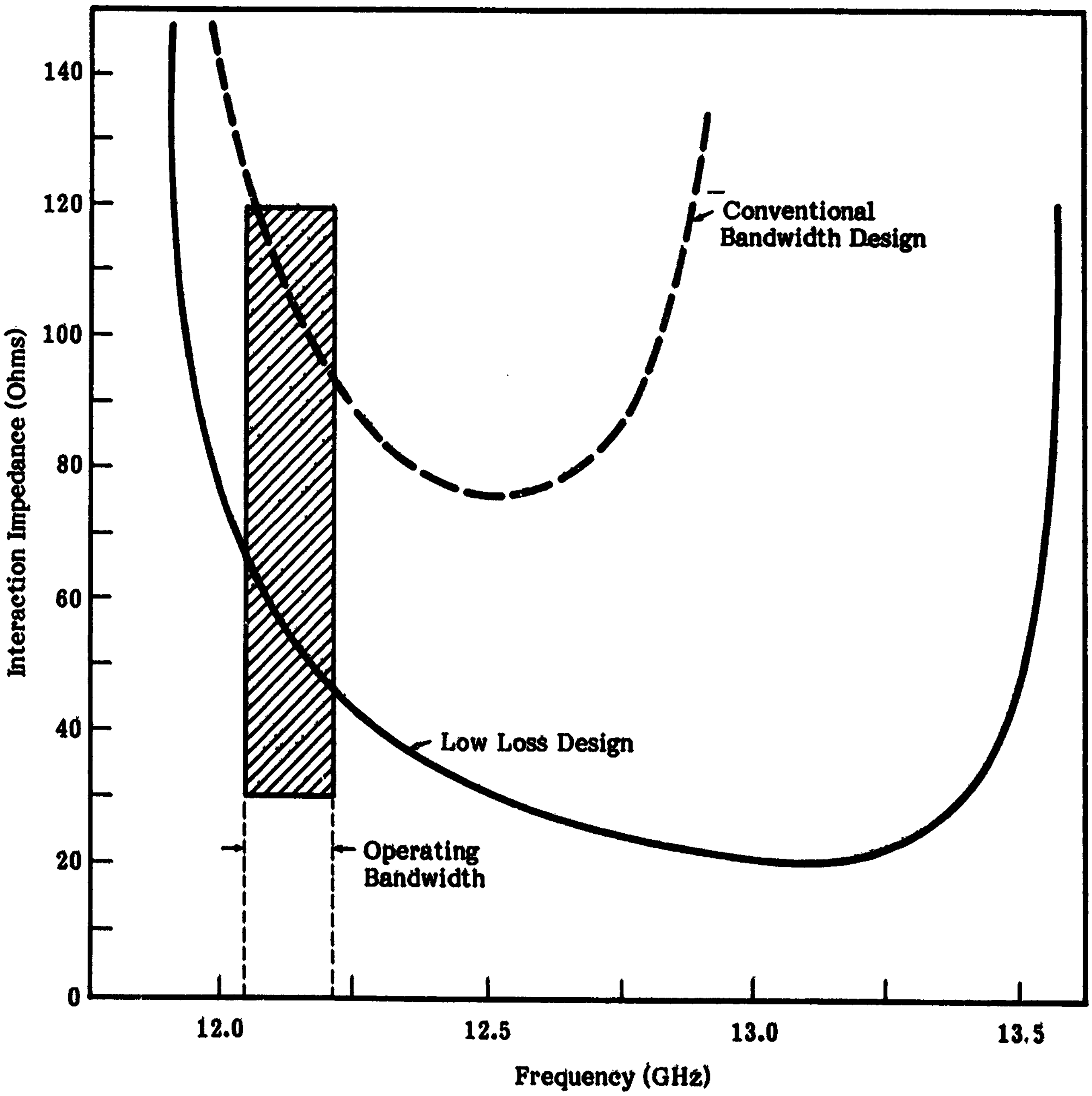

Figure 4-4. Interaction Impedance Relationship

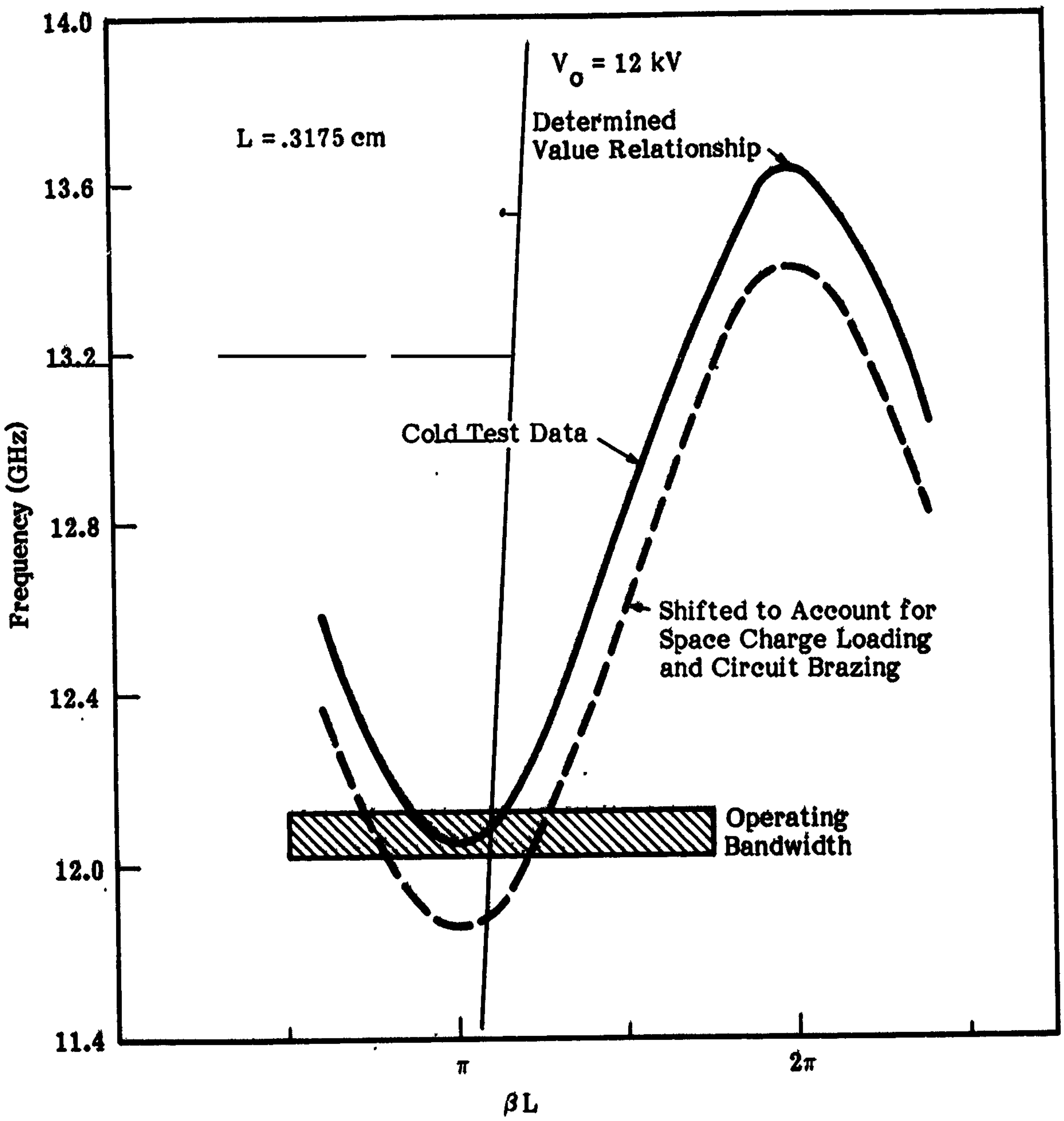

Figure 4-5. Loss vs. Frequency Relationship

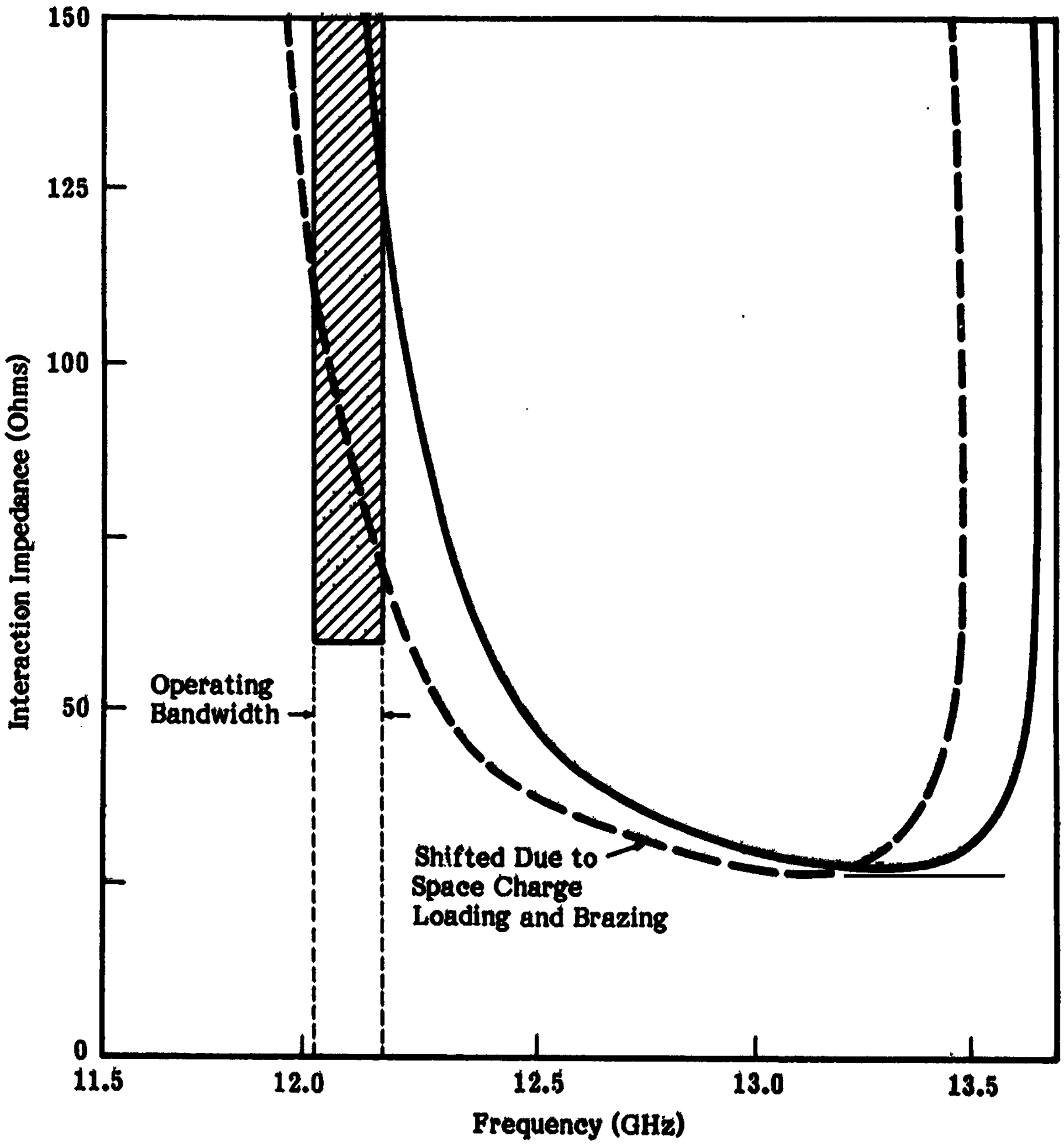

Figure 4-6. Circuit Interaction Impedance

Computer analyis of the large signal interaction also shows that a ten percent reduction in rf power dissipation in the circuit could be obtained, at the cost of approximately one percentage point in basic efficiency, by reducing the number of cavities in the second taper. Part of this efficiency decrease could be recovered by the collector since the spent beam would have additional energy. The predicted values for a tube proposed for fabrication using the values calculated would achieve a basic efficiency of 30 to 32 percent.

The results of the computer analysis for coupling alternatives showed that either a kidney shape or a thin rectangular slot configuration would be acceptable for cavity design. The initial configurations (kidney and thin slot) considered appropriate are shown in figure 4-7. The frequency and voltage versus phase shift characteristic measured for the only completed kidney slot tube is shown in figure 4-8. The rf wave phase velocity expressed in terms of an equivalent or circuit voltage, V_o is also shown. The measured cold interaction impedance and the transmission loss for the kidney shape are plotted in figure 4-9 as a function of the phase shift per cavity. To evaluate the impedance, an effective beam-to-tunnel radius ratio of 0.7 was assumed. A bandwidth of 85 MHz centered at a phase shift of 1.20π corresponds to a phase shift range of 1.12π to 1.26π, and a loss per cavity between 0.17 to 0.12 dB.

The thin slot coupling characteristics for the same parameters with resultant curves are superimposed (shown by dashed lines) on figures 4-8 and 4-9. This is provided to show the comparison of the two alternative configurations. The hot test efficiency comparison for the kidney slot versus the rectangular slot is shown in figure 4-10. The final cavity configuration selected for all tubes (except one) was the thin slot, since stability of the kidney slot circuit was marginal.

The cold bandwidth of the initial units was 1.3 GHz or about 15 times a nominal hot bandwidth of 85 MHz. The passbands of the taper circuits were very close to that of the standard circuit with the operating midband frequency matched up with the corresponding phase shift per cavity. Since the $\omega\beta$ characteristics of the taper circuits and the mid-band values of $\beta L/\pi$ were the same as the standard circuit, straightforward graduations in period between taper sections result in a satisfactory match over the operating band.

A. Kidney Shaped Slot

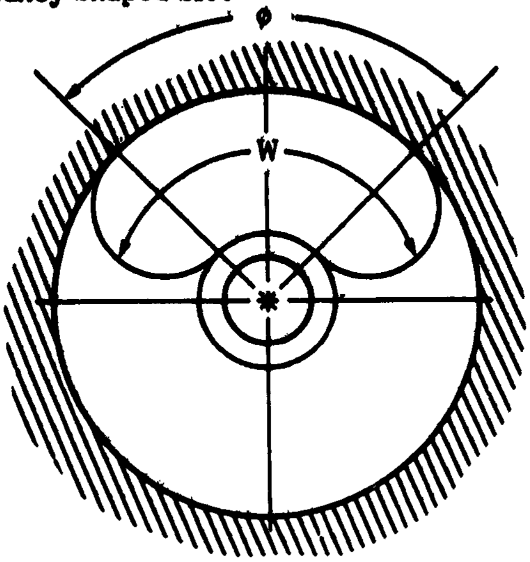

ϕ	8°	24°	30°	UNIT
W	0.686	0.813	0.859	cm
Δf	874	1379	1583	MHz
K_o	220	145	120	Ohms
Loss	0.8	0.2	0.15	dB/cav.

$l_o = .3175$

B. Thin Slot

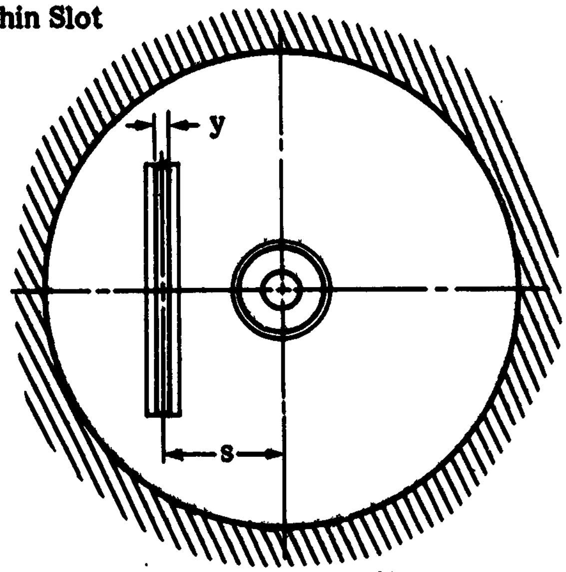

Item	Value	Unit
d1	.127	cm
d2	.279	
d3	1.51	
t	.076	
s	.412	
y	.051	
h	.241	
l_o	.3175	
g	.094k	
Loss	.067	dB/Cav
Δf	1332	GHz

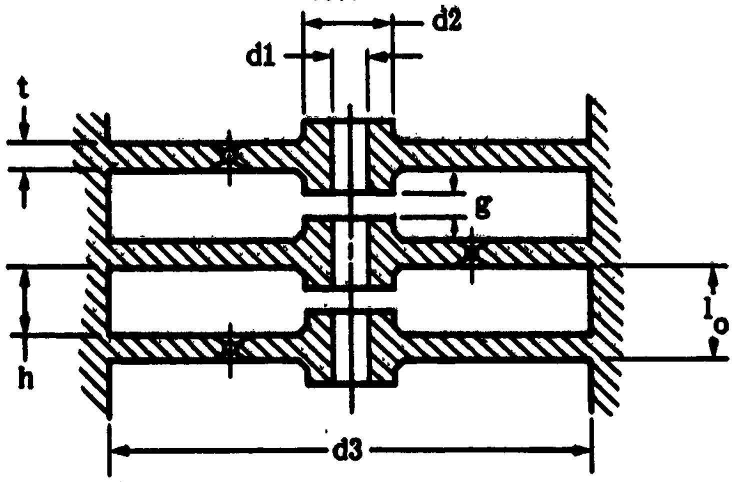

Figure 4-7. Coupling Slot Configuration (Uniform Cavity Sections)

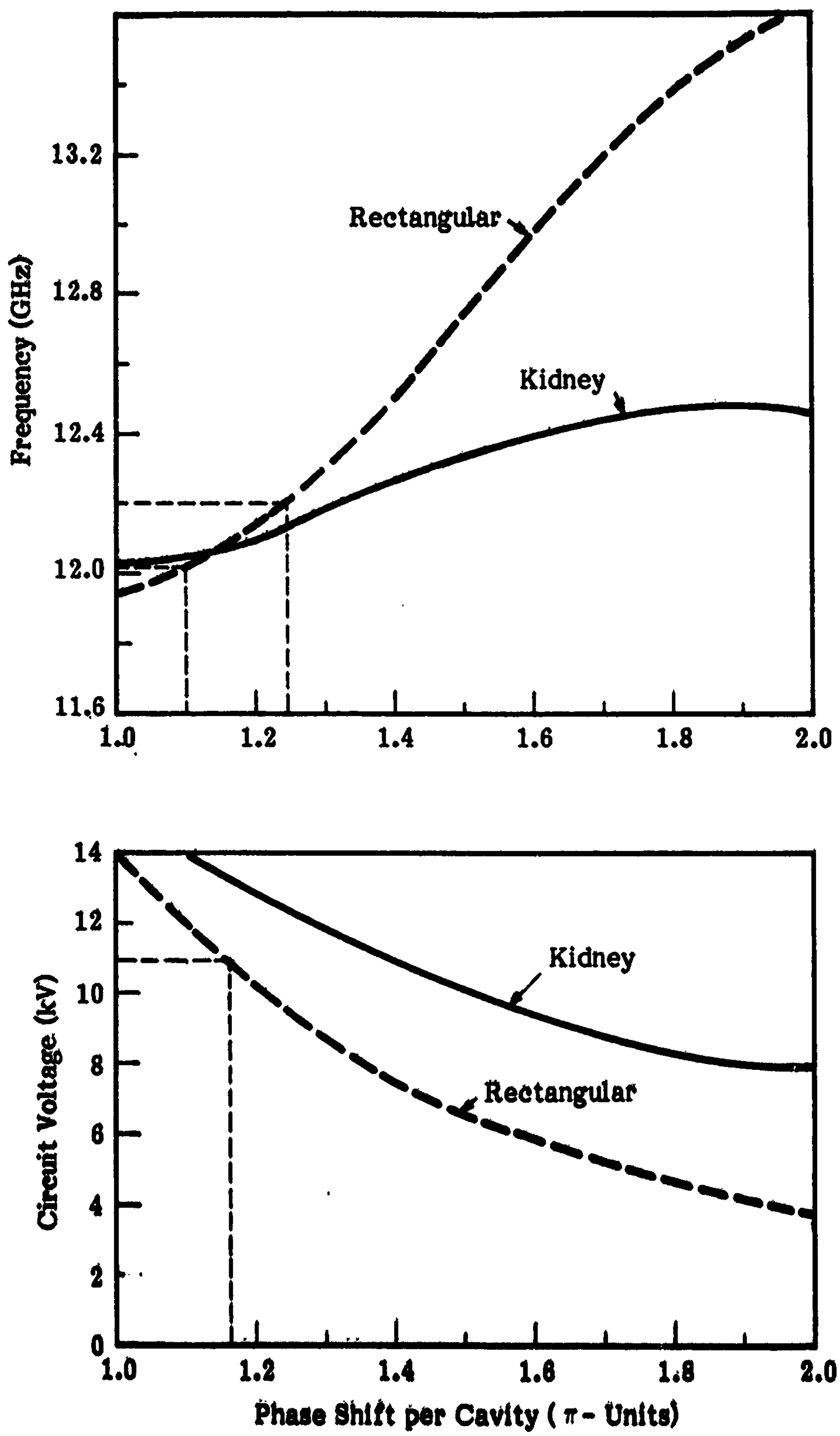

Figure 4-8. Dispersion Characteristics

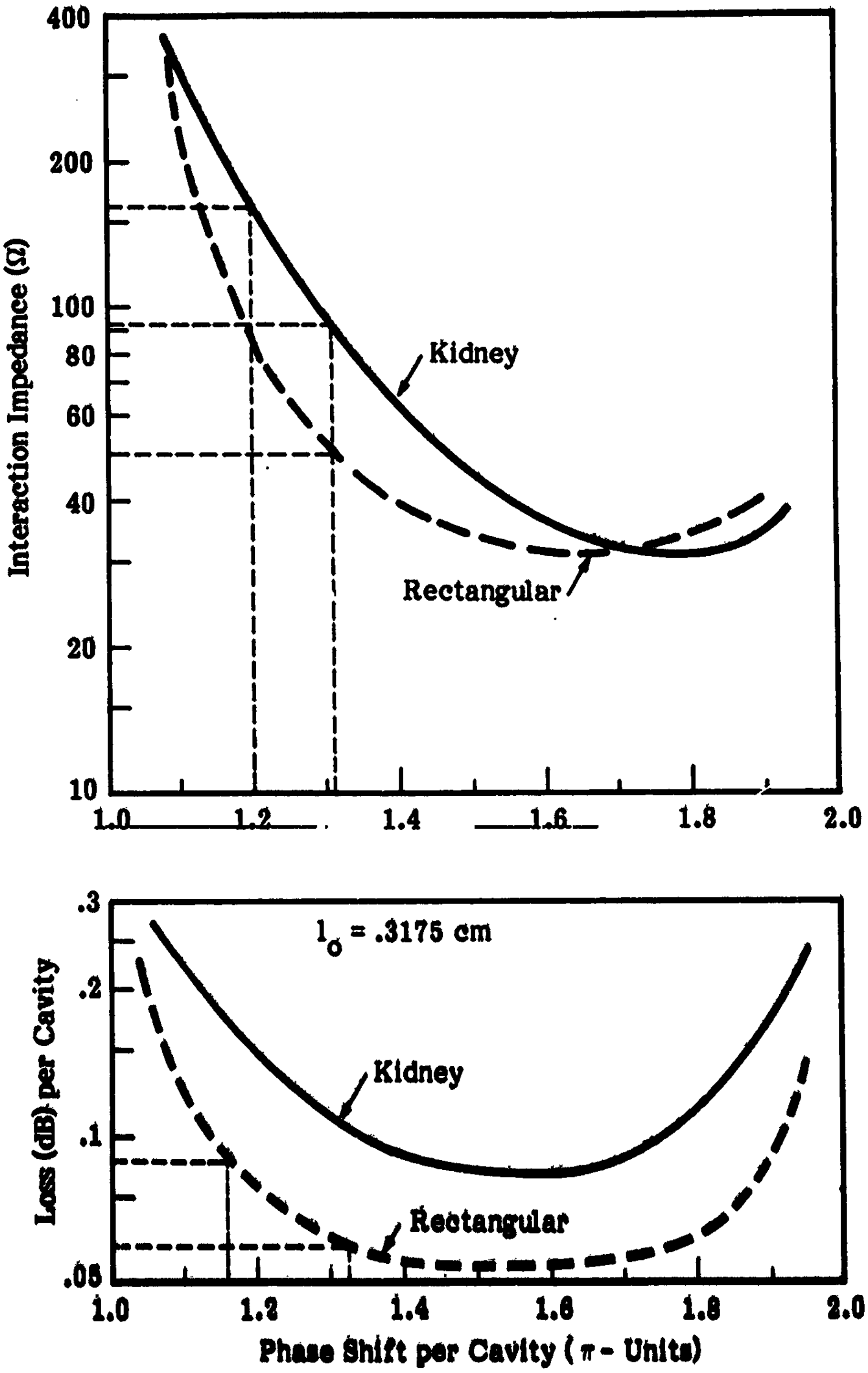

Figure 4-9. Impedance and Loss Characteristics

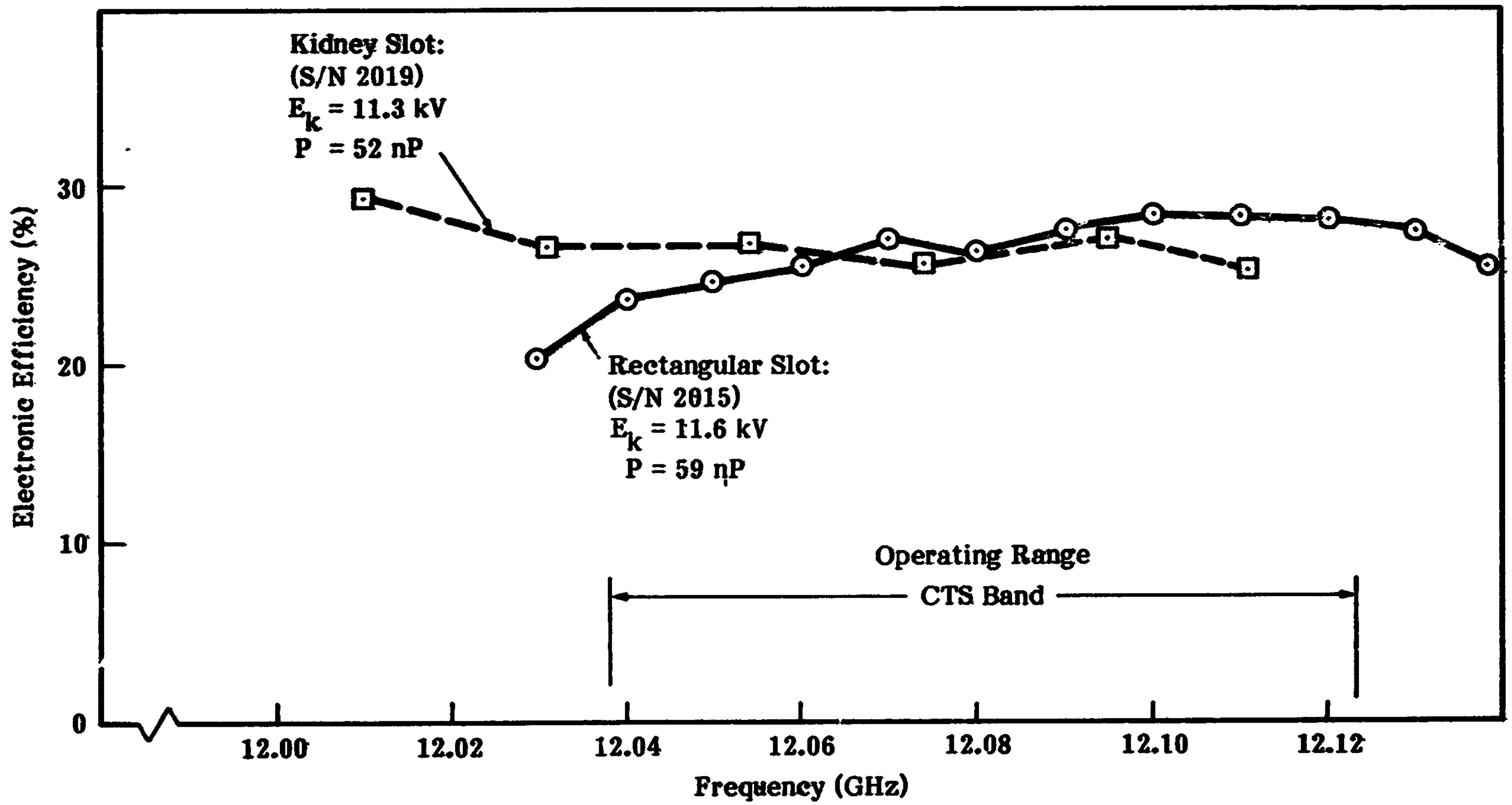

Figure 4-10. Efficiency, Kidney vs. Rectangular Slot

The phase velocity of the standard circuit and two taper circuits in the final design versus frequency is displayed in figure 4-11. The cold interaction impedance is shown in figure 4-12 as a function of phase shift per cavity. An 85 MHz bandwidth about 12.08 GHz corresponds to a phase shift per cavity between 1.15π and 1.25π. The predicted gain variation and insertion loss with respect to frequency is presented in figures 4-13 and 4-14. The parameter has been evaluated using the measured cold circuit characteristics, assuming a beam voltage of 11 kV, a beam current of 67 mA, and other values as shown.

4.3 COMPUTER DESIGN ANALYSIS

The circuit design of the L-5394 was heavily influenced by the analysis of the large signal interaction using a digital computer program. The program that was used is based on a continuous interaction between the electron beam and the first forward space harmonic, and includes the effect of space charge forces due to beam bunching. The beam can be represented mathematically by disks with fixed radius. Such a one-dimensional model of the beam is normally acceptable in cases where the electric rf field varies only slightly over the beam hole area, and where the space charge forces are relatively small. Both of these criteria were satisfied in the tube design due to the small radial propagation parameter γa and the low perveance beam.

The interaction model included the dominant effects and is very convenient to use because of its relative simplicity. Other aspects of the actually more complex interaction process, such as the presence of a backward wave, can be approximated and accounted for by a suitable correction of the basic parameters. The present effective interaction parameters could be determined by using the measured performance of the tube and modifying the calculated projected values previously determined. The observed small signal gain, saturated gain, and saturated efficiency are compared to the projected/modified interaction impedance and phase velocity. These effective interaction parameters are displayed in figures 4-15 and 4-16 as functions of loss and phase shift per cavity. A phase shift range corresponding to approximately 85 MHz about small signal gain maximum is shown with calculations based on the estimated rf loss and a beam-to-hole radius ratio of five tenths. The phase shift/cavity and phase velocity vs. frequency

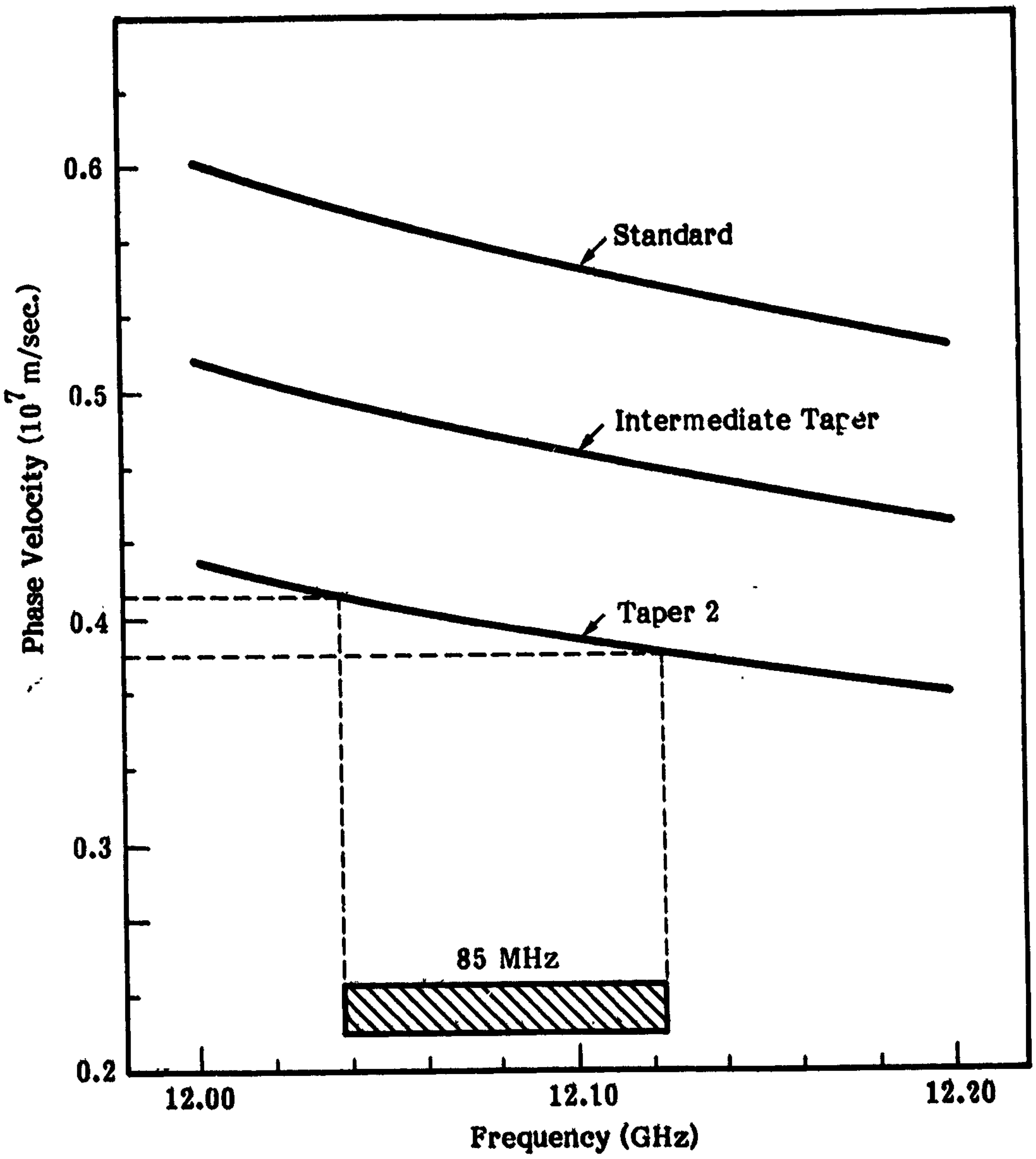

Figure 4-11. Phase Velocity Characteristics

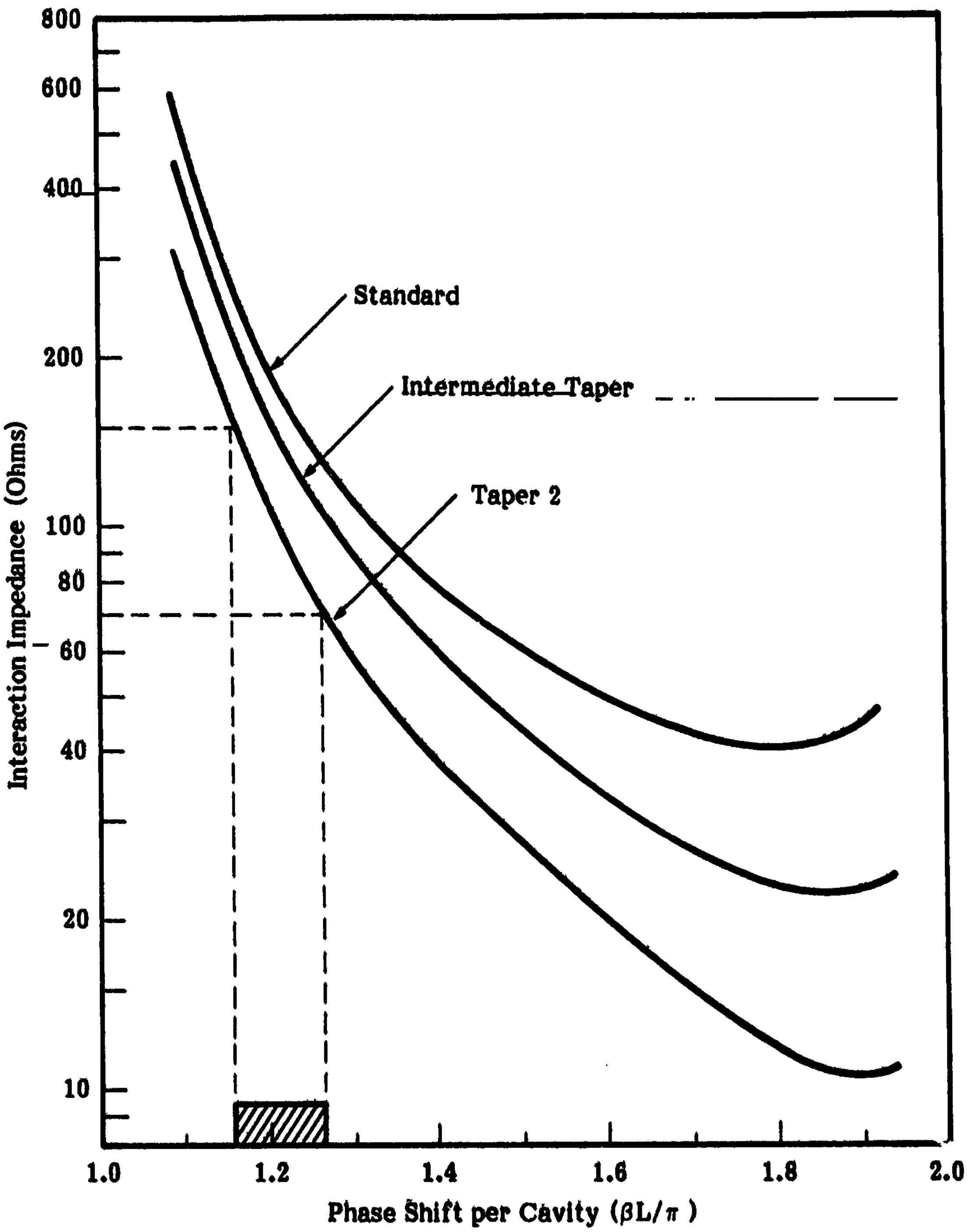

Figure 4-12. Impedance Characteristics

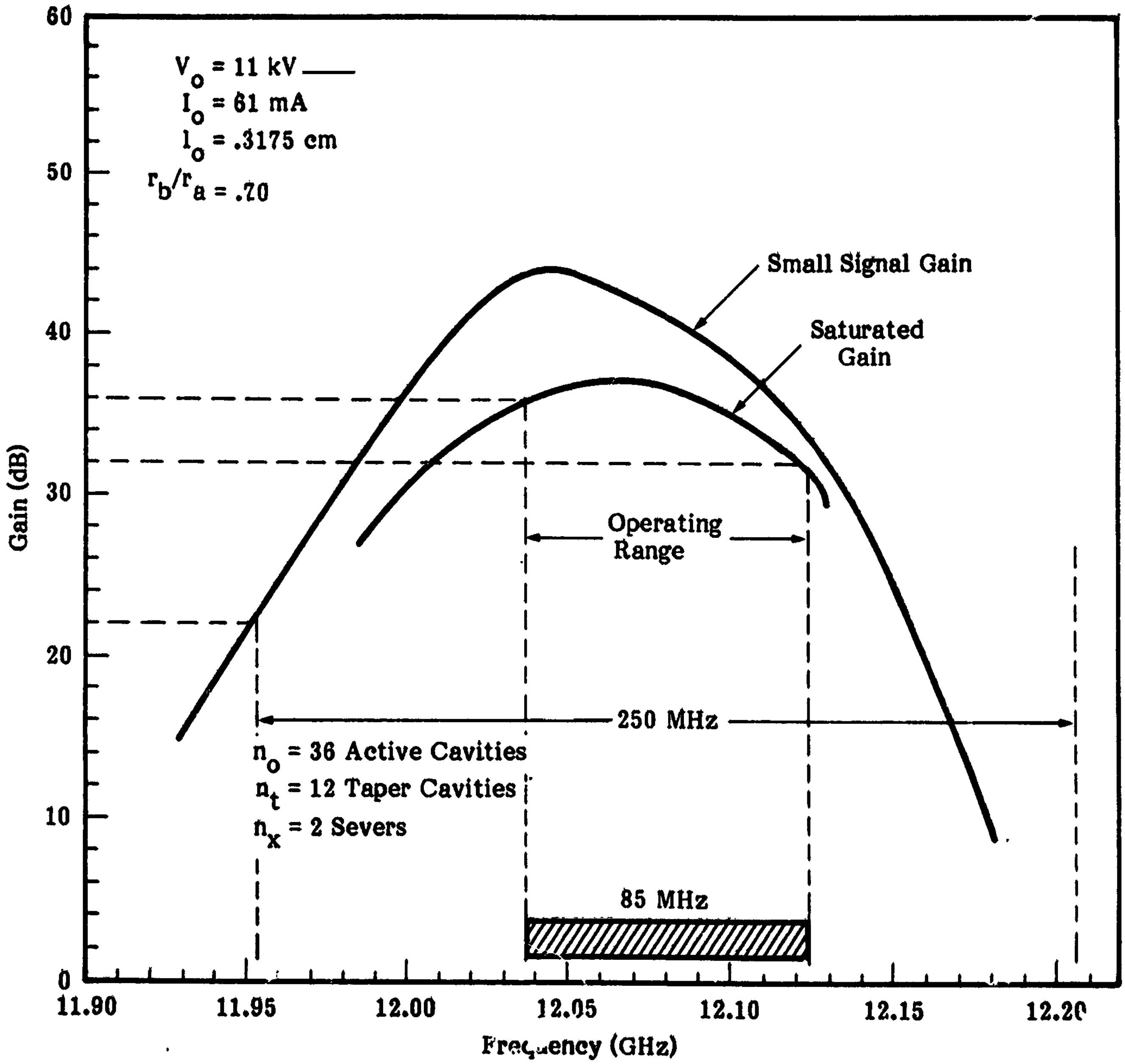

Figure 4-13. Predicted Gain Characteristics

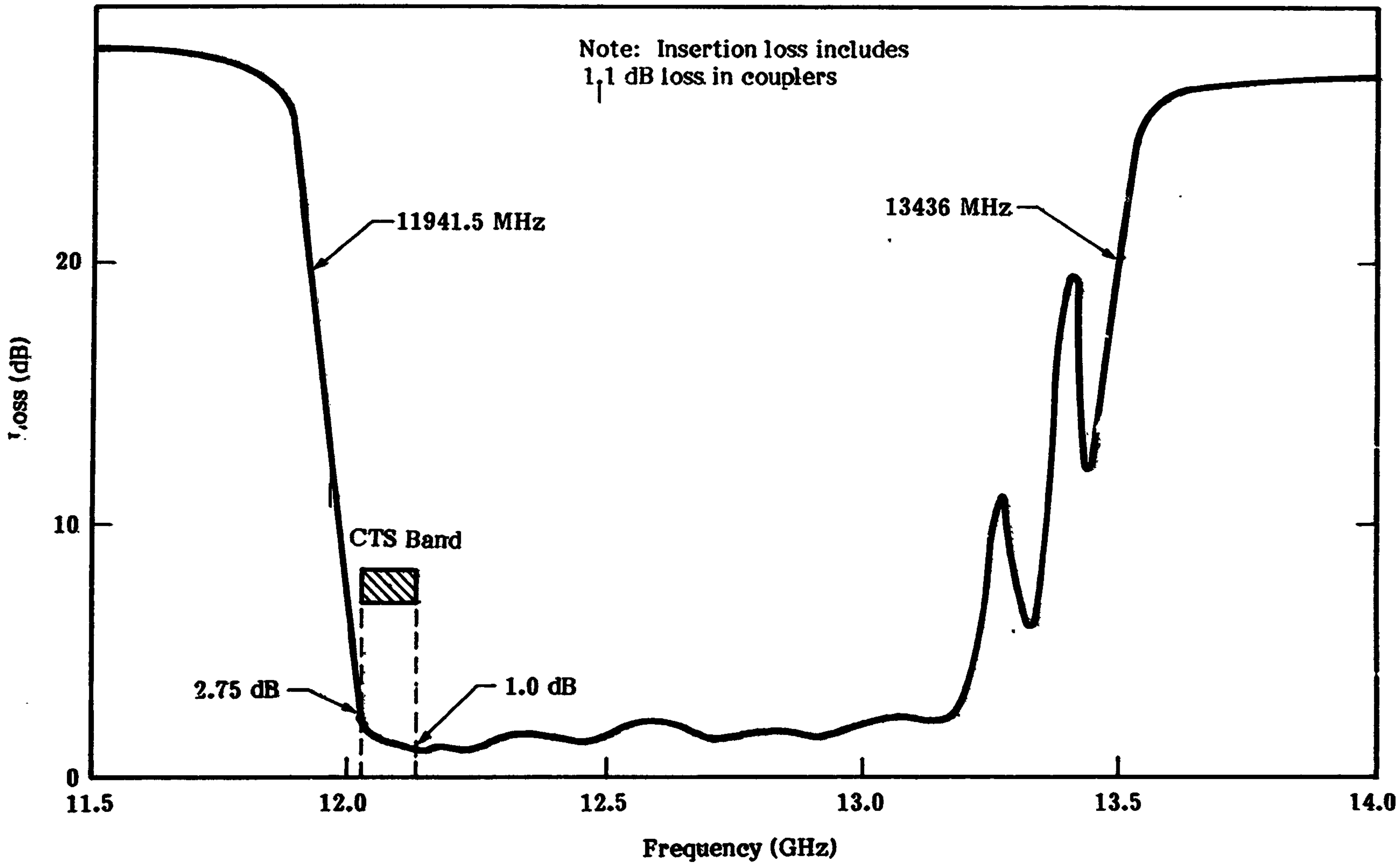

Figure 4-14. Insertion Loss, Center Section

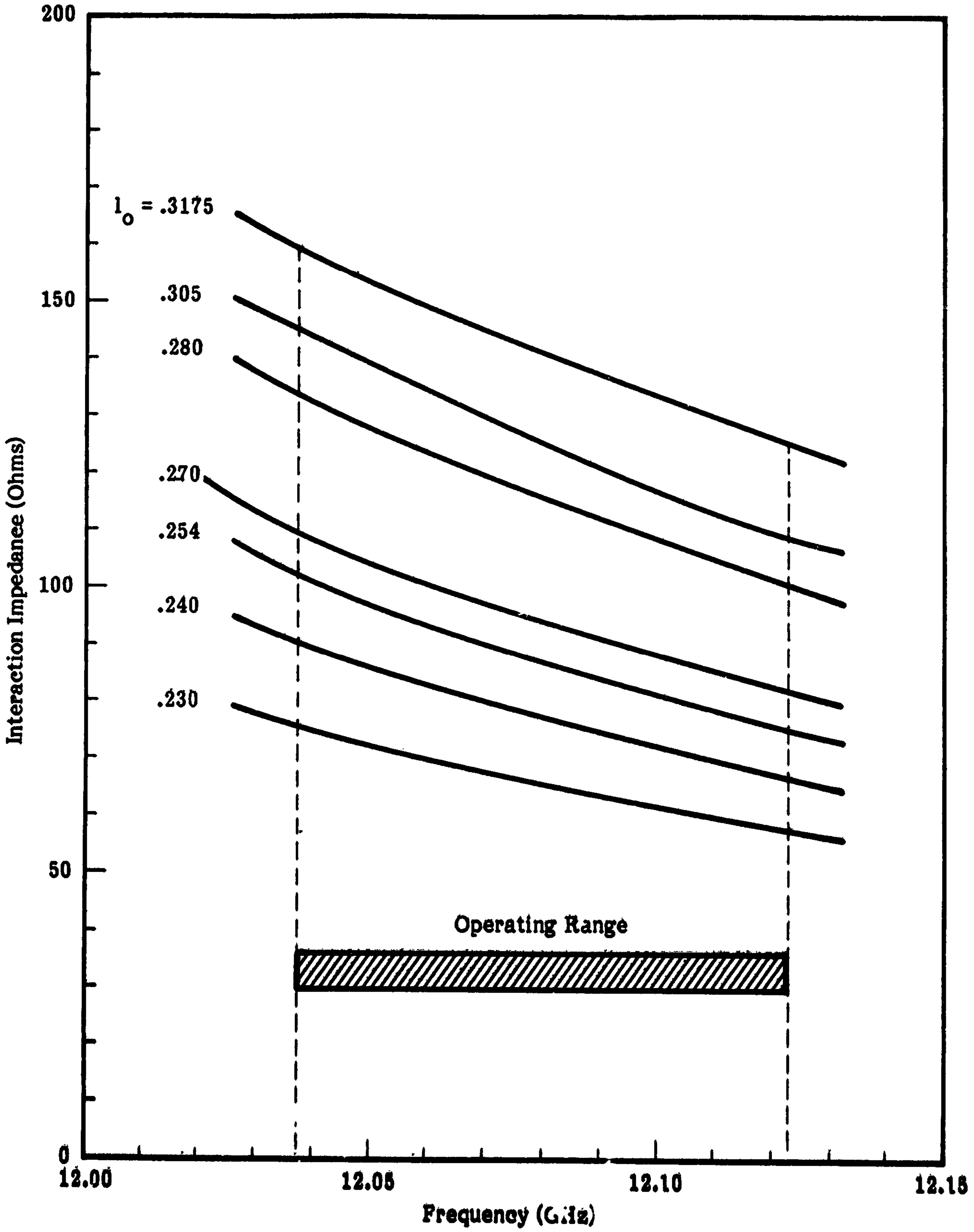

Figure 4-15. Interaction Parameters

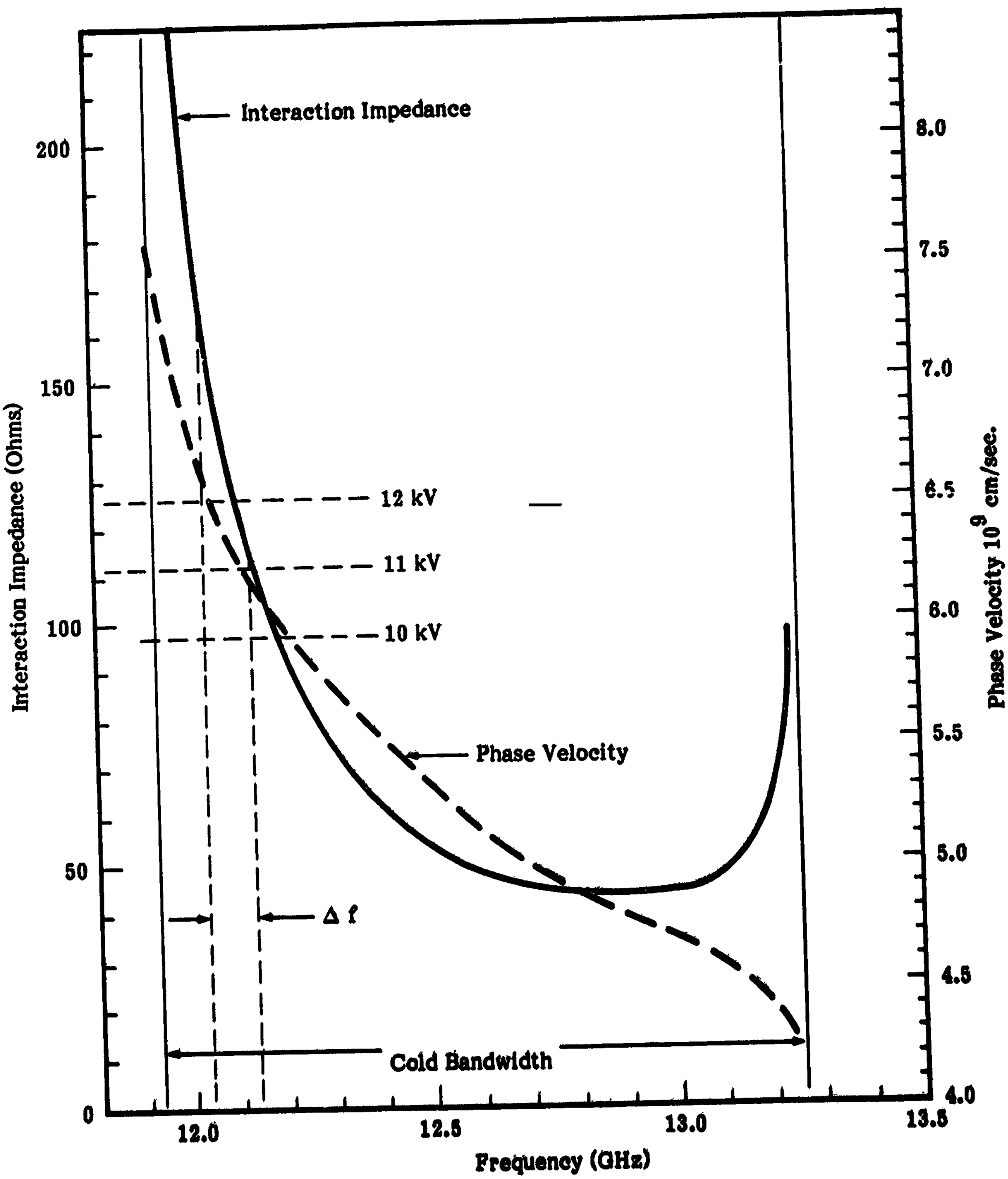

Figure 4-16. Phase Velocity and Interaction Impedance

relationship is shown in figure 4-17 and 4-18.

The rf circuit for the taper was designed utilizing a computer program and by determining the performance at several frequencies over the band for a large number of varying taper configurations. The interaction was calculated over the entire length of the tube (including a sever) at specified drive levels. Phase velocity reductions of 12, 15, and 17 percent in the first taper, and 20, 25, and 30 percent in the second taper were investigated in various combinations. Initially, the increased loss in the tapers was not included. The combination (17, 30) then appeared slightly better than (15, 25). Due to the greater ease in matching a less severe taper, however, the combination (15, 25) was selected. The taper lengths were varied from 6 to 10 cavities in the first taper and 5 to 12 in the second taper. In the initial analysis the optimum lengths were 8 and 7 cavities in the two tapers.

Upon conclusion of the tests for the initial fabricated tube, additional design analysis was performed using the derived effective interaction parameters and the losses measured in the standard cavity sections. The phase velocity in each taper was decreased in proportion to v_T/v_0 where v_T and v_0 are the cold phase velocities of the taper and standard circuits respectively. The interaction impedance was also reduced by the factor $(v_T/v_0)^2$, which corresponded closely to the ratio of the measured cold impedances. The loss in the taper sections was then increased in response to the measured values.

For high basic efficiency, the best taper lengths consisted of 8 cavities in the first taper and 7 cavities in the second taper. The results of a computer run for this configuration at 12.075 GHz and a drive level of 14 dBm are shown in figure 4-19. The calculated gain and efficiency, are plotted versus axial distance, expressed in number of cavities from the input coupler. Also shown is the normalized phase velocity variation. Based on these values, an efficiency of 26 percent is calculated.

The velocity taper profile and configuration as defined at the conclusion of the theoretical design is shown in figure 4-20 and the attendant circuit dimensions in table 4-2. The efficiency degradation and cavity number determination is shown

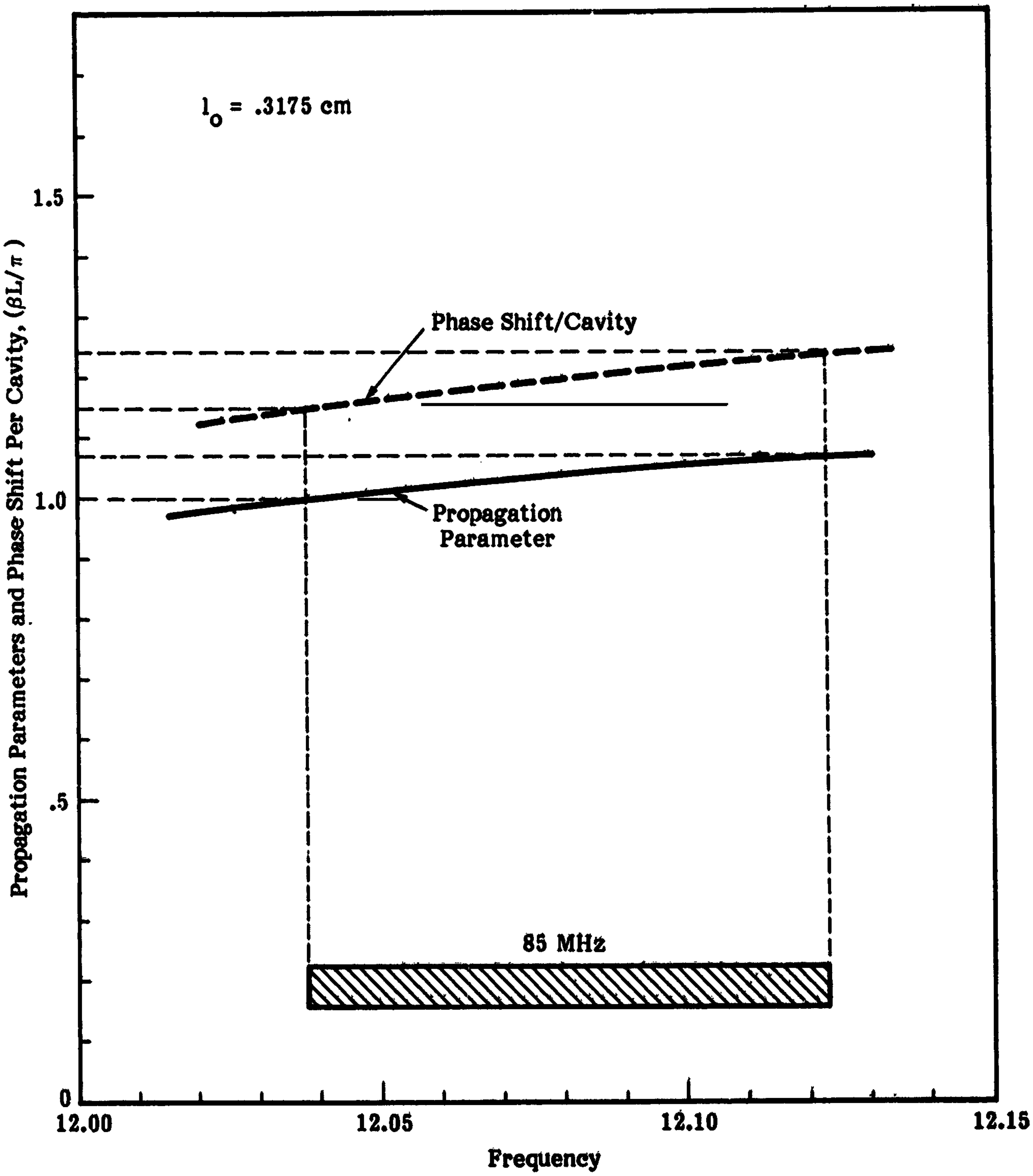

Figure 4-17. Phase Shift and Propagation Parameter

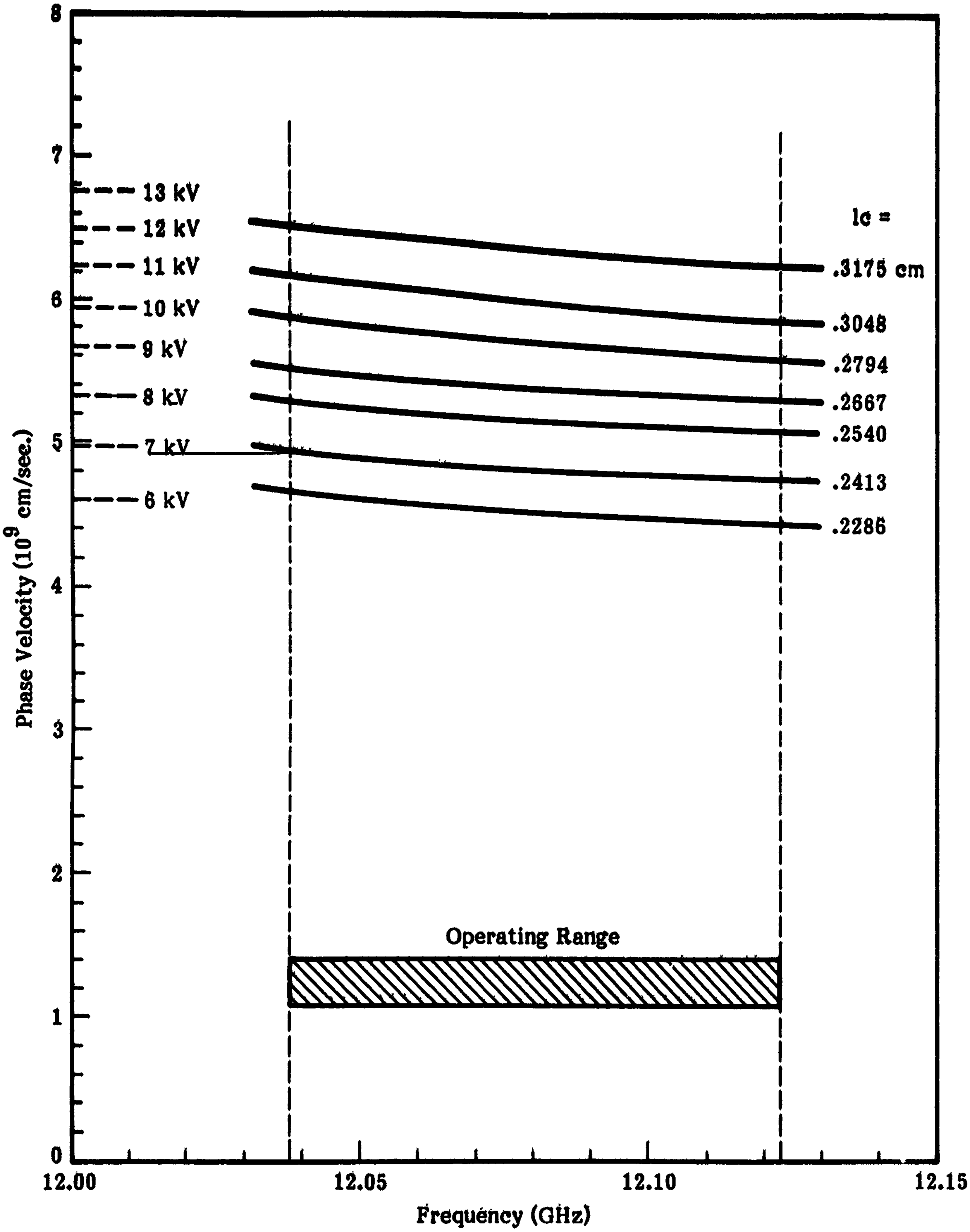

Figure 4-18. Phase Velocity vs. Frequency

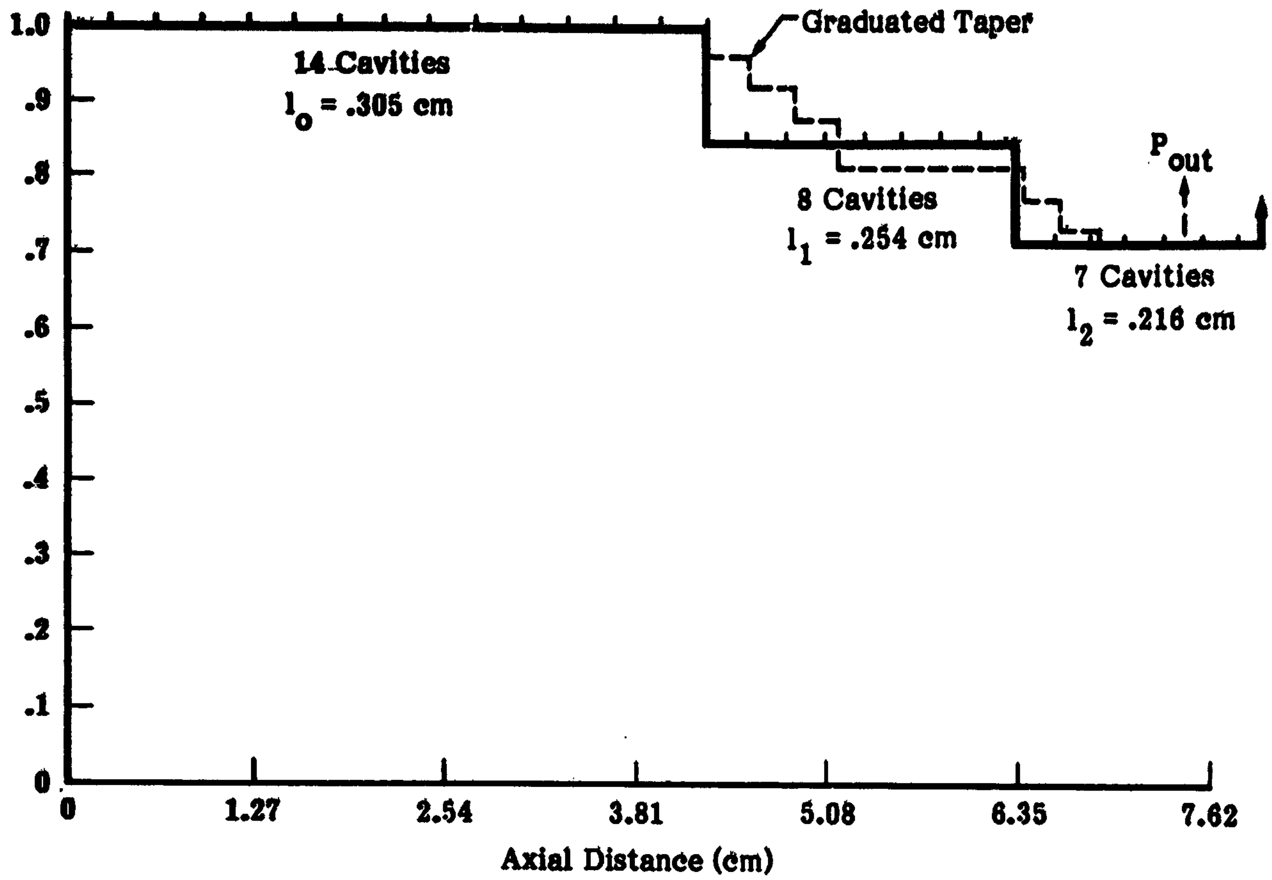

Figure 4-20. Velocity Profile, Output Section

Table 4-2. Output Section Circuit Dimensions (Centimeters)

CIRC.	STD.	T_1	T_2	T_3	T_4	T_5	T_6	T_7	T_8
No.	14X	1X	1X	1X	1X	5X	1X	1X	4X
d_1	.127	—	—	—	—	—	—	—	—
d_2	.280	—	—	—	—	—	—	—	—
d_3	1.511	—	—	—	—	—	—	—	—
t	.076	—	—	—	—	—	—	—	—
l	.305	.298	.292	.280	.267	.254	.241	.228	.216
d/l_o	2.54	2.48	2.44	2.34	2.22	2.09	1.96	1.84	1.83
h	.229	.222	.216	.204	.191	.178	.165	.152	.140
g	.091	.090	.088	.084	.081	.076	.072	.069	.066

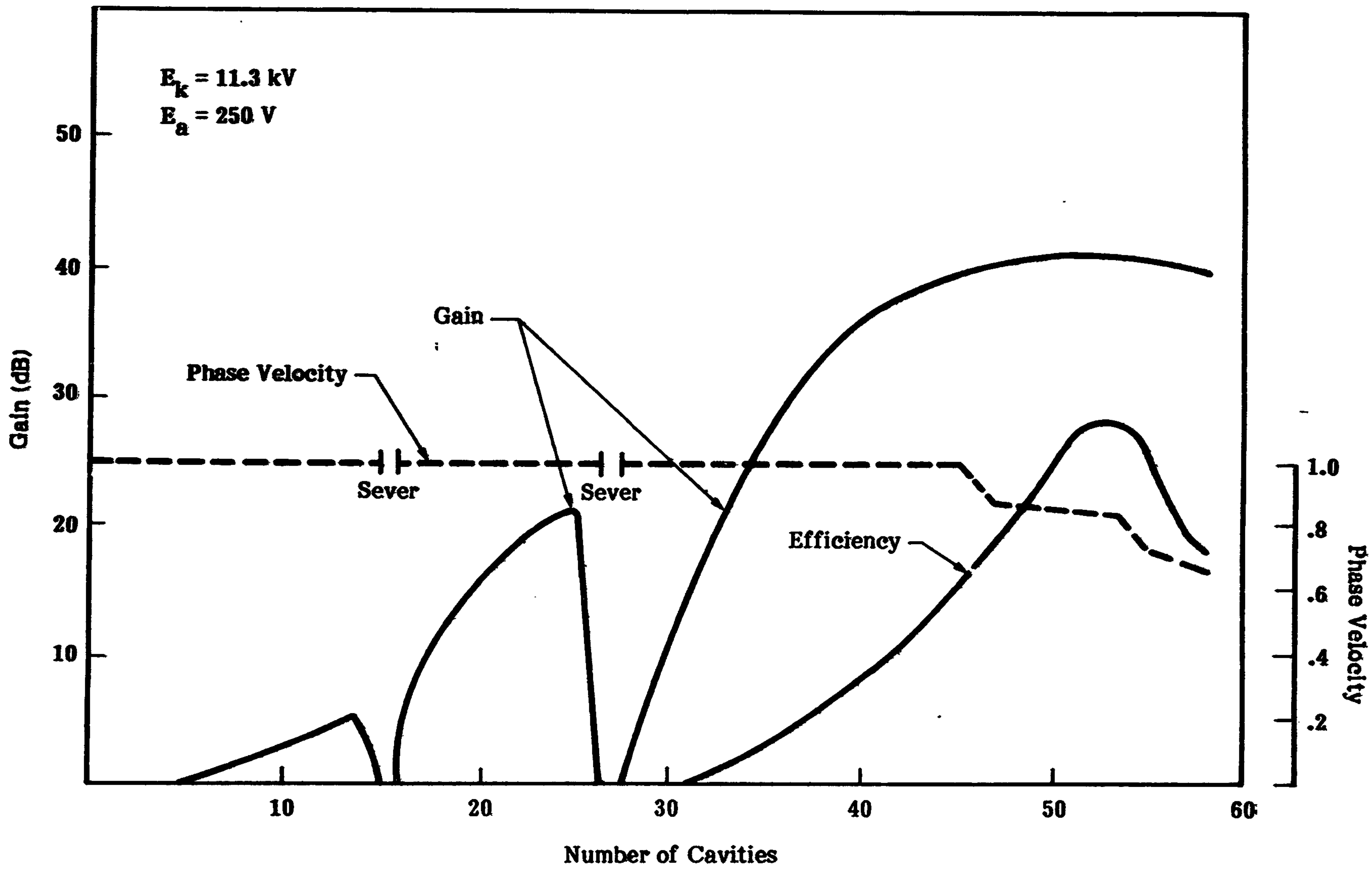

Figure 4-19. Taper Design Performance

in figure 4-21. Figure 4-22 shows the velocity parameter as affected by frequency, over the bandwidth, for three potentials (i.e. 10, 11, 12 kV). Figure 4-23, 4-24, and 4-25 show the calculated tube parameters using a two-step velocity taper at specific input levels.

4.4 FOCUSING SECTION DESIGN ANALYSIS

The analysis associated with the electron beam focusing design was one of the most critical areas in the tube development. It combined the operational requirements and thermal analysis. The maximum operating temperature of the circuit pole piece ferrules and the dissipated power that flows into the base plate structure is directly proportional to the beam current interception on the rf slow wave structure. As such, the beam transmission is an important factor in not only the reliability of the tube but also the adjacent spacecraft components.

Theoretical and experimental evidence determined by previous studies shows that the basic interaction efficiency is a sensitive function of the beam cross-section and the degree of linearity (see Reference 6). It is also known that the collection of the electrons at body potential degrades the overall efficiency of the TWT. Finally, it has been demonstrated that the characteristics of the collector are critically dependent on the electron trajectories of the focused beam near the output of the tube.

The coupled cavity structure provides an excellent circuit for periodic permanent magnet focusing of the electron beam. The cavity walls are fabricated of vacuum quality electrolytic iron that exhibit excellent electrical characteristics as the magnetic pole pieces. The focusing magnets are normally situated between adjacent pole pieces and just outside the copper spacers which form the cavities. In this manner the focusing field is brought into very close proximity to the electron beam. The magnetic pole pieces can be precisely aligned and then brazed in place as part of the circuit assembly sequence, minimizing transverse field effects. In addition, the coupled cavity circuit is thermally rugged as shown in later discussion, making PPM focusing at the specified power level an acceptable design alternative.

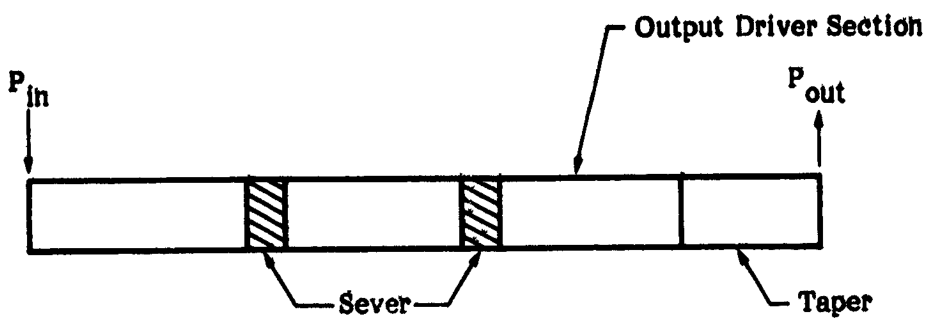

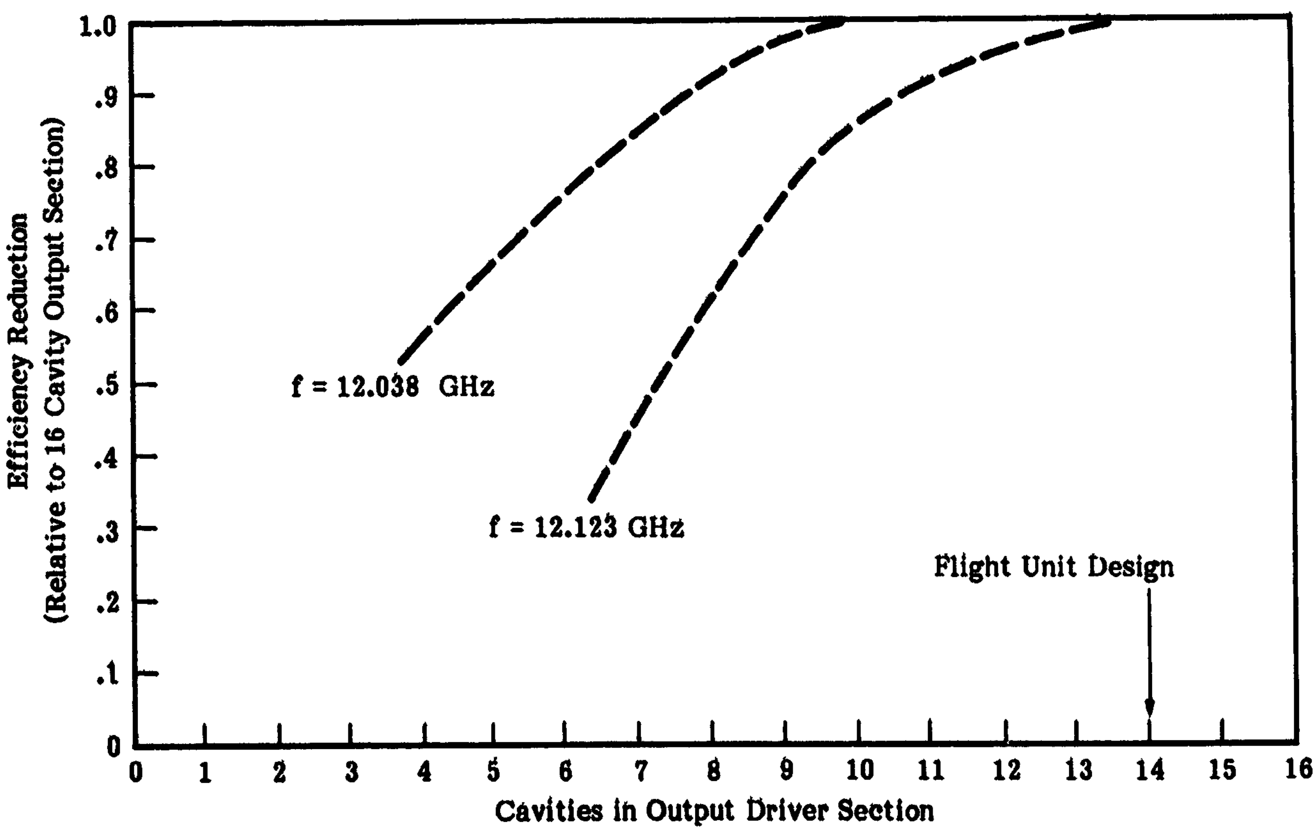

Figure 4-21. Output Cavity Efficiency Curve (Two Step Taper)

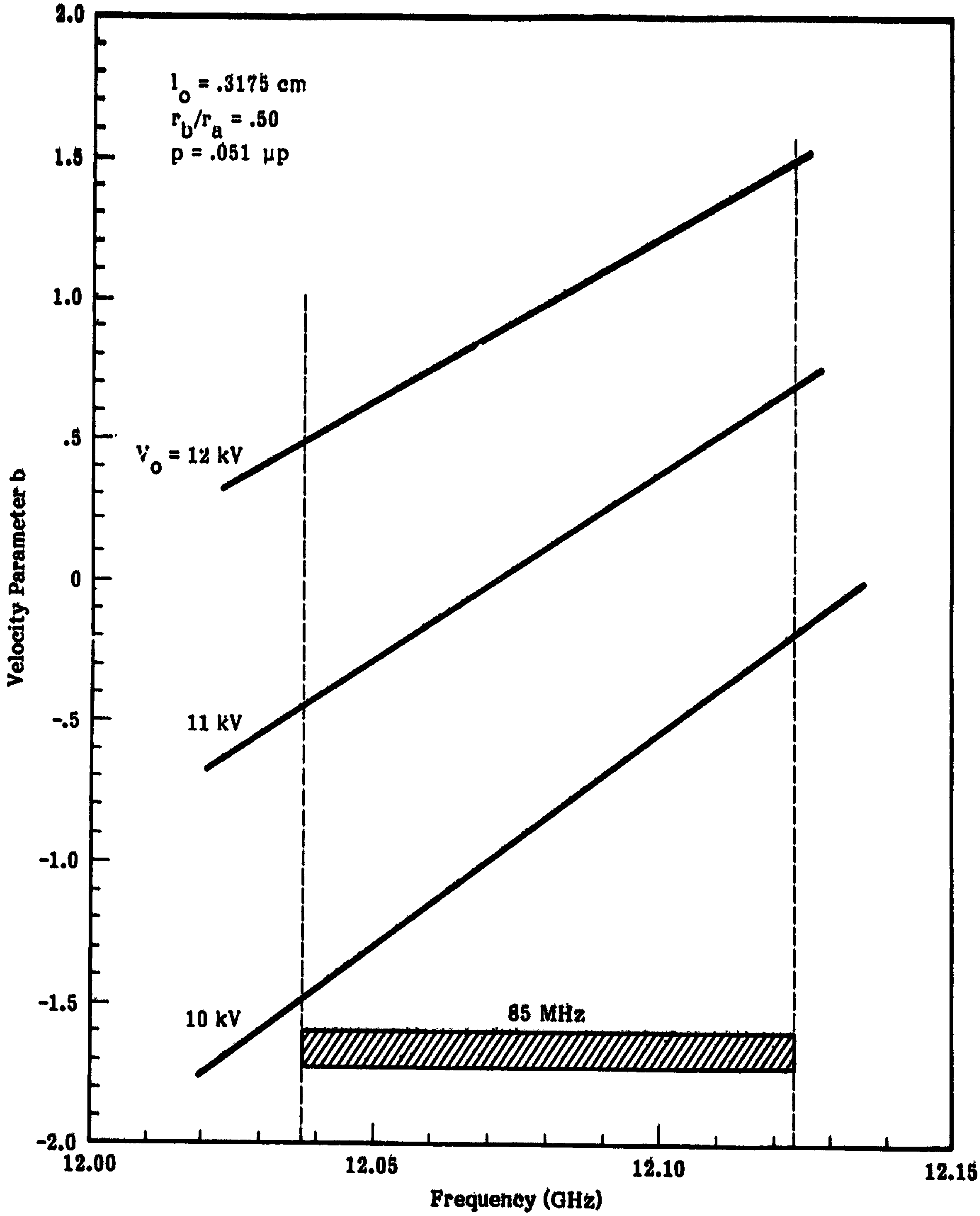

Figure 4-22. Beam Velocity Parameter vs. Frequency

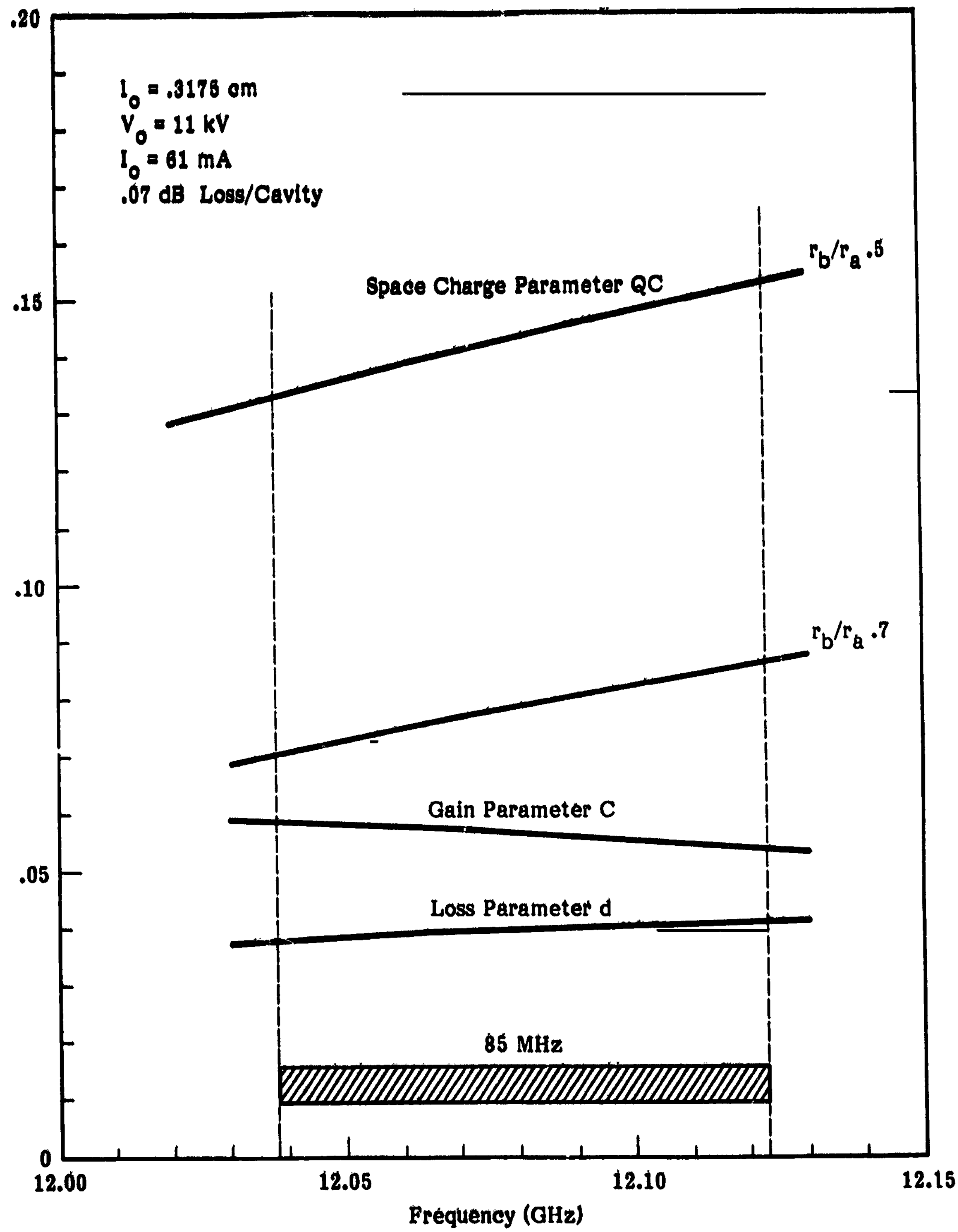

Figure 4-23. Tube Parameters, Two Step Taper (QC, C, d)

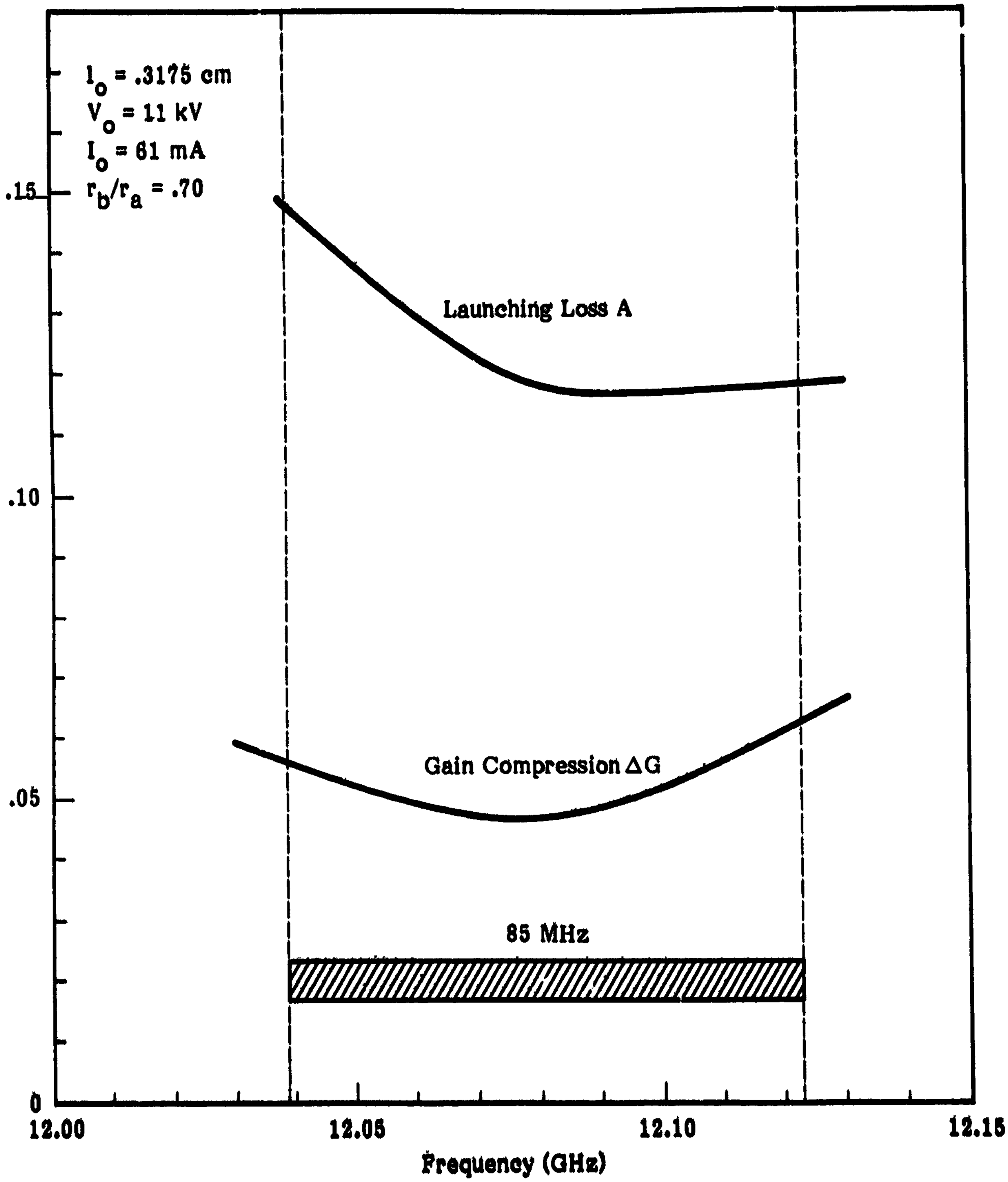

Figure 4-24. Tube Parameters, Two Step Taper (A, ΔG)

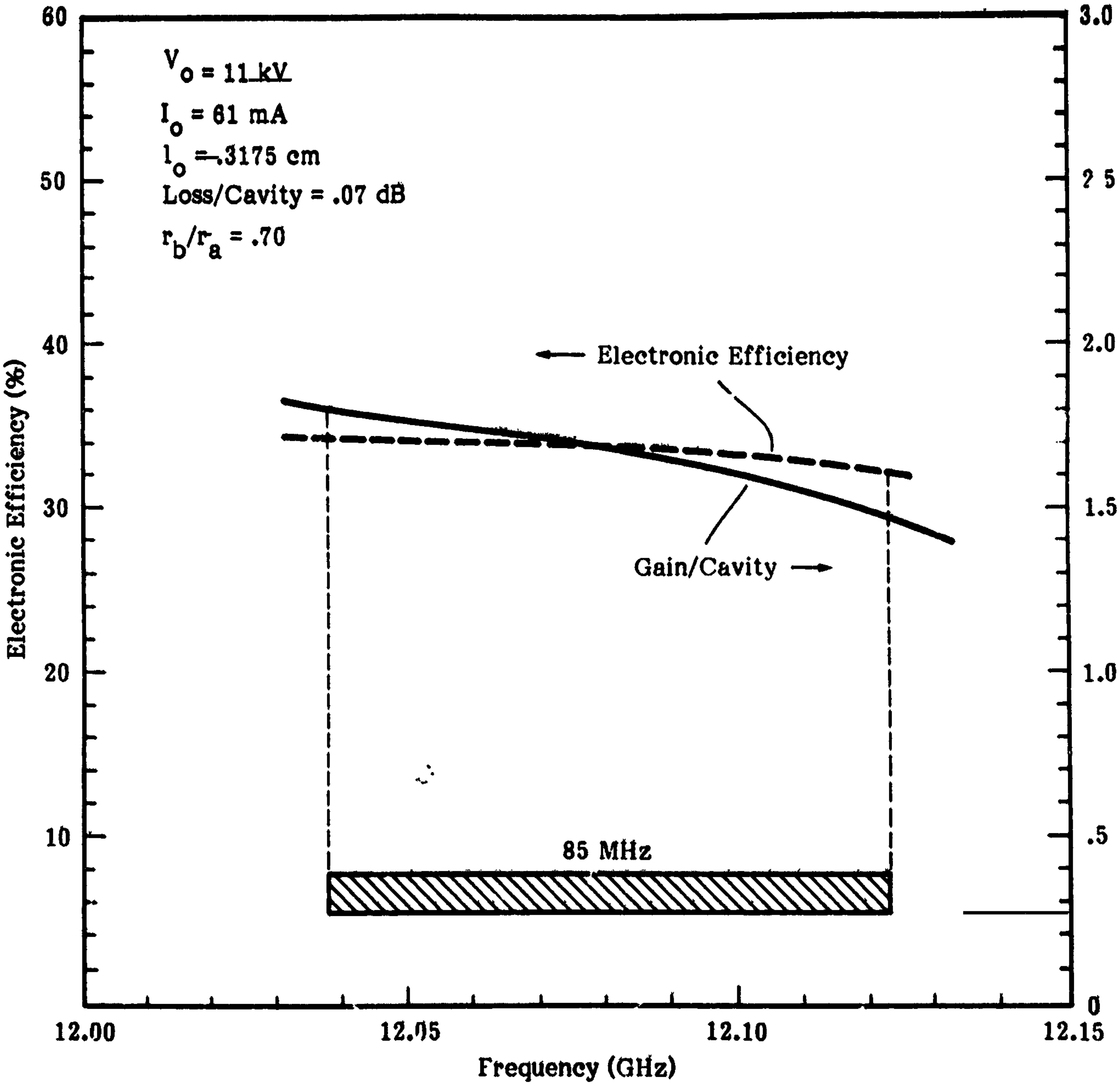

Figure 4-25. Electronic Efficiency and Gain per Cavity

In the L5394 tube, the required axial magnetic field is provided by a double period permanent magnet (PPM) focusing structure as shown in figure 4-26. The axial field distribution plot as measured with typical focusing sections is shown in figure 4-27. The double period PPM focusing used offers a significant advantage over the conventional single period design since a stronger magnetic field can be obtained with a given magnetic material. This is the result of the magnet length per cavity increase, thereby providing a greater magnetizing force between the pole pieces.

By using double period PPM focusing, it was determined that it is possible to use Alnico 8 magnetic material. In the velocity taper position, rare earth magnets (platinum cobalt) were used. These were required to: (1) provide the maximum magnetic focusing field in the vicinity of the tube output where the beam space-charge forces are highest; and (2) achieve this field strength with reduced magnet thickness caused by the velocity taper period reduction. For improved TWT operation at elevated baseplate temperatures, the magnet material in all magnets was changed to samarium cobalt.

Computer analyses using simulation models were completed to optimize the beam focusing with the magnetic field. These computations included the associated thermal velocity effects. In addition, measured magnetic field data, and computer generated plots were developed for various beam envelopes under optimum focusing conditions. The computed result indicated greater than 99 percent transmission without rf drive. The typical dc transmission actually achieved on the tubes was 96 to 99 percent. Beam transmission of 93 to 95 percent was obtained at saturation.

The achievement of this excellent focusing was accomplished with a relative few magnet shunts to maximize transmission. Final mechanical adjustments in focusing were made with the tube operating at 60°C baseplate temperature to account for slight thermal changes in the magnets in the velocity taper. These adjustments also improved the focusing at lower baseplate temperatures.

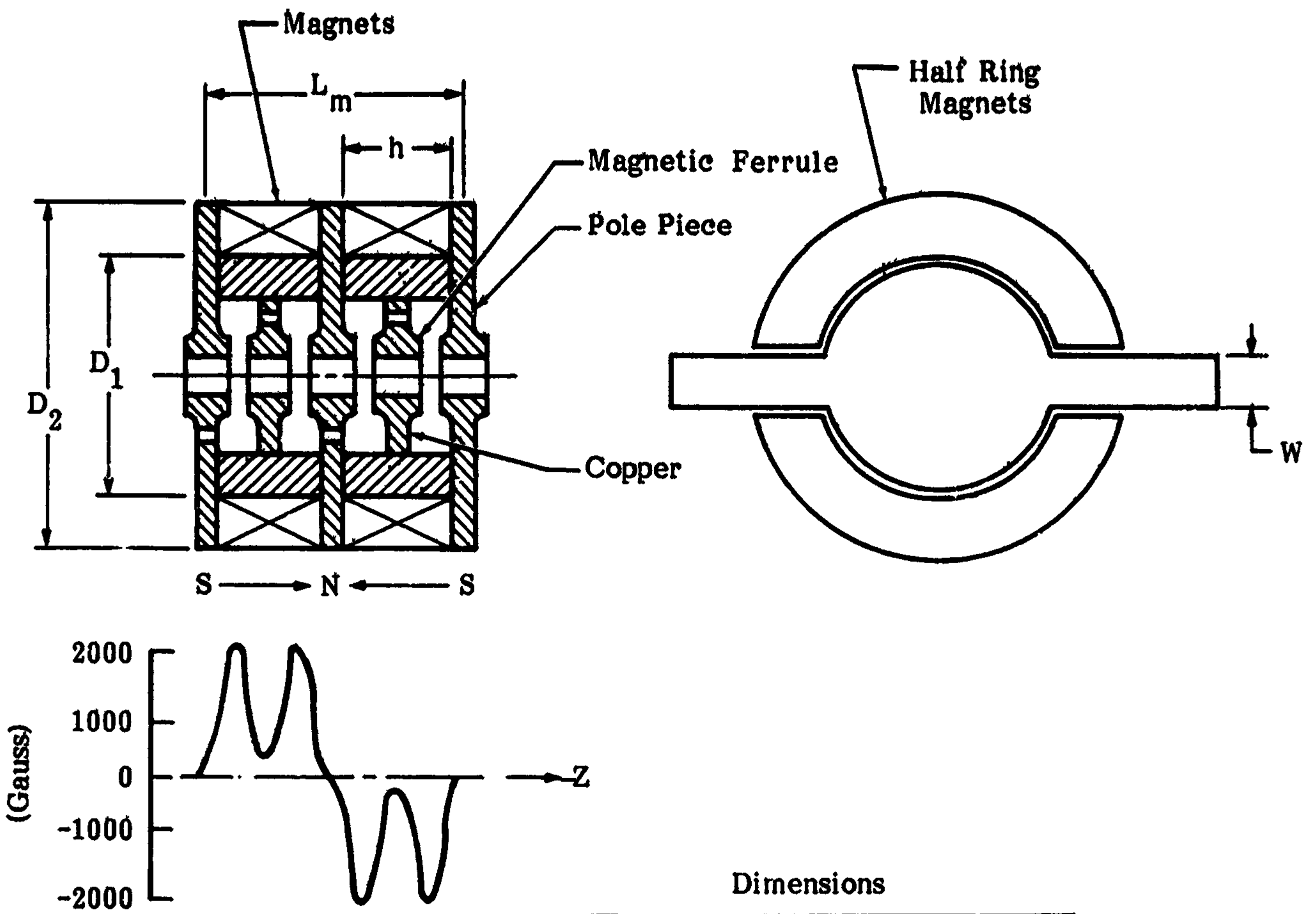

Dimensions

Item	Value (cm)
D_1	2.54
D_2	3.302
h	.533
W	.508
L_m	1.22
l_o	.305

Figure 4-26. Focusing Permanent Magnet Design

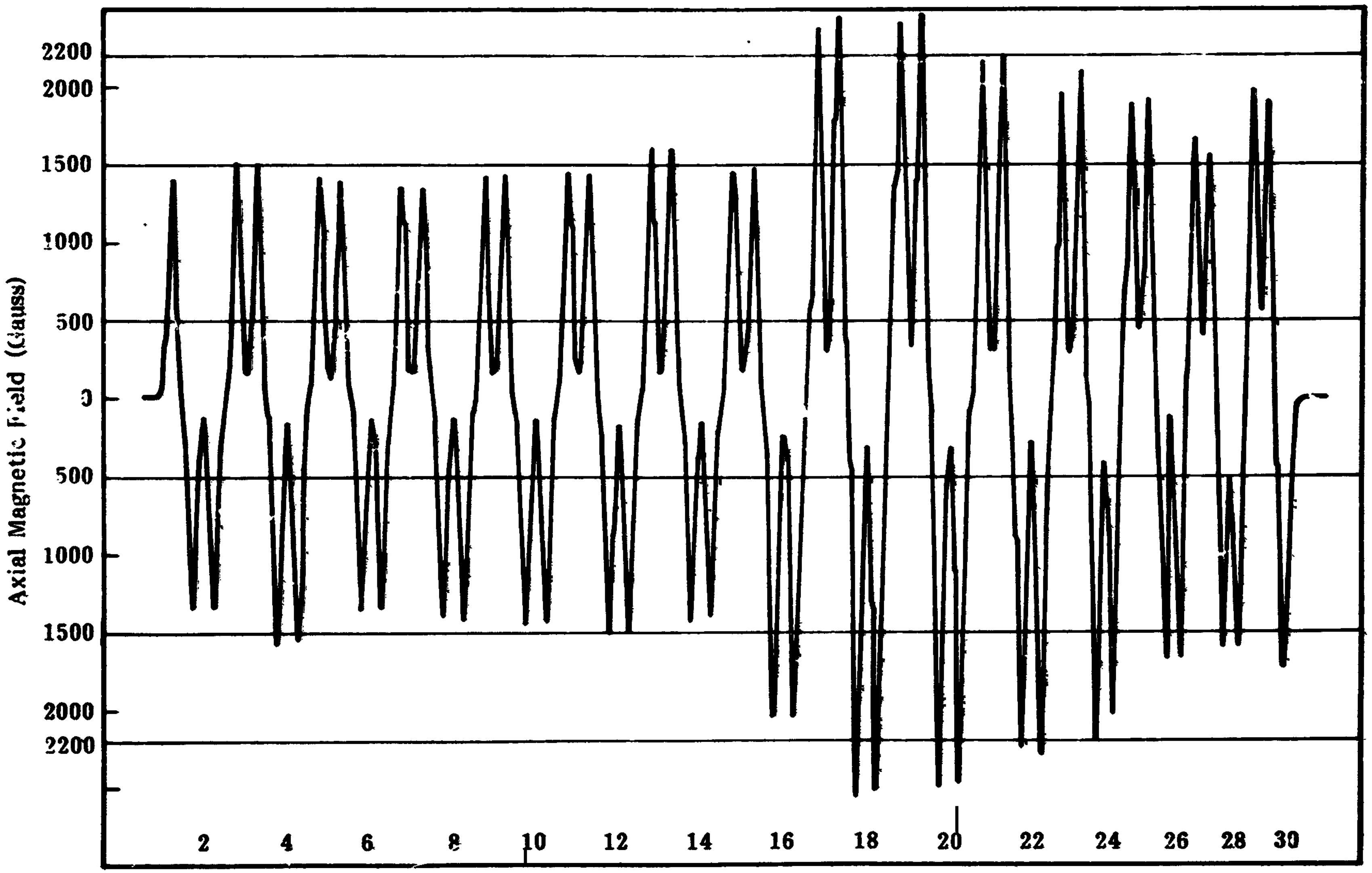

Figure 4-27. Body Magnet Field Plot

4.5 REFOCUSING DESIGN ANALYSIS

To optimize the beam entrance conditions into the multistage depressed collector, it was determined that a refocusing solenoid or a permanent magnet refocusing technique was necessary between the output pole piece and the first collector electrode. The purpose of this refocusing section is to allow the expansion of the spent electron beam, thereby reducing the space charge forces and also minimizing the beam radial velocity components.

The design of the refocusing section was studied in depth at NASA Lewis Research Center (Reference 7) and only a nominal amount of additional analysis was completed at Litton. It was determined by LeRC that the magnitude of the plateau field is also critical with respect to the reduction of the radial rms velocities. The radial velocities can be reduced by nearly a factor of two and sometimes two and one-half with an optimum plateau field design.

The refocusing field was implemented in the tube with permanent magnets. A field reversal between decay field and plateau field was incorporated in order to minimize magnetic leakage fields into the collector. Figure 4-28 shows the axial field distribution calculated for solenoids and permanent magnets. Also shown is the measured values for the permanent magnets used in the design. The axial field distribution for the alternative design utilized in initially fabricated units are shown in figures 4-29 and 4-30.

4.6 MULTISTAGE COLLECTOR ANALYSIS

The multistage collector is considered a key component in achieving high efficiency. The basic analysis, concepts, functioning and the initial design were completed at LeRC. This design consists of multistage depressible collector electrodes as shown in the schematic of figure 4-31. The voltages and positions of the electrodes have been selected to achieve optimum theoretical efficiency enhancement at saturation and to minimize the lens effects of the electrodes. The position of the collector electrodes were calculated to achieve an essentially uniform electrostatic deceleration field in the most negative collector region and a very weakly decelerating field in the vicinity of the collector injection hole.

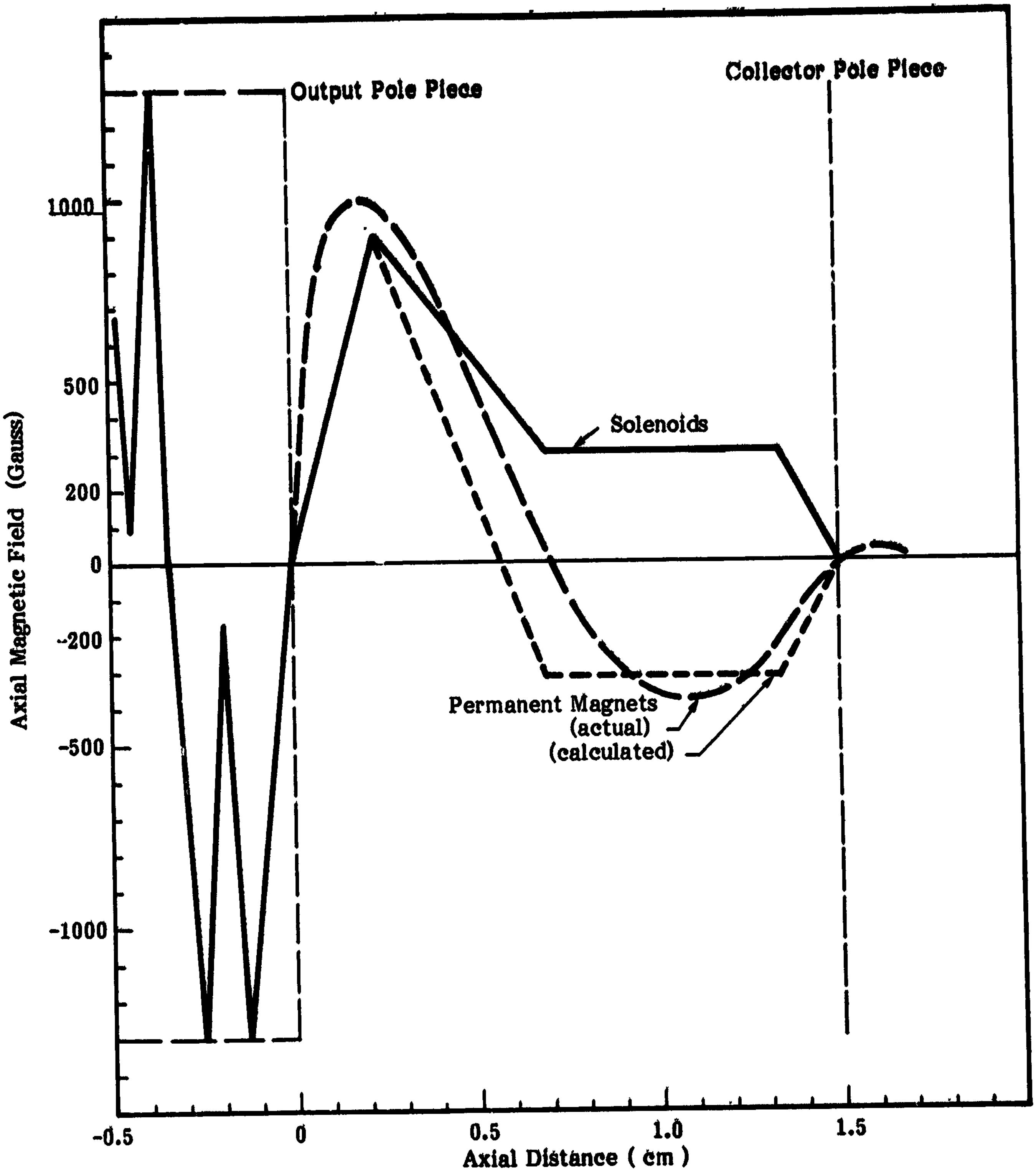

Figure 4-28. Solenoid and Permanent Magnet Comparison

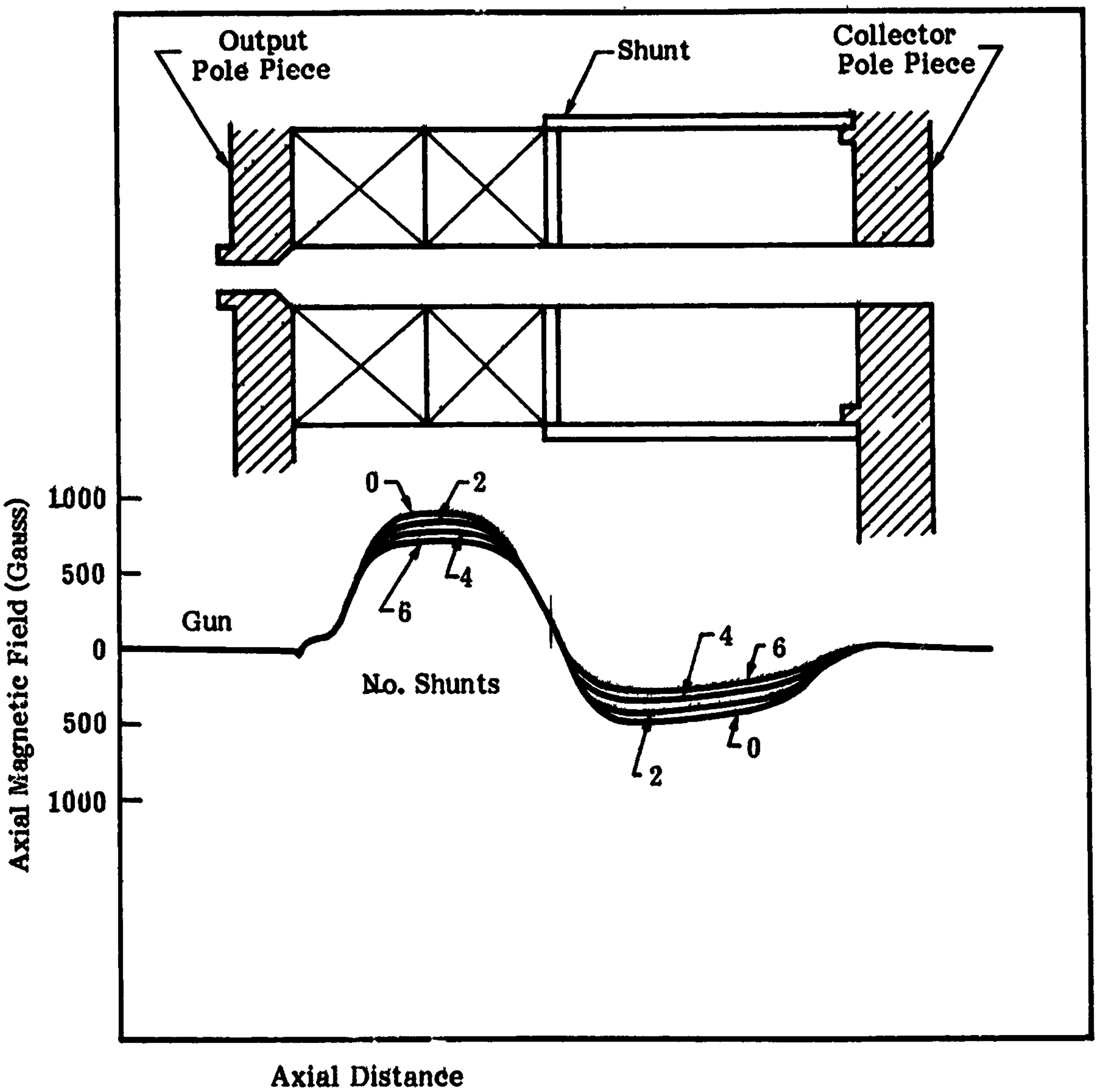

Figure 4-23. Axial Field Distribution

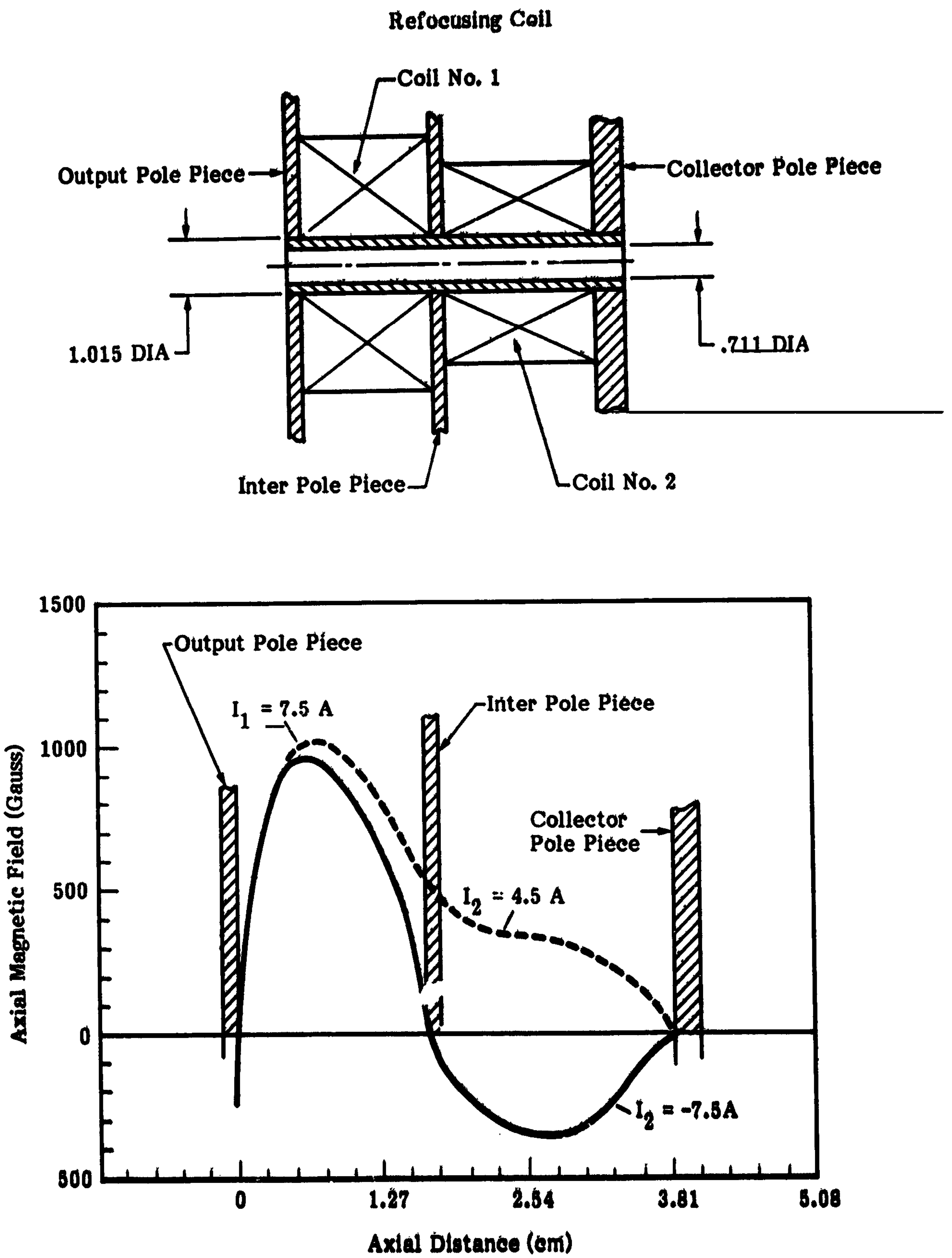

Figure 4-30. Alternative Design, Axial Distribution

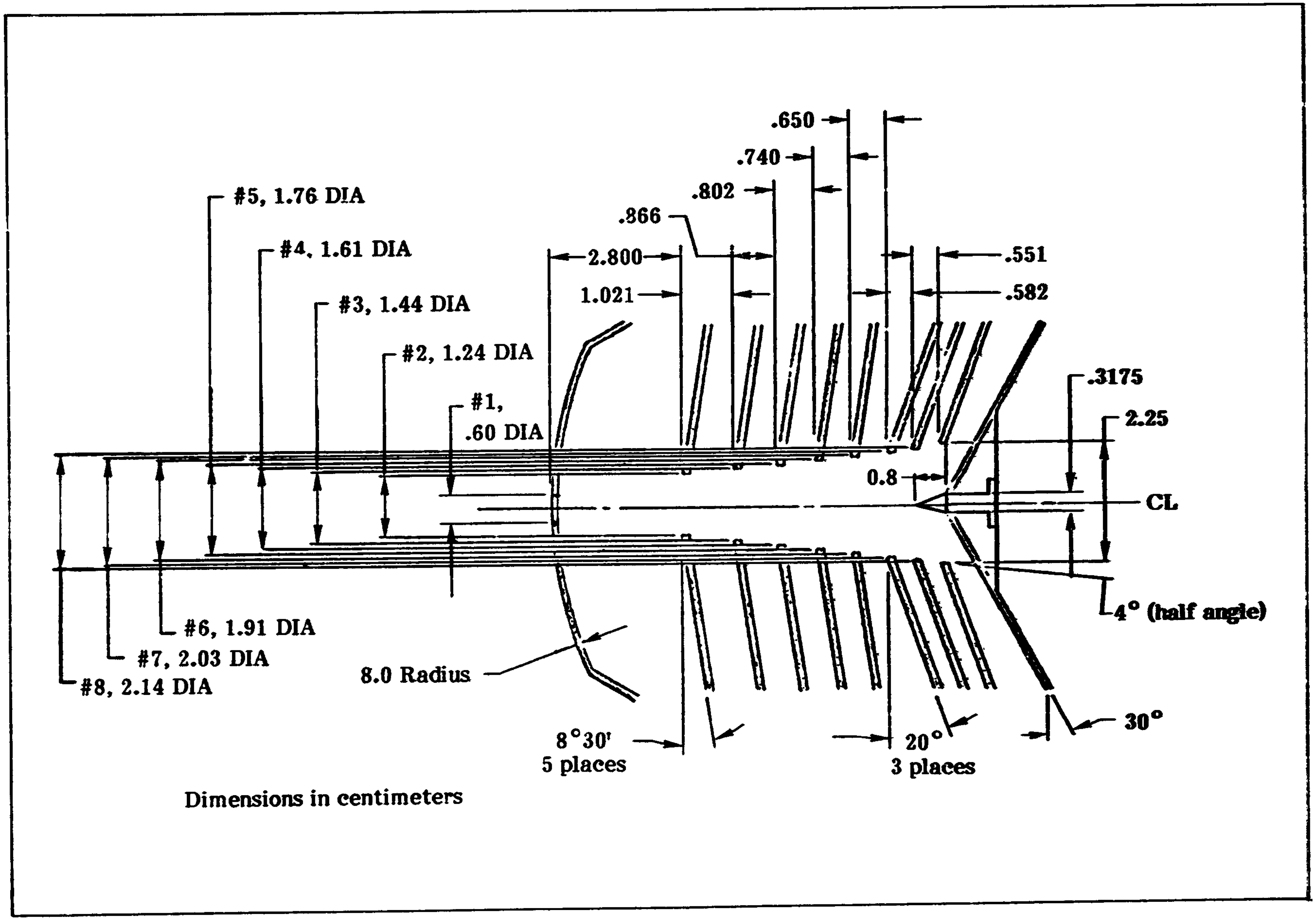

Figure 4-31. Multistage Collector Configuration

The collector efficiency η_{coll} was computed from electrical and steady state thermal measurments of heat dissipation in the initial tube body and the (thermally insulated) collector with carefully calibrated equipment at Lewis Research Center. The collector efficiency, defined as kinetic beam power recovered in the collector over total beam input power into the collector, was determined from two independent measurements:

$$\eta_{coll} = \frac{P_{rec}}{P_{rec} + P_{dis}}$$

$$\eta_{coll} = \frac{P_{rec}}{I_o V_o - P_{rf} - P_{TWT} + P_{heater}}$$

where $P_{rec} = \sum_n I_{cn} V_{cn}$, with I_{cn} and V_{cn} the current and voltage of the n^{th} collector electrode (to body), respectively; P_{dis} is the thermal power dissipated in the collector assembly, and P_{TWT} is the heat power dissipated in the TWT from interception and skin effect losses. The two formulas give agreement within 5 percentage points with the average being 82.5 percent at saturation. This result was achieved with the collector working on a beam having a substantial velocity spread, since approximately 50 percent of the beam power is used up in the tube.

The analyis associated with the mechanical design, electrical limits, and thermal considerations of the collector are discussed additionally in the mechanical design section of this report.

4.7 THERMAL ANALYSIS

The thermal analysis associated with the tube design was primarily concerned with the multistage collector since the thermal characteristics of the MDC directly effect the overall efficiency of the tube, while the thermal characteristics of other sections of the tube have only a secondary effect. A thermal analysis for the tube body was completed, but primarily in support of the mechanical design/assembly of the gun and the focusing section. This is described in Section 5.1, herein.

The preliminary analysis of the radiation cooled multistage depressed collector was accomplished by Mr. A. N. Curren of NASA Lewis Research Center. The computations were performed using a modified version of an existing model thermal analysis computer program. The mechanical model of the MDC was envisioned to consist of flat electrode dishes inside a metal vacuum envelope. It was assumed that there is no heat transfer from the electrodes or the envelope to the support plate. Conservative estimates of the emissivities of the elements (σ = .40) and the envelope (σ = .90) were used. The steady state analysis was performed for two types of OST operation: (1) rf output power of 0 watts (no rf drive) and, (2) tube at saturation; i.e., 200 watts rf output.

The results for condition (1), zero rf output, are shown in figure 4-32. This was determined to be as the worst case condition due to the higher spent beam power and the higher concentration of beam interception on the most depressed elements. The analysis shows that the maximum electrode temperature expected is 570°C, on element number 8. The maximum vacuum envelope temperature shown is 343°C.

The results for condition (2), at saturation, are shown in figure 4-33. The graph on the left part of the figure shows the expected electrode temperature versus radial distance for each of the elements and for the outer surface of the vacuum envelope. The maximum predicted temperature is less than 400°C. The graph on the right provides the vacuum envelope cylinder temperature versus distance along the envelope surface. The maximum expected temperature is 282°C. Based on the results of the initial thermal design, the preliminary mechanical design of the MDC was modified as required to improve the overall collector performance.

One problem that became apparent during the thermal design of the MDC was the reduction of heat conduction from the MDC vacuum envelope to the TWT support plate. Due to the radiation cooling, it was determined that the vacuum envelope operates at several hundred degrees centigrade while the TWT temperature must be maintained below 100°C. Without an effective thermal isolator, a considerable percentage of the collector power dissipation flows back to the body of the TWT, thereby reducing the effectiveness of the radiation cooling approach.

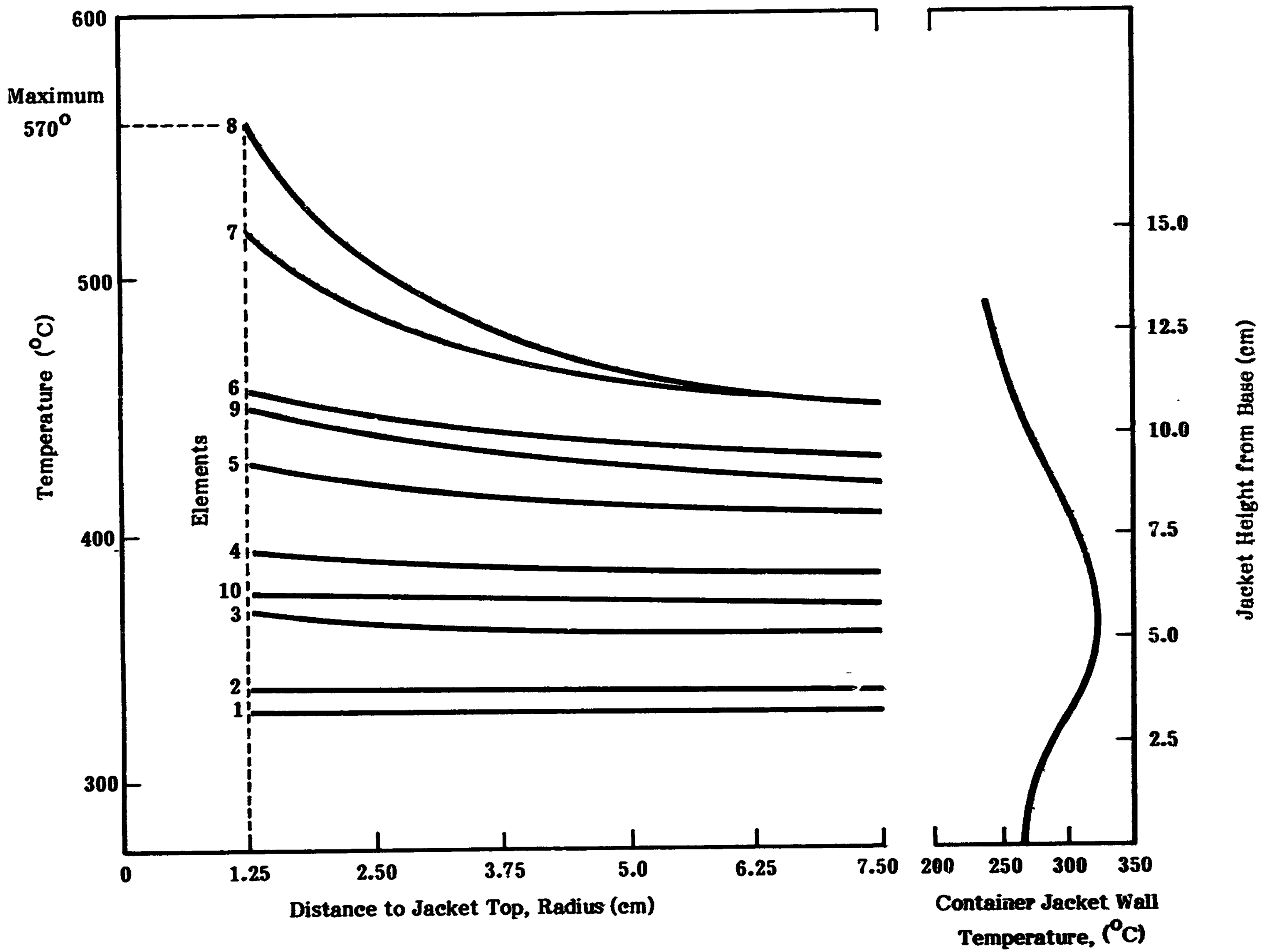

Figure 4-32. MDC Temperature Profile, Zero Output

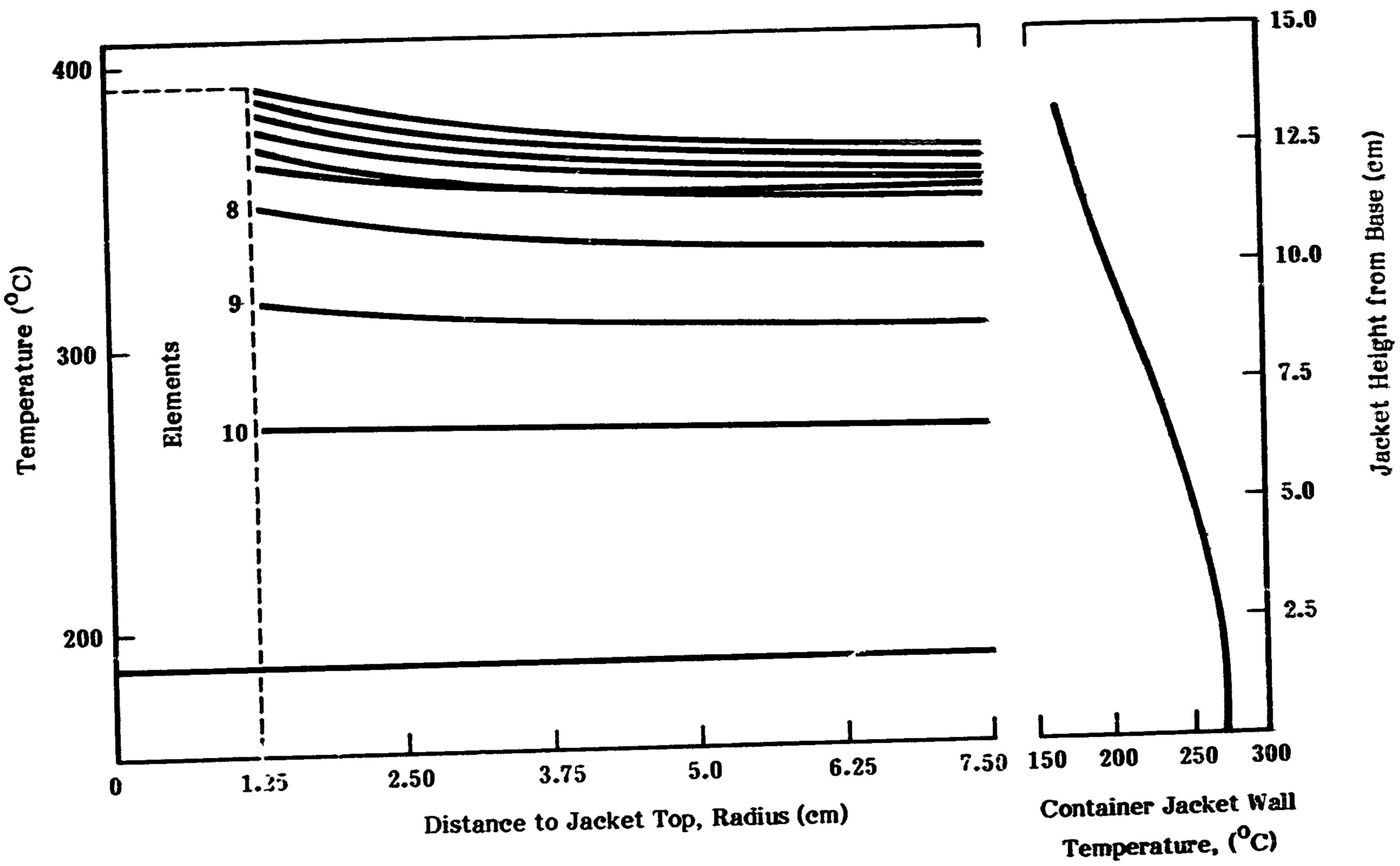

Figure 4-33. MDC Temperature Profile, Saturation

To help solve this problem, an improved thermal isolator was designed. The design consists of a series of concentric thin wall stainless steel cylinders to reduce the effective cross section area and yet provide the necessary mechanical strength to support the electrode assembly. The vacuum integrity of the envelope is maintained by a stainless steel bellows that is welded to the collector jacket support ring and the collector pole piece. The extended conduction path along the length of the bellows acts also as an effective barrier to heat transfer. A simplified drawing of the MDC with the thermal choke is shown in figure 4-34. Additional in-depth thermal analysis was performed by Litton using a simulation 10-node model. This model was later refined and expanded and calculations were made for three conditions; (1) zero rf output, (2) 100 watts output, and (3) 200 watts output.

Figure 4-35 shows the MDC configuration with the effective element position dimension, the physical determination of node location, and the approximation of the thermal choke supports, and the heat reflector in a cross section horizontal orientation. The results obtained from the analysis is presented in tables 4-3 and 4-4. Note that the solar power input was based on the MDC container lateral projected area and that 147 joules/hr.m.^{2} was added on each case. This value has been determined as the expected conditions of the tube in normal space operation.

The analysis associated with the thermal design was as important as the electrical and mechanical designs in determining the final configuration of the radiation cooled multistage depressed collector. Several design trade-offs (and iterations of the thermal analysis) were made between weight, mechanical rigiditiy, size and the operating temperatures before the final configuration was selected. The collector elements in the final configuration are electrically and thermally insulated from each other, from the tube body, and the vacuum envelope. The insulators also provide thermal isolation and mechanical support for the electrodes. Heat is dissipated by radiation to the other electrodes, to the outer surface vacuum envelope, and from there to deep space. With the incorporation of the design features noted and the placement of the reflector between the first electrode and the outside support, less than 6 watts of power soak back is experienced.

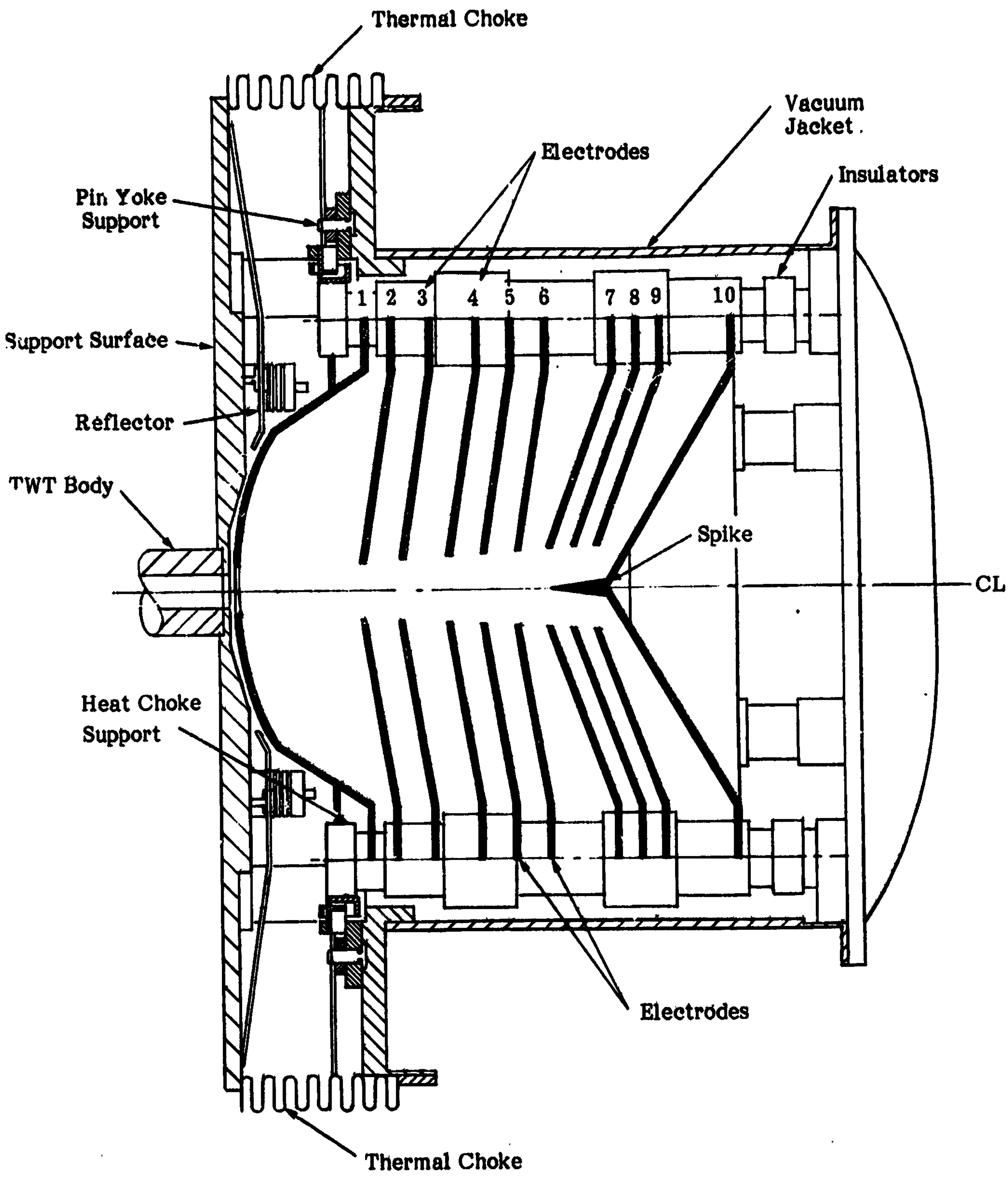

Figure 4-34. Radiation Cooled Collector

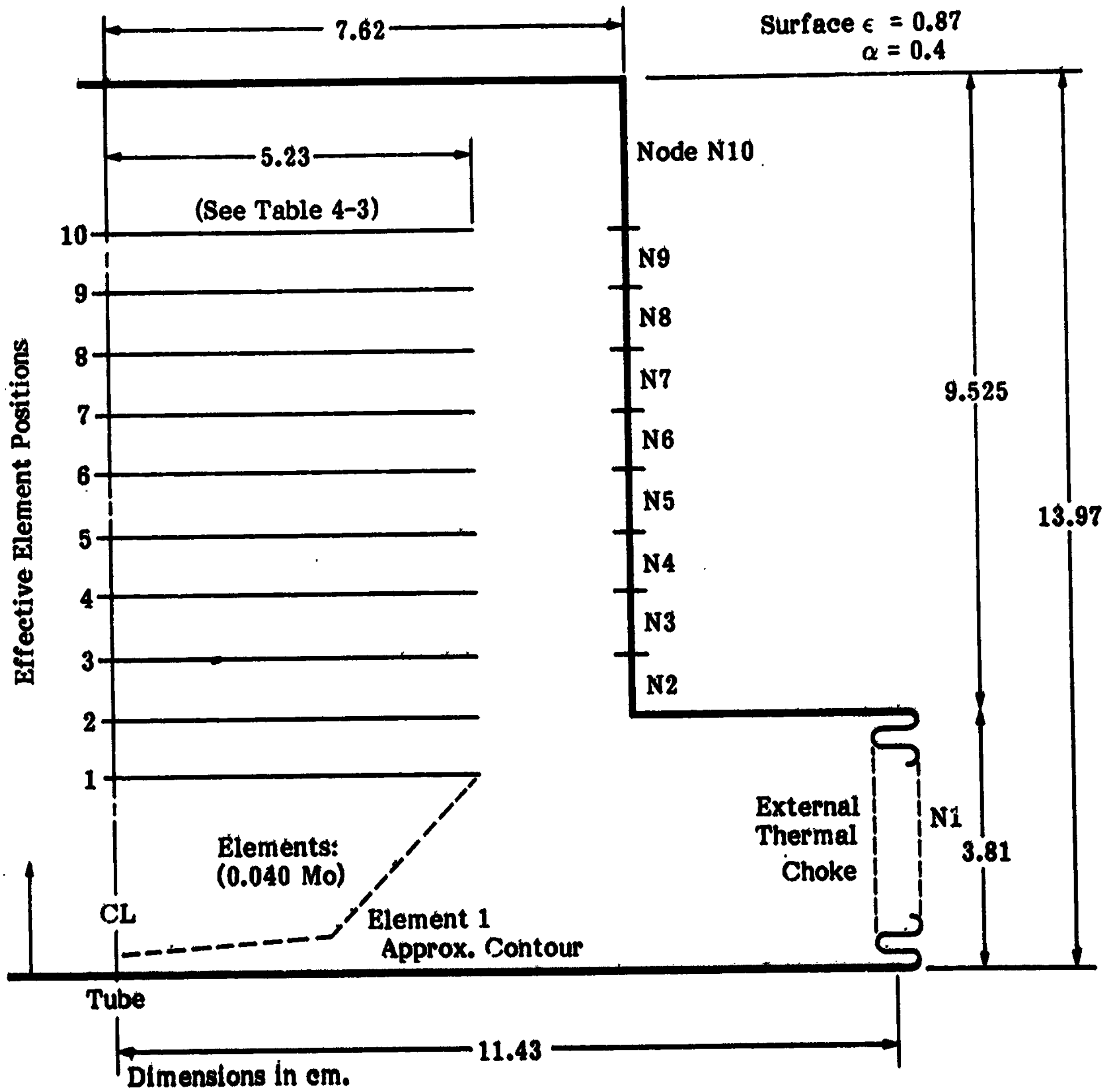

Figure 4-3b. MDC Thermal Configuration

Table 4-3. MDC Thermal Analysis Results; Dissipation

MDC ELEMENT	EFFECTIVE ELEMENT POSITION (Y)	SATURATED OUTPUT 200 WATTS	DC CONDITION 0 WATTS	100W OUTPUT WATTS
1	2.90	4.47	0.17	3.45
2	3.81	6.63	0.60	2.04
3	4.72	16.78	0.74	3.25
4	5.63	22.65	1.12	6.77
5	6.54	11.47	1.74	17.44
6	7.54	5.34	2.30	21.24
7	8.36	4.69	3.46	19.39
8	9.26	4.90	29.90	17.58
9	10.18	11.65	69.67	33.66
10	11.08	0.00	0.00	0.00
TOTAL		88.58	109.70	124.82

Table 4-4. MDC Thermal Analysis Results; Temperature

NODE NO. (Fig. 4-34)	LOCATION, (cm) (Fig. 4-34)	TEMPERATURE, °C AT		
		SATURATED OUTPUT	DC CONDITION	100 WATT OUTPUT
1	2.30	96.7	61.0	90.0
2	4.26	225.0	198.3	245.0
3	5.17	228.9	208.3	255.0
4	6.08	227.8	220.0	263.9
5	7.00	223.3	232.2	271.1
6	7.90	216.1	245.0	274.4
7	8.81	207.8	256.1	273.3
8	9.72	198.9	261.7	267.2
9	10.63	188.9	258.9	257.2
10	13.34	151.7	225.0	211.1

5.0 MECHANICAL DESIGN

The mechanical design of the 200 watt TWT was influenced by numerous factors, including the initial specification parameters, the results obtained during the analytical studies, and the results of tests performed on the preliminary fabricated units. This section of the report is devoted to a discussion of these influencing factors, the initial mechanical design, and the evolution of the current or flight model hardware.

The information is presented in a format similar to the chronological sequence under which it was encountered, that is, system requirement definition, design of components, initial integrating/design problems encountered, problem resolution and design improvements, and the resultant final design/assembly of the tube.

5.1 OST PACKAGE

A. General

The Output Stage Tube (OST) is defined as the combination of the traveling wave tube and the multistage depressed collector. The OST with the addition of the input/output waveguides, power processing system, instrumentation controls and the structural members required to operate in conjunction with an rf driver as an rf power amplifier are identified as the transmitter experiment package (TEP) of the Communication Technology Satellite (CTS) system.

The OST package in the delivered configuration is as shown in figures 2-1 and 3-9. A cross section of the flight tube is as shown in figure 2-6. The tube is mounted to the spacecraft by the tube body support structure so that the collector enclosure protrudes outside the spacecraft thermal envelope and can radiate directly to space. The mechanical and thermal design of the depressed collector are described in another section of this report. The following paragraphs describe the mechanical and thermal design of the tube body. Some of the fabrication problems encountered during tube manufacture are also discussed.

The four major sections of the OST package are discussed in the following paragraphs in a sequence that parallels the electron beam generation and travel; i.e., Electron Gun Assembly, RF Circuit/Body, Refocusing, and Multistage Depressed Collector.

B. Mechanical Design

The tube mechanical design requirements were that the tube body structure support the cantilevered collector through the launch vibration and acceleration environment. The tube body by itself is not designed to carry the structural loads imposed by the cantilevered collector. It was, therefore, necessary to build an exterior structure between the collector and the tube base which would hold the entire structure rigid while transmitting the mechanical loads of the cantilevered collector to the tube body base. The interconnecting structure selected is essentially a box beam truss which surrounds the tube body. The rf input and output waveguides pass through the openings in the truss structure. The design of the truss has not been changed from the original design except for additional diagonals to stiffen some open truss sections.

The rf input and output waveguides were originally supported by lightweight sheetmetal brackets. This waveguide support configuration did not survive vibration test; therefore, it was necessary to redesign the brackets. These were changed to rigid machined aluminum design to insure survival in the flight vibration environment.

C. Thermal Design

The tube body thermal design requirements were that the tube body be required to absorb the heat generated by rf losses in the circuit (≤ 70 watts), by beam interception (≤ 30 watts) and by the cathode heater (6 watts). This heat is conducted by the copper circuit parts to bus bars which are cemented to the length of the tube body with silver epoxy. (Originally these bus bars were bonded to the tube body with Indium solder, but this process was found detrimental to the tube operation). The heat is conducted from the bus bars to the tube base by aluminum saddles which are rigidly bolted to the bus bars and base using Indium foil gaskets. Heat from the baseplate is dissipated in the TEP variable conduction heat pipe radiator system.

A heat choke and heat reflectors between the collector and the tube body are incorporated in the thermal design in order to prevent heat generated in the collector from leaking back to the tube body. The calculated soak back is less than 6 watts. The heat choke consists of a thin stainless steel (low thermal conductivity) bellows vacuum enclosure with the electrode assembly supported on small thin wall stainless steel tubes. Except for the reflector addition, the thermal design of the heat choke and the tube body have remained essentially unchanged from the initial tube design.

D. Interconnections

The major interconnection requirements between the OST and the TEP (Transmitter Experiment Package), which include the interface with the PPS (Power Processing Subsystem) and the spacecraft telemetry system are illustrated in figure 5-1.

E. Production OST Data

The major OST contract specifications are compared to the values measured on the TWT flight unit in table 5-1. This unit is currently operational in the orbiting CTS. In the instances shown, the functional characteristics of the operational unit exceed the requirements stipulated by the specification.

5.2 ELECTRON GUN ASSEMBLY AND FOCUSING

A. Gun Design

The gun design was based on well known methods for Pierce type guns, using the Litton gun trajectory analysis computer program. Because of the low gun perveance, a high area convergence design with good beam laminarity was possible. The high area convergence allowed for relatively low cathode current density, permitting low cathode operating temperature and long life capability.

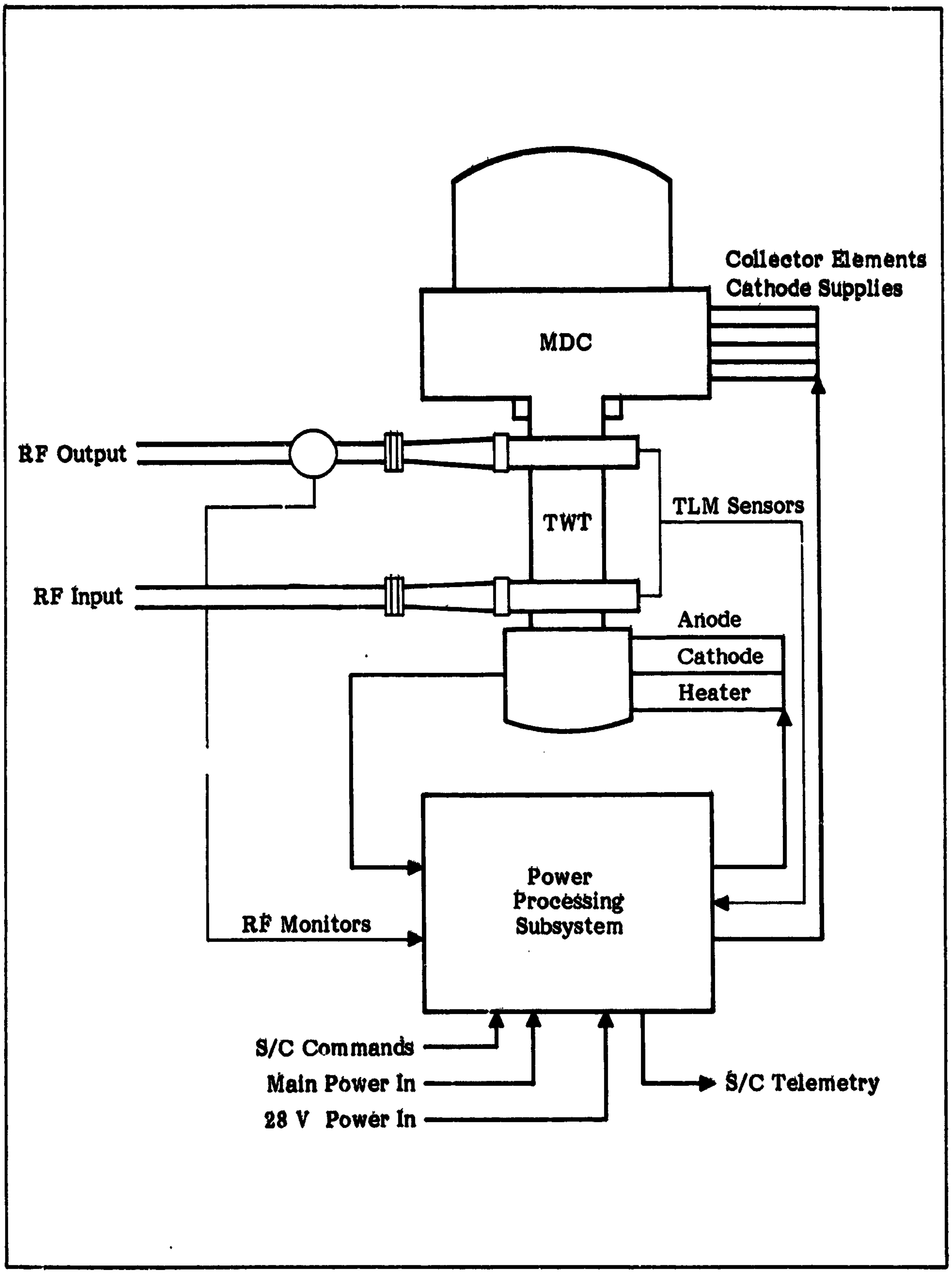

Figure 5-1. TEP/OST Interconnection

A tungsten matrix cathode was chosen because of its suitability for operation in vacuum, since it is very rugged and can be easily reactivated after exposure to air. The tungsten matrix cathode material is also known to be rugged in operation and contributes significantly to extended tube life.

The design included (1) a magnetically shielded gun, and (2) an insulated anode. These design features allowed evaluation of tube performance at various beam currents at constant circuit potential. The design provided for the anode to produce the desired perveance when operating at a slightly elevated voltage (three hundred volts with respect to circuit potential), creating an ion trap to prevent positive ion bombardment of the cathode surface.

A drawing of the gun in the assembled configuration is shown in figure 5-2. The detailed Gun Assembly reference drawing (Litton Dwg. No. 149097) is included in Appendix 1. The gun design parameters with specific values are included in table 5-2.

The initial design of the gun was directed at the 200 watt operation level with a design objective of 0.05 microperveance and an area convergence of approximately 43. The cathode diameter was .417 cm, yielding a cathode current density of 450 mA/cm^2. The trajectory analysis computer program predicted a minimum beam size of .06 cm, located appproximately 0.8 cm from the anode.

Empirical data collected during the R&D phase verifying these parameter approximations are illustrated as follows:

Figure 5-3 "Electrostatic Beam Contours" - three gun assemblies showing the axial distance from the cathode to the beam as a function of beam diameter.

Figure 5-4 "Electrostatic Beam Cross Sections" showing the beam cross section current density at six distances from the anode.

Figure 5-5 "Gun Parameters" showing heater current and cathode current as a function of cathode head temperature.

Table 5-1. Major CTS Specifications and Measured Results
(Flight Unit, S/N 2022)

PARAMETER	SPECIFIED	MEASURED
Active Frequency Band (CTS Band)	12038-12123 MHz	12038-12123 MHz
Minimum Saturated Output Power in CTS Band	180 watts	200 watts
Maximum Saturated Drive Power in CTS Band	23 dBm	22.8 dBm
Maximum Small Signal Gain Variation in CTS Band	3 dB	2.5 dB
Minimum Overall Efficiency in CTS Band	40%	44.1%

Table 5-2. Gun Design Parameters

PARAMETER	VALUE
Aperture Angle	8°
Cathode Diameter	.4166 cm. (0.163")
Perveance	0.052 μP
Cathode Current (V_o = 11 kV, V_a = O)	60 mA
Cathode Emission	450 mA/cm^2
Beam Diameter	.0[illegible] cm. (.025")
Anode to Beam, Minimum	0.76 cm. (0.3")
Area Convergence	43
Cathode Material	Tungsten Matrix (5:3:2 Mole Ratio)
Cathode Temperature (T_c)	<1100°CB
Heater (Potted)	
Voltage	3.5 Volts
Current	1.35 amps
Power	4.7 watts

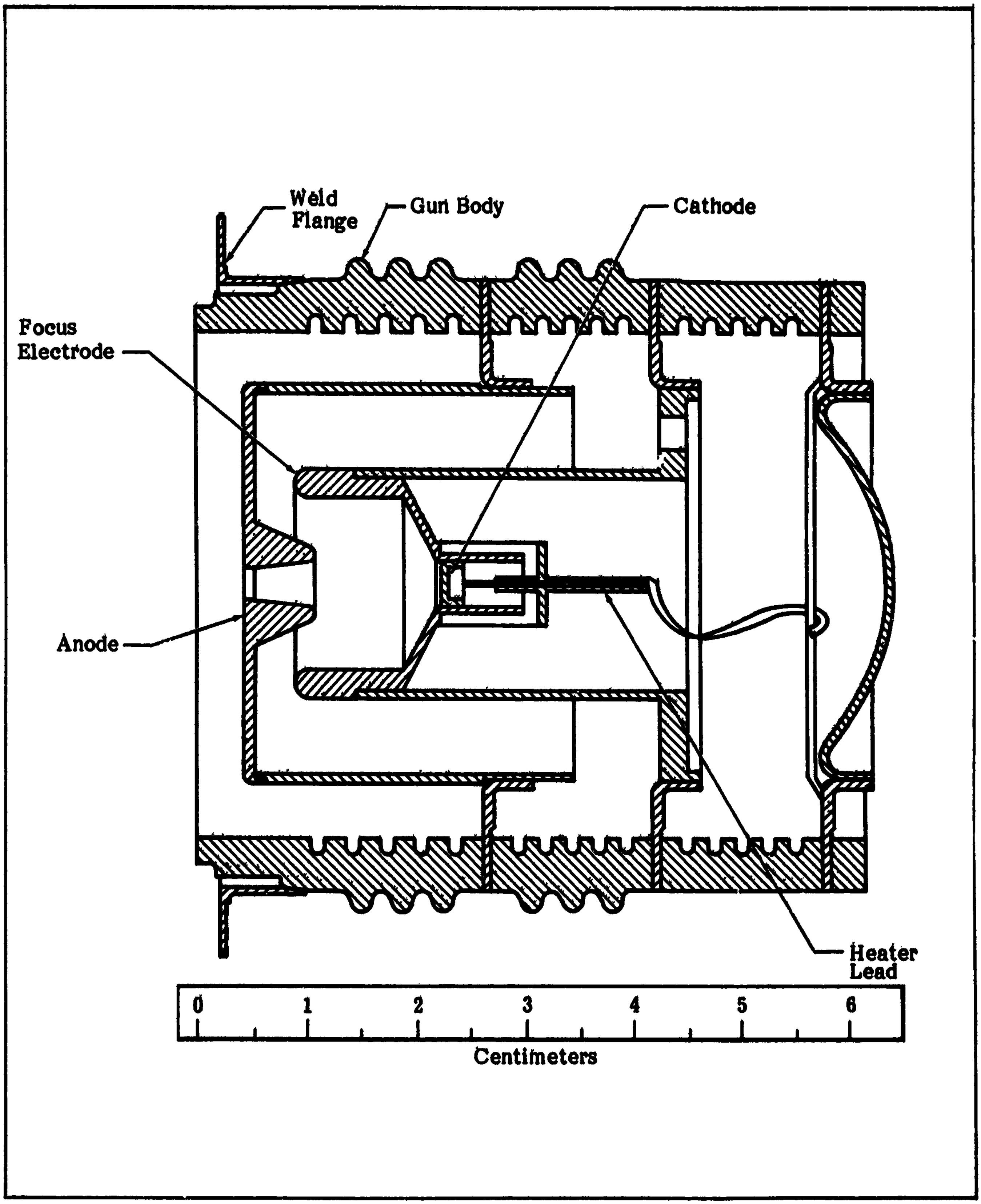

Figure 5-2. Gun Assembly Cross Section

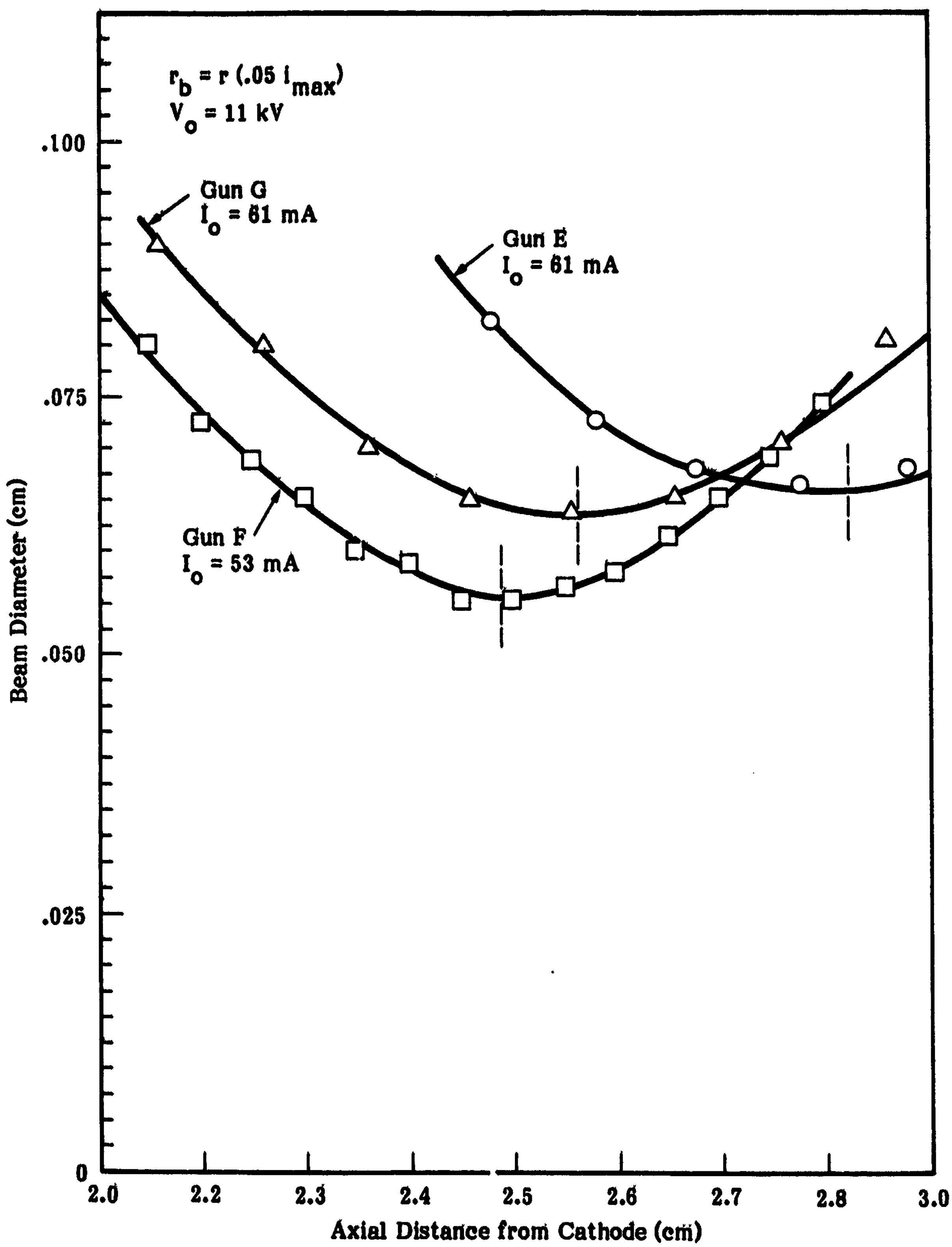

Figure 5-3. Electrostatic Beam Contours

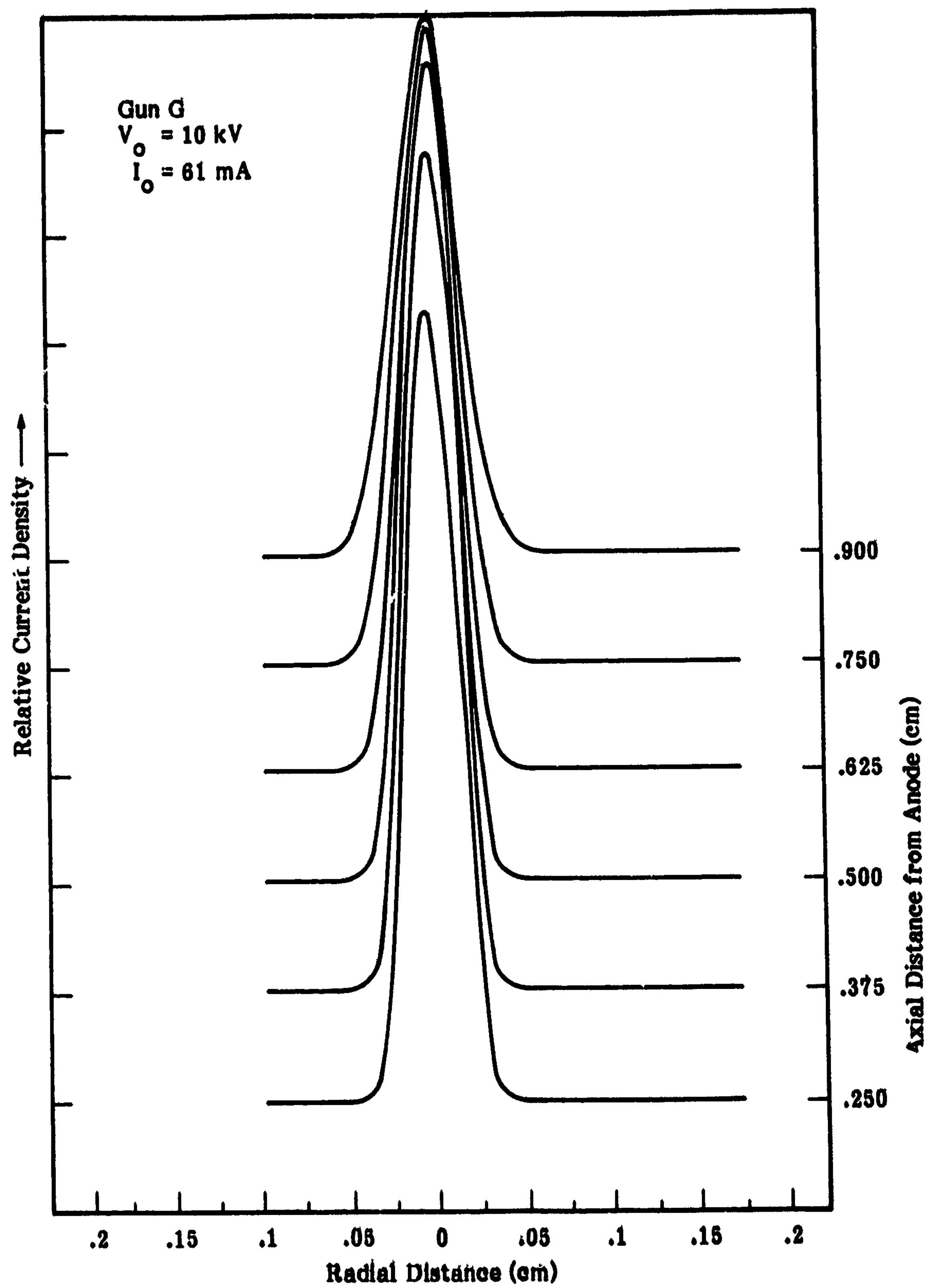

Figure 5-4. Electrostatic Beam Cross Sections

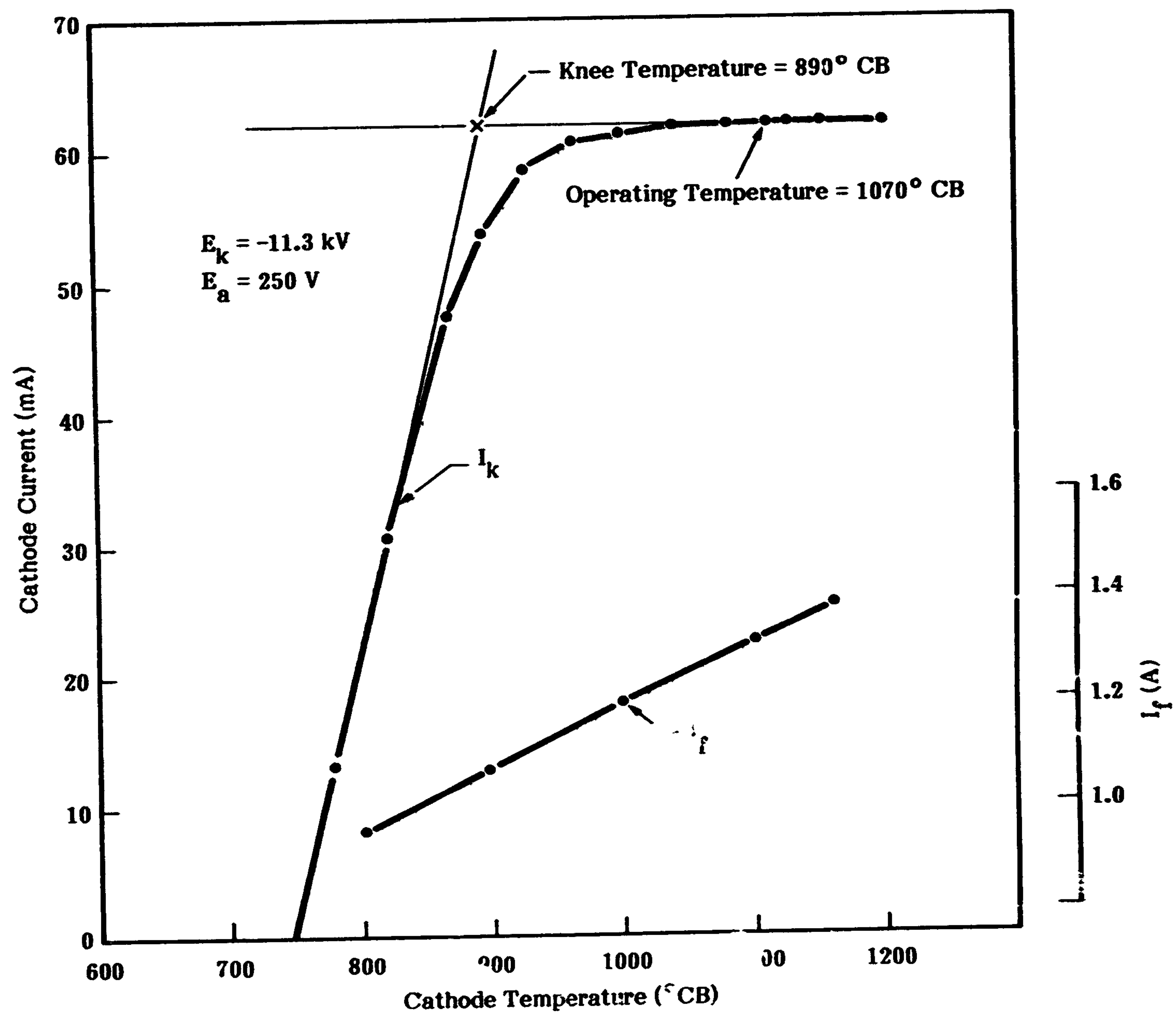

Figure 5-5. Heater Parameters, Flight Unit

B. Focusing Design

The magnetic focusing was designed with half ring magnets which extend over two cavity periods. This double period configuration is commonly used in PPM focused coupled cavity tubes and achieves higher peak fields with smaller transverse perturbation fields due to the coupling slots than single period focusing. The focusing stability is generally assumed to be equal to that of single period focusing. For this design, the focusing stability goal of six was high. The magnet material is samarium cobalt, and the required peak field is in the order of 1500 gauss in the input and center sections, and 2200 gauss in the output section. The design proved to be sensitive in the area of beam alignment; however, when proper alignment and focus was accomplished, beam transmission into the collector was typically 98 percent without rf, and 94 percent at saturation.

C. Gun Assembly Problems/Solutions

During the development of the flight version OST from the R&D phase tubes, a series of gun and cathode problems became apparent. These problems and their effected solutions are summarized below.

1. Redesign of the cathode structure

The original cathode structure in the R&D phase tubes employed a Spectramat type "B" impregnated tungsten cathode pellet contained in a molybdenum sleeve which was 0.0025 cm thick, 0.419 cm in diameter and about 0.766 cm high. This type cathode was used in all the initial tubes fabricated. During that initial period, one tube developed unstable electron emission problems during testing. When it was dismantled for examination, the molybdenum sleeve, which is very brittle, revealed several fractures. This result, plus the possibility that the brittle cathode sleeve might not withstand vibration testing, led to a redesign. The revised design substituted a molybdenum (50%) - rhenium (50%) sleeve .0025 cm thick for the molybdenum. This alloy, which is ductile, offered a satisfactory solution to the problem. When this change was initiated, an in-house capability of making impregnated cathodes was utilized so that the complete cathode structure was fabricated within Litton. All the cathodes that went into the OST's after that change had an impregnated cathode inserted into a molybdenum-rhenium sleeve.

2. Preparation and processing of guns and cathodes

Because of the stringent life requirements of the space OST in the CTS program, it was obvious early in the program that the processing of the cathodes should be carefully controlled to give maximum life. An examination of the processing schedule for electron guns, instituted early in the production program, showed that the cathodes were subjected to a number of rigorous processing procedures which could adversely affect life. The two most important procedures were:

- After assembly, the cathodes in the gun were subjected to three heating cycles, (cathode preglow, gun assembly preglow and beam analyzer activation) each of which was followed by exposure to air before storage.

- Stringent activation schedules which subjected the cathodes to very high temperatures of 1200°C for three hours or more. These were reviewed and revised so that essential needs were met and the adverse effects were minimized. The changes adopted were:

  - After assembly, the cathodes in the gun were subjected to only two heating cycles by eliminating the cathode assembly preglow. This step was further revised, later in the program by eliminating beam analyzer tests so that only one heating cycle was employed before exhaust.

  - The activation schedule was changed so that the activation procedure consisted of heating the cathode to 1200°C for only five or ten minutes at a time (hot shotting) for a maximum of one hour.

3. Operating cathode temperature during life

The R&D phase tubes were operating with cathode temperatures near 1200°CB to maintain emission of 0.5A/cm^2. This is not an unusual occurrence in commercial terrestial tubes but was considered a real problem for the OST because output could be adversely affected over the two year life period. Decisions were made to improve processing so that high temperature and gas effects could be minimized. As a result, a basic requirement for the OST was established which stated that the cathode has to operate below 1100°C in order that the minimum of two years operational life could be expected.

D. Production Gun Data

During the production phase, gun assemblies for the twenty-seven (27) production OST units plus additional gun assemblies for test and spares were fabricated by Litton. To illustrate the performance that was experienced from these units, the operating characteristics of three representative gun assemblies are presented in table 5-3. These gun assemblies are in the OST units designated for: life test, (S/N 2020); flight (S/N 2022); and prime flight back up (S/N 2025).

Table 5-3. Gun Assembly Operating Characteristics (Installed in OST Designated)

CHARACTERISTIC OR PARAMETER	LIFE TEST OST	OST FLIGHT UNIT	FLIGHT BACK-UP
Analyzer Data			
Perveance (nP)	56.0	61.5	60.0
T_{knee} (°CB)	868	890	965
Anode to Beam Min. (cm)	.78 (.312")	.93 (.37")	.88 (.353")
Hot Test-CW Mode			
Perveance (nP)	57.4	62.6	59.5
E_k (kV)	11.4	11.3	11.5
E_a (V)	450	450	250
T_k (°CB)	1090	1050	1050
T_{knee} (°CB)	945	990	983

5.3 RF CIRCUIT/BODY

A. General

The design of the rf circuit/body is described in NASA TN D-7709 (Reference 9), with minor changes as discussed in the following paragraphs. A drawing of the RF Circuit/Body is shown in figure 5-6 and the breakdown reference drawing (Litton Dwg. No. 147935) is included in Appendix 1.

B. Cavity Design

In the cavity design lower cutoff frequencies were aligned to provide the 85 MHz wide CTS band in all sections of the tube. The number of active cavities in each section is shown in figure 5-7. The three gain sections are separated by severs. The velocity taper sections are separated by transition regions in which the phase velocity (periodic length) changes gradually from one cavity to the next. Each sever consists of two modified cavities each containing tuning stubs and silicon carbide-beryllium oxide loads. Forward and backward circuit waves are completely terminated at a sever since there is no coupling slot in the wall between the two sever cavities. Two additional cavities adjacent to the input and output couplers and on each side of the two severs are modified for impedance matching purposes. These cavities have extra long coupling slots and thus extra wide cold bandwidth, and provide a reduced contribution to the gain of the tube.

C. Waveguide Window

A poker chip type waveguide window (WR-75) was scaled from similar existing X-Band window designs. High purity alumina was chosen because of its very low rf loss and superior brazing strength. A schematic of the window design and its performance characteristics are shown in figure 5-8. The voltage reflection coefficient is found to be 2% or less throughout the 10 GHz to 14 GHz range. A ghost mode was identified at 16.3 GHz but it was of little concern since the circuit is not capable of propagation at that frequency.

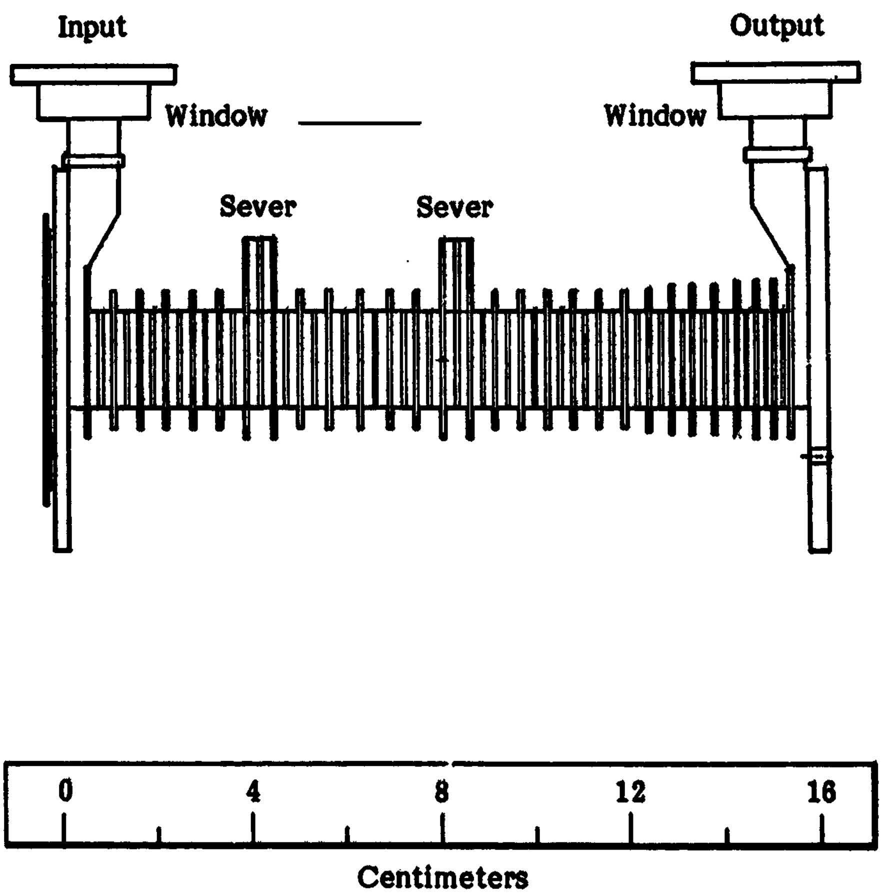

Figure 5-6. RF Circuit/Body Assembly

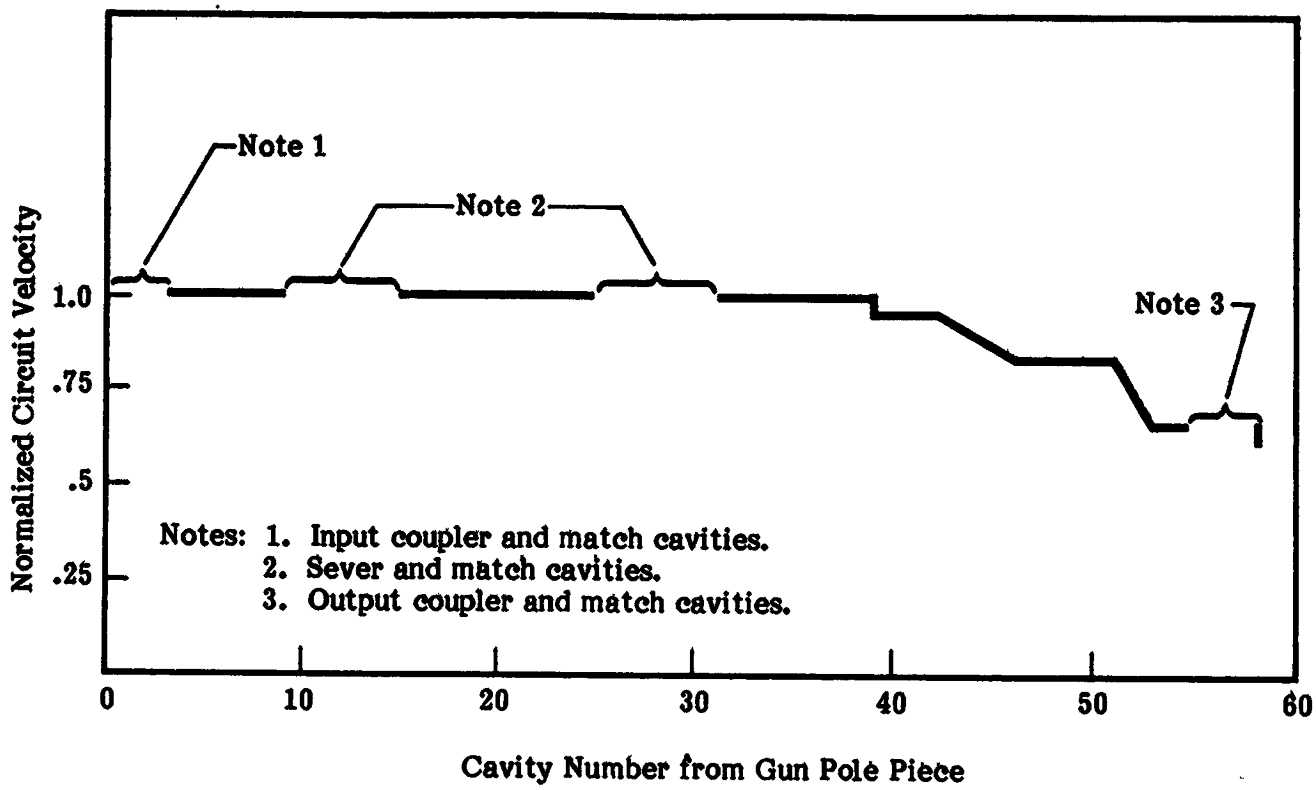

Circuit Periods and Cavity Count

SECTION	PERIOD (cm)	No. of Cavities
Input	0.318	10
Input Sever	0.368	2
Center	0.318	14
Output Sever	0.368	2
Output Driver #1	0.318	10
Output Driver #2	0.304	3
T1	0.298	1
T2	0.292	1
T3	0.280	1
T4	0.267	1*
T5	0.254	5*
T6	0.241	1
T7	0.228	1
T8	0.216	4

* Number of cavities reversed in tubes fabricated after flight units for stability improvement.

Figure 5-7. Normalized Circuit Velocity vs. Cavity Number

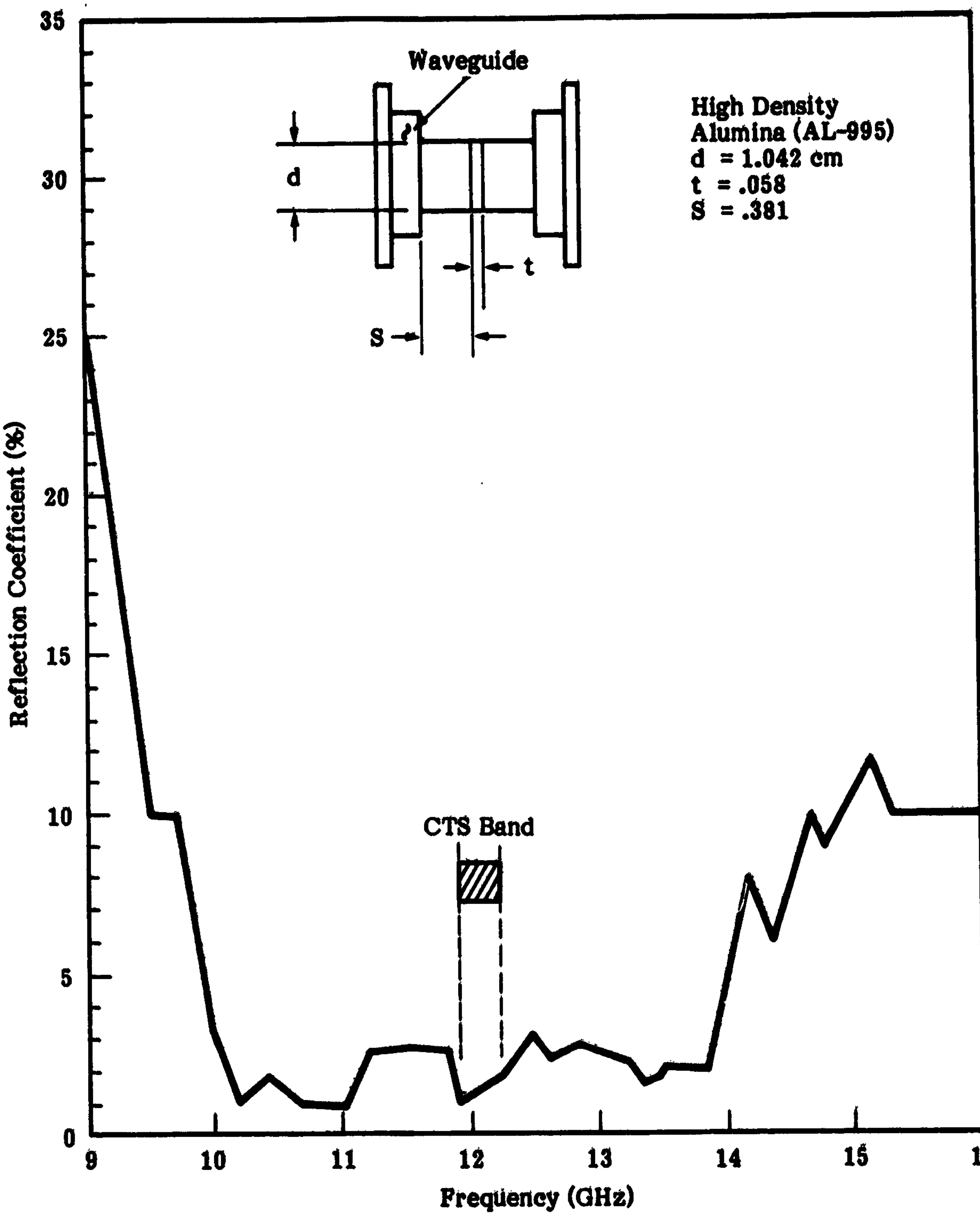

Figure 5-8. Waveguide Window Characteristics

D. Waveguide Step Transformer

A four step waveguide transformer was designed to provide an impedance match between the standard input and output waveguide heights and the reduced height waveguides of the couplers. The design was based on quarter wavelength transformer theory and included step susceptance corrections. A Litton computer program was used which allows specification of bandwidth and number of steps. Step dimensions and resultant VSWR are then given. The final design configuration and the performance curve of the transformer are shown in figure 5-9.

E. RF Circuit Assembly Problems/Solutions

As compared to the design defined in NASA TN D-7709 (Reference 9), some minor changes in parts, dimensions, and fabrication procedures were required to achieve the desired placement of the CTS hot band within the circuit cold pass band. Tubes produced early in the program had a tendency to have maximum gain and efficiency below the CTS band and small signal gain varying rapidly with frequency across the CTS band. Furthermore, the frequency response characteristics were rather unrepeatable from tube to tube. Cold test measurements indicated that the circuit passband shifted downward, by a nonrepeatable amount, during each braze operation. Because additional braze operations were used to repair leaks and other defects, the number of times a particular circuit section was brazed varied from three to as many as five. Even prior to the first braze cold test measurements showed a misalignment of up to 150 MHz between the circuit passbands in different sections of the tube.

The nonrepeatability was reduced by improved parts quality control and standardization of the braze operation. Repair brazes were no longer allowed. Thereafter, the downward shift of the circuit passband due to the two allowed braze operations was a fairly consistent 50 ±10 MHz. The circuit passband in various tube sections was raised or lowered as required by altering cavity diameter by amounts up to 0.25 mm. Output circuits were designed for lower cutoff frequencies of about 50 MHz higher than the input or center sections in

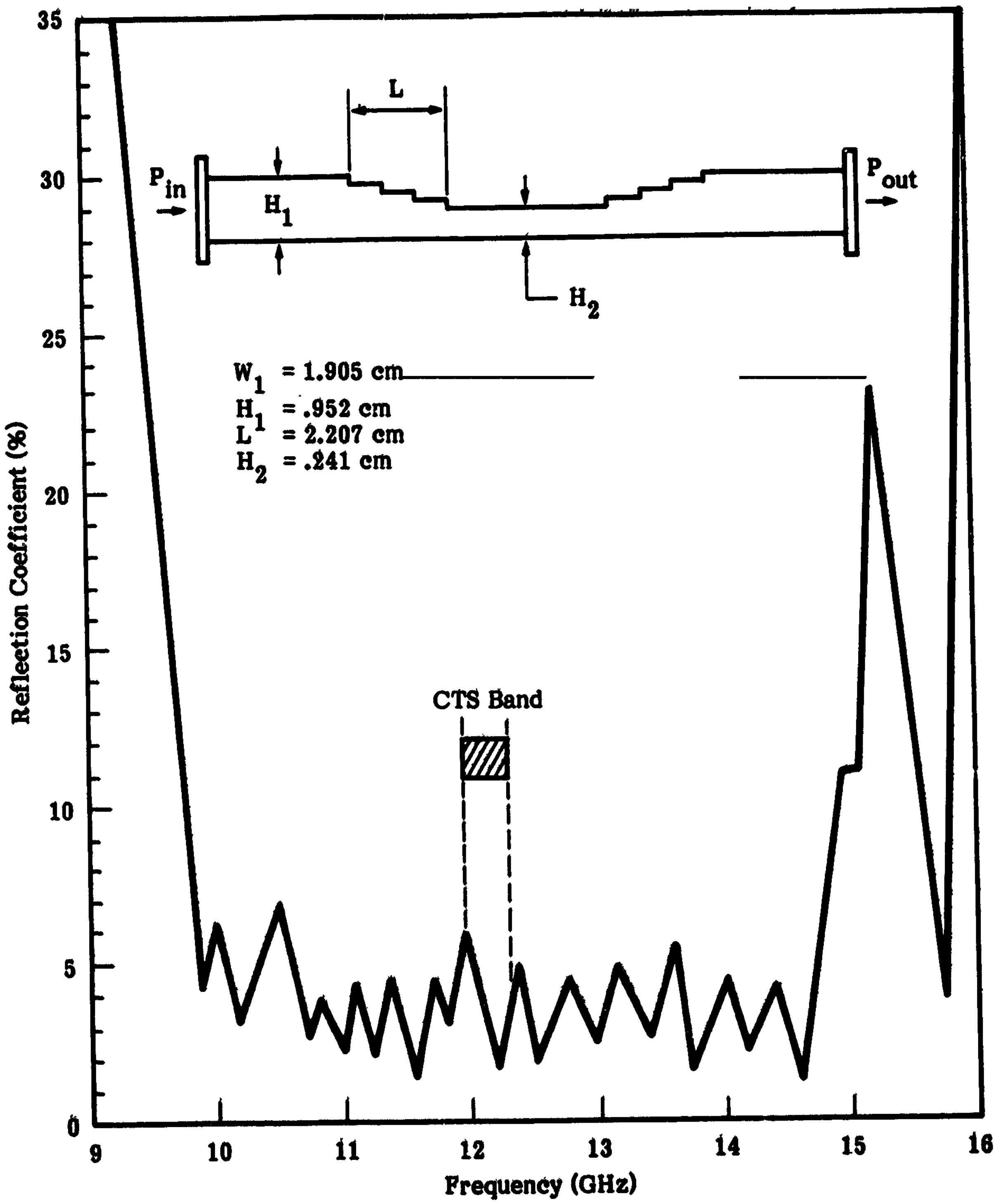

Figure 5-9. Waveguide Transformer Characteristics

the first half of production tubes. For units thereafter, the circuit passband, before braze, was aligned throughout the tube about 50 MHz higher than the desired final frequency range. This resulted in a flat gain over the passband.

F. Production RF Circuit Body Data

As a result of the corrective actions implemented as indicated in the preceding paragraph, the following performance improvements were achieved:

- Improved small signal gain flatness as shown in figure 5-10.
- Improved saturation output power in the CTS operating band as shown in figure 5-11.
- Improved alignment of lower cutoff frequencies as shown in figure 5-12 for flight model OST's.

5.4 REFOCUSING

A. General

In order for the multistage collector (discussed in paragraph 5-5) to yield maximum energy recovery, the spent beam must be reconditioned before entrance into the collector. This is accomplished in the refocusing section by means of a specified magnetic field distribution. This distribution allows the spent beam to first expand and thereby reduce its space charge forces, after which it is refocused to cause the electron trajectories to become more parallel for more effective velocity sorting in the collector.

The refocusing section that was utilized was originated and designed at NASA Lewis Research Center and is essential for the highly efficient operation of multistage collectors. Its operation is described in NASA TN D-7660 (Reference 15).

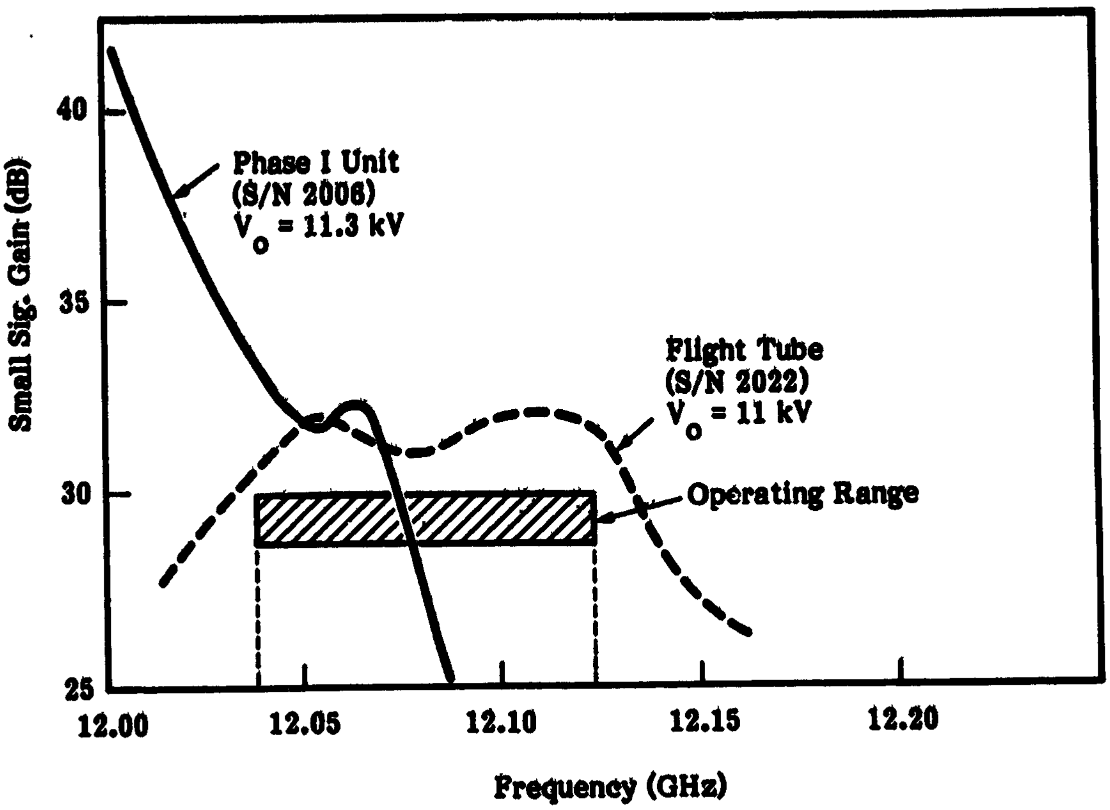

Figure 5-10. Small Signal Gain vs. Frequency

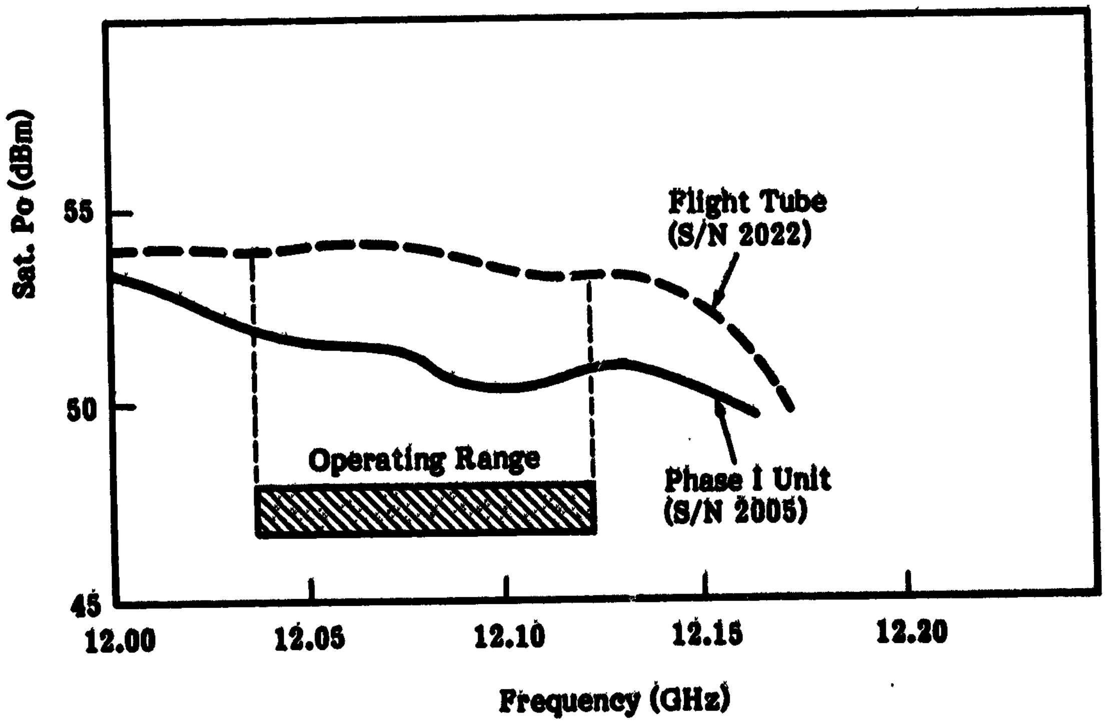

Figure 5-11. Saturated Output Power vs. Frequency

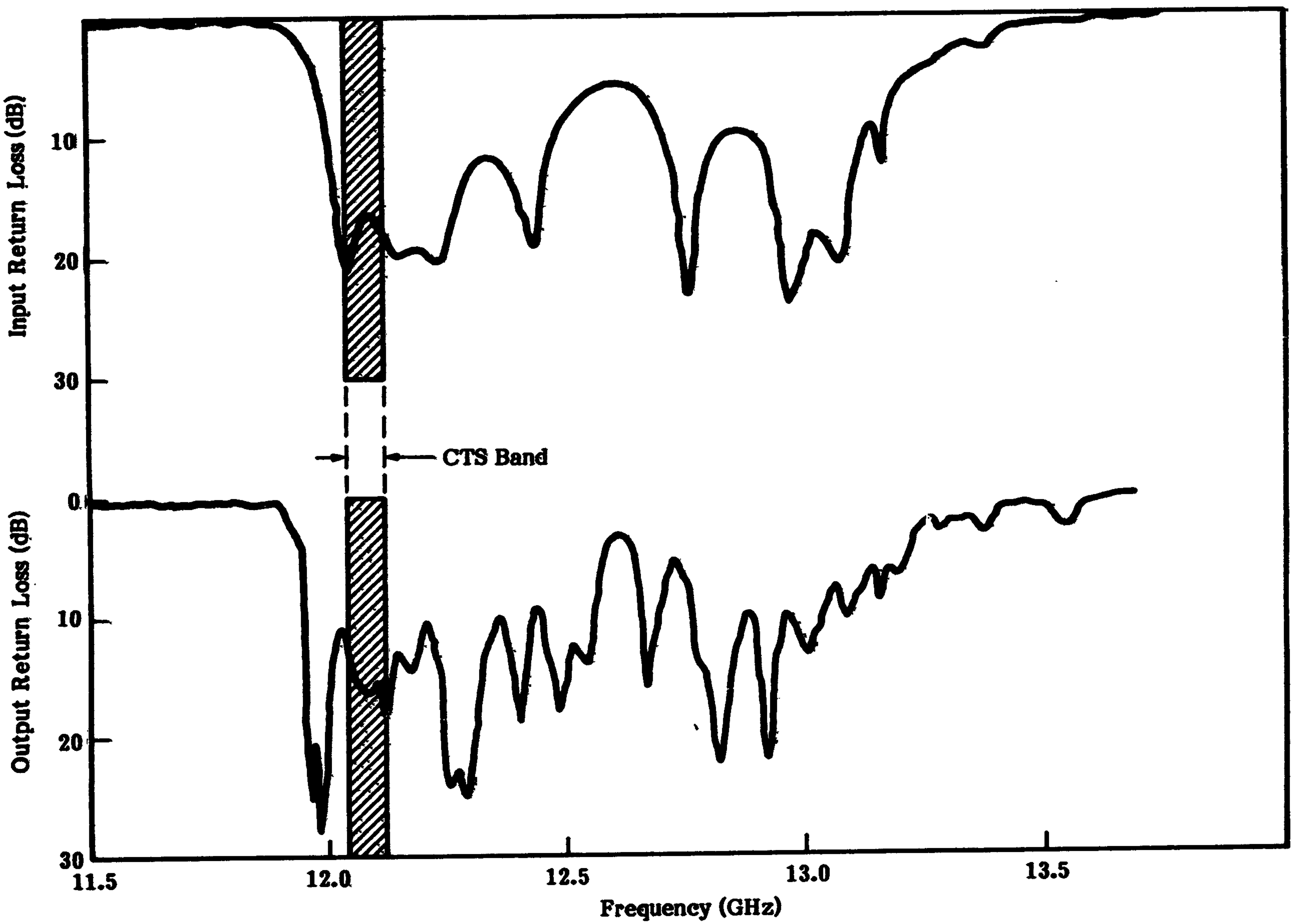

Figure 5-12. VSWR, Match After Final Braze (S/N 2022 Cold Test Data)

B. Theoretical Design

In the refocusing section, the magnetic focusing field is gradually reduced over a significant length, such that the corresponding beam expansion can be considered adiabatic. The field decay is followed by a short plateau field which is terminated at the entrance plane of the collector. The refocusing section has two important functions:

1. Beam expansion - The spent beam is allowed to expand so that its space charge forces become small. This will improve velocity sorting in the multistage collector due to space charge effects.

2. Refocusing - The expanded spent beam is refocused such that it enters the collector essentially with parallel trajectories. Properly arranged adiabatic expansion of the beam reduces radial velocity components of the spent beam and thus makes the velocity sorting of the collector more effective. The configuration of the refocusing magnet and of a typical refocused field plot are shown in figure 5-13.

C. Mechanical Design

The refocusing field was implemented in the flight tubes exclusively with permanent magnets, and without the use of solenoids. A field reversal between decay field and plateau field was incorporated in order to minimize magnetic leakage fields into the collector. Empirical data collected was substantial, and verified the analytical design configuration. It was demonstrated that reversed plateau and decaying fields as realized from permanent magnets are as effective in refocusing the beams as are unreversed fields established with solenoids.

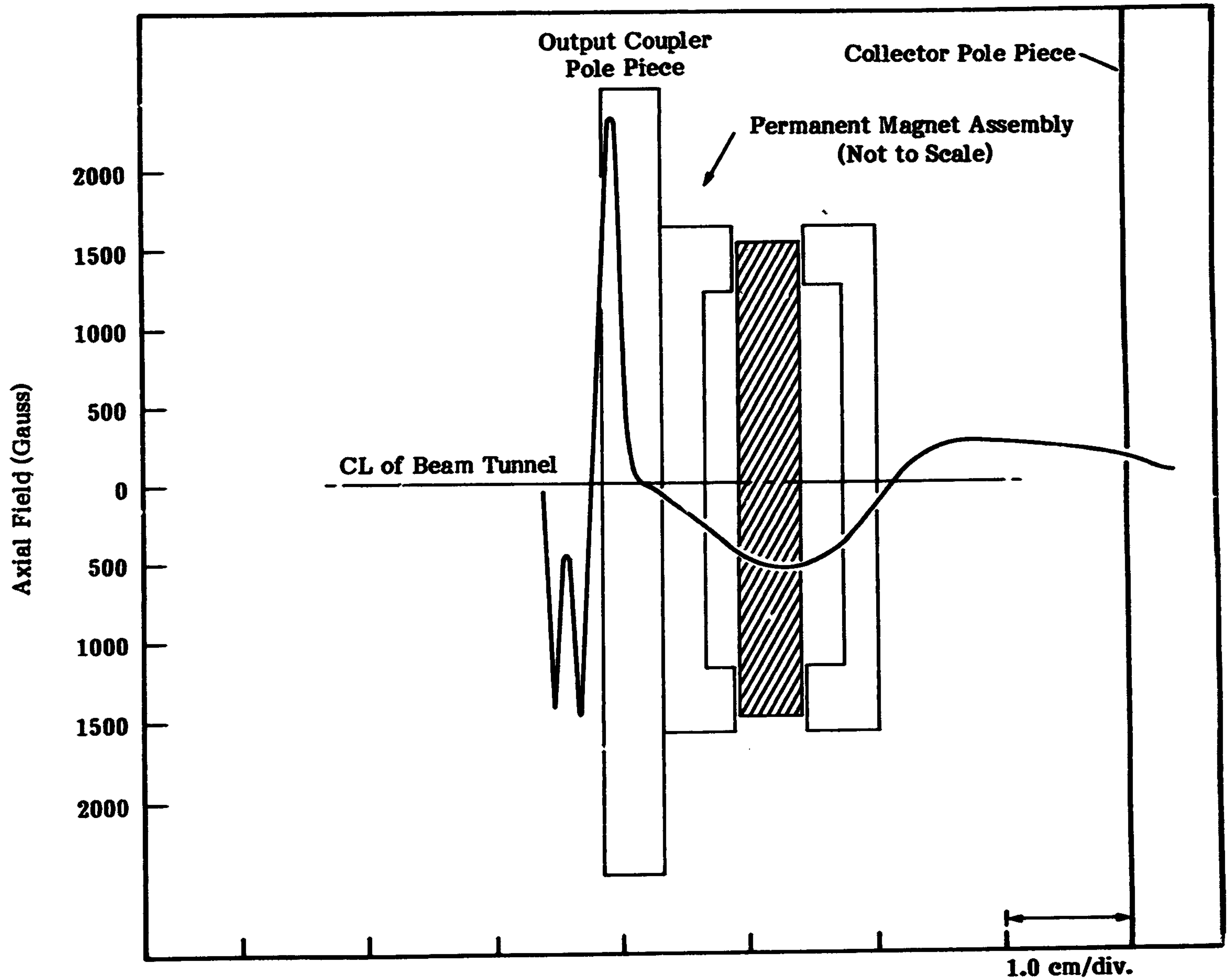

Figure 5-13. Refocusing Magnet Schematic with Field Plot

5.5 MULTISTAGE DEPRESSED COLLECTOR

A. General

The multistage depressed collector (MDC) is a key component in achieving high efficiency. Its basic concepts and functioning are described in NASA TN D-7709 (Reference 9). It consists of nine depressible collector electrodes as shown in figure 5-14. The MDC is designed to operate at optimum efficiency under saturated conditions with minimum lens effects developed by the electrodes. The Collector Assembly reference drawing (Litton Dwg. No. 148739) is included in Appendix 1.

B. Initial Electrical Design

For the initial electrical design of the collector, the voltages and positions of the electrodes were selected to achieve the following:

1. Optimum efficiency enhancement at saturation - The voltages of the available number of collector electrodes were selected to achieve maximum efficiency enhancement at saturation. This was determined by the kinetic energy distribution of the spent beam.

2. Minimize lens effects of the electrodes - The position of the collector electrodes was selected to achieve essentially a uniform electrostatic deceleration field in the most negative collector region and a very weak decelerating field in the vicinity of the injection hole at the collector pole piece. The length of the trajectories is much larger than the radius of the beam at injection which makes the beam appear as a point source. The number of collector elements was chosen as ten in order to compensate for uncertainties in predicting the spent beam distribution at the time of conceptual design. After experimental evaluation, it was determined probable that elimination of four electrodes (with the lowest current levels) would reduce the collector efficiency by only a few percentage points.

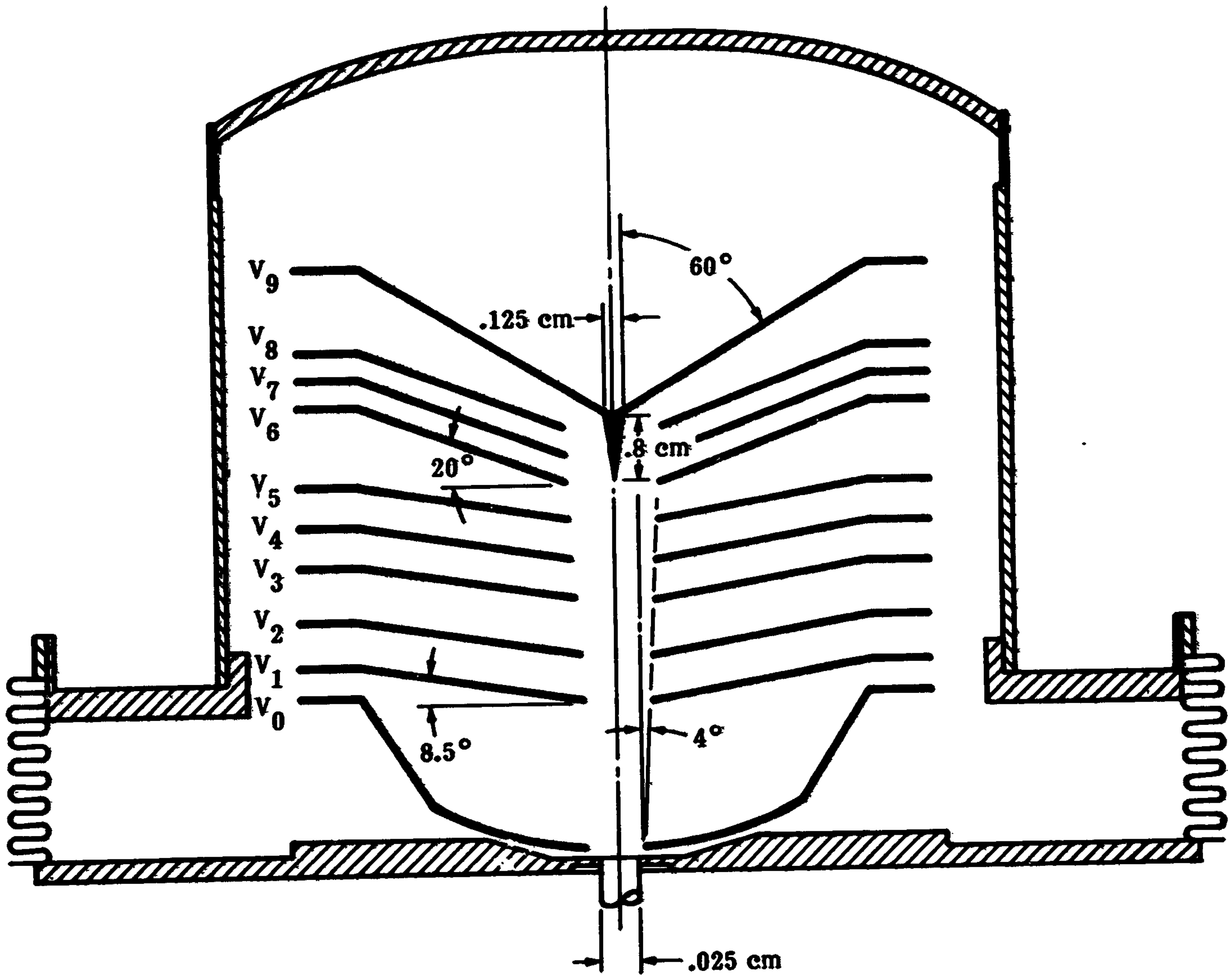

Figure 5-14. MDC Schematic (Cross Section)

This loss could, in turn, be partially recovered by an improved collector design. This design alternative was not tested nor implemented in the design.

A computer analysis was used to determine the spent beam characteristics as a function of normalized current and voltage for the collector electrodes. These summary results of this analysis are displayed in the curve shown in figure 5-15.

C. Design for Efficiency

The collector was designed with the goal of producing the maximum efficiency possible. The design was accomplished considering several factors. The radial deflection forces induced by the electric fields of the collector provide the necessary velocity sorting of the electron beam. The spike at cathode potential provides additional radial deflection which acts mainly on the high energy electrons. Secondary electrons back streaming is almost absent because of automatic suppression in negative fields, as defined in NASA TN D-6093 (Reference 7). At saturation, the highest collector efficiency was 84 percent, which was achieved in an initial tube (S/N 2006). Nominal overall efficiency was slightly over 50 percent. The aperture cone, that is the conical surface on which the openings in the electrodes terminate, was assigned two experimental values: 6° and 4°. From these two values, a single one which produced the best efficiency was to be selected for the flight design. The value of 6° produced the best efficiency for the initial design, and was selected from the single cavity calculation of electron trajectories for the tube. When computing trajectories, a reduction of radial velocities due to the action of the refocusing section was taken into account. At the time of the conceptual design of the tube, it was estimated that the circuit losses would amount to approximately 10 to 20 percent of the internally generated rf power. In reality, this number was as high as 30 to 40 percent. This appreciable amount of loss had several adverse effects. First, the electronic

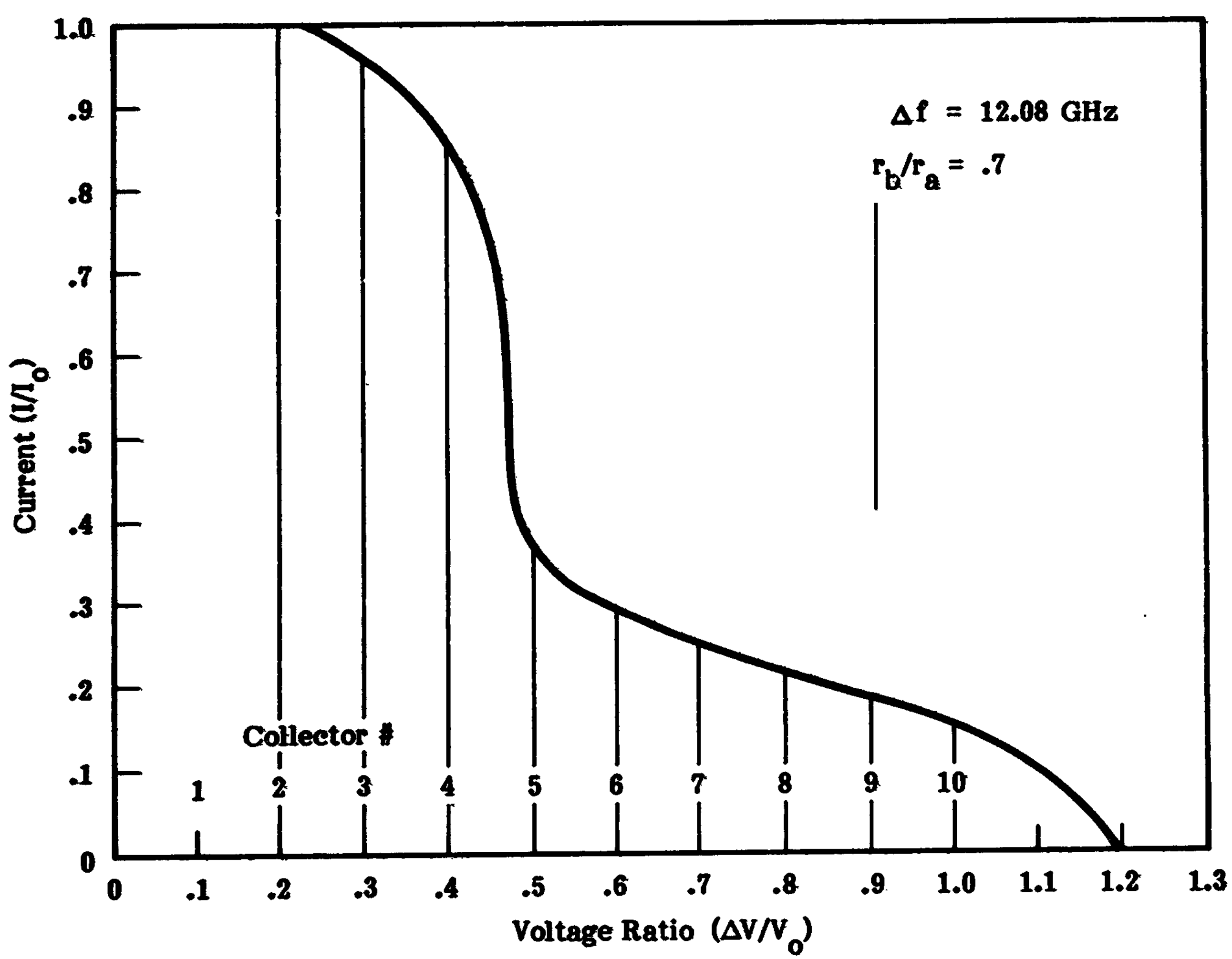

Figure 5-15. Spent Beam Characteristics (Computed)

efficiency (total conversion of dc into rf power) was approximately 45 percent while the useful rf efficiency decreased to 20 to 30 percent over a portion of the band (this latter number was achieved in S/N 2006). This increase in the internal power conversion efficiency resulted in more axial and radial velocity dispersion than originally estimated. After the completion of the R&D phase, it became evident that aperture angles of approximately 7°, even more than the 6° originally estimated, might be required for optimum performance.

During the R&D phase, four (4) tubes were fabricated, two with 4° and two with 6° apertures by each of the two R&D contractors, Litton and Hughes. Of the four tubes delivered by Litton, two were fully operable and both had 6° apertures. The Hughes operational tube had a 4° aperture. Because of significant differences in perveance and basic tube design, a proper interpretation of performance results was only partially possible. The MDC on the Litton tubes had slightly higher efficiency than the collector on the Hughes tube. Also, the Hughes tube had a perveance of 0.12×10^{-6}, (twice that of Litton's design), thus having larger space charge spreading which seemed to indicate the need for apertures larger than Litton's design.

Typical MDC electrode currents, input powers, and dissipation under saturated conditions and without rf drive power are illustrated in figures 5-16 and 5-17, respectively. Negative current reading for electrode No. 10 indicates secondary emissions to electrode No. 9. When the tube is operated with the PPS, this current subtracts from the cathode current, and reduces the apparent cathode supply current. In the laboratory tests, these currents were considered and measured separately. Power recovered by electrode No. 10 was set to zero whenever a negative current value was observed.

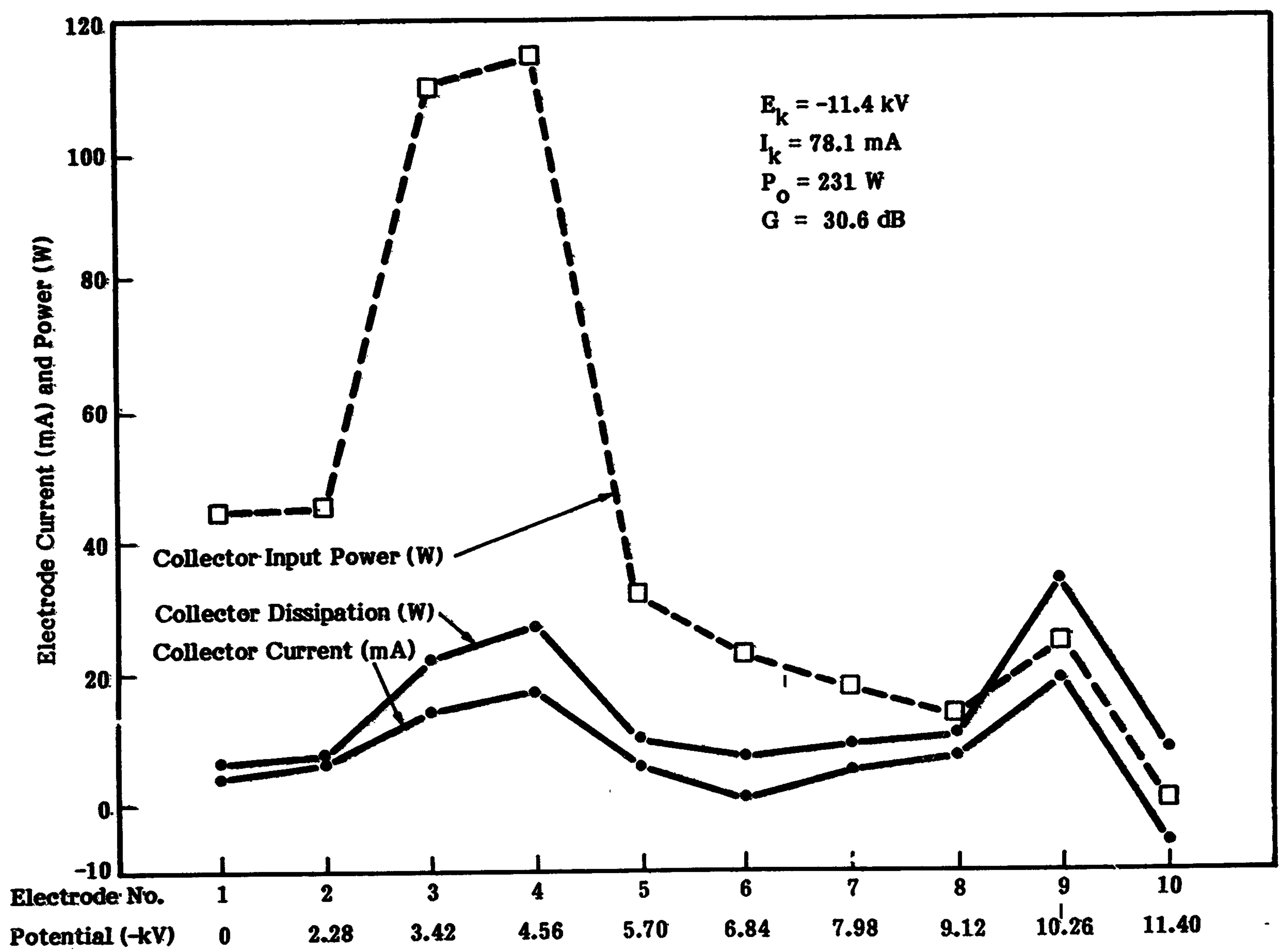

Figure 5-16. Collector Current and Power Distribution (Typical, Midband Saturation)

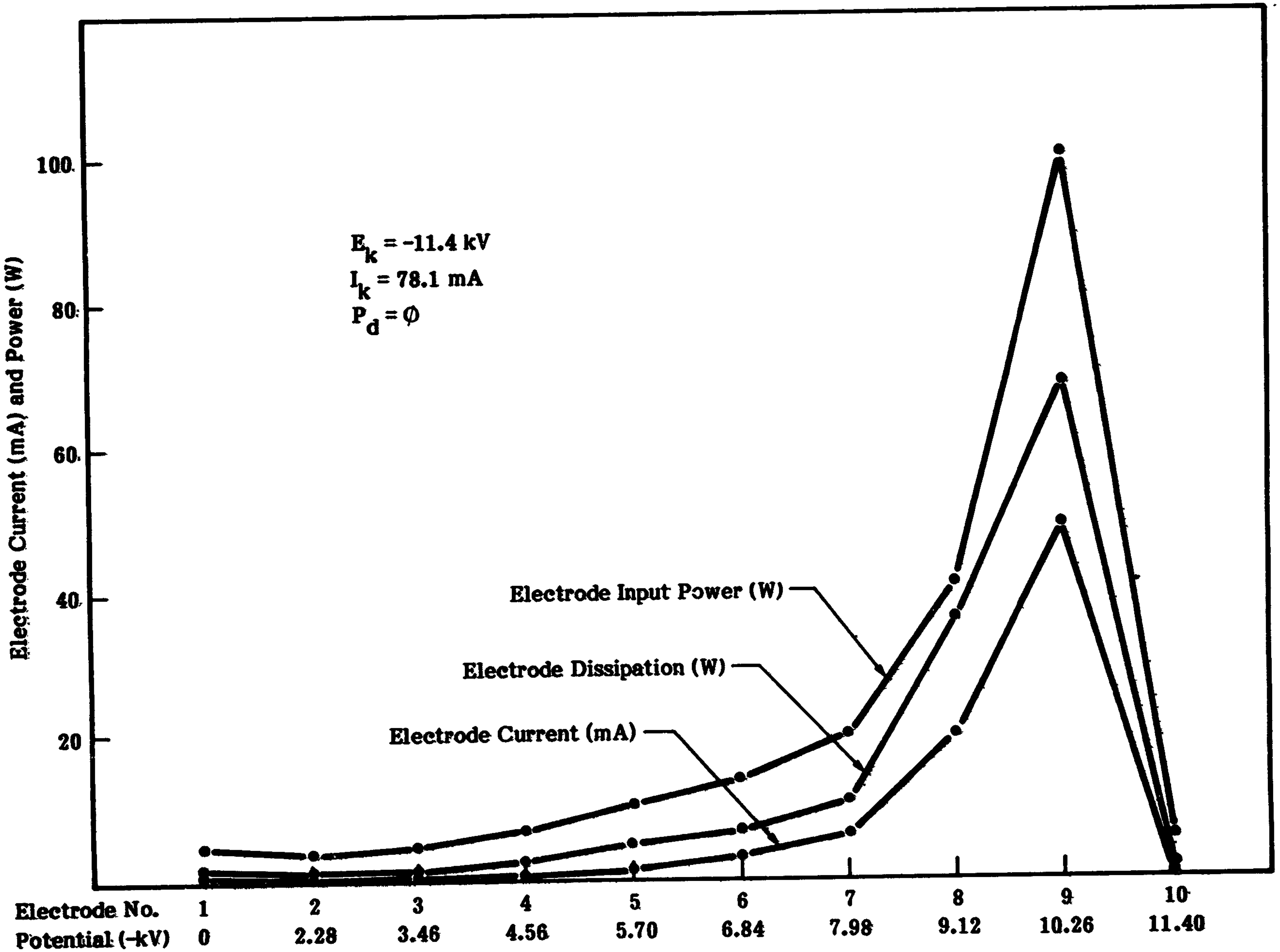

Figure 5-17. Current and Power Distribution (Typical, Zero Drive)

D. Design Freeze

Due to schedule constraints, a design freeze was initiated without an additional evaluation of the 4° apertures. A decision was made to incorporate the unproven 4° aperture size as the final design based on considerations from the available data on tube S/N 2007. After more test results became available, it was decided that the 6° design would probably have been a better choice than the 4° design. Subsequently, measured collector efficiencies never quite attained the values established with the collector having the larger cone angle of 6°, but were as high as 82 percent.

Except for the aforementioned change in the aperture angle to 4°, and freezing the length of the spike to 0.8 cm, the collector electrical design is identical to that initially defined by the program. Some additional performance details for the selected design are included in NASA TN D-7709.

E. Potential Improvements

The evaluation of collector performance and newer analytical results indicate that the design and, very likely, the performance of the collector could be improved by incorporating the implementation of the following three simple changes:

1. Increase the aperture angle from 4° to 7°.

2. Increase the angle of the conical electrode at cathode potential from 60° to 70°, thus making the design less dispersive for the high energy classes and, consequently, more efficient in the rf as well as the dc mode.

3. Optimize efficiency by adjusting collector potentials. (Early in the program it was determined that voltages would be set in the PPS as fixed percentages of total cathode voltage.)

F. Mechanical Design

The nine (9) depressible collector electrodes are circular plates spaced about 1 cm apart (see figure 5-14) and held in position by six equally spaced alumina ceramic insulation posts. This collector plate assembly is attached to a cyclindrical vacuum enclosure by supports at each end of each of the six ceramic rods.

The mechanical design requirements for the collector support system are that it transfers a steady state peak acceleration load of 16 g's along the collector axis and 3.5 g's laterally. The collector support system is also required to withstand vibration environments in which the peak lateral acceleration force at the collector is 35 g's between 110 and 120 Hz. The collector support system also should not have resonant frequencies which would couple with the satellite vibration input frequencies. In addition, the collector support system needs to withstand the operational and vacuum bakeout temperature excursions and their accompanying thermal distortions of up to 0.13 cm (52 mils) differential diametral expansion and up to 0.065 cm (26 mils) differential longitudinal expansion between the collector and its supporting vacuum enclosure.

The original collector support design consisted of stainless steel U-tabs welded between cyclinders brazed to the ceramic rods of the collector and the vacuum enclosure at each end of the collector as shown in figure 5-18. These collector supports allowed the collector to expand freely both diametrically and longitudinally with respect to the enclosure. However, the collector system vibration natural frequency was too low with respect to that of the entire tube assembly and high amplification factors were recorded on the collector during vibration. During vibration qualification, the U-tab supports cracked. A design modification was incorporated to overcome this problem.

The collector support system was redesigned and successfully met the requirements of high natural frequency coupled with free radial and logitudinal expansion. The redesign consisted of fixing the base of the collector (plates #1 and #2) in longitudinal position by means of six radially pointing pins at each of

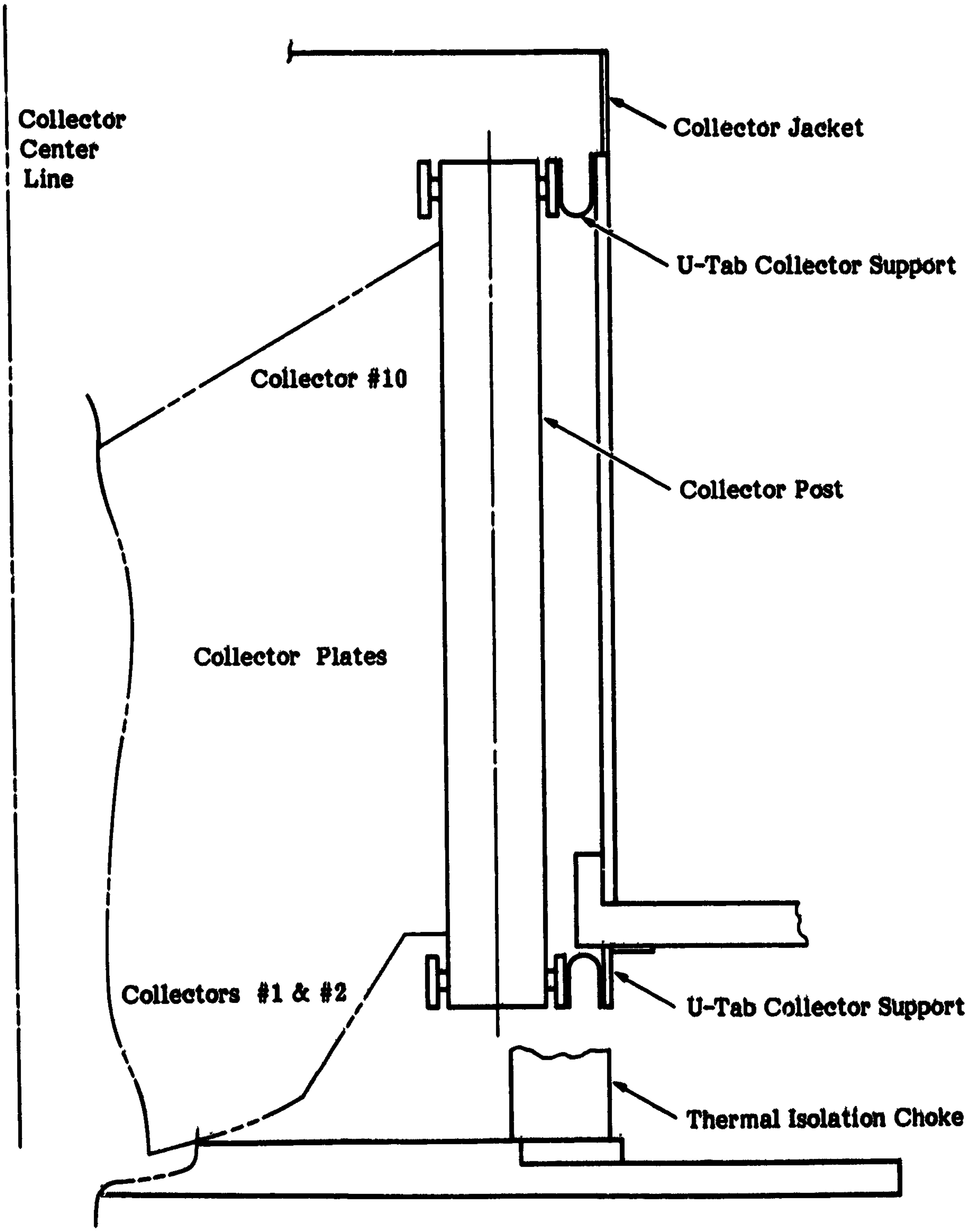

Figure 5-18. Collector Support Design

the six collector ceramic rods as detailed in figure 5-19. This allows free radial expansion but no longitudinal or rocking motion of the collector. Radial pointing forks, as shown in figure 5-20, are used in contact with the ceramic rods at the opposite end of the collector, plate number 10. These forks restrain the collector laterally but not radially or longitudinally. Thus the collector can freely expand and contract both radially and longitudinally with respect to the collector support enclosure, but has high resonant natural frequencies (greater than 800 Hz) in both directions.

Since the pins and the forks of the support system act as bearings during thermal cycling, good vacuum bearing materials had to be used. Tungsten pins in Zirconium-copper bushings were used at the pinned collector and precision stainless steel forks riding directly on the centerless ground alumina ceramic rod were used at the opposite collector end.

G. Thermal Design

The primary thermal design requirement for the collector is that it radiates up to 170 watts of heat dissipated by the spent electron beam. This thermal energy is radiated from the collector plates to the collector vacuum enclosure and then reradiated to space. Since the spent electron beam velocity distribution varies for a saturated electron beam as opposed to a beam without rf drive, the collector plates are required to radiate the nonuniform heat loads and the collector structure must be capable of withstanding the nonuniform thermal stresses created by this heat loading. Local hot spots on the collector plates were estimated to have temperatures up to 400°C. The collector vacuum enclosure operates at approximately 200°C in a space environment. The collector structure and collector support system were also designed to withstand one or more vacuum bakeouts at 600°C.

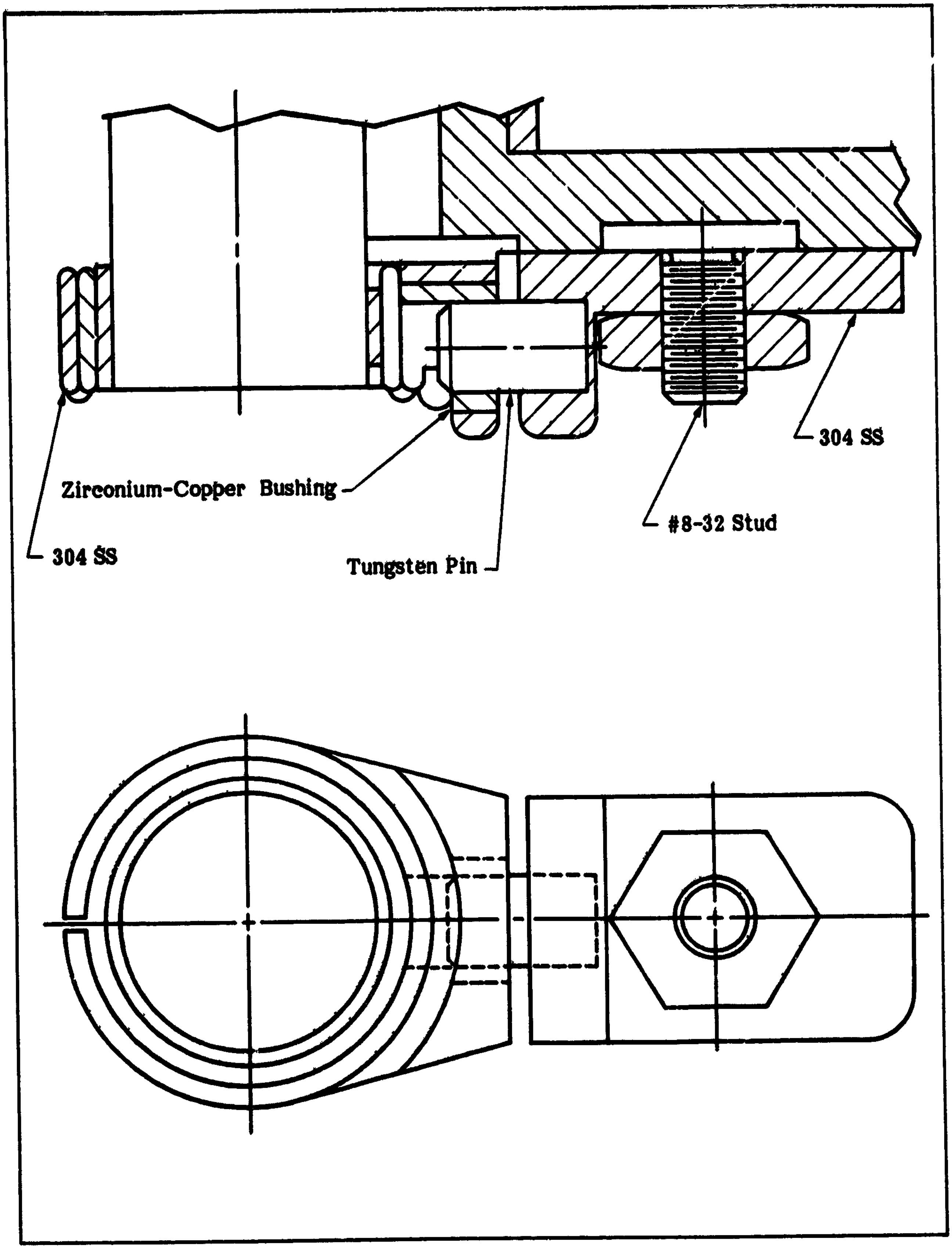

Figure 5-19. Collector Support, Plates No. 1 and No. 2

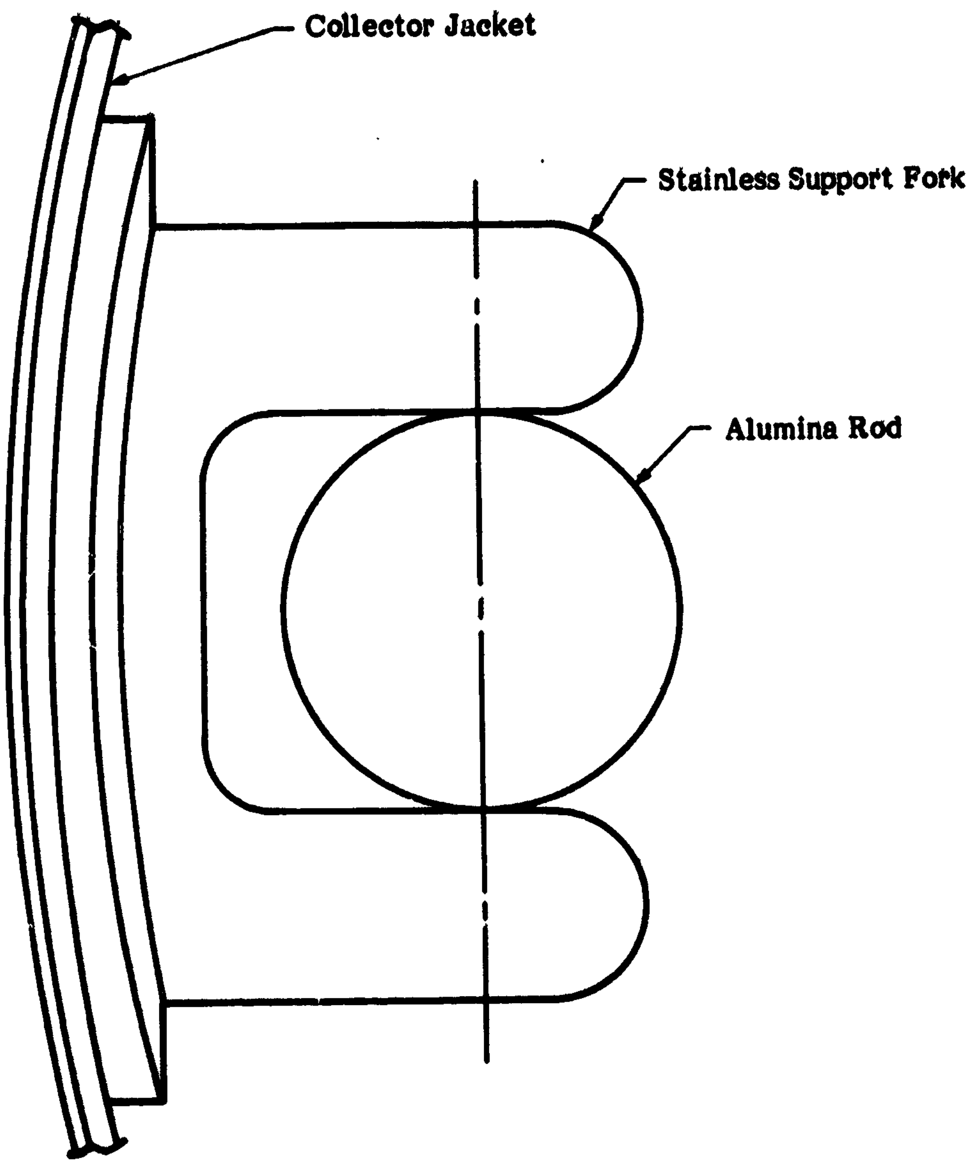

Figure 5-20. Collector Support, Plate No. 10

6.0 FABRICATION, QUALITY AND RELIABILITY RESULTS

The L-5394 tubes were fabricated, assembled, tested, and inspected in accordance with the standards and procedures developed by Litton exclusively for this program. Design and selection of parts, subassemblies, and assemblies were controlled by the standard configuration management procedures maintained at Litton, and inspected/documented in accordance with the standard Quality Procedures. The quality and the reliability programs were enacted in accordance with the specific plans developed for this program.

6.1 FABRICATION METHODS

The fabrication methods for each subassembly and assembly were developed specifically for this program. In most cases, these methods and procedures are adaptations of normal in-house practices utilized by Litton on similar programs and related hardware fabrication. These methods and processes were prepared and released in accordance with the standard manufacturing procedures manual. They were updated as necessary, maintained current, and provided the detailed steps of completing the fabrication of piece parts from released drawings through the completed assembly.

The fabrication of the tubes was accomplished by the manufacturing of individual detailed piece parts, assembling these parts into minor subassemblies, assembling the minor subassemblies into the major subassemblies, and then assembling the major subassemblies into the tube assembly. The piece parts comprising the subassemblies are shown in Appendix 1, the reference drawings for the gun, body, and collector subassemblies. The processes utilized in the subassembly and tube fabrication are shown in figure 6-1. These included several recently developed manufacturing methods including the laser weld and the Tig weld processes used in the gun assembly and the integrated tube assembly.

A breakdown of the assembly and associated inspection processes flow chart for one of the major subassemblies, the gun, is shown in figure 6-2. Each block of the figure represents an independent operation in the overall process. Each block was described in a manufacturing standard or in the case of inspection steps, in the quality manual. Similar descriptions of the other subassembly processes were generated and used during manufacture of the production units.

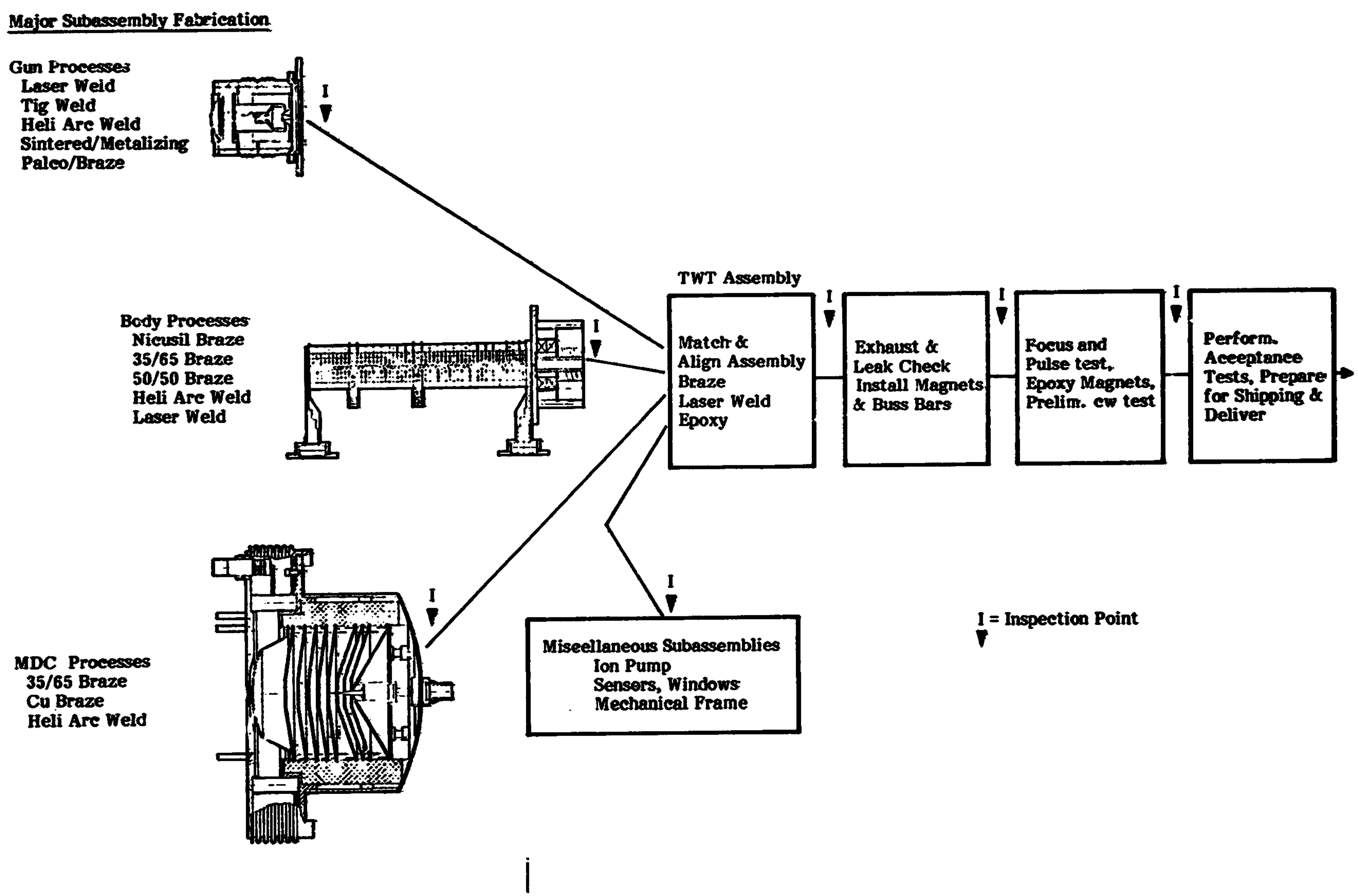

Figure 6-1. Fabrication Processes

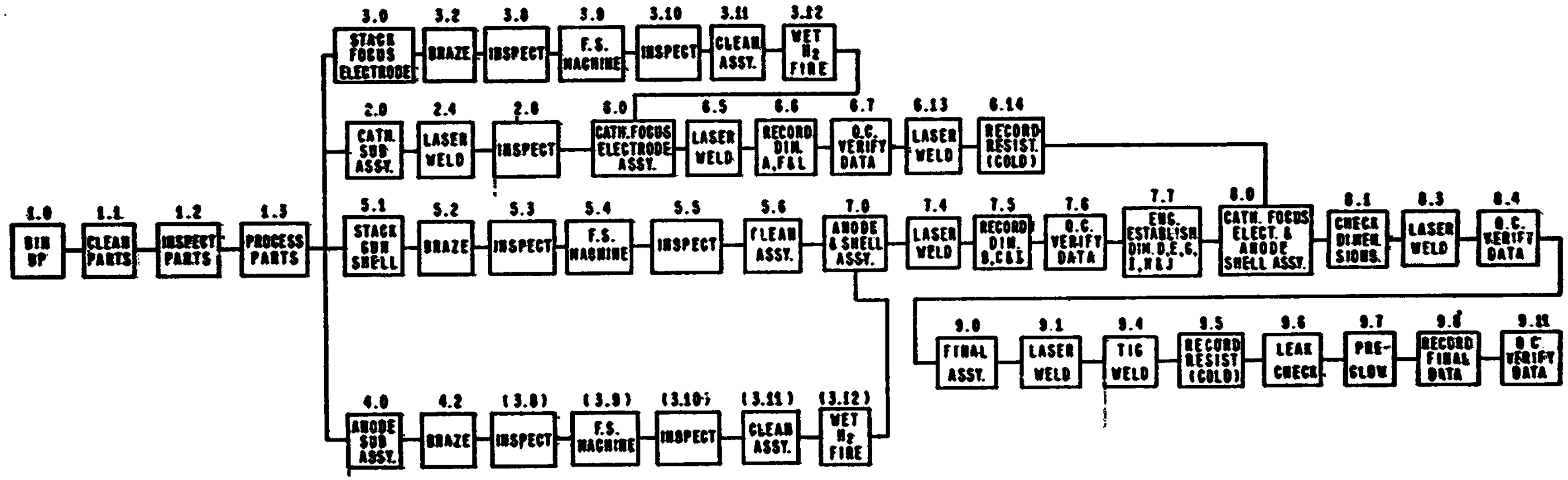

Note: Numbers above blocks refer to production procedure step.

Figure 6-2. Gun Assembly Flow Chart

Additional process standards were generated for tube level processes, including tube exhaust methods, rework procedures in case of specific faults, painting, packaging, and shipping. These procedures are maintained current by the normal release methods. Many of the techniques described within these manufacturing standards are considered company proprietary. The baseline document for the qualification and flight units which provides details of tube assembly and test requirements is shown in Appendix 4.

6.2 PRODUCTION TEST METHODS

The OST's are produced utilizing a controlled production flow process with predetermined operations, tests, and quality monitor points identified. The simplified flow chart showing the complete tube assembly, together with the test/inspection and monitor points is shown in figure 6-3. The detailed procedure associated with each step is noted on the flow chart.

As shown by the flow chart, upon completion of the production fabrication processes, each OST was subjected to a series of operational tests and inspections to insure compliance with the specification requirements. These tests included the inspections/measurements designated by the assembly processes and as defined by the final data package instructions. The requirements for the final data package are contained herein, as Appendix 5. The final rf test circuit arrangements, together with applicable test equipment are shown in figures 6-4 and 6-5. The voltages and current levels for operating the circuit during test are shown in figure 6-6.

Results of the acceptance tests of four tubes; the vibration test unit, the flight unit, the prime flight backup unit, and one other flight backup unit are shown in Section 7.0.

6.3 TUBE PROCESSING METHODS

In the early stages of the program, tubes were sealed off and shipped to NASA without the benefit of rigorous processing procedures considered necessary for

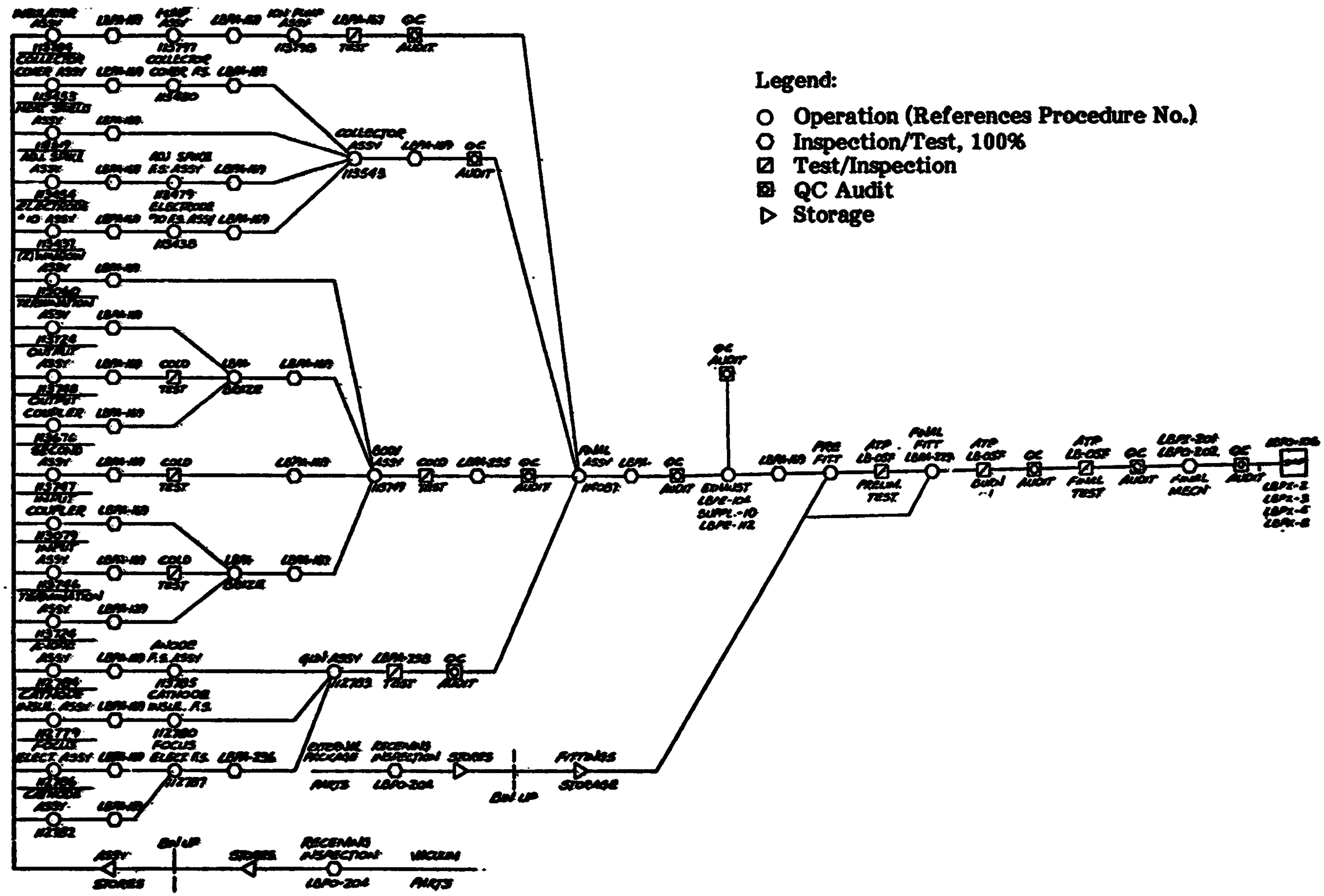

Figure 6-3. Production Flow Chart

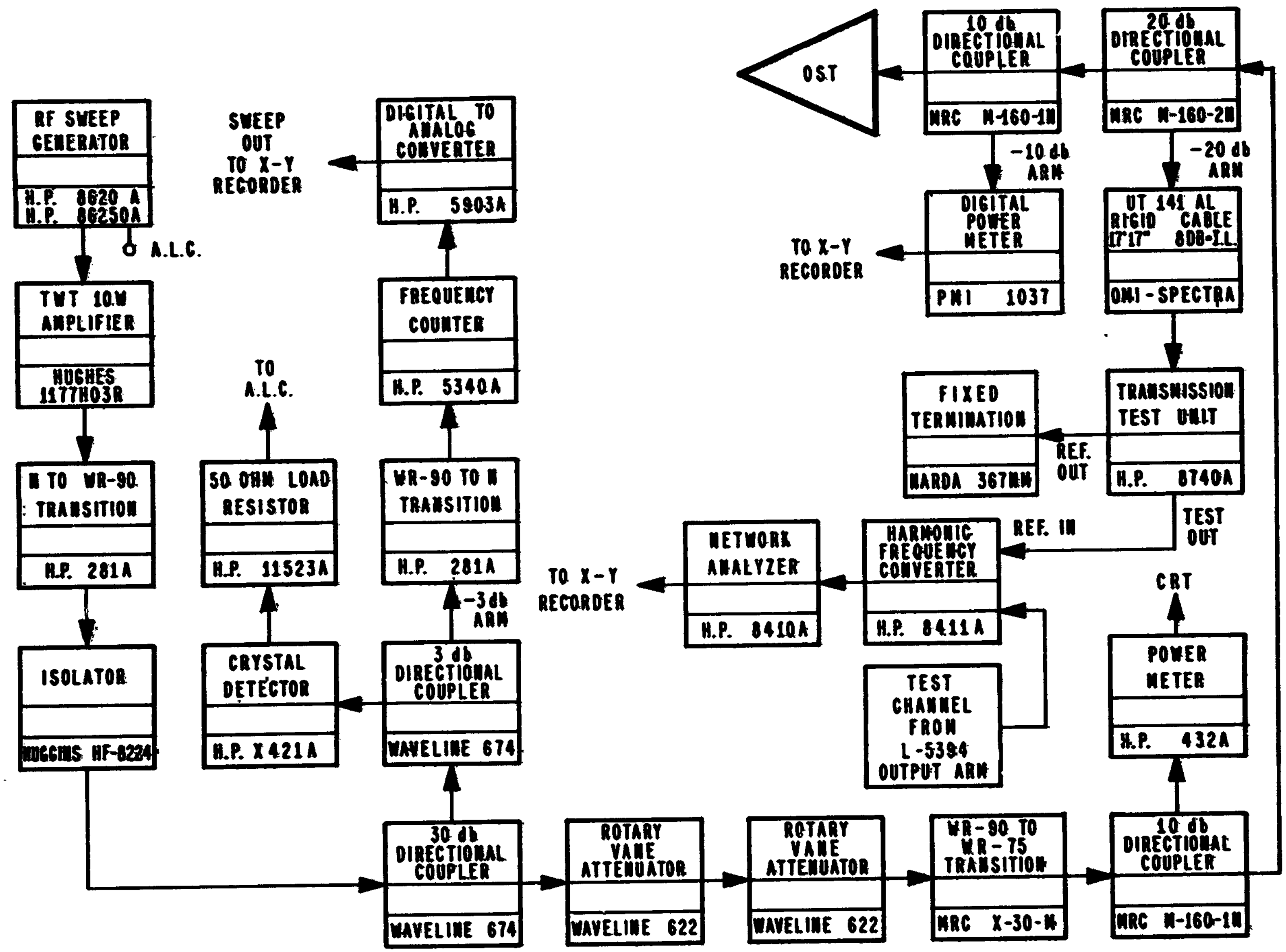

Figure 6-4. OST Input Test Arrangement

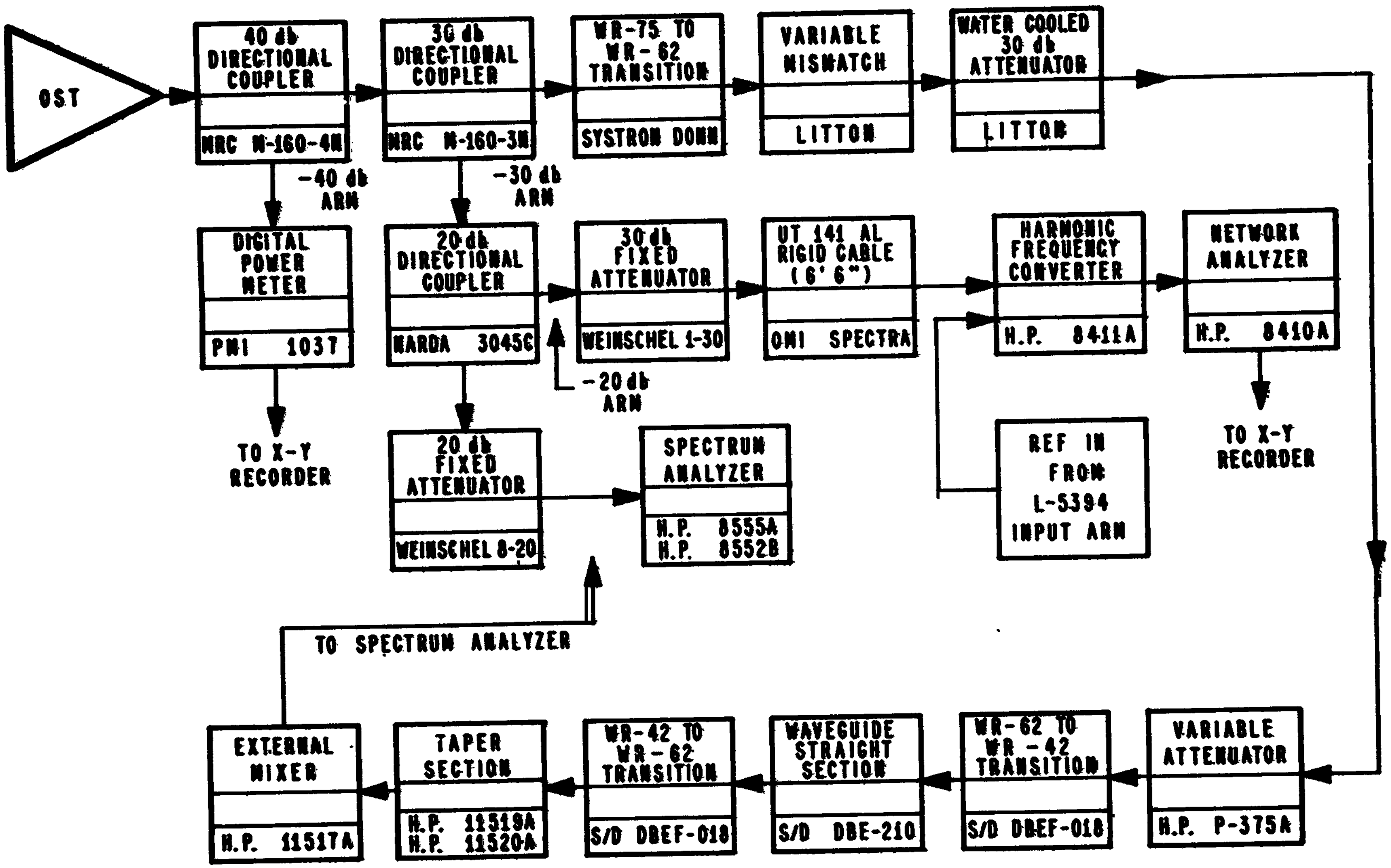

Figure 6-5. OST Output Test Arrangement

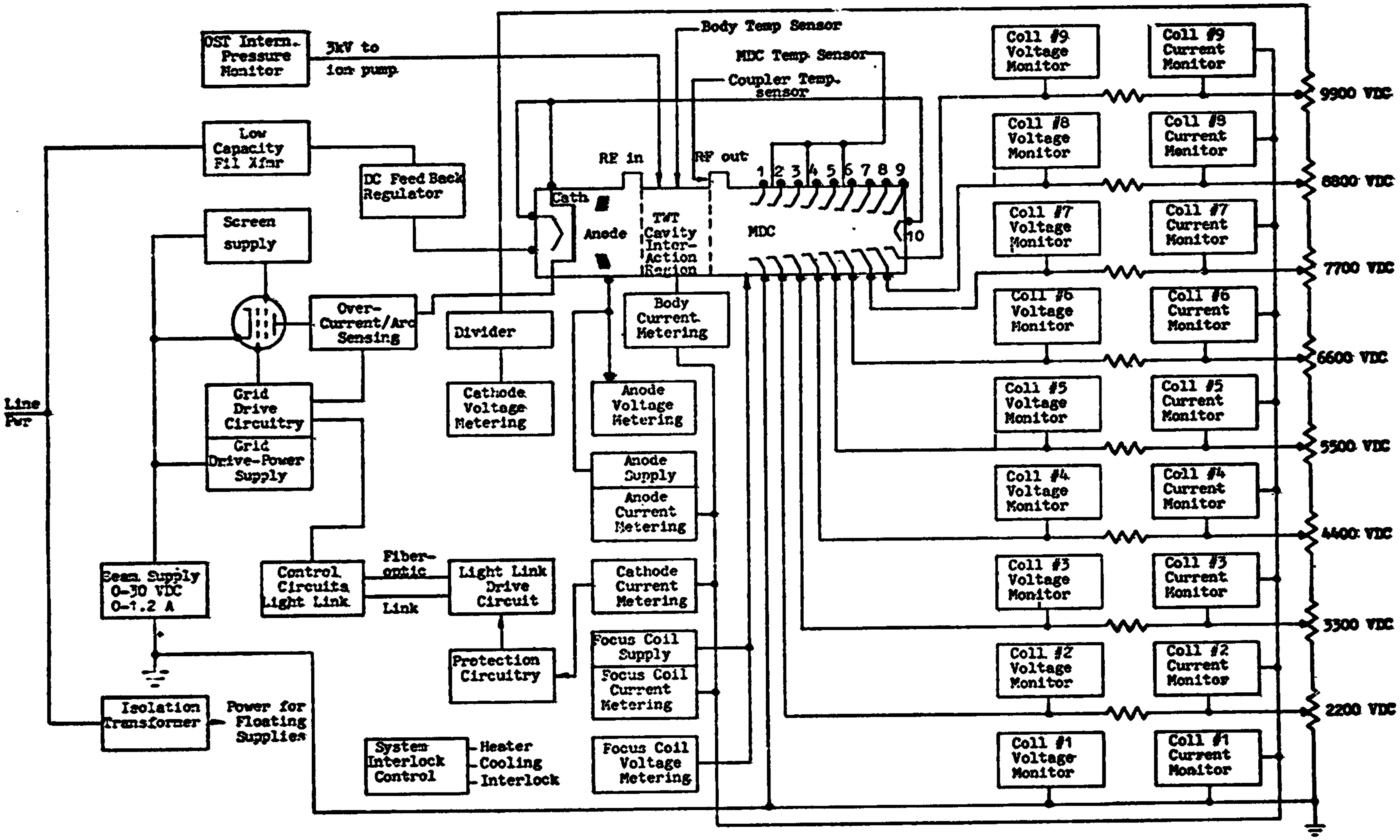

Figure 6-6. Test Voltages and Current Levels

space applications. This fact was recognized in the early fabricated units because considerable arcing and gas evolution problems arose during bench testing. These problems became more prevelant when the testing proceeded from open air to a vacuum tank environment. The subsequent heating and gas evolution in the OST made some of these early tubes inoperative during thermal vacuum testing.

This problem was solved by establishing rigorous processing schedules and procedures for the flight qualification model units as identified previously. After the assembly process, the tubes were baked-out at 450° C for at least 24 hours while the collector jacket was simultaneously heated to 600° C. After pinching off the tube at the bakeout station, the cathode was activated and the beam focused. The tube was then electrically processed by a pulsing technique, starting at 0.1% duty cycle and gradually increasing the cycle. The OST was aged by slowly increasing the duty cycle as the tube degassed and cw operation was attained. At this point the collector jacket temperature was slowly increased to a maximum of 300°C using external heaters and the collector jacket was degassed further. If the gas evolution was still too high at cw operation during this procedure, pulse techniques were reemployed until the tube was ultimately degassed. The final criterion for operation, before the tube was sealed off from the processing vacuum pump, was that the tube must operate with no arcing under cw conditions, with the collector jacket at 300°C, and the gas pressure less than 1 x 10^{-8} Torr as measured in the 0.1 liter/second ion pump.

6.4 FAILURES DISCUSSION

The following listing and discussion shows the variety of problems, discrepancies, and failures encountered during the production and test of the TWT's. The listing does not identify the particular unit on which the failure occurred or time of occurrence, since the discussion is intended to show the type of specific problems or failures that were identified, together with the response or corrective action taken to remedy the problem. In most cases, these problems were identified at the time of occurence, documented via the Litton Failure Analysis Report procedure, and provided to the NASA project manager on a monthly basis.

In a portion of the discussion or listing shown herein, a group or category of faults and/or failures are described together with the appropriate changes, alterations or fixes accomplished to be all encompassing for those failures. Not included in the listing are simple workmanship errors, insignificant problems associated with piece parts or subassembly test failures, and discrepancies not directly associated with tube functional characteristics or design parameters. Also, in the corrective action discussion, no mention is made of the numerous minor changes and improvements that were initiated just to simplify or better control the tube fabrication process. The problems/discrepancies are arranged in categories relating to the major subassemblies of the tube, and are presented in the following general sequence; (1) gun (2) body or rf circuit, (3) MDC and (4) miscellaneous items.

Several other problems of lesser importance were encountered during the program, but their resolution was not the result of a single design change or fabrication modification. These included the type of problem that one might expect to encounter in a state of the art hardware fabrication program. The resolution of these problems was the result of an accumulative experimental and test activity whereby numerous alternatives or combination of several partial modifications were utilized to overcome a single problem. This type of resolution can best be described as a result of the "learning curve" experienced by the program technical staff.

Table 6-1. Production and Test Discrepancies

PROBLEM/DISCREPANCY	CORRECTIVE ACTION/COMMENT
Spot weld failure in the gun allowed the cathode to break free from the support ring. This resulted in high cathode peak current.	A design change was implemented whereby the cathode to support ring spot weld process was replaced by a continuous laser weld.
No emission from the cathode assembly during the gun assembly test in the beam analyzer. Subsequent failure analysis revealed that there was insufficient barium impregnation in the cathode heater.	The particular faulty unit was reworked with a new cathode. In addition, an improved control technique was developed for the barium-cathode impregnation process of the gun fabrication.
The cathode operating temperature for Phase I units was considered excessively high to meet the expected design life.	Revised processing procedures to limit maximum cathode operating temperatures to 1100 °C.
The cathode molybdenum support sleeve fractured during initial shock and vibration tests.	Revised the sleeve design and changed material to molybdenum/rhenium. Changed from a vendor supplied cathode to an inhouse manufactured impregnated cathode.
Second termination failed cold test after brazing due to collapse of the assembly and subsequent narrowing of the gap between ferrules.	Particular assembly was redimensioned, and subsequent units incorporated a design change that increased the wall thickness for added strength.
Leak detected in the input match pole piece and the termination pole piece.	A design change was implemented that replaced the stainless steel adapter with one made of monel alloy.
Slight misalignment of beam hole after completion of body brazing.	The fabrication process was modified to include an additional quality check point of perpendicularity alignment within the body and severs, prior to brazing process.
An unacceptable impedance match existed for an output section after the brazing of the subassembly had been completed.	It was determined that the section was only marginally acceptable prior to braze. The assembly process was modified to insure that marginal piece-part or subassemblies are not utilized in fabrication of the next higher assembly.

Table 6-1. Production and Test Discrepancies (Continued)

PROBLEM/DISCREPANCY	CORRECTIVE ACTION/COMMENT
Misalignment of the termination assembly with body after brazing.	Altered the brazing process and added a brazing fixture to better position and stack parts prior to the brazing operation.
Inadequate thermal conductivity between the body assembly and the mechanical supports.	Altered the technique by which the tube body is attached to the bus bars from torch soldering with Indium to a bonding method utilizing silver-loaded epoxy with high thermal conductivity.
Fillets between ferrules and copper pole pieces vary after braze operation.	Procedures were modified to provide additional controls and inspection steps during brazing. This resulted in better workmanship and uniformity.
Notch filter center frequency shifted downward about 10 MHz in temperature/vacuum exposure.	Replaced aluminum cavity tuners with Kovar tuners.
Incorrect frequency positioning with the tendency of the power and gain peak to be below the lower band edge and power and gain deficiency at the high frequency end.	The corrective action associated with this problem included the definition of a final tube cavity layout, with precise control of lower cutoff frequency of each circuit section.
The small signal gain variation across the frequency band was about 10 dB, in excess of the specification requirement.	Several slight design modifications including alteration to the taper region, ferrule modification, and improved subassembly test for the tube body.
Output circuit oscillations for beam voltages near the specification range.	Improved control of lower cutoff frequency of each cavity and repositioned certain output section cavities.
The lead insulator for the tenth electrode in a MDC fractured at the braze joint at conclusion of the heliarc welding process.	Analysis showed that the fixture was too tight and the heat shock during welding caused the ceramic to fracture. The brazing fixture and the procedure were modified.

Table 6-1. Production and Test Discrepancies (Continued)

PROBLEM/DISCREPANCY	CORRECTIVE ACTION/COMMENT
The ceramic standoff support in the MDC fractured as a result of a weld heat shock.	A design change was initiated that altered the support sleeve configuration and material to Kovar. A centerless grinding process was added to the individual insulators for improved heat expansion match.
Arcing between electrodes in the MDC. Results of analysis showed that arcing was caused by outgassing Alumina due to impregnation residue from the collector finishing process.	Changed material of 10th electrode to spun molybdenum and altered the finishing process to include iron shot peening of the electrodes. Resulted in improved finish and the reduction in arcing.
Waveguide coupler diodes fail or change output with respect to time, temperature, and vacuum.	Altered design with a redesigned coupler and procured improved diodes from a different vendor.
Vacuum leaks in tubes after brazing.	Implemented a procedure for stringent control of brazing and related rework.

7.0 TEST RESULTS

This section presents the results of final tests performed on four representative units produced during the production phase of the program. The four units include the life test unit (ETM-3), the flight unit (QF-4), the prime flight backup unit (QF-3), and another flight backup unit designated QF-5. These units are considered representative of the tube configurations produced during the Phase II qualification/production contract. They also represent units of prime importance from the standpoint of application or functional observability.

The data presented herein has been extracted from that information supplied to NASA in the final test data report, as associated with the respective unit. The data as presented, is in the exact format as it appeared in the delivered document, and reflects the reporting requirements stipulated in the final data package requirements (contained herein as Appendix 5). For purposes of clarity, the curves and plots have not been included as part of this report.

The information is presented in the tube sequence designated above, and contains the test data identified for each tube. The number of pages included with the presentation for each tube is noted below. In each case the summary data sheet is provided, and then a variable quantity of backup data is provided based on the relative importance associated with the particular unit. The following listing shows the tube designator, the tube application, and the number of data pages included.

Tube Ident. (Serial No.)	Application	Data Pages
ETM-3 (2020)	LeRC Life Test	5
QF-4 (2022)	Flight Unit	25
QF-3 (2025)	Flight Backup (Prime)	13
QF-5 (2030)	Flight Backup	3

PRECEDING PAGE BLANK NOT FILMED

7.1 ETM-3 TEST DATA (LeRC Life Test Unit, S/N 2020)

FINAL TEST DATA SUMMARY
(Table I)

Cathode Voltage	E_k	11400	Volts
Cathode Current	I_k	74.0	mA
Anode Voltage	E_A	450	Volts
Heater Voltage	E_f	3.47	Volts
Heater Current	I_f	1.28	Amps

MDC Electrode No.	1	2	3	4	5
Electrode Voltage (kv) (Relative to Gnd)	0.0	2.26	3.39	4.52	5.65
	6	7	8	9	10
	6.78	7.91	9.04	10.17	11.4

Frequency (MHz)	12040	12080	12120
Sat. Output Power (W)	197.4	163.1	177.1
Sat. Drive Power (dBm)	23.1	22.0	23.7
(mW)	203.8	159.3	232.5
Sat. Gain (dB)	29.9	30.1	28.8
Body Current, Sat(mA)	7.8	5.2	7.0
Transmission, Sat.(%)	89.5	93.0	90.5
Overall Eff., Sat(%)	38.6	34.3	36.6
Total DC Input Power, Sat. (W)	507.5	471.5	480.2
Second Harmonic, Sat. (dBm)	+24.0	+10.1	+0.9
Third Harmonic, Sat. (dBm)	<15	<15	<15

NOTES

A. Dummy gain equalizer installed. IL = 0.2 dB (Fig. 19)

B. MCS Model M-11424, S/N 6 waveguide coupler installed.

(Fig. 20)			
Insertion Loss (dB)	0.3	0.3	0.3
Frequency (MHz)	12040	12080	12120

C. Small Signal Gain @ 11.930 MHz = 38.5 dB (e_k = 11.0 kV

D. OST weight 25.0 lb.

E. Thermistor R/T Calibration (Figs. 23 and 24).

F. OST processed over frequency range of 12020 to 12130 MHz for CW operation. Limit duty to 10% outside of this frequency range.

/VAUG102H/ 1-5394 DATA REDUCTION (VERSION 10/1/74): 10/09 15:48
MOD. FOR ALEXOVICH CIRCUIT
TUBE # 539#2020. TEST DATE 9OCT74(1)
BENCH # 1. OPERATOR RIP/LWB

NAS 3-15830

CONC. #		1	2	3	4	5	6
1. FREQUENCY, GHZ		12.030	12.030	12.040	12.049	12.061	12.270
2. CATHODE VOLTS		11420	11400	11400	11400	11400	11400
3. MA		.4	74.4	73.7	74.4	73.7	73.7
4. BEAM WATTS		4.1	848.5	840.1	848.5	840.1	840.1
5. MOD ANODE VOLTS		450	450	450	450	451	451
6. MA		.0	.0	.0	.0	.0	.0
7. WATTS		.0	.0	.0	.0	.0	.0
8. HEATER VOLTS		.0	3.30	3.30	3.30	3.30	3.30
9. AMPS		.0	1.26	1.26	1.26	1.26	1.26
10. WATTS		.0	4.16	4.16	4.16	4.16	4.16
11. NASA OUTPUT SENSOR	MV	.0	-50.1	-46.7	-41.9	-34.4	-29.6
12. NASA REVERSE SENSOR	MV	-.301	-.302	-.398	-.492	-.607	-.705
13. REVERSE POWER SIGNAL	MV	.0	.0	.0	.0	.0	.0
14. VACUUM(VALUES=LOG(X/10^3))		12.2	12.9	15.9	15.9	15.9	15.9
15. BASEPLATE CALORIMETER	W	53.2	25.7	10.0	8.3	9.1	19.1
16. RF OUTPUT CALORIMETER	W	.0	182.3	182.3	157.4	124.3	134.7
17. RF DRIVE DBM		23.3	24.0	23.1	23.1	21.7	21.9
18. MW		212.3	253.0	203.4	204.9	149.2	156.3
19. OUTPUT POWER DBM		10.5	53.0	53.0	52.7	52.3	52.0
20. WATTS		.0	200.8	197.4	185.4	168.4	158.7
21. GAIN DB		.0	29.0	29.9	29.6	30.5	30.1
22. TOTAL COLLECTOR MA		-.5	68.3	68.2	68.0	69.4	70.0
BODY LOSSES:							
23. INTERCEPTION MA		.1	7.9	7.4	8.2	6.5	5.5
24. WATTS		.5	54.1	53.2	54.6	44.6	37.6
25. RF LOSS WATTS		.0	70.3	69.1	64.9	56.9	55.5
26. TOTAL WATTS		.5	124.4	122.3	119.5	103.5	93.2
27. RESIDUAL BEAM POWER AT COLLECTOR WATTS		3.6	523.4	520.4	543.7	561.1	588.2
28. TOTAL HV INPUT WATTS		.4	502.8	507.5	507.7	488.7	483.1
29. OUTPUT+INTCPT+LOSS W		.5	325.1	319.7	304.9	272.0	251.9
30. COLLECTOR DISSIP. W		.3	184.7	187.9	202.8	216.7	231.2
31. AVGE. IMPACT VOLTS		-639	2704	2755	2905	3124	3301
32. COLLECTOR EFFICIENCY PCT		90.8	64.7	63.9	62.7	61.9	60.7
33. OVERALL EFFIC INCL HTR		1.4	39.1	38.6	36.2	34.2	32.6
35. ELECTRONIC EFFIC.	PCT	.4	31.9	31.7	29.5	27.1	25.5
36. NASA DEF.	PCT	.3	23.7	23.3	21.8	20.0	18.9
37. THERMISTOR NO. 1	MV	619.1	225.1	216.3	200.2	234.0	430.3
38. THERMISTOR NO. 2	MV	11.4	7.8	7.2	5.6	4.6	3.2
39. THERMISTOR NO. 3	MV	801.7	727.2	717.6	701.0	696.9	735.2
40. THERMISTOR NO. 4	MV	692.1	724.7	720.1	723.1	744.6	797.7

128. 5. BASEPLATE 50.0C

All Vidar Data: NASA forward and reverse sensors are not connected.
Col. 1: E_b = 0 Volts; Col. 2 to 6: Saturated output power
All Vidar Data except Table II (a) Col 1: Actual filament voltage measured at socket is 3.47 Volts. Actual filament current measured with standard is 1.28 Amps. Cathode current is 74.0 mA actual.

TABLE II (a)

TUBE # 539#2020. TEST DATE 9OCT74(1). SHEET 2

NAS 3-15830

COLLECTOR VOLTAGES RELATIVE TO CATHODE:

NO.						
1	11420	11047	11016	11072	11075	11039
2	9142	9136	9123	9122	9129	9112
3	8032	7965	7946	7942	7959	7944
4	6873	6790	6793	6808	6803	6793
5	5726	5560	5542	5673	5672	5654
6	4591	4515	4513	4534	4537	4512
7	3505	3279	3232	3218	3190	3168
8	2344	2174	2155	2173	2157	2135
9	1275	1019	1023	1039	1031	1024
10	0	0	0	0	0	0

COLLECTOR CURRENTS, MA:

NO.						
1	.0	4.0	4.0	3.9	3.9	3.8
2	.0	5.8	6.0	5.6	5.5	5.7
3	.0	25.2	25.2	24.8	23.1	22.3
4	.0	5.9	5.9	6.2	6.5	6.9
5	.0	3.8	3.7	4.4	4.6	5.6
6	.0	5.0	4.2	5.4	5.7	6.8
7	.0	5.9	5.6	5.1	5.6	5.6
8	.0	4.7	5.5	5.7	6.8	7.2
9	.0	8.1	7.6	7.1	7.4	6.3
10	-.5	-.0	.0	.1	.1	-.1

COLLECTOR INPUT POWERS, WATTS:

NO.						
1	.0	44.4	44.2	43.3	43.2	42.4
2	.0	52.7	54.3	50.6	49.9	52.1
3	.0	200.6	200.0	196.9	184.1	177.1
4	.0	40.2	40.3	40.5	44.8	46.9
5	.0	21.3	20.7	24.8	26.2	31.7
6	.0	22.7	22.0	24.4	26.0	30.6
7	.0	19.4	17.9	16.3	17.6	17.9
8	.0	10.2	11.7	12.5	14.8	15.3
9	.0	8.2	7.7	7.4	7.6	6.4
10	.0	.0	.0	.0	.0	.0

COLLECTOR DISSIPATIONS, WATTS:

NO.						
1	.0	13.9	11.0	11.7	12.2	12.7
2	.0	15.6	15.4	16.6	17.1	18.9
3	.0	68.1	69.3	74.0	72.3	73.4
4	.0	16.0	16.3	17.8	20.6	22.8
5	.0	10.2	10.1	13.0	14.4	18.5
6	.0	13.6	13.4	18.1	17.9	22.4
7	.0	16.0	15.3	15.2	17.5	18.6
8	.0	12.7	15.0	17.1	21.4	23.6
9	.0	21.8	20.3	21.3	23.1	26.7
10	6.5	26.9	27.7	31.2	31.6	32.5

TABLE II (b)

NAS 3-15830

TUBE # 539402020. TEST DATE 9OCT74(1). SHEET 3

COL. #:	1	2	3	4	5	6
1. FREQUENCY, GHZ	12.079	12.090	12.102	12.111	12.120	12.129
2. CATHODE VOLTS	11400	11400	11380	11320	11360	11400
3. MA	73.7	73.0	73.0	72.2	72.2	73.0
4. BEAM WATTS	840.1	831.7	830.2	821.8	821.8	831.7
5. MOD ANODE VOLTS	450	450	450	450	450	450
6. MA	.0	.0	.0	.0	.0	.0
7. WATTS	.0	.0	.0	.0	.0	.0
8. HEATER VOLTS	3.30	3.30	3.30	3.30	3.30	3.30
9. AMPS	1.26	1.26	1.26	1.26	1.26	1.26
10. WATTS	4.16	4.16	4.15	4.15	4.16	4.16
11. NASA OUTPUT SENSOR MV	-31.4	-24.5	-27.8	-28.3	-30.2	-28.8
12. NASA REVERSE SENSOR MV	-.791	-.899	-1.000	-1.109	-1.201	-1.293
13. REVERSE POWER SIGNAL MV	.0	.0	.0	.0	.0	.0
14. VACUUM(VAUGS=LOG(5/V^3))	15.9	15.9	15.9	15.9	15.9	15.9
15. BASEPLATE CALORIMETER W	15.8	27.4	17.4	15.8	13.3	17.4
16. RF OUTPUT CALORIMETER W	124.3	243.6	116.0	[illegible]	140.9	165.7
17. RF DRIVE DBM	22.0	22.7	23.9	23.7	23.7	23.6
18. MW	159.3	167.9	245.0	234.8	232.5	229.5
19. OUTPUT POWER DBM	52.1	52.0	52.1	52.2	52.5	52.7
20. WATTS	163.1	156.7	162.8	166.4	177.1	187.6
21. GAIN DB	30.1	29.2	28.2	28.5	28.8	29.1
22. TOTAL COLLECTOR MA	70.3	70.4	68.4	67.9	67.2	67.6
BODY LOSSES:						
23. INTERCEPTION MA	5.2	5.1	5.9	6.5	7.0	7.3
24. WATTS	35.4	34.7	39.7	44.3	47.7	49.6
25. RF LOSS WATTS	57.1	54.8	57.0	58.2	62.0	65.7
26. TOTAL WATTS	92.5	89.5	96.7	102.6	109.7	115.2
27. RESIDUAL BEAM POWER AT COLLECTOR WATTS	584.5	585.4	570.7	552.8	535.0	528.8
28. TOTAL HV INPUT WATTS	471.5	467.0	471.0	473.5	480.2	485.3
29. OUTPUT+INTCPT+LOSS W	255.6	246.2	259.5	269.0	286.7	302.8
30. COLLECTOR DISSIP. W	215.9	220.8	211.4	204.5	193.4	182.5
31. AVGE. IMPACT VOLTS	3070	3137	3373	3013	2678	2698
32. COLLECTOR EFFICIENCY PCT	63.1	62.3	63.0	63.0	63.8	65.5
33. OVERALL EFFIC INCL HTR	34.3	33.3	34.3	34.8	36.6	38.3
35. ELECTRONIC EFFIC. PCT	26.2	25.4	26.5	27.3	29.1	30.5
36. NASA DEF. PCT	19.4	18.8	19.6	20.3	21.5	22.6
37. THERMISTOR NO. 1 MV	393.8	393.6	237.4	289.3	295.9	344.4
38. THERMISTOR NO. 2 MV	2.9	2.7	2.5	2.6	2.3	10.6
39. THERMISTOR NO. 3 MV	731.3	725.0	720.4	717.3	709.5	700.2
40. THERMISTOR NO. 4 MV	763.2	764.8	769.8	752.7	751.5	749.9

Col. 1 to 6: Saturated Output Power
All Vidar Data: Vacuum readings suspect. Vidar reading ground currents.
Actual pressure is less than 10^{-9} Torr.

TABLE II (c)

NAS 3-15830

TUBE # 539402020. TEST DATE 9OCT74(1). SHEET 4

COLLECTOR VOLTAGES RELATIVE TO CATHODE: NO.						
1	11065	11099	11100	11099	11017	10682
2	9113	9129	9294	9134	9095	9113
3	7956	7988	7939	7950	7944	7978
4	6764	6760	6729	6724	6730	6817
5	5540	5629	5568	5571	5568	5698
6	4504	4487	4419	4420	4411	4558
7	3194	3245	3155	3192	3178	3269
8	2103	2128	2025	2029	2021	2152
9	993	1033	918	928	923	1073
10	0	0	0	0	0	0
COLLECTOR CURRENTS, MA: NO.						
1	3.7	3.7	3.7	3.7	3.8	3.7
2	5.3	5.3	5.2	5.2	5.6	6.1
3	20.4	19.2	19.5	19.8	20.6	20.8
4	7.5	7.5	7.2	6.7	6.0	5.7
5	6.3	6.5	6.7	6.0	5.3	4.8
6	7.5	7.9	8.0	7.4	7.0	6.4
7	5.9	6.2	6.3	6.6	6.6	6.6
8	8.0	6.3	8.0	8.5	8.6	9.1
9	6.0	5.8	5.1	4.8	4.4	4.0
10	-.1	.0	-.9	-.8	-.9	.4
COLLECTOR INPUT POWERS, WATTS: NO.						
1	40.5	41.2	41.5	41.3	41.8	40.3
2	48.1	47.9	47.0	47.0	51.0	55.9
3	162.4	153.7	154.6	157.5	164.0	165.6
4	50.7	50.6	48.4	44.9	40.6	39.0
5	35.4	36.5	37.1	33.3	29.2	27.0
6	33.8	35.6	35.4	32.8	31.0	29.4
7	19.0	20.1	19.8	21.1	21.6	21.5
8	15.7	17.6	15.2	17.3	17.4	19.6
9	5.9	6.0	4.7	4.5	4.0	4.3
10	.0	.0	.0	.0	.0	.0
COLLECTOR DISSIPATIONS, WATTS: NO.						
1	11.2	11.6	11.5	11.2	10.9	10.0
2	16.2	15.5	15.9	15.5	16.1	16.5
3	62.7	60.4	59.9	59.7	59.4	56.0
4	23.0	23.4	22.1	20.1	17.4	15.4
5	19.2	20.3	20.5	18.0	15.1	12.8
6	23.0	24.9	24.5	22.4	20.2	17.4
7	18.2	19.4	19.3	19.9	19.5	17.6
8	24.4	25.9	24.5	25.5	24.8	24.5
9	18.3	15.2	15.4	14.6	12.6	10.8
10	30.4	31.4	26.1	27.5	26.1	29.0

TABLE II (d)

MADG102H/ L-5394 DATA REDUCTION (VERSION 10/1/74): 10/15 13:12
MOD. FOR ALEXOVICH CIRCUIT
TUBE # 5394#2020, TEST DATE 9OCT74(1)
BENCH # 1. OPERATOR RIP/LRB

NAS 3-15830

CUE. #	1	2	3	4	5	6
1. FREQUENCY, GHZ	12.030	12.040	12.050	12.060	12.069	12.080
2. CATHODE VOLTS	11401	11400	11401	11337	11350	11330
3. MA	75.0	75.0	75.8	75.0	75.0	75.8
4. BEAM WATTS	854.9	854.9	863.5	853.4	862.1	862.1
5. MOD ANODE VOLTS	450	451	451	451	450	450
6. MA	.0	.0	.0	.0	.0	.0
7. WATTS	.0	.0	.0	.0	.0	.0
8. HEATER VOLTS	.73	.00	.00	.00	.00	.00
9. AMPS	.00	.00	.00	.00	.00	.00
10. WATTS	.00	.00	.00	.00	.00	.00
11. NASA OUTPUT SENSOR MV	-1.0	-.9	-.7	-.6	-.5	-.6
12. NASA REVERSE SENSOR MV	-.300	-.398	-.496	-.602	-.663	-.797
13. REVERSE POWER SIGNAL MV	.0	.0	.0	.0	.0	.0
14. VACUUM(VAUMS=LOG(1/M**3))	15.9	15.9	15.9	15.9	15.9	15.9
15. BASEPLATE CALORIMETER W	23.4	19.9	19.1	15.6	22.4	33.7
16. RF OUTPUT CALORIMETER W	.0	.0	.0	.0	.0	.0
17. RF DRIVE DBM	11.1	10.0	9.4	9.0	9.0	9.7
18. MW	12.7	10.0	8.7	7.9	7.9	9.3
19. OUTPUT POWER DBM	43.0	42.9	42.7	42.2	42.0	42.0
20. WATTS	19.9	19.6	18.5	16.8	15.9	16.0
21. GAIN DB	31.9	32.9	33.3	33.3	33.0	32.4
22. TOTAL COLLECTOR MA	73.7	73.7	73.4	73.5	74.1	74.0
BODY LOSSES:						
23. INTERCEPTION MA	1.7	1.7	1.6	1.6	1.6	1.6
24. WATTS	11.7	11.7	11.2	10.7	10.6	10.9
25. RF LOSS WATTS	7.0	5.9	6.5	5.9	5.6	5.6
26. TOTAL WATTS	18.7	18.6	17.7	16.5	16.4	16.5
27. RESIDUAL BEAM POWER AT COLLECTOR WATTS	816.4	816.7	827.3	820.1	829.8	829.6
28. TOTAL RF INPUT WATTS	229.5	227.4	224.0	221.2	220.6	222.6
29. OUTPUT+INTCPT+LOSS %	38.5	38.2	36.2	33.3	32.3	32.5
30. COLLECTOR DISSIP. %	190.9	189.2	187.8	187.9	188.3	170.0
31. AVGE. IMPACT VOLTS	2543	2569	2551	2556	2540	2557
32. COLLECTOR EFFICIENCY PCT	76.6	76.8	77.3	77.1	77.3	77.1
33. OVERALL EFFIC INCL HTR	8.7	8.6	8.3	7.6	7.2	7.2
35. ELECTRONIC EFFIC. PCT	3.1	3.1	2.9	2.7	2.5	2.5
36. NASA DEF. PCT	2.3	2.3	2.1	2.0	1.8	1.9
37. THERMISTOR NO. 1 MV	503.7	498.7	500.1	504.8	507.9	507.7
38. THERMISTOR NO. 2 MV	10.1	9.5	8.9	8.0	7.5	7.0
39. THERMISTOR NO. 3 MV	749.5	748.2	747.8	744.8	744.4	743.0
40. THERMISTOR NO. 4 MV	831.3	827.9	828.2	827.7	825.1	824.1

Col. 1 to 6: Saturated Output Power -10 dBm.

All Varian Data except Table II (a) Col. 1: Actual filament voltage measured at socket is 3.47 Volts.

Actual filament current measured with standard is 1.28 Amps. Cathode current is 74.0 mA actual.

TABLE II (e)

TUBE # 5394#2020, TEST DATE 9OCT74(1), SHEET 2

NAS 3-15830

COLLECTOR VOLTAGES RELATIVE TO CATHODE:

NO.						
1	11399	11399	11399	11379	11379	11370
2	9192	9191	9191	9177	9173	9177
3	8145	8142	8143	8133	8128	8132
4	6873	6870	6855	6854	6847	6844
5	5700	5701	5679	5682	5672	5673
6	4528	4513	4495	4502	4494	4494
7	3240	3238	3237	3241	3255	3243
8	2034	2023	2025	2036	2058	2054
9	1018	1004	1007	1019	1042	1042
10	0	0	0	0	0	0

COLLECTOR CURRENTS, MA:

NO.						
1	.9	.9	.9	.9	.9	.9
2	.7	.7	.7	.7	.7	.7
3	1.0	1.0	1.0	.9	.9	.9
4	1.5	1.5	1.4	1.4	1.3	1.4
5	3.4	3.4	3.2	3.1	3.0	3.1
6	8.9	8.8	8.7	8.4	8.2	8.5
7	14.0	13.8	13.2	12.9	12.7	12.9
8	26.3	26.4	26.5	26.8	27.1	26.5
9	16.7	17.2	17.8	18.3	18.7	18.5
10	.4	.3	.3	.1	.7	.7

COLLECTOR INPUT POWERS, WATTS:

NO.						
1	10.0	10.1	10.0	10.0	9.6	9.9
2	6.3	6.2	6.2	6.1	6.0	6.1
3	8.0	7.9	7.7	7.6	7.3	7.6
4	10.2	10.2	9.7	9.3	9.1	9.5
5	19.5	19.1	18.4	17.7	17.1	17.8
6	40.2	39.9	39.9	37.4	36.8	38.1
7	45.3	43.6	42.7	41.9	41.3	41.8
8	53.5	53.3	53.7	54.6	55.7	54.4
9	16.9	17.3	17.9	18.6	19.5	19.3
10	.0	.0	.0	.0	.0	.0

COLLECTOR DISSIPATIONS, WATTS:

NO.						
1	2.3	2.3	2.2	2.3	2.2	2.2
2	1.8	1.7	1.7	1.7	1.7	1.7
3	2.4	2.5	2.4	2.4	2.3	2.4
4	3.8	3.8	3.5	3.5	3.4	3.6
5	8.9	8.6	8.3	8.0	7.7	8.0
6	23.0	22.7	22.1	21.4	20.8	21.7
7	36.2	34.5	33.5	31.1	32.2	33.3
8	60.2	61.7	61.5	62.6	66.6	60.0
9	43.2	44.3	45.4	45.7	47.5	47.5
10	26.2	25.5	26.3	25.9	27.2	27.5

TABLE II (f)

ORIGINAL PAGE IS
OF POOR QUALITY

NAS-3-15830

TUBE # 5394#2020, TEST DATE 9OCT74(1), SHEET 3

COL. #		1	2	3	4	5	6
1. FREQUENCY, GHZ		12.090	12.100	12.110	12.120	12.130	12.197
2. CATHODE VOLTS		11380	11380	11381	11400	11340	11380
3. MA		75.4	75.8	75.3	75.8	75.6	75.0
4. BEAM WATTS		862.1	862.1	862.1	863.4	862.1	853.4
5. MOD ANODE VOLTS		450	450	450	451	450	451
6. MA		.0	.0	.0	.0	.0	.0
7. WATTS		.0	.0	.0	.0	.0	.0
8. HEATER VOLTS		.00	.00	.00	.00	.00	.00
9. AMPS		.00	.00	.00	.00	.00	.00
10. WATTS		.00	.00	.00	.00	.00	.00
11. NASA OUTPUT SENSOR	MV	-.5	-.6	-.5	-.5	-.7	.0
12. NASA REVERSE SENSOR	MV	-.899	-.998	-1.102	-1.200	-1.303	-1.296
13. REVERSE POWER SIGNAL	MV	.0	.0	.0	.0	.0	.0
14. VACUUM(VAUMS=LOG(1/M**3))		15.9	15.9	15.7	15.9	15.9	15.9
15. BASEPLATE CALORIMETER	W	17.4	17.4	34.9	20.8	17.4	18.3
16. RF OUTPUT CALORIMETER	W	.0	.0	.0	.0	.0	.0
17. RF DRIVE DBM		10.7	11.9	12.9	13.5	13.8	-23.7
18. MW		11.9	15.5	19.2	22.3	24.2	.0
19. OUTPUT POWER DBM		41.9	42.1	42.2	42.5	42.6	2.9
20. WATTS		15.5	16.1	16.5	17.7	18.1	.0
21. GAIN DB		31.2	30.2	29.4	29.0	28.7	.0
22. TOTAL COLLECTOR MA		73.7	73.0	73.2	73.6	73.7	73.9
BODY LOSSES:							
23. INTERCEPTION MA		1.6	1.7	1.7	1.7	1.7	1.3
24. WATTS		11.2	11.3	11.4	11.6	11.6	9.1
25. RF LOSS WATTS		5.4	5.6	5.8	6.2	6.3	.0
26. TOTAL WATTS		15.6	17.0	17.2	17.7	17.9	9.1
27. RESIDUAL BEAM POWER AT COLLECTOR WATTS		831.0	829.1	828.3	829.2	826.6	844.3
28. TOTAL HV INPUT WATTS		225.1	224.3	225.2	229.9	230.3	186.3
29. OUTPUT+INTCPT+LOSS W		32.1	33.0	33.8	35.4	36.0	9.1
30. COLLECTOR DISSIP. W		193.0	191.2	191.4	194.5	194.3	177.2
31. AVGE. IMPACT VOLTS		2618	2619	2615	2641	2635	2397
32. COLLECTOR EFFICIENCY PCT		76.8	76.9	76.9	76.5	76.5	79.0
33. OVERALL EFFIC INCL HTR		6.9	7.2	7.4	7.7	7.9	.0
35. ELECTRONIC EFFIC.	PCT	2.4	2.5	2.5	2.6	2.8	.0
36. NASA DEF.	PCT	1.8	1.9	1.9	2.1	2.1	.0
37. THERMISTOR NO. 1	MV	506.6	505.5	502.3	492.3	487.4	499.3
38. THERMISTOR NO. 2	MV	5.7	5.4	5.0	4.5	4.3	4.2
39. THERMISTOR NO. 3	MV	740.4	741.7	740.2	737.5	738.6	734.0
40. THERMISTOR NO. 4	MV	825.1	824.7	825.7	824.3	826.6	832.0

Col. 1 to 5: Saturated Output Power -10 dBm.

Col. 6: No drive power

TABLE II (g)

NAS-3-15830

TUBE # 5394#2020, TEST DATE 9OCT74(1), SHEET 4

COLLECTOR VOLTAGES RELATIVE TO CATHODE:

NO.						
1	11379	11379	11379	11394	11379	11379
2	9175	9169	9179	9192	9168	9173
3	8127	8119	8132	8134	8117	8123
4	6631	6456	6851	6570	6854	6868
5	5683	5582	5687	5697	5351	5706
6	4484	4505	4505	4518	4513	4550
7	3323	3214	3237	3227	3217	3226
8	2014	2023	2031	2044	2043	2017
9	995	995	995	1005	1012	931
10	0	0	0	0	0	0

COLLECTOR CURRENTS, MA:

NO.						
1	.9	.9	.9	1.0	1.0	.6
2	.7	.7	.7	.8	.7	.5
3	1.0	1.0	1.0	1.1	1.1	.7
4	1.5	1.5	1.5	1.6	1.6	1.0
5	3.3	3.2	3.1	3.1	3.3	2.0
6	8.9	8.7	8.6	8.8	8.7	4.9
7	13.5	13.8	14.6	15.1	15.1	8.7
8	25.7	24.9	24.0	23.4	23.5	26.0
9	18.1	18.1	18.4	18.5	16.5	27.0
10	.3	.3	.4	.3	.3	.3

COLLECTOR INPUT POWERS, WATTS:

NO.						
1	10.4	10.5	10.6	11.3	11.3	8.9
2	6.3	6.4	6.5	6.9	6.8	4.9
3	8.2	8.2	8.3	8.8	8.9	5.8
4	10.2	10.4	10.4	10.9	11.2	7.1
5	16.5	17.9	17.5	17.7	18.6	11.4
6	39.1	39.3	38.7	39.8	39.1	22.2
7	43.4	44.5	47.2	49.8	48.4	27.9
8	51.7	50.3	46.7	47.8	47.9	56.5
9	18.0	18.0	18.3	18.6	18.7	26.4
10	.0	.0	.0	.0	.0	.0

COLLECTOR DISSIPATIONS, WATTS:

NO.						
1	2.4	2.4	2.4	2.6	2.6	1.9
2	1.8	1.8	1.9	2.0	1.9	1.2
3	2.5	2.6	2.7	2.9	2.9	1.7
4	3.9	4.0	4.0	4.2	4.3	2.5
5	6.6	6.2	6.0	6.2	6.6	4.4
6	23.2	22.9	22.5	23.2	22.8	11.7
7	35.3	35.2	36.1	40.0	39.7	20.7
8	67.1	65.1	62.7	61.8	61.8	67.2
9	47.3	47.3	48.2	46.6	48.7	64.5
10	26.9	26.9	27.1	27.2	27.2	24.8

7.2 QF-4 TEST DATA (Flight Unit, S/N 2022)

10.0 Specifications Parameter		QF Design Specification	Actual Value
10.1 Saturation Characteristics			12.038-12.123
10.1.1 Frequency	(GHz)	12.038-12.123	12.040-12.120 (for Table II & III data)
10.1.2 Gain	(dB)	30^{+2}_{-1}	29.8 (min) Table II(k)
10.1.3 Output Power, Pos, Min.	(W)	180	191 (min) Table II(k)
10.1.4 Overall Efficiency, Min.	(%)	40	44.5 (min) Table II(k)
10.1.5 DC Input Power, Max.	(W)	500	474 (max) Table II(i)
10.1.6 Beam Transmission @ 50°C Baseplate, Min.	(%)	92	93.7 (min) @ 55°C Table III(k)
10.1.7 AM/PM (pos to Pos -2dB)	(°/dB)	6	6.74*
10.1.8 Second Order Phase Deviation Max.	($^\circ$/MHz^2)	0.3	Not computed
10.1.9 Harmonic Output Power, 2nd and 3rd, Max.	(dBm)	+23	+18 (max) Table I(a)
10.1.10 Thermal Input to Baseplate, Max.	(W)	150	105 (max) Table II(i)
10.2 Small Signal Characteristics (Po = saturation Po -10 dB)			
10.2.1 Gain Variation, peak to peak	(dB)	5	2.9
10.2.2 Gain-Below 11.928 GHz, Max.	(dB)	20	<20
10.3 Noise Figure, Max.	(dB)	40	35.5
10.4 Differential Gain (3 to 23 dB below Pos)	(dB)	0.7	1.0
10.5 Spurious Output Power (Pd = 0 and Pds, excluding harmonically related signals)			
a. In any 4 kHz band between 14.0 and 14.3 GHz	(dBm)	-10	<-10
b. In any 100 MHz band between 10.0 and 18.0 GHz	(dBm)	-10	<-10

10.0 Specifications (continued)

Parameter		QF Design Specification	Actual Value
10.6 Overdrive without OST damage, Continuous, Max.	(dBm)	+29	No Test
Short Term, ≤ 0.5 sec, Max.	(dBm)	+43.4	No Test
10.7 Power Processor Requirements (Set to OST decal values)			
10.7.1 Cathode Voltage with respect to ground.	(kV)	-11.3 ±0.3	11.2
10.7.2 Anode Voltage with respect to ground.	(V)	350 ±200	250
10.7.3 Anode Current, Max.	(mA)	0.1	<0.1
10.7.4 Heater Current, (constant current supply).	(A)	1.3 ±0.1	1.29
10.7.5 Heater Voltage with respect to cathode, Max.	(V)	4.2	3.29
10.7.6 Body Current Overload Trip	(mA)	10	10
10.7.7 Ion Pump Supply Voltage	(kV)	2.3 - 3.3	3.0
10.7.8 Ion Pump Current Overload Trip (sum of two pumps)	(μA)	10	10
10.7.9 Collector Voltages, Electrode #1 - #10 (% of cathode voltage)		0, 20, 30, 40, 50, 60, 70, 80 90 and 100	OK
10.7.10 Baseplate Temperature			
Operating	(°C)	0 to +58	35 to 55
At Turn on	(°C)	-15 to +58	No test
Non-Operating	(°C)	-20 to +65	No Test
10.8 Refocusing Magnetic Field		PM	PM
10.9 Weight OST	(lb)	26.02 Max.	26.24
10.10 Design Life	(yr)	2	2
10.11 Waveguide Type		WR-75	WR-75

FINAL TEST DATA SUMMARY

(Table Ia)

Cathode Voltage	E_k		11,200			Volts
Cathode Current	I_k		76.0			mA
Anode Voltage	E_A		250			Volts
Heater Voltage	E_f		3.29			Volts
Heater Current	I_f		1.29			Amps
Cathode Temperature	T_k		1075			Deg.C
MDC Electrode No.	1	2	3	4	5	
Electrode Voltage (kV)	0.0	2.24	3.36	4.48	5.60	
(Relative to Gnd)	6	7	8	9	10	
	6.72	7.84	8.96	10.08	11.20	

Frequency (MHz)	12040	12080	12120
Sat. Output Power (dBm)	53.8	53.6	52.8
Sat. Output Power (W)	239	227	191
Sat. Drive Power (dBm)	23	23	23
(mW)	200	201	198
Sat. Gain (dB)	30.8	30.5	29.8
Body Current,Sat (mA)	3.1	3.4	3.0
Transmission,Sat (%)	95.9	95.5	96.0
Overall Eff.,Sat (%)	50.6	48.6	44.5
Total DC Power,Sat (W)	470	463	425
Second Harmonic,Sat (dBm)	@ F=24080 +18	@F=24160 +7	@F=24240 +6
Third Harmonic, Sat (dBm)	@ F=36120 <-15	@f=36240 <-15	@F=36360 <-15
Notch Filter IL (dB)	0.9	0.5	0.25
MCS Waveguide Coupler IL (dB)	0.25	0.20	0.20

NOTES

A. Thermistor R/T Calibration.

B. RF System NASA #1 Certificate of Calibration Western Automatic Test Services on 4/18/75.

C. Total Filament Hours 631.1 on 4/28/75.

D. Total Cathode Pulse Hours 161.7 on 4/28/75.

E. Total Cathode CW Hours 307.5 on 4/28/75. (plus ~1300 at LeRC)

F. Base Plate Temperature is 38°C.

FINAL TEST DATA SUMMARY

(Table Ib)

Cathode Voltage	E_k		11,200			Volts
Cathode Current	I_k		76.0			mA
Anode Voltage	E_A		250			Volts
Heater Voltage	E_f		3.29			Volts
Heater Current	I_f		1.20			Amps
Cathode Temperature	T_k		1075			Deg.C
MDC Electrode No.	1	2	3	4	5	
Electrode Voltage (kV)	0.0	2.24	3.36	4.48	5.60	
(Relative to Gnd)	6	7	8	9	10	
	6.72	7.84	8.96	10.08	11.2	

Frequency (MHz)	12040	12080	12120
Sat. Output Power (dBm)	53.6	53.4	52.5
Sat. Output Power (W)	229	216	179
Sat. Drive Power (dBm)	23	23	23
(mW)	200	201	198
Sat. Gain (dB)	30.6	30.3	29.6
Body Current,Sat. (mA)	4.1	4.5	3.6
Transmission,Sat. (%)	94.6	94.1	95.3
Overall Eff.,Sat. (%)	47.4	45.8	41.9
Total DC Power,Sat. (W)	479	468	422

NOTE

A. Base Plate Temperature is 55°C.

/VAUG1021/ L-5394 DATA REDUCTION (VERSION 12/6/74) 04/25 09:48
MOD. FOR ALEXOVICH [illegible]
TUBE # L-5394 #2022R-1 . TEST DATE 23APR75 (2)
BENCH # 1. OPERATOR RIP-LRB

NAS 3-15830

COL. #:	1	2	3	4	5	6
1. FREQUENCY, GHZ	12.030	12.040	12.050	12.060	12.070	12.080
2. CATHODE VOLTS	11197	11218	11197	11197	11197	11218
3. MA	76.0	76.0	76.0	76.0	76.0	76.0
4. BEAM WATTS	850.8	852.3	850.8	850.8	850.8	852.3
5. MOD ANODE VOLTS	250	250	251	251	251	250
6. MA	-.0	-.0	-.0	-.0	-.0	-.0
7. WATTS	.0	.0	.0	.0	.0	.0
8. HEATER VOLTS	3.29	3.29	3.29	3.29	3.29	3.29
9. AMPS	1.29	1.29	1.29	1.29	1.29	1.29
10. WATTS	4.24	4.24	4.24	4.24	4.24	4.24
11. NASA OUTPUT SENSOR MV	-.1	-.1	-.1	-.1	-.1	-.1
12. NASA REVERSE SENSOR MV	.0	.0	-.1	-.1	.0	.0
13. REVERSE POWER SIGNAL DBM	.0	.0	-.0	.0	.0	.0
14. VACUUM(VAUNS=LOG(N/M^3))	14.5	14.4	14.5	14.5	14.5	14.5
15. BASEPLATE CALORIMETER W	.0	.0	.0	.0	.0	.0
16. RF OUTPUT CALORIMETER W	192.0	192.0	183.5	166.6	153.9	137.0
17. RF DRIVE DBM	27.6	27.6	27.6	27.6	27.7	27.6
18. MW	576.8	576.8	580.8	580.8	582.1	578.1
19. OUTPUT POWER DBM	53.0	53.0	52.7	52.3	52.1	51.7
20. WATTS	198.2	197.7	184.1	170.8	161.1	147.0
21. GAIN DB	25.4	25.4	25.0	24.7	24.4	24.1
22. TOTAL COLLECTOR MA	69.6	69.5	69.0	68.6	68.1	67.7
BODY LOSSES:						
23. INTERCEPTION MA	6.8	6.9	7.5	8.0	8.4	8.7
24. WATTS	45.6	46.6	50.2	53.7	56.4	58.7
25. RF LOSS WATTS	69.4	69.2	64.4	59.8	56.4	51.5
26. TOTAL WATTS	115.0	115.8	114.6	113.5	112.8	110.1
27. RESIDUAL BEAM POWER AT COLLECTOR WATTS	537.7	538.8	552.1	566.5	576.9	595.1
28. TOTAL HV INPUT WATTS	463.5	466.4	458.8	448.6	438.4	428.6
29. OUTPUT+INTCPT+LOSS W	313.1	313.5	298.7	284.3	273.9	257.2
30. COLLECTOR DISSIP. W	152.4	152.9	160.1	164.3	164.5	171.4
31. AVGE. IMPACT VOLTS	2191	2201	2320	2394	2415	2532
32. COLLECTOR EFFICIENCY PCT	71.7	71.6	71.0	71.0	71.5	71.2
33. OVERALL EFFIC INCL HTR	42.2	42.0	39.8	37.7	36.4	34.0
35. ELECTRONIC EFFIC. PCT	31.4	31.3	29.2	27.1	25.6	23.3
36. NASA DEF. PCT	23.3	23.2	21.6	20.1	18.9	17.3
37. THERMISTOR NO. 1 DEG C	66.3	64.9	64.8	64.9	65.2	65.6
38. THERMISTOR NO. 2 DEG C	285.1	274.1	285.1	285.1	285.1	285.1
39. THERMISTOR NO. 3 DEG C	56.9	57.0	57.1	57.2	57.2	57.2
40. THERMISTOR NO. 4 DEG C	67.8	69.3	69.8	69.8	69.6	69.0

LITTON 18 REV. A

COL. 1 SAT. DRIVE POWER + 4.5DD.
COL. 2 38.5 DEGREE BASE PLATE

P_d = +27.5 dBm Col. 1 to Col. 6

TABLE II(a)

TUBE # L-5394 #2022R-1 . TEST DATE 23APR75 (2). SHEET 2

NAS 3-15830

COLLECTOR VOLTAGES RELATIVE TO CATHODE:

NO.						
1	11172	11192	11172	11175	11175	11198
2	8935	8956	8944	8942	8948	8972
3	7793	7817	7808	7817	7830	7859
4	6693	6723	6714	6725	6710	6752
5	5593	5614	5604	5623	5588	5629
6	4496	4508	4480	4514	4470	4541
7	3400	3459	3392	3485	3392	3392
8	2305	2318	2265	2259	2256	2231
9	1096	1115	1076	1101	1129	1111
10	0	0	0	0	0	0

COLLECTOR CURRENTS, MA:

NO.						
1	3.4	3.5	3.4	3.1	3.0	2.7
2	4.2	4.2	4.0	3.6	3.4	3.0
3	12.6	12.9	12.4	11.0	9.9	8.5
4	13.3	12.8	12.0	11.2	10.1	9.6
5	6.3	5.8	5.6	5.6	5.3	5.1
6	7.5	7.5	7.6	8.0	8.2	8.6
7	8.5	9.0	9.6	10.6	11.6	11.9
8	6.2	6.1	6.7	7.8	9.3	11.0
9	13.4	12.6	11.0	9.5	8.6	8.4
10	-5.8	-4.9	-3.1	-1.7	-1.2	-1.1

COLLECTOR INPUT POWERS, WATTS:

NO.						
1	38.3	38.6	37.5	34.3	33.0	30.6
2	37.2	37.4	35.7	32.2	30.2	27.0
3	98.1	100.9	96.4	85.7	77.5	66.4
4	89.3	85.9	80.7	75.0	67.5	65.1
5	35.0	32.7	31.4	31.4	29.5	28.7
6	33.8	33.9	33.9	36.3	36.7	38.7
7	28.8	31.1	32.5	36.1	39.3	40.5
8	14.3	14.1	15.1	17.7	21.1	24.6
9	14.7	14.0	11.8	10.4	9.7	9.3
10	.0	.0	.0	.0	.0	.0

COLLECTOR DISSIPATIONS, WATTS:

NO.						
1	7.5	7.6	7.8	7.3	7.1	6.9
2	9.1	9.2	9.3	8.6	8.1	7.6
3	27.6	28.4	28.7	26.2	23.9	21.4
4	29.2	28.1	27.9	26.7	24.3	24.4
5	13.7	12.8	13.0	13.4	12.7	12.9
6	16.5	16.6	17.5	19.2	19.9	21.7
7	18.5	19.8	22.3	25.4	28.0	30.2
8	13.6	13.4	15.5	18.8	22.6	27.9
9	29.4	27.7	25.4	22.6	20.8	21.2
10	12.8	10.7	7.2	4.0	2.9	2.8

LITTON 18 REV. A

II(b)

TUBE # L-5394 #2022R-1 , TEST DATE 23APR75 (2), SHEET 3 NAS 3-15230

COL. #:	1	2	3	4	5	6
1. FREQUENCY, GHZ	12.090	12.100	12.110	12.120	12.130	12.080
2. CATHODE VOLTS	11197	11218	11197	11197	11197	11197
3. MA	76.0	76.0	76.0	76.0	76.0	76.0
4. BEAM WATTS	850.9	852.3	850.9	850.9	850.9	850.9
5. MOD ANODE VOLTS	250	250	250	250	251	250
6. MA	-.0	-.0	.0	-.0	.0	-.0
7. WATTS	.0	.0	.0	.0	.0	.0
8. HEATER VOLTS	3.29	3.29	3.29	3.29	3.29	3.29
9. AMPS	1.29	1.29	1.29	1.29	1.29	1.29
10. WATTS	4.24	4.24	4.24	4.24	4.24	4.24
11. NASA OUTPUT SENSOR MV	-.1	-.1	.0	-.1	-.1	-.1
12. NASA REVERSE SENSOR MV	.0	.0	.0	-.1	-.1	.0
13. REVERSE POWER SIGNAL DBM	.0	.0	.0	.0	.0	.0
14. VACUUM(VAUNS=LOG(N/M^3))	14.5	14.4	14.5	14.5	14.5	14.5
15. BASEPLATE CALORIMETER W	.0	.0	.0	.0	.0	.0
16. RF OUTPUT CALORIMETER W	120.1	111.6	107.4	107.4	103.2	200.4
17. RF DRIVE DBM	27.6	27.6	27.6	27.6	27.6	26.0
18. MW	579.4	580.8	571.5	572.8	570.2	400.9
19. OUTPUT POWER DBM	51.2	50.8	50.6	50.6	50.6	53.1
20. WATTS	130.3	120.7	115.1	114.8	115.6	205.1
21. GAIN DB	23.5	23.2	23.0	23.0	23.1	27.1
22. TOTAL COLLECTOR MA	67.7	67.6	68.0	68.5	69.4	69.8
BODY LOSSES:						
23. INTERCEPTION MA	8.9	8.8	8.6	8.1	7.3	6.7
24. WATTS	59.7	59.4	57.6	54.7	48.8	44.8
25. RF LOSS WATTS	45.6	42.3	40.3	40.2	40.5	71.8
26. TOTAL WATTS	105.3	101.6	97.9	94.9	89.2	116.6
27. RESIDUAL BEAM POWER AT COLLECTOR WATTS	615.3	630.0	638.0	641.2	646.0	529.2
28. TOTAL HV INPUT WATTS	413.5	406.6	399.8	394.4	382.9	470.7
29. OUTPUT+INTCPT+LOSS W	235.6	222.3	212.9	209.7	204.9	321.7
30. COLLECTOR DISSIP. W	177.9	184.2	186.9	184.7	178.0	149.0
31. AVGE. IMPACT VOLTS	2629	2723	2750	2697	2566	2136
32. COLLECTOR EFFICIENCY PCT	71.1	70.8	70.7	71.2	72.4	71.8
33. OVERALL EFFIC INCL HTR	31.2	29.4	28.5	28.8	29.9	43.2
35. ELECTRONIC EFFIC. PCT	20.7	19.1	18.3	18.2	18.3	32.5
36. NASA DEF. PCT	15.3	14.2	13.5	13.5	13.6	24.1
37. THERMISTOR NO. 1 DEG C	66.0	66.4	66.6	66.5	65.9	65.4
38. THERMISTOR NO. 2 DEG C	285.1	285.1	285.1	285.1	285.1	285.1
39. THERMISTOR NO. 3 DEG C	57.3	57.2	57.2	57.2	57.3	56.9
40. THERMISTOR NO. 4 DEG C	68.4	67.6	67.0	66.4	66.0	70.5

REV A

Col. 1 to 5 Sat. Drive +4.5 dB

Col. 1 to 6 38.6°C Base Plate

Col. 6 - Reference Only

II(c)

TUBE # L-5394 #2022R-1 , TEST DATE 23APR75 (2), SHEET 4 NAS 3-15230

COLLECTOR VOLTAGES RELATIVE TO CATHODE: NO.						
1	11180	11201	11182	11181	11182	11168
2	8959	8961	8960	8956	8960	8931
3	7858	7869	7865	7858	7865	7795
4	6714	6749	6720	6743	6743	6693
5	5583	5612	5585	5625	5627	5615
6	4452	4488	4444	4493	4493	4509
7	3393	3415	3390	3384	3414	3445
8	2204	2225	2201	2185	2189	2294
9	1115	1147	1118	1084	1093	1154
10	0	0	0	0	0	0
COLLECTOR CURRENTS, MA: NO.						
1	2.6	2.4	2.4	2.4	2.3	3.6
2	2.7	2.5	2.5	2.5	2.4	4.7
3	7.0	6.1	6.0	6.0	5.9	15.0
4	8.7	8.1	8.1	8.3	8.5	14.1
5	5.0	5.0	4.8	4.6	4.5	4.3
6	9.0	9.5	9.5	9.5	9.5	5.6
7	12.4	12.8	12.7	12.0	10.8	8.0
8	13.1	14.2	14.3	14.3	14.8	7.1
9	8.3	8.0	8.6	10.0	11.7	8.4
10	-1.0	-.9	-.9	-1.0	-1.1	-.9
COLLECTOR INPUT POWERS, WATTS: NO.						
1	28.7	27.2	26.9	27.2	26.1	40.4
2	24.5	22.5	22.1	22.0	21.5	41.9
3	54.9	48.1	47.3	47.2	46.5	116.6
4	58.1	54.9	54.3	55.8	57.5	94.6
5	27.9	28.1	26.7	25.7	25.3	24.0
6	40.0	42.5	42.4	42.7	42.7	25.1
7	41.9	43.6	43.1	40.5	36.9	27.4
8	28.8	31.5	31.5	31.3	32.4	16.2
9	9.3	9.1	9.6	10.9	12.8	9.7
10	.0	.0	.0	.0	.0	.0
COLLECTOR DISSIPATIONS, WATTS: NO.						
1	6.8	6.6	6.5	6.6	6.0	7.7
2	7.2	6.8	6.8	6.6	6.2	10.0
3	18.4	16.6	16.5	16.2	15.2	32.0
4	22.7	22.2	22.2	22.3	21.9	30.2
5	13.1	13.6	13.1	12.3	11.5	9.1
6	23.6	25.8	26.2	25.6	24.4	11.9
7	32.5	34.8	34.9	32.3	27.7	17.0
8	34.3	38.6	39.3	38.6	38.0	15.1
9	21.9	21.7	23.7	27.0	30.0	18.0
10	2.6	2.5	2.6	2.8	2.8	2.0

REV A

II(d)

TUBE # L-5394 #2022R-1 , TEST DATE 23APR75 (2), SHEET 5 NAS 3-15830

COL. #:	1	2	3	4	5	6
1. FREQUENCY, GHZ	12.030	12.040	12.050	12.060	12.070	12.080
2. CATHODE VOLTS	11218	11197	11197	11197	11218	11197
3. MA	76.0	76.0	76.0	76.0	76.0	76.0
4. BEAM WATTS	852.4	851.0	850.9	850.9	852.5	851.0
5. MOD ANODE VOLTS	250	250	250	250	251	250
6. MA	.0	-.0	.0	-.0	-.0	.0
7. WATTS	.0	.0	.0	.0	.0	.0
8. HEATER VOLTS	3.29	3.29	3.29	3.29	3.29	3.29
9. AMPS	1.29	1.29	1.29	1.29	1.29	1.29
10. WATTS	4.24	4.24	4.24	4.24	4.24	4.24
11. NASA OUTPUT SENSOR MV	-.1	-.1	.0	-.1	-.1	-.1
12. NASA REVERSE SENSOR MV	.0	.0	-.1	.0	-.1	-.1
13. REVERSE POWER SIGNAL DBM	.0	.0	.0	.0	.0	.0
14. VACUUM(VAURS=LOG(N/M^3))	14.5	14.4	14.5	14.5	14.5	14.5
15. BASEPLATE CALORIMETER W	.0	.0	.0	.0	.0	.0
16. RF OUTPUT CALORIMETER W	225.8	230.0	230.0	225.8	221.6	204.7
17. RF DRIVE DBM	26.0	26.0	26.0	26.0	26.0	26.0
18. MW	398.1	399.0	401.8	401.8	401.8	401.8
19. OUTPUT POWER DBM	53.6	53.7	53.6	53.5	53.4	53.2
20. WATTS	230.7	233.3	227.0	222.8	220.3	209.9
21. GAIN DB	27.6	27.7	27.5	27.4	27.4	27.2
22. TOTAL COLLECTOR MA	71.7	71.7	71.2	71.0	70.7	70.3
BODY LOSSES:						
23. INTERCEPTION MA	4.8	4.8	5.2	5.6	5.9	6.2
24. WATTS	32.0	32.2	34.8	37.6	39.6	41.8
25. RF LOSS WATTS	80.7	81.7	79.4	78.0	77.1	73.5
26. TOTAL WATTS	112.7	113.9	114.2	115.6	116.7	115.3
27. RESIDUAL BEAM POWER AT COLLECTOR WATTS	509.0	503.7	509.7	512.4	515.5	525.9
28. TOTAL HV INPUT WATTS	486.3	485.7	484.5	480.5	476.7	469.9
29. OUTPUT+INTCPT+LOSS #	343.4	347.3	341.2	338.5	337.0	325.1
30. COLLECTOR DISSIP. #	142.9	138.5	143.2	142.1	139.6	144.7
31. AVG. IMPACT VOLTS	1993	1932	2013	2000	1976	2059
32. COLLECTOR EFFICIENCY PCT	71.9	72.5	71.9	72.3	72.9	72.5
33. OVERALL EFFIC INCL HTR	47.3	47.6	46.4	46.0	45.8	44.3
35. ELECTRONIC EFFIC. PCT	36.5	37.0	36.0	35.4	34.9	33.3
36. NASA DEF. PCT	27.1	27.4	26.7	26.2	25.8	24.7
37. THERMISTOR NO. 1 DEG C	64.2	62.7	62.3	62.5	62.9	63.6
38. THERMISTOR NO. 2 DEG C	285.1	274.1	285.1	285.1	285.1	285.1
39. THERMISTOR NO. 3 DEG C	57.8	57.9	57.9	57.8	58.1	58.1
40. THERMISTOR NO. 4 DEG C	73.9	74.6	74.8	74.8	74.7	74.2

COL. 1 SAT DRIVE POWER +3DB
COL. 2 38.6 DEGREES C BASE PLATE

LITTON 10 REV. A

Col. 1 to 6 Sat Drive Power +3 dB = +26 dBm

II(e)

TUBE # L-5394 #2022R-1 , TEST DATE 23APR75 (2), SHEET 6 NAS 3-15830

COLLECTOR VOLTAGES RELATIVE TO CATHODE:

NO.						
1	11205	11184	11185	11185	11207	11187
2	8949	8936	8935	8937	8944	8935
3	7854	7821	7818	7820	7824	7826
4	6715	6701	6706	6705	6741	6709
5	5611	5595	5604	5605	5634	5609
6	4530	4509	4519	4512	4545	4504
7	3428	3387	3363	3376	3359	3361
8	2296	2246	2248	2237	2257	2213
9	1066	1032	1058	1067	1092	1082
10	0	0	0	0	0	0

COLLECTOR CURRENTS, MA:

NO.						
1	4.0	4.0	4.0	3.9	3.8	3.7
2	5.2	5.3	5.3	5.1	5.0	4.8
3	15.7	16.5	16.5	16.5	16.1	15.2
4	17.2	16.6	16.3	15.6	15.0	14.6
5	5.7	5.4	5.1	4.8	4.6	4.3
6	5.4	5.5	5.0	5.0	5.2	5.6
7	5.9	6.0	6.5	7.0	7.4	7.7
8	4.1	3.8	3.9	4.4	5.4	6.9
9	15.8	15.4	13.5	10.9	9.6	8.5
10	-7.3	-6.8	-5.0	-2.2	-1.3	-.9

COLLECTOR INPUT POWERS, WATTS:

NO.						
1	44.5	45.0	44.6	43.5	42.5	40.9
2	46.4	47.4	47.0	45.8	44.4	43.0
3	123.4	129.1	129.3	129.1	125.6	119.1
4	115.6	111.0	109.2	104.5	101.3	97.7
5	31.8	30.0	28.4	27.0	25.6	24.0
6	24.6	24.7	22.8	22.7	23.6	25.0
7	20.2	20.4	22.1	23.6	24.8	25.9
8	9.5	8.6	8.8	9.9	12.2	15.3
9	17.2	15.9	14.3	11.6	10.5	9.2
10	.0	.0	.0	.0	.0	.0

COLLECTOR DISSIPATIONS, WATTS:

NO.						
1	7.9	7.8	8.0	7.8	7.5	7.5
2	10.3	10.2	10.6	10.3	9.8	9.9
3	31.3	31.9	33.3	33.0	31.7	31.3
4	34.3	32.0	32.8	31.2	29.7	30.0
5	11.3	10.4	10.2	9.6	9.0	8.8
6	10.8	10.6	10.1	10.1	10.3	11.4
7	11.7	11.6	13.1	14.0	14.6	15.9
8	8.2	7.4	7.9	8.8	10.7	14.2
9	31.5	29.7	27.2	21.9	18.9	17.5
10	14.5	13.1	10.0	4.5	2.6	1.9

LITTON 10 REV. A

II(f)

TUBE # L-5394 #2022R-1 . TEST DATE 23APR75 (2). SHEET 7 W/S 3-15000

	COL. #	1	2	3	4	5
1.	FREQUENCY, GHZ	12.090	12.100	12.110	12.120	12.130
2.	CATHODE VOLTS	11218	11218	11197	11197	11218
3.	MA	76.0	76.0	76.0	76.0	76.0
4.	BEAM WATTS	852.5	852.5	851.0	851.0	852.5
5.	MOD ANODE VOLTS	250	250	251	250	250
6.	MA	.0	-.0	-.0	-.0	-.0
7.	WATTS	.0	.0	.0	.0	.0
8.	HEATER VOLTS	3.29	3.29	3.29	3.29	3.29
9.	AMPS	1.29	1.29	1.29	1.29	1.29
10.	WATTS	4.24	4.24	4.24	4.24	4.24
11.	NASA OUTPUT SENSOR MV	-.1	-.1	-.1	-.1	-.1
12.	NASA REVERSE SENSOR MV	.0	.0	.0	-.1	-.1
13.	REVERSE POWER SIGNAL DBM	.0	.0	.0	.0	.0
14.	VACUUM(VAUNS=LOG(W/W*3))	14.5	14.5	14.5	14.5	14.5
15.	BASEPLATE CALORIMETER W	.0	.0	.0	.0	.0
16.	RF OUTPUT CALORIMETER W	196.2	183.5	175.1	166.6	158.1
17.	RF DRIVE DBM	26.0	26.0	26.0	26.0	26.0
18.	MW	401.8	400.9	396.3	395.4	395.4
19.	OUTPUT POWER DBM	53.0	52.7	52.5	52.3	52.1
20.	WATTS	198.2	187.9	175.9	169.7	160.5
21.	GAIN DB	26.9	26.7	26.5	26.3	26.1
22.	TOTAL COLLECTOR MA	70.1	70.3	70.6	71.2	71.8
	BODY LOSSES:					
23.	INTERCEPTION MA	6.4	6.2	5.9	5.3	4.6
24.	WATTS	42.9	42.0	39.8	35.8	31.0
25.	RF LOSS WATTS	69.4	65.8	61.6	59.4	56.2
26.	TOTAL WATTS	112.3	107.8	101.3	95.2	87.2
27.	RESIDUAL BEAM POWER AT COLLECTOR WATTS	542.1	556.8	573.7	586.1	604.8
28.	TOTAL HV INPUT WATTS	464.1	453.4	441.5	425.5	408.8
29.	OUTPUT+INTCPT+LOSS W	310.4	295.7	277.3	264.9	247.8
30.	COLLECTOR DISSIP. W	153.6	157.7	164.3	160.6	161.0
31.	AVG. IMPACT VOLTS	2192	2243	2327	2257	2242
32.	COLLECTOR EFFICIENCY PCT	71.7	71.7	71.4	72.6	73.4
33.	OVERALL EFFIC INCL HTR	42.3	41.1	39.5	39.5	38.9
35.	ELECTRONIC EFFIC. PCT	31.4	29.8	27.9	26.9	25.4
36.	NASA DEF. PCT	23.2	22.0	20.7	19.9	18.8
37.	THERMISTOR NO. 1 DEG C	64.0	64.4	64.5	64.1	63.3
38.	THERMISTOR NO. 2 DEG C	285.1	285.1	285.1	285.1	285.1
39.	THERMISTOR NO. 3 DEG C	58.0	57.8	57.6	57.7	57.8
40.	THERMISTOR NO. 4 DEG C	73.8	73.2	72.5	71.9	71.2

Col. 1 to Col. 6 Sat Drive Power +3 dB = +26 dBm

Col. 1 to Col. 6 38.6°C Base Plate

II(g)

TUBE # L-5394 #2022R-1 . TEST DATE 23APR75 (2). SHEET 8 W/S 3-15000

COLLECTOR VOLTAGES RELATIVE TO CATHODE:

NO.	1	2	3	4	5
1	11208	11209	11190	11190	11213
2	8963	8962	8948	8946	8970
3	7848	7849	7836	7830	7859
4	6733	6742	6731	6731	6748
5	5617	5605	5600	5598	5617
6	4504	4465	4463	4477	4486
7	3367	3367	3334	3337	3365
8	2240	2236	2219	2206	2205
9	1146	1137	1142	1122	1118
10	0	0	0	0	0

COLLECTOR CURRENTS, MA:

NO.	1	2	3	4	5
1	3.5	3.2	3.2	3.0	2.9
2	4.5	4.1	3.9	3.6	3.4
3	14.7	14.1	13.7	13.3	12.5
4	13.4	12.0	11.3	11.0	10.5
5	4.5	4.9	4.9	4.4	4.2
6	6.2	7.0	7.3	7.4	7.7
7	8.1	8.8	9.0	8.6	7.9
8	8.4	9.1	9.9	11.3	12.5
9	7.7	7.7	8.4	9.5	11.1
10	-.8	-.8	-.9	-.9	-.9

COLLECTOR INPUT POWERS, WATTS:

NO.	1	2	3	4	5
1	39.3	37.1	35.4	33.6	32.7
2	40.0	36.9	34.7	32.2	30.8
3	115.1	110.7	107.4	104.0	98.1
4	90.3	81.2	76.2	74.0	70.7
5	25.1	27.5	27.2	24.6	23.6
6	27.7	31.4	32.8	33.1	34.5
7	27.4	29.6	30.0	28.6	26.7
8	18.8	20.3	21.9	25.0	27.6
9	8.8	8.8	9.6	10.6	12.4
10	.0	.0	.0	.0	.0

COLLECTOR DISSIPATIONS, WATTS:

NO.	1	2	3	4	5
1	7.7	7.4	7.4	6.8	6.5
2	9.8	9.2	9.0	8.1	7.7
3	32.2	31.6	31.9	30.0	28.0
4	29.4	27.0	26.3	24.8	23.5
5	9.8	11.0	11.3	9.9	9.4
6	13.5	15.7	17.0	16.7	17.3
7	17.8	19.7	21.0	19.4	17.8
8	16.4	20.3	23.0	25.6	28.0
9	16.8	17.4	19.5	21.3	24.8
10	1.7	1.7	2.1	2.0	2.0

II(h)

TUBE # L-5394 #2022R-1 . TEST DATE 23APR75 (2). SHEET 9 NAS 3-15830

COL. #:	1	2	3	4	5	6
1. FREQUENCY, GHZ	12.030	12.040	12.050	12.060	12.070	12.080
2. CATHODE VOLTS	11218	11218	11197	11218	11218	11218
3. MA	76.0	76.0	76.0	76.0	76.0	76.0
4. BEAM WATTS	852.5	852.5	851.1	852.5	852.5	852.5
5. 2ND ANODE VOLTS	251	251	251	251	251	251
6. MA	-.0	-.0	-.0	-.0	-.0	-.0
7. WATTS	.0	.0	.0	.0	.0	.0
8. HEATER VOLTS	3.29	3.29	3.29	3.29	3.29	3.29
9. AMPS	1.29	.29	1.29	1.29	1.29	1.29
10. WATTS	4.24	4.24	4.24	4.24	4.24	4.24
11. NASA OUTPUT SENSOR MV	-.1	.0	-.1	-.1	.0	-.1
12. NASA REVERSE SENSOR MV	.0	.0	.0	-.1	.0	.0
13. REVERSE POWER SIGNAL DBM	.0	-.0	.0	.0	.0	.0
14. VACUUM(VAUNS=LOG(A/M^3))	14.5	14.5	14.5	14.5	14.5	14.5
15. BASEPLATE CALORIMETER W	.0	.0	.0	.0	.0	.0
16. RF OUTPUT CALORIMETER W	230.0	234.2	236.5	234.2	230.0	225.8
17. RF DRIVE DBM	23.0	23.0	23.0	23.0	23.0	23.0
18. MW	198.7	199.7	201.1	200.9	201.3	201.3
19. OUTPUT POWER DBM	53.8	53.8	53.7	53.6	53.6	53.6
20. WATTS	237.5	239.6	232.8	231.3	229.0	227.4
21. GAIN DB	30.8	30.8	30.6	30.6	30.6	30.5
22. TOTAL COLLECTOR MA	73.4	72.5	73.5	73.4	73.2	73.3
BODY LOSSES:						
23. INTERCEPTION MA	3.2	3.1	3.2	3.2	3.4	3.4
24. WATTS	21.5	21.1	21.2	21.7	22.7	23.1
25. RF LOSS WATTS	83.1	83.8	81.5	80.9	80.1	79.6
26. TOTAL WATTS	104.7	105.0	102.7	102.7	102.8	102.7
27. RESIDUAL BEAM POWER AT COLLECTOR WATTS	510.3	508.0	515.7	518.6	520.7	522.5
28. TOTAL HV INPUT WATTS	472.9	469.6	474.0	471.5	467.9	463.8
29. OUTPUT+INTCPT+LOSS W	342.2	344.5	335.5	333.9	331.8	330.0
30. COLLECTOR DISSIP. W	130.6	125.0	138.5	137.5	136.1	133.8
31. AVGE. IMPACT VOLTS	1780	1726	1865	1874	1859	1826
32. COLLECTOR EFFICIENCY PCT	74.4	75.4	73.1	73.5	73.9	74.4
33. OVERALL EFFIC INCL HTR	49.8	50.6	48.7	48.6	48.5	48.6
35. ELECTRONIC EFFIC. PCT	37.6	37.9	36.9	36.6	36.3	36.0
36. NASA DEF. PCT	27.9	28.1	27.3	27.1	26.9	26.7
37. THERMISTOR NO. 1 DEG C	60.0	59.6	59.4	59.2	59.2	59.3
38. THERMISTOR NO. 2 DEG C	285.1	285.1	300.1	300.1	300.1	285.1
39. THERMISTOR NO. 3 DEG C	57.9	57.9	58.1	58.2	58.1	58.3
40. THERMISTOR NO. 4 DEG C	73.8	74.1	74.3	74.4	74.4	74.3

REV. A

Col. 1 to Col. 6 Sat Drive Power-+23 dBm

Col. 1 to Col. 6 38.6°C Base Plate

II(i)

TUBE # L-5394 #2022R-1 . TEST DATE 23APR75 (2). SHEET 10 NAS 3-15830

COLLECTOR VOLTAGES RELATIVE TO CATHODE:

NO.						
1	11195	11194	11174	11195	11195	11194
2	8959	8957	8934	8954	8953	8952
3	7853	7852	7831	7850	7848	7846
4	6723	6691	6691	6736	6737	6717
5	5630	5595	5611	5668	5665	5628
6	4531	4480	4502	4546	4538	4496
7	3329	3349	3337	3349	3340	3350
8	2259	2268	2253	2258	2249	2277
9	1100	1061	1047	1078	1087	1138
10	0	0	0	0	0	0

COLLECTOR CURRENTS, MA:

NO.						
1	4.0	4.1	4.2	4.1	4.1	4.0
2	5.4	5.8	6.0	6.0	6.0	5.9
3	15.0	15.9	16.4	16.3	16.5	16.3
4	18.6	18.7	18.9	18.5	17.8	17.1
5	6.2	4.9	4.6	4.2	3.9	4.0
6	3.8	3.5	3.3	3.5	3.7	4.1
7	5.4	4.4	4.2	4.4	4.5	4.7
8	6.2	4.8	4.8	5.1	5.6	6.7
9	14.8	17.1	17.2	16.1	14.0	11.7
10	-6.1	-6.7	-6.0	-4.8	-2.8	-1.2

COLLECTOR INPUT POWERS, WATTS:

NO.						
1	44.9	46.2	46.9	46.0	45.3	44.7
2	48.4	51.6	53.4	53.3	53.6	53.1
3	118.1	124.8	128.7	128.0	129.3	127.5
4	125.2	125.1	125.1	124.7	120.0	114.9
5	34.8	27.2	25.8	23.9	22.3	22.7
6	17.3	15.6	15.0	16.0	16.9	18.3
7	18.1	14.9	14.1	14.6	14.9	15.6
8	13.9	10.8	10.7	11.4	12.5	15.2
9	16.2	18.1	18.0	17.4	15.2	13.3
10	.0	.0	.0	.0	.0	.0

COLLECTOR DISSIPATIONS, WATTS:

NO.						
1	7.1	7.1	7.9	7.7	7.5	7.3
2	9.6	9.9	11.3	11.1	11.1	10.8
3	26.8	27.4	31.0	30.4	30.6	29.7
4	33.2	32.3	35.5	34.7	33.1	31.2
5	11.0	8.4	8.6	7.9	7.3	7.4
6	6.8	6.0	6.3	6.6	6.9	7.4
7	9.7	7.7	8.0	8.2	8.3	8.5
8	11.0	8.2	9.0	9.5	10.3	12.2
9	26.3	29.5	32.3	30.2	26.1	21.4
10	10.8	11.5	11.3	8.9	5.3	2.2

REV. A

II(j)

TUBE # L-5394 #2022R-1 . TEST DATE 23APR75 (2). SHEET 11 NAS 3-15830

	COL. #:	1	2	3	4	5
1.	FREQUENCY, GHZ	12.089	12.100	12.110	12.120	12.130
2.	CATHODE VOLTS	11197	11218	11197	11197	11197
3.	MA	76.0	76.0	76.0	76.0	76.0
4.	BEAM WATTS	851.0	852.6	851.0	851.0	851.0
5.	MOD ANODE VOLTS	250	250	251	250	251
6.	MA	-.0	-.0	-.0	-.0	-.0
7.	WATTS	.0	.0	.0	.0	.0
8.	HEATER VOLTS	3.29	3.29	3.29	3.29	3.29
9.	AMPS	1.29	1.29	1.29	1.29	1.29
10.	WATTS	4.24	4.24	4.24	4.24	4.24
11.	NASA OUTPUT SENSOR MV	-.1	-.1	-.1	-.1	-.1
12.	NASA REVERSE SENSOR MV	-.1	.0	.0	-.1	-.1
13.	REVERSE POWER SIGNAL DBM	-.0	.0	-.0	.0	-.0
14.	VACUUM(VAURS=LOG(N/M^3))	14.5	14.5	14.5	14.4	14.5
15.	BASEPLATE CALORIMETER W	.0	.0	.0	.0	.0
16.	RF OUTPUT CALORIMETER W	221.6	217.3	208.9	187.7	166.6
17.	RF DRIVE DBM	23.0	23.0	23.0	23.0	23.0
18.	MW	201.2	200.4	201.0	198.3	197.7
19.	OUTPUT POWER DBM	53.5	53.5	53.3	52.8	52.3
20.	WATTS	223.6	222.0	213.6	190.9	169.3
21.	GAIN DB	30.5	30.4	30.3	29.8	29.3
22.	TOTAL COLLECTOR MA	73.1	73.2	73.4	73.6	74.1
	BODY LOSSES:					
23.	INTERCEPTION MA	3.5	3.5	3.3	3.0	2.7
24.	WATTS	23.7	23.7	22.2	20.0	17.9
25.	RF LOSS WATTS	78.3	77.7	74.8	66.8	59.2
26.	TOTAL WATTS	102.0	101.4	96.9	86.8	77.2
27.	RESIDUAL BEAM POWER AT COLLECTOR WATTS	525.4	529.2	540.5	573.3	604.5
28.	TOTAL HV INPUT WATTS	463.1	464.3	450.5	424.6	395.5
29.	OUTPUT+INTCPT+LOSS W	325.6	323.4	310.5	277.7	246.5
30.	COLLECTOR DISSIP. W	137.5	140.9	140.0	146.9	149.0
31.	AVGE. IMPACT VOLTS	1882	1925	1908	1995	2011
32.	COLLECTOR EFFICIENCY PCT	73.8	73.4	74.1	74.4	75.4
33.	OVERALL EFFIC INCL HTR	47.8	47.4	47.0	44.5	42.4
35.	ELECTRONIC EFFIC. PCT	35.5	35.2	33.9	30.3	26.9
36.	NASA DEF. PCT	26.3	26.0	25.1	22.4	19.9
37.	THERMISTOR NO. 1 DEG C	59.7	60.1	60.4	60.2	59.4
38.	THERMISTOR NO. 2 DEG C	265.1	300.1	285.1	285.1	285.1
39.	THERMISTOR NO. 3 DEG C	58.3	58.1	56.2	58.2	57.9
40.	THERMISTOR NO. 4 DEG C	74.2	74.1	73.8	73.3	72.4

Col. 1 to Col. 6 Set Drive Power- +23 dBm

Col. 1 to Col. 6 38.6°C Base Plate

REV. A

II(k)

TUBE # L-5394 #2022R-1 . TEST DATE 23APR75 (2). SHEET 12 NAS 3-15830

COLLECTOR VOLTAGES RELATIVE TO CATHODE:

NO.					
1	11175	11196	11177	11180	11182
2	8933	8949	8933	8941	8960
3	7823	7835	7814	7820	7856
4	6707	6733	6717	6725	6735
5	5620	5637	5614	5608	5586
6	4490	4497	4470	4461	4462
7	3306	3314	3286	3283	3316
8	2243	2266	2260	2220	2179
9	1140	1166	1162	1126	1074
10	0	0	0	0	0

COLLECTOR CURRENTS, MA:

NO.					
1	4.0	3.9	3.7	3.5	3.2
2	5.9	5.8	5.3	4.6	4.0
3	16.3	17.4	17.4	15.8	13.7
4	16.5	15.1	13.7	12.3	10.8
5	4.1	3.9	4.0	4.0	4.1
6	4.5	4.9	5.4	5.8	6.4
7	5.0	5.5	5.7	5.7	5.6
8	7.5	8.1	9.0	10.7	12.4
9	10.2	9.4	10.2	12.1	14.8
10	-.9	-.8	-.9	-1.0	-1.0

COLLECTOR INPUT POWERS, WATTS:

NO.					
1	44.4	44.0	41.6	38.8	35.6
2	53.0	51.8	47.2	41.4	36.2
3	127.7	136.0	135.6	123.7	107.6
4	110.3	101.5	92.0	82.7	72.8
5	23.2	21.7	22.5	22.7	23.0
6	20.3	22.1	24.0	25.8	28.8
7	16.4	18.4	18.7	18.8	18.6
8	16.8	18.4	20.3	23.8	27.0
9	11.6	11.0	11.9	13.6	15.9
10	.0	.0	.0	.0	.0

COLLECTOR DISSIPATIONS, WATTS:

NO.					
1	7.5	7.6	7.1	6.9	6.4
2	11.2	11.1	10.1	9.2	8.1
3	30.7	33.4	33.1	31.6	27.5
4	31.0	29.0	26.1	24.5	21.7
5	7.8	7.4	7.6	8.1	8.3
6	8.5	9.4	10.2	11.5	12.9
7	9.3	10.7	10.8	11.4	11.3
8	14.1	15.6	17.1	21.4	24.9
9	19.2	18.1	19.5	24.1	29.8
10	1.6	1.5	1.7	1.9	2.0

REV. A

II(1)

TUBE # L-5394 #2022R-1 . TEST DATE 23APR75 (2). SHEET 13 NAS 3-15830

COL. #:	1	2	3	4	5	6
1. FREQUENCY, GHZ	12.030	12.040	12.050	12.061	12.070	12.080
2. CATHODE VOLTS	11197	11197	11218	11218	11218	11218
3. MA	76.0	76.0	76.0	76.0	76.0	76.0
4. BEAM WATTS	850.9	850.9	852.4	852.4	852.4	852.4
5. MOD ANODE VOLTS	250	250	250	250	250	250
6. MA	.0	.0	-.0	-.0	.0	.0
7. WATTS	.0	.0	.0	.0	.0	.0
8. HEATER VOLTS	3.29	3.29	3.29	3.29	3.29	3.29
9. AMPS	1.29	1.29	1.29	1.29	1.29	1.29
10. WATTS	4.24	4.24	4.24	4.24	4.24	4.24
11. NASA OUTPUT SENSOR MV	.0	-.1	-.1	-.1	-.1	-.1
12. NASA REVERSE SENSOR MV	.0	-.1	.0	.0	.0	-.1
13. REVERSE POWER SIGNAL DBM	.0	.0	.0	.0	-.0	.0
14. VACUUM(VAUNS=LOG(N/M^3))	14.5	14.5	14.5	14.5	14.5	14.5
15. BASEPLATE CALORIMETER W	.0	.0	.0	.0	.0	.0
16. RF OUTPUT CALORIMETER W	103.2	103.2	86.3	77.8	82.0	86.3
17. RF DRIVE DBM	15.4	15.4	15.4	15.4	15.5	15.4
18. MW	34.6	34.8	34.8	35.0	35.1	35.1
19. OUTPUT POWER DBM	50.9	50.9	50.3	49.8	50.1	50.3
20. WATTS	123.3	122.5	106.3	95.7	102.9	107.1
21. GAIN DB	35.5	35.5	34.8	34.4	34.7	34.8
22. TOTAL COLLECTOR MA	74.9	74.8	75.0	75.1	75.2	74.9
BODY LOSSES:						
23. INTERCEPTION MA	2.0	1.9	1.8	1.8	1.8	1.8
24. WATTS	13.4	13.0	12.2	11.6	12.1	12.4
25. RF LOSS WATTS	43.2	42.9	37.2	33.5	36.0	37.5
26. TOTAL WATTS	56.6	55.9	49.5	45.3	48.1	49.9
27. RESIDUAL BEAM POWER AT COLLECTOR WATTS	671.0	672.5	696.7	711.4	701.4	695.5
28. TOTAL HV INPUT WATTS	314.9	313.8	296.5	287.1	294.9	299.9
29. OUTPUT+INTCPT+LOSS "	179.9	178.4	155.7	141.0	151.0	156.9
30. COLLECTOR DISSIP. "	135.0	135.4	140.7	146.1	143.9	142.9
31. AVGE. IMPACT VOLTS	1803	1810	1277	1944	19.4	1907
32. COLLECTOR EFFICIENCY PCT	79.9	79.9	79.8	79.5	79.5	79.4
33. OVERALL EFFIC INCL HTR	36.6	38.5	35.3	32.8	34.4	35.2
35. ELECTRONIC EFFIC. PCT	19.6	19.4	16.8	15.2	16.3	17.0
36. NASA DEF. PCT	14.5	14.4	12.5	1 .2	12.1	12.6
37. THERMISTOR NO. 1 DEG C	51.2	51.5	51.4	5 .2	51.0	51.0
38. THERMISTOR NO. 2 DEG C	285.1	265.1	295.1	285.1	300.1	295.1
39. THERMISTOR NO. 3 DEG C	54.3	54.5	54.5	54.5	54.4	54.4
40. THERMISTOR NO. 4 DEG C	58.5	58.8	58.6	58.3	58.1	58.1

REV. A

Col. 1 to Col. 6 Sat Drive -3 dB = +15.4 dBm

Col. 1 to Col. 6 38.6°C Base Plate

II(m)

TUBE # L-5394 #2022R-1 . TEST DATE 23APR75 (2). SHEET 14 NAS 3-15830

COLLECTOR VOLTAGES RELATIVE TO CATHODE:

NO.	1	2	3	4	5	6
1	11190	11190	11213	11214	11213	11213
2	8921	8923	8950	8949	8944	8949
3	7843	7844	7874	7885	7871	7874
4	6681	6686	6715	6716	6715	6709
5	5571	5571	5587	5590	5591	5593
6	4447	4449	4457	4455	4463	4466
7	3368	3350	3343	3345	3350	3367
8	2196	2184	2205	2210	2234	2236
9	1125	1150	1142	1131	1125	1127
10	0	0	0	0	0	0

COLLECTOR CURRENTS, MA:

NO.	1	2	3	4	5	6
1	2.2	2.1	1.9	1.5	1.8	1.9
2	2.2	2.1	1.8	1.6	1.7	1.8
3	4.3	4.4	3.2	2.7	3.2	3.8
4	9.2	9.0	8.0	7.5	8.1	8.5
5	4.1	4.0	3.9	4.0	4.0	4.0
6	6.4	6.3	6.9	7.1	6.8	6.5
7	10.8	11.1	12.4	12.9	12.8	12.4
8	22.3	24.3	23.4	22.0	20.0	18.4
9	14.3	12.4	14.4	16.5	17.2	18.2
10	-1.1	-.8	-.7	-.5	-.5	-.5

COLLECTOR INPUT POWERS, WATTS:

NO.	1	2	3	4	5	6
1	24.6	23.9	20.1	18.3	20.2	21.5
2	19.4	19.0	15.8	14.2	15.4	16.5
3	33.9	34.6	24.8	20.9	24.8	29.7
4	61.5	60.1	53.8	50.2	54.6	57.0
5	22.8	22.5	21.7	22.1	22.3	22.3
6	28.5	27.8	30.5	31.5	30.4	28.9
7	36.5	37.1	41.3	43.0	43.0	41.8
8	49.1	53.0	51.5	48.5	44.6	41.1
9	16.1	14.2	16.5	19.6	19.4	20.5
10	.0	.0	.0	.0	.0	.0

COLLECTOR DISSIPATIONS, WATTS:

NO.	1	2	3	4	5	6
1	4.0	3.9	3.4	3.2	3.4	3.7
2	3.9	3.9	3.3	3.1	3.3	3.5
3	7.8	8.0	5.9	5.2	6.0	7.2
4	16.6	16.3	15.0	14.5	15.6	16.2
5	7.4	7.3	7.3	7.7	7.6	7.6
6	11.6	11.3	12.9	13.7	13.0	12.3
7	19.5	20.0	23.2	25.0	24.6	23.7
8	40.3	43.9	43.9	42.7	38.3	35.1
9	25.8	22.5	27.1	32.0	33.0	34.8
10	1.9	1.5	1.2	1.0	.9	1.0

REV. A

II(n)

TUBE # L-5394 #2022R-1 . TEST DATE 23APR75 (2). SHEET 15 NAS 3-15330

COL. #	1	2	3	4	5
1. FREQUENCY, GHZ	12.090	12.100	12.110	12.120	12.130
2. CATHODE VOLTS	11197	11218	11197	11197	11218
3. MA	76.0	76.0	76.0	76.0	76.0
4. BEAM WATTS	850.8	852.3	850.9	850.8	852.3
5. MOD ANODE VOLTS	250	251	251	250	250
6. MA	.0	.0	-.0	.0	-.0
7. WATTS	.0	.0	.0	10	.0
8. HEATER VOLTS	3.29	3.29	3.29	3.29	3.29
9. AMPS	1.29	1.29	1.29	1.29	1.29
10. WATTS	4.24	4.24	4.24	4.24	4.24
11. NASA OUTPUT SENSOR MV	-.1	-.1	-.1	.0	-.1
12. NASA REVERSE SENSOR MV	.0	-.1	10	-.1	10
13. REVERSE POWER SIGNAL DBM	.0	-.0	10	.0	.0
14. VACUUM(VAUNS=LOG(N/M^3))	14.5	14.5	14.5	14.5	14.5
15. BASEPLATE CALORIMETER W	.0	.0	.0	10	10
16. RF OUTPUT CALORIMETER W	82.0	86.3	86.3	56.7	18.6
17. RF DRIVE DBM	15.4	15.4	15.4	15.4	15.4
18. MW	35.0	35.0	34.5	34.5	34.4
19. OUTPUT POWER DBM	50.2	50.3	50.1	48.9	46.8
20. WATTS	104.1	106.1	102.9	78.5	47.6
21. GAIN DB	34.7	34.8	34.7	33.6	31.4
22. TOTAL COLLECTOR MA	74.9	74.9	74.9	75.0	75.2
BODY LOSSES:					
23. INTERCEPTION MA	1.9	1.9	1.9	1.8	1.7
24. WATTS	12.5	12.5	12.4	12.4	11.3
25. RF LOSS WATTS	36.4	37.1	36.0	27.5	16.7
26. TOTAL WATTS	48.9	49.6	48.4	39.8	28.0
27. RESIDUAL BEAM POWER AT COLLECTOR WATTS	697.8	696.6	699.5	732.5	776.7
28. TOTAL HV INPUT WATTS	293.5	296.8	296.9	268.3	227.1
29. OUTPUT+INTCPT+LOSS W	153.0	155.7	151.3	118.3	75.6
30. COLLECTOR DISSIP. W	140.5	141.1	145.6	149.9	151.5
31. AVGE. IMPACT VOLTS	1875	1883	1944	1999	2014
32. COLLECTOR EFFICIENCY PCT	79.9	79.7	79.2	79.5	80.5
33. OVERALL EFFIC INCL HTR	35.0	35.2	34.2	28.8	20.6
35. ELECTRONIC EFFIC. PCT	16.5	16.8	16.3	12.5	7.5
36. NASA DEF. PCT	12.2	12.4	12.1	9.2	5.6
37. THERMISTOR NO. 1 DEG C	50.9	50.9	51.1	51.0	50.4
38. THERMISTOR NO. 2 DEG C	285.1	285.1	300.1	300.1	285.1
39. THERMISTOR NO. 3 DEG C	54.3	54.3	54.3	54.2	54.1
40. THERMISTOR NO. 4 DEG C	58.0	57.9	57.8	57.3	56.4

Col. 1 to Col. 6 Sat Drive -3 dB = +15.4 dBm

Col. 1 to Col. 6 38.6°C Base Plate

Rev A

II(o)

TUBE # L-5394 #2022R-1 . TEST DATE 23APR75 (2). SHEET 16 NAS 3-15330

COLLECTOR VOLTAGES RELATIVE TO CATHODE:

NO.					
1	11192	11212	11191	11193	11220
2	8927	8945	8922	8929	8957
3	7849	7861	7833	7862	7895
4	6684	6708	6689	6700	6771
5	5561	5594	5578	5572	5609
6	4427	4470	4462	4447	4485
7	3331	3372	3333	3343	3362
8	2233	2267	2242	2239	2243
9	1082	1091	1055	1056	1053
10	0	0	0	0	0

COLLECTOR CURRENTS, MA:

NO.					
1	1.9	2.0	2.0	1.7	1.1
2	1.9	1.9	1.9	1.5	.9
3	3.9	4.5	4.7	2.5	1.3
4	8.4	8.7	9.1	7.4	3.4
5	3.9	3.9	4.0	3.8	3.4
6	6.3	6.1	5.9	6.1	6.0
7	11.9	11.1	10.5	11.0	10.7
8	15.9	13.9	13.6	15.4	18.1
9	21.5	23.6	23.9	26.5	30.9
10	-.6	-.6	-.6	-.6	-.5

COLLECTOR INPUT POWERS, WATTS:

NO.					
1	21.5	22.0	22.3	18.5	12.1
2	16.5	17.1	17.2	13.5	8.0
3	30.6	35.1	36.4	19.3	10.6
4	56.3	58.6	61.1	49.2	22.7
5	21.5	21.6	22.5	21.0	18.8
6	28.0	27.2	26.2	27.2	26.7
7	39.5	37.3	34.9	36.7	36.0
8	35.6	31.4	30.4	34.4	40.6
9	23.2	25.7	25.2	28.0	32.6
10	.0	.0	.0	.0	.0

COLLECTOR DISSIPATIONS, WATTS:

NO.					
1	3.6	3.7	3.9	3.3	2.2
2	3.5	3.6	3.8	3.0	1.8
3	7.3	8.4	9.0	4.9	2.7
4	15.8	16.4	17.7	14.7	6.8
5	7.2	7.3	7.9	7.5	6.8
6	11.8	11.5	11.4	12.2	12.0
7	22.3	20.8	20.4	21.9	21.6
8	29.8	26.1	26.4	30.7	36.5
9	40.3	44.4	46.4	53.0	62.3
10	1.1	1.1	1.2	1.3	1.1

Rev A

II(p)

TUBE # L-5394 #2022R-1 . TEST DATE 23APR75 (2). SHEET 17

NAS 3-15330

COL. #		1	2	3	4	5	6
1.	FREQUENCY. GHZ	12.030	12.039	12.050	12.060	12.070	12.080
2.	CATHODE VOLTS	11218	11218	11218	11218	11238	11218
3.	MA	76.0	76.0	76.0	76.0	76.0	76.0
4.	BEAM WATTS	852.3	852.2	852.3	852.3	853.8	852.2
5.	MOD ANODE VOLTS	250	250	250	250	250	250
6.	MA	-.0	-.0	.0	-.0	.0	.0
7.	WATTS	.0	.0	.0	.0	.0	.0
8.	HEATER VOLTS	3.29	3.29	3.29	3.29	3.29	3.29
9.	AMPS	1.29	1.29	1.29	1.29	1.29	1.29
10.	WATTS	4.24	4.24	4.24	4.24	4.24	4.24
11.	NASA OUTPUT SENSOR MV	.0	-.1	.0	.0	-.1	-.1
12.	NASA REVERSE SENSOR MV	.0	-.1	.0	-.1	.0	-.1
13.	REVERSE POWER SIGNAL DBM	.0	-.0	.0	.0	.0	-.0
14.	VACUUM(VAUNS=LOG(N/M^3))	14.5	14.5	14.5	14.4	14.4	14.5
15.	BASEPLATE CALORIMETER W	.0	.0	.0	.0	.0	.0
16.	RF OUTPUT CALORIMETER W	.0	.0	.0	.0	.0	.0
17.	RF DRIVE DBM	8.8	8.9	8.9	8.9	8.9	8.9
18.	KW	7.6	7.7	7.7	7.7	7.7	7.7
19.	OUTPUT POWER DBM	44.1	44.0	43.4	42.5	42.5	43.2
20.	WATTS	25.7	25.1	21.9	17.6	17.6	21.0
21.	GAIN DB	35.3	35.1	34.6	33.6	33.6	34.3
22.	TOTAL COLLECTOR MA	75.4	75.5	75.5	75.6	75.5	75.5
	BODY LOSSES:						
23.	INTERCEPTION MA	1.6	1.6	1.6	1.5	1.5	1.5
24.	WATTS	10.5	10.6	10.4	10.2	10.0	9.9
25.	RF LOSS WATTS	9.0	8.8	7.7	6.2	6.2	7.3
26.	TOTAL WATTS	19.5	19.4	18.1	16.4	16.1	17.2
27.	RESIDUAL BEAM POWER AT COLLECTOR WATTS	807.1	807.6	812.3	818.3	820.1	814.0
28.	TOTAL HV INPUT WATTS	194.4	195.0	190.3	179.3	183.5	185.5
29.	OUTPUT+INTCPT+LOSS #	45.2	44.6	40.0	34.0	33.7	38.2
30.	COLLECTOR DISSIP. W	149.2	150.5	150.3	145.3	149.8	147.3
31.	AVGE. IMPACT VOLTS	1979	1994	1991	1923	1984	1952
32.	COLLECTOR EFFICIENCY PCT	81.5	81.4	81.5	82.2	81.7	81.9
33.	OVERALL EFFIC INCL HTR	12.9	12.6	11.3	9.6	9.4	11.1
35.	ELECTRONIC EFFIC. PCT	4.1	4.0	3.5	2.8	2.8	3.3
36.	NASA DEF. PCT	3.3	2.9	2.6	2.1	2.1	2.5
37.	THERMISTOR NO. 1 DEG C	44.5	44.6	44.5	44.4	44.3	44.2
38.	THERMISTOR NO. 2 DEG C	285.1	285.1	285.1	285.1	285.1	285.1
39.	THERMISTOR NO. 3 DEG C	51.4	51.4	51.4	51.4	51.4	51.3
40.	THERMISTOR NO. 4 DEG C	46.0	46.0	45.9	45.9	45.8	45.8

LITTON 10 REV. A

Col. 1 to Col. 6 Sat Drive -10 dB = +8.82 dBm

Col. 1 to Col. 6 38.6°C Base Plate

II(q)

TUBE # L-5394 #2022R-1 . TEST DATE 23APR75 (2). SHEET 18

NAS 3-15330

COLLECTOR VOLTAGES RELATIVE TO CATHODE:

NO.						
1	11224	11226	11224	11275	11246	11210
2	8958	8971	8972	8965	8983	8964
3	7898	7917	7917	7908	7925	7907
4	6784	6812	6778	6798	6816	6799
5	5607	5641	5603	5619	5647	5624
6	4464	4506	4466	4497	4516	4493
7	3359	3423	3443	3409	3428	3383
8	2190	2174	2195	2138	2260	2247
9	1087	1069	1096	1021	1124	1106
10	0	0	0	0	0	0

COLLECTOR CURRENTS, MA:

NO.						
1	.6	.6	.6	.5	.5	.5
2	.5	.5	.4	.4	.4	.4
3	.6	.6	.6	.5	.5	.6
4	1.0	1.0	.9	.9	.8	.9
5	1.7	1.7	1.5	1.5	1.5	1.5
6	4.3	4.4	4.0	3.5	3.4	3.7
7	8.2	7.8	6.5	5.6	6.1	7.8
8	31.2	31.7	32.3	31.4	29.0	26.9
9	28.1	27.8	29.2	31.7	33.6	33.5
10	-.6	-.7	-.6	-.5	-.3	-.3

COLLECTOR INPUT POWERS, WATTS:

NO.						
1	9.5	6.7	6.3	5.9	5.7	6.1
2	4.1	4.2	3.9	3.7	3.6	3.8
3	4.9	5.0	4.7	4.3	4.3	4.5
4	6.6	6.6	6.2	5.8	5.7	6.1
5	9.4	9.6	8.8	8.3	8.2	8.5
6	19.0	19.8	17.7	15.9	15.2	16.4
7	27.5	26.7	22.5	18.9	20.9	26.3
8	68.3	69.0	70.9	67.1	65.5	60.4
9	30.5	29.7	32.0	32.4	37.8	37.0
10	.0	.0	.0	.0	.0	.0

COLLECTOR DISSIPATIONS, WATTS:

NO.						
1	1.1	1.2	1.1	1.0	1.0	1.1
2	.9	.9	.9	.8	.8	.8
3	1.2	1.3	1.2	1.0	1.1	1.1
4	1.9	1.9	1.8	1.6	1.7	1.7
5	3.3	3.4	3.1	2.8	2.9	3.0
6	8.4	8.8	7.9	6.8	6.7	7.1
7	16.2	15.6	13.0	10.7	12.1	15.2
8	61.8	63.3	64.3	60.4	57.5	52.5
9	55.5	55.5	58.1	61.0	66.7	65.3
10	1.2	1.3	1.2	.9	.6	.5

LITTON 10 REV. A

II(r)

TUBE # L-5394 #2022R-1 . TEST DATE 23APR75 (2). SHEET 19 NAS 3-15830

COL. #:	1	2	3	4	5
1. FREQUENCY, GHZ	12.089	12.100	12.110	12.120	12.130
2. CATHODE VOLTS	11238	11238	11218	11238	11218
3. MA	76.0	76.0	76.0	76.0	76.0
4. BEAM WATTS	853.7	853.7	852.3	853.8	852.2
5. MOD ANODE VOLTS	250	250	250	250	250
6. MA	.0	-.0	-.0	.0	-.0
7. WATTS	.0	.0	.0	.0	.0
8. HEATER VOLTS	3.29	3.29	3.29	3.29	3.29
9. AMPS	1.29	1.29	1.29	1.29	1.29
10. WATTS	4.24	4.24	4.24	4.24	4.24
11. NASA OUTPUT SENSOR MV	-.1	-.1	-.1	-.1	-.1
12. NASA REVERSE SENSOR MV	-.1	-.1	-.1	.0	-.1
13. REVERSE POWER SIGNAL DBM	.0	.0	.0	.0	.0
14. VACUUM(VAUNS=LOG(1/M^3))	14.5	14.5	14.4	14.5	14.5
15. BASEPLATE CALORIMETER W	.0	.0	.0	.0	.0
16. RF OUTPUT CALORIMETER W	.0	.0	.0	.0	.0
17. RF DRIVE DBM	8.9	8.9	8.8	8.8	8.8
18. MW	7.7	7.7	7.6	7.6	7.6
19. OUTPUT POWER DBM	43.3	43.0	42.5	41.3	38.9
20. WATTS	21.5	20.0	17.9	13.6	7.8
21. GAIN DB	34.4	34.1	33.7	32.5	30.1
22. TOTAL COLLECTOR MA	75.5	75.2	74.9	75.6	75.6
BODY LOSSES:					
23. INTERCEPTION MA	1.5	1.5	1.5	1.5	1.5
24. WATTS	9.9	9.8	10.0	10.0	9.8
25. RF LOSS WATTS	7.5	7.0	6.3	4.8	2.7
26. TOTAL WATTS	17.4	16.8	16.2	14.7	12.6
27. RESIDUAL BEAM POWER AT COLLECTOR WATTS	814.8	816.9	818.2	825.5	831.8
28. TOTAL HV INPUT WATTS	186.8	181.5	177.0	176.2	165.5
29. OUTPUT+INTCPT+LOSS W	38.9	36.8	34.1	28.4	20.4
30. COLLECTOR DISSIP. W	147.9	144.7	142.9	147.9	145.1
31. AVGE. IMPACT VOLTS	1959	1924	1908	1957	1921
32. COLLECTOR EFFICIENCY PCT	81.9	82.3	82.5	82.1	82.6
33. OVERALL EFFIC INCL HTR	11.2	10.8	9.9	7.5	4.6
35. ELECTRONIC EFFIC. PCT	3.4	3.2	2.8	2.2	1.2
36. NASA DEF. PCT	2.5	2.3	2.1	1.6	.9
37. THERMISTOR NO. 1 DEG C	44.2	44.2	44.2	44.1	43.9
38. THERMISTOR NO. 2 DEG C	285.1	285.1	285.1	285.1	285.1
39. THERMISTOR NO. 3 DEG C	51.3	51.2	51.2	51.2	51.1
40. THERMISTOR NO. 4 DEG C	45.7	45.7	45.6	45.4	45.2

LITTON 18 REV. A

Col. 1 to Col. 6 Sat Drive -10 dB = 8.82 dBm

Col. 1 to Col. 6 38.6°C Base Plate

II(s)

TUBE # L-5394 #2022R-1 . TEST DATE 23APR75 (2). SHEET 20 NAS 3-15830

COLLECTOR VOLTAGES RELATIVE TO CATHODE:					
NO. 1	11245	11243	11224	11245	11225
2	8965	8991	8962	8984	8968
3	7928	7933	7903	7927	7913
4	6813	6828	6795	6816	6807
5	5638	5649	5621	5644	5639
6	4507	4513	4485	4514	4507
7	3393	3408	3380	3418	3437
8	2266	2188	2165	2218	2195
9	1110	1006	997	1023	998
10	0	0	0	0	0
COLLECTOR CURRENTS, MA:					
NO. 1	.6	.6	.6	.5	.5
2	.4	.4	.4	.4	.4
3	.6	.6	.6	.6	.5
4	.9	.9	.9	.9	.8
5	1.5	1.6	1.5	1.5	1.3
6	3.8	4.2	3.7	3.6	3.2
7	8.3	8.6	8.2	7.4	4.9
8	25.4	23.8	23.1	22.9	23.7
9	34.2	34.8	36.1	38.0	40.5
10	-.2	-.2	-.2	-.2	-.2
COLLECTOR INPUT POWERS, WATTS:					
NO. 1	6.2	6.2	6.5	6.0	5.5
2	4.0	3.8	3.8	3.7	3.3
3	4.6	4.6	4.6	4.4	4.0
4	6.1	6.2	6.1	5.9	5.4
5	8.7	9.2	8.7	8.6	7.6
6	17.1	19.0	16.7	16.1	14.2
7	28.0	29.1	27.7	25.2	16.7
8	57.6	52.0	50.4	50.9	52.1
9	38.0	35.0	35.9	38.9	40.4
10	.0	.0	.0	.0	.0
COLLECTOR DISSIPATIONS, WATTS:					
NO. 1	1.1	1.1	1.1	1.0	.9
2	.9	.8	.8	.8	.7
3	1.1	1.1	1.1	1.1	1.0
4	1.8	1.8	1.7	1.7	1.5
5	3.0	3.1	2.9	3.0	2.6
6	7.4	8.1	7.1	7.0	6.1
7	16.2	16.5	15.6	14.4	9.3
8	49.8	43.7	44.0	44.9	45.6
9	67.1	67.0	68.8	74.4	77.8
10	.5	.4	.4	.4	.4

LITTON 18 REV. A

II(t)

ORIGINAL PAGE IS OF POOR QUALITY

TUBE # L-5394 #2022R-1 . TEST DATE 23APR75 (2). SHEET 21

NAS 3-15830

	COL. #:	1
1.	FREQUENCY, GHZ	12.080
2.	CATHODE VOLTS	11218
3.	MA	76.0
4.	BEAM WATTS	852.2
5.	ADD ANODE VOLTS	250
6.	MA	.0
7.	WATTS	.0
8.	HEATER VOLTS	3.29
9.	AMPS	1.29
10.	WATTS	4.24
11.	NASA OUTPUT SENSOR MV	-.1
12.	NASA REVERSE SENSOR MV	.0
13.	REVERSE POWER SIGNAL DBM	.0
14.	VACUUM(VAUNS=LOG(A/M^3))	14.5
15.	BASEPLATE CALORIMETER W	.0
16.	RF OUTPUT CALORIMETER W	1.7
17.	RF DRIVE DBM	-75.2
18.	MW	.0
19.	OUTPUT POWER DBM	-31.7
20.	WATTS	.0
21.	GAIN DB	.0
22.	TOTAL COLLECTOR MA	75.7
	BODY LOSSES:	
23.	INTERCEPTION MA	1.4
24.	WATTS	9.5
25.	RF LOSS WATTS	.0
26.	TOTAL WATTS	9.5
27.	RESIDUAL BEAM POWER AT COLLECTOR WATTS	842.7
28.	TOTAL HV INPUT WATTS	139.0
29.	OUTPUT+INTCPT+LOSS W	9.5
30.	COLLECTOR DISSIP. W	129.5
31.	AVGE. IMPACT VOLTS	1710
32.	COLLECTOR EFFICIENCY PCT	84.6
33.	OVERALL EFFIC INCL HTR	.0
35.	ELECTRONIC EFFIC. PCT	.0
36.	NASA DEF. PCT	.0
37.	THERMISTOR NO. 1 DEG C	43.7
38.	THERMISTOR NO. 2 DEG C	285.1
39.	THERMISTOR NO. 3 DEG C	51.1
40.	THERMISTOR NO. 4 DEG C	44.9

COL. 1 NO DRIVE CASE

Col. 1 39.6°C Base Plate

REV. A

II(u)

TUBE # L-5394 #2022R-1 . TEST DATE 23APR75 (2). SHEET 22

NAS 3-15830

COLLECTOR VOLTAGES RELATIVE TO CATHODE:

NO.	
1	11227
2	8964
3	7910
4	6799
5	5629
6	4506
7	3467
8	2256
9	934
10	0

COLLECTOR CURRENTS, MA:

NO.	
1	.4
2	.3
3	.4
4	.6
5	1.1
6	2.2
7	3.1
8	14.2
9	53.6
10	-.2

COLLECTOR INPUT POWERS, WATTS:

NO.	
1	4.4
2	2.6
3	3.2
4	4.4
5	6.0
6	9.8
7	10.9
8	32.0
9	50.0
10	.0

COLLECTOR DISSIPATIONS, WATTS:

NO.	
1	.7
2	.5
3	.7
4	1.1
5	1.8
6	3.7
7	5.4
8	24.3
9	91.7
10	.3

REV. A

II(v)

GO TO 120

/VAUG1021/ L-5394 DATA REDUCTION (VERSION 12/6/74); 04/24 ?:30
MOD. FOR ALEXOVICH CIRCUIT
TUBE # L-5394 #2022R-1, TEST DATE 23APR75 (1)
BENCH # 1, OPERATOR RIP LRB KR DC

NAS 3-15830

COL. #:	1	2	3	4	5	6
1. FREQUENCY, GHZ	12.030	12.040	12.050	12.059	12.070	12.080
2. CATHODE VOLTS	11177	11177	11177	11177	11177	11197
3. MA	76.0	76.0	76.0	76.0	76.0	76.0
4. BEAM WATTS	848.9	849.0	848.9	849.0	849.0	850.6
5. MOD ANODE VOLTS	251	252	251	252	251	252
6. MA	-.0	.0	-.0	-.0	-.0	-.0
7. WATTS	.0	.0	.0	.0	.0	.0
8. HEATER VOLTS	3.29	3.29	3.29	3.29	3.29	3.29
9. AMPS	1.29	1.29	1.29	1.29	1.29	1.29
10. WATTS	4.24	4.24	4.24	4.24	4.24	4.24
11. NASA OUTPUT SENSOR MV	.0	-.1	-.1	-.1	-.1	-.1
12. NASA REVERSE SENSOR MV	-.1	-.1	.0	-.1	.0	.0
13. REVERSE POWER SIGNAL DBM	.0	-.0	-.0	.0	-.0	.0
14. VACUUM(VAUNS=LOG(A/M^3))	14.5	14.5	14.5	14.5	14.5	14.5
15. BASEPLATE CALORIMETER W	.0	.0	.0	.0	.0	.0
16. RF OUTPUT CALORIMETER W	175.1	170.8	162.4	149.7	137.0	120.1
17. RF DRIVE DBM	27.5	27.5	27.5	27.5	27.5	27.5
18. MW	562.3	563.6	562.3	566.2	566.2	567.5
19. OUTPUT POWER DBM	52.6	52.5	52.3	51.9	51.6	51.2
20. WATTS	183.0	178.0	169.6	153.4	144.0	130.6
21. GAIN DB	25.1	25.0	24.8	24.3	24.1	23.6
22. TOTAL COLLECTOR MA	68.2	67.9	67.3	67.2	67.1	67.2
BODY LOSSES:						
23. INTERCEPTION MA	8.3	8.7	9.1	9.4	9.5	9.5
24. WATTS	55.9	58.4	61.1	62.7	63.5	63.6
25. RF LOSS WATTS	64.0	62.3	59.3	53.7	50.4	45.7
26. TOTAL WATTS	120.0	120.7	120.4	116.4	113.9	109.3
27. RESIDUAL BEAM POWER AT COLLECTOR WATTS	546.0	550.4	558.9	579.2	591.1	610.7
28. TOTAL HV INPUT WATTS	464.1	462.4	453.8	444.3	432.1	420.9
29. OUTPUT+INTCPT+LOSS W	303.0	298.6	299.0	269.8	257.9	239.8
30. COLLECTOR DISSIP. W	161.2	163.8	153.8	174.4	174.2	181.1
31. AVGE. IMPACT VOLTS	2365	2411	2433	2596	2597	2695
32. COLLECTOR EFFICIENCY PCT	70.5	70.2	70.7	69.9	70.5	70.4
33. OVERALL EFFIC INCL HTR	39.1	38.1	37.0	34.2	33.0	30.7
35. ELECTRONIC EFFIC. PCT	29.1	28.3	27.0	24.4	22.9	20.7
36. NASA DEF. PCT	21.6	21.0	20.0	18.1	17.0	15.4
37. THERMISTOR NO. 1 DEG C	88.8	88.6	88.7	88.7	88.8	88.9
38. THERMISTOR NO. 2 DEG C	217.7	217.7	217.7	217.7	217.7	220.4
39. THERMISTOR NO. 3 DEG C	63.8	63.8	63.9	64.0	64.0	64.0
40. THERMISTOR NO. 4 DEG C	70.2	71.0	71.3	71.4	71.2	70.8

Rev. A

Col. 1 to 6 Set Drive Power +4.5 dBm = +27.5 dBm

Col. 1 to 6 55 Degree C Base Plate

Table IIIa

TUBE # L-5394 #2022R-1, TEST DATE 23APR75 (1), SHEET 2

NAS 3-15830

COLLECTOR VOLTAGES RELATIVE TO CATHODE: NO.						
1	11168	11168	11169	11170	11170	11194
2	8899	8898	8894	8898	8904	8930
3	7760	7761	7753	7768	7782	7813
4	6672	6682	6684	6704	6692	6730
5	5536	5552	5551	5568	5542	5592
6	4445	4449	4440	4465	4432	4487
7	3366	3349	3331	3325	3323	3329
8	2243	2259	2239	2244	2243	2224
9	1009	1048	1048	1080	1049	1105
10	0	0	0	0	0	0
COLLECTOR CURRENTS, MA: NO.						
1	3.3	3.3	3.2	3.0	2.8	2.6
2	4.1	4.0	3.8	3.5	3.2	2.9
3	11.6	11.5	10.7	9.8	8.7	7.2
4	12.3	11.7	10.9	9.9	9.2	8.8
5	6.0	5.8	5.5	5.3	5.1	5.1
6	8.1	7.9	7.9	8.2	8.4	8.9
7	9.2	9.6	10.3	11.2	11.9	12.2
8	6.1	6.6	7.3	8.7	10.6	12.2
9	12.6	11.7	10.5	8.9	8.3	8.3
10	-5.0	-3.9	-2.7	-1.4	-1.0	-.9
COLLECTOR INPUT POWERS, WATTS: NO.						
1	36.7	36.3	35.3	33.3	31.5	29.0
2	36.2	35.5	34.1	31.4	28.8	25.5
3	89.7	89.2	82.6	76.1	67.4	56.1
4	81.7	77.9	72.7	66.3	61.2	59.0
5	33.3	31.9	30.4	29.7	29.2	28.6
6	35.8	34.9	35.2	36.6	37.2	40.0
7	31.0	32.2	34.3	37.2	39.6	40.6
8	13.6	14.9	16.4	19.6	23.7	27.1
9	12.7	12.2	11.0	9.7	8.7	9.2
10	.0	.0	.0	.0	.0	.0
COLLECTOR DISSIPATIONS, WATTS: NO.						
1	7.8	7.8	7.7	7.7	7.3	7.0
2	9.6	9.6	9.3	9.2	8.4	7.7
3	27.3	27.7	25.9	25.4	22.5	19.4
4	29.0	28.1	26.4	25.7	23.8	23.6
5	14.2	13.9	13.3	13.8	13.2	13.8
6	19.1	18.9	19.3	21.3	21.8	24.0
7	21.8	23.2	29.0	29.0	31.0	32.8
8	14.4	15.9	17.8	22.7	27.4	32.9
9	29.7	28.1	25.4	23.2	21.5	22.5
10	11.7	9.5	6.5	3.5	2.6	2.5

Rev. A

III(b)

TUBE # L-5394 #2022R-1, TEST DATE 23APR75 (1), SHEET 3 NAS 3-15830

COL. #:	1	2	3	4	5
1. FREQUENCY, GHZ	12.090	12.100	12.110	12.121	12.131
2. CATHODE VOLTS	11177	11177	11177	11177	11177
3. MA	76.0	76.0	76.0	76.0	76.0
4. BEAM WATTS	849.0	849.0	849.1	849.0	849.0
5. MOD ANODE VOLTS	252	252	252	251	252
6. MA	-.0	-.0	-.0	-.0	-.0
7. WATTS	.0	.0	.0	.0	.0
8. HEATER VOLTS	3.29	3.29	3.29	3.29	3.29
9. AMPS	1.29	1.29	1.29	1.29	1.29
10. WATTS	4.24	4.24	4.24	4.24	4.24
11. NASA OUTPUT SENSOR MV	-.1	-.1	-.1	-.1	-.1
12. NASA REVERSE SENSOR MV	.0	.0	.0	.0	.0
13. REVERSE POWER SIGNAL DBM	.0	.0	.0	-.0	.0
14. VACUUM(VAUNS=LOG(N/M^3))	14.5	14.5	14.5	14.5	14.5
15. BASEPLATE CALORIMETER W	.0	.0	.0	.0	.0
16. RF OUTPUT CALORIMETER W	107.4	103.2	103.2	98.9	98.9
17. RF DRIVE DBM	27.5	27.5	27.5	27.5	27.5
18. MW	567.5	564.9	558.5	559.8	557.2
19. OUTPUT POWER DBM	50.8	50.6	50.3	50.4	50.4
20. WATTS	120.2	114.3	107.8	108.7	109.5
21. GAIN DB	23.3	23.1	22.9	22.9	22.9
22. TOTAL COLLECTOR MA	67.2	67.1	67.6	68.4	69.1
BODY LOSSES:					
23. INTERCEPTION MA	9.4	9.2	9.0	8.4	7.4
24. WATTS	62.8	61.6	60.2	56.4	49.7
25. RF LOSS WATTS	42.1	40.0	37.7	38.1	38.3
26. TOTAL WATTS	104.9	101.7	97.9	94.5	88.0
27. RESIDUAL BEAM POWER AT COLLECTOR WATTS	623.9	633.0	643.4	645.8	651.5
28. TOTAL HV INPUT WATTS	407.9	400.5	395.6	389.3	375.2
29. OUTPUT+INTCPT+LOSS W	225.1	216.0	205.7	203.2	197.5
30. COLLECTOR DISSIP. W	182.8	184.5	189.9	186.1	177.7
31. AVGE. IMPACT VOLTS	2720	2752	2608	2722	2573
32. COLLECTOR EFFICIENCY PCT	70.7	70.9	70.5	71.2	72.7
33. OVERALL EFFIC INCL HTR	29.2	28.2	27.0	27.6	28.9
35. ELECTRONIC EFFIC. PCT	19.1	18.2	17.1	17.3	17.4
36. NASA DEF. PCT	14.2	13.5	12.7	12.8	12.9
37. THERMISTOR NO. 1 DEG C	88.9	88.9	88.9	88.8	88.1
38. THERMISTOR NO. 2 DEG C	217.7	217.7	217.7	217.7	217.7
39. THERMISTOR NO. 3 DEG C	64.0	64.1	64.0	64.0	63.9
40. THERMISTOR NO. 4 DEG C	70.3	69.8	69.4	68.9	68.7

COL.3-> SAT DRIVE +4.5DB (27.5DBM)

COL. 1 to 5 55°C Base Plate

11101 10 REV. A

III(c)

TUBE # L-5394 #2022R-1, TEST DATE 23APR75 (1), SHEET 4 NAS 3-15830

COLLECTOR VOLTAGES RELATIVE TO CATHODE:					
NO. 1	11172	11173	11173	11173	11173
2	8911	8916	8913	8912	8911
3	7805	7808	7815	7803	7803
4	6717	6716	6706	6712	6712
5	5571	5560	5557	5566	5574
6	4454	4439	4431	4443	4446
7	3287	3317	3313	3301	3306
8	2180	2209	2193	2180	2170
9	1078	1116	1076	1049	1024
10	0	0	0	0	0
COLLECTOR CURRENTS, MA:					
NO. 1	2.4	2.3	2.4	2.3	2.3
2	2.6	2.4	2.4	2.4	2.4
3	6.2	5.6	5.6	5.6	5.7
4	8.2	7.9	7.9	8.3	8.3
5	5.1	5.0	4.7	4.6	4.5
6	9.3	9.6	9.5	9.7	9.5
7	12.5	12.8	12.5	11.4	10.3
8	13.5	14.3	14.5	14.2	14.8
9	8.2	7.9	9.1	10.8	12.4
10	-.9	-.8	-.8	-1.0	-1.0
COLLECTOR INPUT POWERS, WATTS:					
NO. 1	27.1	26.1	26.4	25.9	25.5
2	22.9	21.6	21.5	21.1	20.9
3	48.5	43.8	43.5	43.6	44.3
4	55.3	53.3	52.9	55.7	55.6
5	26.6	27.6	26.1	25.8	25.0
6	41.4	42.6	42.2	43.1	42.3
7	41.1	42.3	41.2	37.7	33.9
8	29.4	31.6	31.7	30.9	32.1
9	8.9	8.8	9.8	11.3	12.7
10	.0	.0	.0	.0	.0
COLLECTOR DISSIPATIONS, WATTS:					
NO. 1	6.6	6.4	6.6	6.3	5.9
2	7.0	6.7	6.8	6.5	6.0
3	16.9	15.4	15.6	15.2	14.6
4	22.4	21.8	22.2	22.6	21.3
5	14.0	13.7	13.2	12.6	11.5
6	25.3	26.4	26.8	26.4	24.5
7	34.0	35.1	35.0	31.1	26.4
8	36.7	39.4	40.6	38.6	38.1
9	22.3	21.8	25.5	29.4	31.9
10	2.3	2.2	2.3	2.6	2.5

11101 10 REV. A

III(d)

TUBE # L-5394 #2022R-1, TEST DATE 23APR75 (1), SHEET 5 NAS 3-15330

COL. #:	1	2	3	4	5	6
1. FREQUENCY, GHZ	12.030	12.040	12.050	12.060	12.070	12.080
2. CATHODE VOLTS	11197	11177	11177	11197	11197	11177
3. MA	76.0	76.0	76.0	76.0	76.0	76.0
4. BEAM WATTS	850.7	849.1	849.1	850.7	850.7	849.1
5. MOD ANODE VOLTS	252	251	252	252	252	252
6. MA	-.0	.0	-.0	-.0	-.0	-.0
7. WATTS	.0	.0	.0	.0	.0	.0
8. HEATER VOLTS	3.29	3.29	3.29	3.29	3.29	3.29
9. AMPS	1.29	1.29	1.29	1.29	1.29	1.29
10. WATTS	4.24	4.24	4.24	4.24	4.24	4.24
11. NASA OUTPUT SENSOR MV	-.1	.0	-.1	-.1	.0	.0
12. NASA REVERSE SENSOR MV	.0	.0	.0	.0	.0	-.1
13. REVERSE POWER SIGNAL DBM	.0	.0	.0	.0	.0	.0
14. VACUUM(VAUNS=LOG(N/M^3))	14.5	14.5	14.5	14.5	14.5	14.5
15. BASEPLATE CALORIMETER W	.0	.0	.0	.0	.0	.0
16. RF OUTPUT CALORIMETER W	213.1	217.3	213.1	204.7	196.2	187.7
17. RF DRIVE DBM	26.0	26.0	26.0	26.0	26.0	26.0
18. MW	398.1	399.9	401.8	401.8	400.9	399.9
19. OUTPUT POWER DBM	53.4	53.4	53.2	53.1	53.0	52.8
20. WATTS	216.3	216.8	208.4	204.2	200.0	189.7
21. GAIN DB	27.4	27.3	27.2	27.1	27.0	26.8
22. TOTAL COLLECTOR MA	70.1	70.0	69.9	69.3	68.9	68.8
BODY LOSSES:						
23. INTERCEPTION MA	6.4	6.6	7.0	7.4	7.6	7.8
24. WATTS	42.7	44.5	47.1	49.4	51.1	52.2
25. RF LOSS WATTS	75.7	75.9	73.0	71.5	70.0	66.4
26. TOTAL WATTS	118.4	120.4	120.1	120.8	121.1	118.6
27. RESIDUAL BEAM POWER AT COLLECTOR WATTS	516.0	512.0	520.6	525.6	529.6	540.8
28. TOTAL HV INPUT WATTS	484.0	484.6	483.5	480.1	473.4	465.8
29. OUTPUT+INTCPT+LOSS W	334.6	337.2	328.6	325.0	321.1	308.3
30. COLLECTOR DISSIP. W	149.4	147.4	155.0	155.1	152.3	157.5
31. AVGE. IMPACT VOLTS	2130	2108	2218	2237	2212	2289
32. COLLECTOR EFFICIENCY PCT	71.1	71.2	70.2	70.5	71.2	70.9
33. OVERALL EFFIC INCL HTR	44.3	44.3	42.7	42.2	41.9	40.4
35. ELECTRONIC EFFIC. PCT	34.3	34.5	33.1	32.4	31.7	30.2
36. NASA DEF. PCT	25.4	25.5	24.5	24.0	23.5	22.3
37. THERMISTOR NO. 1 DEG C	88.6	87.9	87.4	87.2	87.3	87.4
38. THERMISTOR NO. 2 DEG C	217.7	217.7	217.7	215.3	217.7	217.7
39. THERMISTOR NO. 3 DEG C	64.3	64.4	64.4	64.4	64.5	64.4
40. THERMISTOR NO. 4 DEG C	74.7	75.1	75.4	75.5	75.5	75.3

COL. 1 TO 6 Set Drive Power +3 dB = +26 dBm

COL. 1 TO 6 55.0°C Base Plate

LITTON 1B Rev A

III(e)

TUBE # L-5394 #2092R-1, TEST DATE 23APR75 (1), SHEET 6 NAS 3-15330

COLLECTOR VOLTAGES RELATIVE TO CATHODE:

NO.						
1	11165	11165	11165	11185	11187	11167
2	8894	8869	8874	8902	8895	8873
3	7739	7765	7708	7745	7731	7712
4	6664	6642	6641	6667	6673	6660
5	5563	5531	5532	5558	5567	5556
6	4482	4444	4444	4466	4471	4453
7	3346	3334	3365	3373	3345	3277
8	2259	2257	2247	2265	2275	2223
9	992	997	989	1053	1084	1055
10	0	0	0	0	0	0

COLLECTOR CURRENTS, MA:

NO.						
1	3.9	3.9	3.8	3.8	3.6	3.5
2	5.0	5.1	5.0	4.9	4.6	4.5
3	15.4	16.0	16.0	15.6	15.0	14.2
4	15.5	15.0	14.7	13.9	13.5	12.9
5	5.7	5.4	5.1	4.8	4.6	4.5
6	5.8	5.7	5.3	5.5	5.6	6.1
7	6.3	6.6	7.0	7.5	7.9	8.3
8	4.1	4.1	4.4	5.1	6.2	7.7
9	14.8	13.8	12.1	10.0	8.8	7.9
10	-6.3	-5.4	-3.5	-1.7	-1.0	-.8

COLLECTOR INPUT POWERS, WATTS:

NO.						
1	43.1	43.3	42.8	42.2	40.4	39.2
2	44.8	44.9	44.0	43.2	41.3	39.6
3	118.9	123.1	123.4	121.1	115.9	109.3
4	103.2	99.4	97.6	92.9	90.0	85.8
5	31.8	29.6	28.0	26.7	25.4	24.9
6	26.1	25.4	23.6	24.3	24.9	27.0
7	21.0	21.8	23.6	25.4	26.6	27.3
8	9.3	9.2	10.0	11.5	14.2	17.2
9	14.7	13.7	11.9	10.5	9.6	8.3
10	.0	.0	.0	.0	.0	.0

COLLECTOR DISSIPATIONS, WATTS:

NO.						
1	8.2	8.2	8.5	8.4	8.0	8.0
2	10.7	10.7	11.0	10.8	10.3	10.2
3	32.7	33.7	35.5	35.0	33.2	32.4
4	33.0	31.5	32.6	31.2	29.8	29.5
5	12.2	11.3	11.2	10.7	10.1	10.3
6	12.4	12.1	11.8	12.2	12.3	13.9
7	13.4	13.8	15.5	16.8	17.6	19.1
8	8.8	8.6	9.8	11.4	13.8	17.7
9	31.5	29.0	26.8	22.4	19.6	18.1
10	13.5	11.3	7.8	3.8	2.3	1.7

LITTON 1B Rev A

III(f)

TUBE # L-5394 #2022R-1, TEST DATE 23APR75 (1), SHEET 7 NAS 3-15830

COL. #:	1	2	3	4	5
1. FREQUENCY, GHZ	12.090	12.100	12.110	12.121	12.130
2. CATHODE VOLTS	11177	11197	11197	11197	11197
3. MA	76.0	76.0	76.0	76.0	76.0
4. BEAM WATTS	849.1	850.7	850.7	850.7	850.8
5. MOD ANODE VOLTS	252	252	252	252	251
6. MA	-.0	.0	-.0	-.0	-.0
7. WATTS	.0	.0	.0	.0	.0
8. HEATER VOLTS	3.29	3.29	3.29	3.29	3.29
9. AMPS	1.29	1.29	1.29	1.29	1.29
10. WATTS	4.24	4.24	4.24	4.24	4.24
11. NASA OUTPUT SENSOR MV	-.1	-.1	-.1	-.1	-.1
12. NASA REVERSE SENSOR MV	-.1	-.1	-.1	-.1	.0
13. REVERSE POWER SIGNAL DBM	.0	.0	.0	.0	.0
14. VACUUM(VAUNS=LOG(N/M^3))	14.5	14.4	14.5	14.5	14.4
15. BASEPLATE CALORIMETER W	.0	.0	.0	.0	.0
16. RF OUTPUT CALORIMETER W	175.1	166.6	162.4	158.1	145.5
17. RF DRIVE DBM	26.0	26.0	26.0	26.0	26.0
18. MW	400.9	401.8	395.4	395.4	394.5
19. OUTPUT POWER DBM	52.5	52.3	52.1	52.0	51.7
20. WATTS	178.8	171.6	162.1	156.9	147.7
21. GAIN DB	26.5	26.3	26.1	26.0	25.7
22. TOTAL COLLECTOR MA	68.8	68.9	69.6	70.3	71.3
BODY LOSSES:					
23. INTERCEPTION MA	7.8	7.5	6.9	6.1	5.2
24. WATTS	52.2	50.5	46.6	40.7	35.0
25. RF LOSS WATTS	62.6	60.1	56.7	54.9	51.7
26. TOTAL WATTS	114.7	110.6	103.3	95.6	86.7
27. RESIDUAL BEAM POWER AT COLLECTOR WATTS	555.6	568.5	585.3	598.2	616.4
28. TOTAL HV INPUT WATTS	456.2	447.3	435.5	417.7	399.1
29. OUTPUT+INTCPT+LOSS W	293.5	282.2	265.4	252.5	234.4
30. COLLECTOR DISSIP. W	162.7	165.1	170.1	165.3	164.7
31. AVGE. IMPACT VOLTS	2364	2395	2444	2352	2309
32. COLLECTOR EFFICIENCY PCT	70.7	71.0	70.9	72.4	73.3
33. OVERALL EFFIC INCL HTR	38.8	38.0	36.9	37.2	36.6
35. ELECTRONIC EFFIC. PCT	28.4	27.2	25.7	24.9	23.4
36. NASA DEF. PCT	21.1	20.2	19.1	18.4	17.4
37. THERMISTOR NO. 1 DEG C	87.6	87.8	87.7	87.4	86.4
38. THERMISTOR NO. 2 DEG C	215.3	217.7	217.7	215.3	217.7
39. THERMISTOR NO. 3 DEG C	64.4	64.3	64.3	64.2	64.1
40. THERMISTOR NO. 4 DEG C	74.9	74.3	73.9	73.4	72.8

COL.1-5 SAT DRIVE+3DB(SET TO+26.0DBM)

COL. 1 TO 5 55.0 DEGREE C BASE PLATE

LITTON REV. A

III(g)

TUBE # L-5394 #2022R-1, TEST DATE 23APR75 (1), SHEET 8 NAS 3-15830

NO.					
COLLECTOR VOLTAGES RELATIVE TO CATHODE:					
1	11168	11189	11190	11191	11192
2	8883	8908	8902	8913	8912
3	7725	7745	7731	7754	7756
4	6673	6688	6688	6696	6686
5	5559	5562	5554	5571	5555
6	4457	4457	4433	4450	4433
7	3299	3312	3308	3313	3338
8	2219	2230	2218	2204	2213
9	1062	1089	1081	1058	1053
10	0	0	0	0	0
COLLECTOR CURRENTS, MA:					
1	3.3	3.1	3.0	2.9	2.8
2	4.1	3.8	3.6	3.4	3.2
3	13.3	12.9	12.9	12.4	11.4
4	12.0	10.9	10.5	10.4	9.9
5	4.7	4.9	4.6	4.3	4.2
6	6.7	7.5	7.4	7.4	7.8
7	8.9	9.3	9.2	8.5	8.1
8	9.1	9.6	10.5	12.1	13.1
9	7.4	7.6	8.6	9.7	11.6
10	-.6	-.7	-.8	-.8	-.8
COLLECTOR INPUT POWERS, WATTS:					
1	37.2	35.1	33.7	32.1	31.2
2	36.3	34.2	32.4	30.2	28.7
3	102.7	100.2	99.9	96.1	88.5
4	79.8	72.6	70.4	69.6	66.3
5	25.9	27.1	25.7	23.7	23.1
6	29.9	33.3	32.9	32.9	34.7
7	29.3	30.7	30.5	28.2	27.0
8	20.2	21.5	23.3	26.7	28.9
9	7.9	8.3	9.3	10.3	12.3
10	.0	.0	.0	.0	.0
COLLECTOR DISSIPATIONS, WATTS:					
1	7.9	7.5	7.4	6.8	6.4
2	9.7	9.2	8.9	8.0	7.4
3	31.4	31.0	31.6	29.1	26.3
4	28.3	26.0	25.7	24.5	22.9
5	11.0	11.7	11.3	10.0	9.6
6	15.9	17.9	18.1	17.4	18.1
7	21.0	22.2	22.5	20.0	18.7
8	21.5	23.1	25.6	28.5	30.1
9	17.5	18.3	20.9	22.8	26.9
10	1.5	1.7	1.9	1.8	1.9

LITTON REV. A

III(h)

TUBE # L-5394 #2022R-1, TEST DATE 23APR75 (1), SHEET 9 NAS 3-15330

COL. #:	1	2	3	4	5	6
1. FREQUENCY, GHZ	12.030	12.039	12.050	12.060	12.071	12.080
2. CATHODE VOLTS	11197	11177	11177	11197	11197	11197
3. MA	76.0	76.0	76.0	76.0	76.0	76.0
4. BEAM WATTS	850.6	849.1	849.0	850.7	850.7	850.7
5. MOD ANODE VOLTS	252	252	251	251	251	251
6. MA	-.0	-.0	-.0	-.0	-.0	-.0
7. WATTS	.0	.0	.0	.0	.0	.0
8. HEATER VOLTS	3.29	3.29	3.29	3.29	3.29	3.29
9. AMPS	1.29	1.29	1.29	1.29	1.29	1.29
10. WATTS	4.24	4.24	4.24	4.24	4.24	4.24
11. NASA OUTPUT SENSOR MV	-.1	-.1	-.1	-.1	.0	-.1
12. NASA REVERSE SENSOR MV	-.1	.0	-.1	.0	-.1	-.1
13. REVERSE POWER SIGNAL DBM	-.0	.0	-.0	.0	.0	.0
14. VACUUM(VAUNS=LOG(1/M^3))	14.6	14.6	14.5	14.5	14.4	14.5
15. BASEPLATE CALORIMETER W	.0	.0	.0	.0	.0	.0
16. RF OUTPUT CALORIMETER W	225.8	225.8	225.8	225.8	221.6	217.3
17. RF DRIVE DBM	23.0	23.0	23.0	23.0	23.0	23.0
18. MW	199.7	199.8	201.6	201.0	201.1	201.4
19. OUTPUT POWER DBM	53.6	53.6	53.5	53.4	53.4	53.4
20. WATTS	229.3	229.4	222.8	220.6	221.1	216.3
21. GAIN DB	30.6	30.6	30.4	30.4	30.4	30.3
22. TOTAL COLLECTOR MA	72.6	72.5	72.1	72.5	72.2	72.1
BODY LOSSES:						
23. INTERCEPTION MA	4.1	4.1	4.1	4.2	4.4	4.5
24. WATTS	27.5	27.2	27.2	28.2	29.3	30.1
25. RF LOSS WATTS	80.3	80.3	78.0	77.2	77.4	75.7
26. TOTAL WATTS	107.8	107.6	105.2	105.4	106.7	105.8
27. RESIDUAL BEAM POWER AT COLLECTOR WATTS	513.5	512.1	521.0	524.6	522.9	528.6
28. TOTAL HV INPUT WATTS	480.3	479.3	477.7	474.4	471.6	468.5
29. OUTPUT+INTCPT+LOSS W	337.1	337.0	328.0	326.0	327.7	322.1
30. COLLECTOR DISSIP. W	143.2	142.4	149.7	148.4	143.9	146.4
31. AVGE. IMPACT VOLTS	1974	1962	2075	2048	1994	2030
32. COLLECTOR EFFICIENCY PCT	72.1	72.2	71.3	71.7	72.5	72.3
33. OVERALL EFFIC INCL HTR	47.3	47.4	46.2	46.1	46.5	45.8
35. ELECTRONIC EFFIC. PCT	36.4	36.5	35.4	35.0	35.1	34.3
36. NASA DEF. PCT	27.0	27.0	26.2	25.9	26.0	25.4
37. THERMISTOR NO. 1 DEG C	81.8	84.4	81.1	81.0	81.0	81.2
38. THERMISTOR NO. 2 DEG C	217.7	217.7	217.7	217.7	217.7	220.4
39. THERMISTOR NO. 3 DEG C	63.0	63.0	63.1	63.1	63.1	63.2
40. THERMISTOR NO. 4 DEG C	74.5	74.7	74.9	74.9	75.0	74.9

LTTO1 10 REV-A

COL. 1 TO 6 SAT: DRIVE POWER (+23 dBm)

COL. 1 TO 6 55°C BASE PLATE

III(i)

TUBE # L-5394 #2022R-1, TEST DATE 23APR75 (1), SHEET 10 NAS 3-15330

COLLECTOR VOLTAGES RELATIVE TO CATHODE:

NO.						
1	11191	11171	11172	11191	11191	11192
2	8951	8934	8926	8949	8953	8952
3	7837	7819	7810	7833	7843	7844
4	6681	6663	6690	6691	6689	6704
5	5541	5532	5568	5565	5560	5573
6	4443	4430	4435	4452	4444	4460
7	3378	3358	3376	3379	3390	3376
8	2267	2249	2261	2254	2255	2204
9	1067	1061	1078	1090	1104	1084
10	0	0	0	0	0	0

COLLECTOR CURRENTS, MA:

NO.						
1	4.2	4.3	4.3	4.2	4.1	4.0
2	5.8	5.9	6.0	6.1	6.1	6.0
3	15.7	16.2	16.6	16.7	16.5	16.3
4	18.2	18.6	18.2	17.5	16.7	16.3
5	5.1	4.6	4.0	3.7	3.6	3.7
6	3.8	3.6	3.5	3.7	4.0	4.3
7	4.9	4.3	4.4	4.6	4.8	5.0
8	5.0	4.2	4.4	4.9	5.7	6.6
9	15.6	16.7	15.9	14.5	12.5	10.9
10	-5.8	-5.7	-5.1	-3.2	-1.8	-.9

COLLECTOR INPUT POWERS, WATTS:

NO.						
1	47.3	47.7	47.8	46.8	46.3	45.1
2	51.8	53.0	53.8	54.2	54.4	53.4
3	123.4	126.7	129.6	130.4	129.7	127.5
4	121.9	123.9	121.8	116.8	111.5	109.0
5	28.2	25.2	22.0	20.4	20.2	20.8
6	16.9	15.7	15.3	16.4	17.6	19.0
7	16.4	14.4	14.9	15.7	16.4	17.0
8	11.4	9.5	9.9	11.0	12.7	14.5
9	17.2	17.7	17.2	15.8	13.8	11.8
10	.0	.0	.0	.0	.0	.0

COLLECTOR DISSIPATIONS, WATTS:

NO.						
1	8.3	8.4	8.9	8.6	8.3	8.2
2	11.4	11.6	12.5	12.4	12.1	12.1
3	31.1	31.8	34.4	34.1	33.0	33.0
4	36.0	36.5	37.8	35.8	33.2	33.0
5	10.0	8.9	8.2	7.5	7.3	7.6
6	7.5	7.0	7.2	7.5	7.9	8.7
7	9.6	8.4	9.2	9.5	9.6	10.2
8	9.9	8.3	9.1	10.0	11.3	13.4
9	30.9	32.7	33.0	29.6	24.9	22.1
10	11.5	11.3	10.6	6.6	3.6	1.9

LTTO1 10 REV-A

III(j)

TUBE # L-5394 #2022R-1, TEST DATE 23APR75 (1), SHEET 11 NAS 3-15330

COL. #:	1	2	3	4	5
1. FREQUENCY, GHZ	12.091	12.100	12.111	12.120	12.130
2. CATHODE VOLTS	11197	11197	11177	11197	11197
3. MA	76.0	76.0	76.0	76.0	76.0
4. BEAM WATTS	850.6	850.7	849.1	850.7	850.7
5. MOD ANODE VOLTS	252	252	251	251	251
6. MA	-.0	-.0	-.0	-.0	-.0
7. WATTS	.0	.0	.0	.0	.0
8. HEATER VOLTS	3.29	3.29	3.29	3.29	3.29
9. AMPS	1.29	1.29	1.29	1.29	1.29
10. WATTS	4.24	4.24	4.24	4.24	4.24
11. NASA OUTPUT SENSOR MV	.0	-.1	-.1	-.1	-.1
12. NASA REVERSE SENSOR MV	.0	.0	.0	-.1	-.1
13. REVERSE POWER SIGNAL DBM	-.0	-.0	.0	-.0	-.0
14. VACUUM(VAUNS=LOG(N/M^3))	14.5	14.5	14.5	14.5	14.5
15. BASEPLATE CALORIMETER W	.0	.0	.0	.0	.0
16. RF OUTPUT CALORIMETER W	213.1	208.9	196.2	183.5	153.9
17. RF DRIVE DBM	23.0	23.0	23.0	23.0	23.0
18. MW	200.8	201.0	198.4	197.8	197.7
19. OUTPUT POWER DBM	53.3	53.2	52.9	52.5	51.9
20. WATTS	212.5	209.7	192.8	178.8	156.2
21. GAIN DB	30.2	30.2	29.9	29.6	29.0
22. TOTAL COLLECTOR MA	71.9	72.1	72.6	73.0	73.6
BODY LOSSES:					
23. INTERCEPTION MA	4.7	4.5	4.1	3.6	3.2
24. WATTS	31.4	30.4	27.2	24.0	21.2
25. RF LOSS WATTS	74.4	73.4	67.5	62.6	54.7
26. TOTAL WATTS	105.8	103.8	94.7	86.6	75.9
27. RESIDUAL BEAM POWER AT COLLECTOR WATTS	532.3	537.1	561.6	585.3	618.5
28. TOTAL HV INPUT WATTS	468.9	464.5	444.3	422.0	389.4
29. OUTPUT+INTCPT+LOSS W	318.3	313.6	287.5	265.4	232.2
30. COLLECTOR DISSIP. W	150.6	150.9	156.8	156.6	157.2
31. AVGE. IMPACT VOLTS	2095	2092	2160	2145	2136
32. COLLECTOR EFFICIENCY PCT	71.7	71.9	72.1	73.2	74.6
33. OVERALL EFFIC INCL HTR	44.9	44.7	43.0	41.9	39.7
35. ELECTRONIC EFFIC. PCT	33.7	33.3	30.7	28.4	24.8
36. NASA EFF. PCT	25.0	24.7	22.7	21.0	18.4
37. THERMISTOR NO. 1 DEG C	81.5	81.9	82.0	81.7	80.8
38. THERMISTOR NO. 2 DEG C	217.1	217.1	217.7	217.7	217.1
39. THERMISTOR NO. 3 DEG C	63.2	63.2	63.2	63.2	63.2
40. THERMISTOR NO. 4 DEG C	74.1	74.5	74.3	73.7	73.0

COL. 5 SAT DRIVE=+23.0DBM

COL. 1 TO 6 55 DEGREE C BASE PLATE

LITTON 1B REV. A

III(k)

TUBE # L-5394 #2022R-1, TEST DATE 23APR75 (1), SHEET 12 NAS 3-15330

COLLECTOR VOLTAGES RELATIVE TO CATHODE:

NO.					
1	11200	11192	11173	11194	11202
2	8950	8951	8940	8969	8975
3	7831	7826	7810	7846	7866
4	6701	6708	6698	6721	6743
5	5556	5562	5539	5554	5567
6	4432	4442	4414	4420	4424
7	3354	3375	3337	3357	3358
8	2230	2235	2194	2206	2189
9	1137	1130	1104	1126	1082
10	0	0	0	0	0

COLLECTOR CURRENTS, MA:

NO.					
1	4.0	3.8	3.6	3.4	3.1
2	5.8	5.6	5.0	4.6	3.9
3	16.5	17.2	16.6	15.2	12.6
4	15.4	14.2	12.7	11.6	10.3
5	3.8	3.7	3.9	3.9	4.0
6	4.7	5.1	5.6	6.0	6.7
7	5.5	5.8	6.1	5.9	5.8
8	7.5	8.1	9.4	11.1	12.9
9	9.5	9.4	10.5	12.3	15.3
10	-.7	-.7	-.9	-.9	-.9

COLLECTOR INPUT POWERS, WATTS:

NO.					
1	44.5	42.9	40.4	37.8	34.3
2	52.3	49.7	45.1	41.0	34.9
3	129.1	134.5	129.8	119.2	99.3
4	103.1	94.9	85.0	78.0	69.5
5	20.9	20.8	21.3	21.4	22.0
6	20.9	22.7	24.5	26.3	29.7
7	18.4	19.7	20.5	19.9	19.6
8	16.6	18.1	20.7	24.5	28.2
9	10.8	10.6	11.6	13.8	16.5
10	.0	.0	.0	.0	.0

COLLECTOR DISSIPATIONS, WATTS:

NO.					
1	8.3	8.0	7.8	7.2	6.5
2	12.2	11.6	10.9	9.8	8.3
3	34.5	35.9	35.9	32.6	27.0
4	32.2	29.6	27.4	24.9	22.0
5	7.9	7.8	8.3	8.3	8.5
6	9.9	10.7	12.0	12.8	14.3
7	11.5	12.2	13.3	12.7	12.5
8	15.6	16.9	20.3	23.8	27.6
9	19.9	19.6	22.7	25.4	32.6
10	1.5	1.4	1.9	1.8	2.0

LITTON 1B REV. A

III(l)

TUBE # L-5394 #2022R-1, TEST DATE 23APR75 (1), SHEET 13 NAS 3-15330

	COL. #:	1	2	3	4	5	6
1.	FREQUENCY, GHZ	12.031	12.040	12.049	12.060	12.070	12.080
2.	CATHODE VOLTS	11197	11197	11197	11218	11197	11197
3.	MA	76.0	76.0	76.0	76.0	76.0	76.0
4.	BEAM WATTS	850.6	850.6	850.4	852.0	850.6	850.6
5.	MOD ANODE VOLTS	251	251	251	251	251	252
6.	MA	.0	-.0	-.0	.0	.0	-.0
7.	WATTS	.0	.0	.0	.0	.0	.0
8.	HEATER VOLTS	3.29	3.29	3.29	3.29	3.29	3.29
9.	AMPS	1.29	1.29	1.29	1.29	1.29	1.29
10.	WATTS	4.24	4.24	4.24	4.24	4.24	4.24
11.	NASA OUTPUT SENSOR MV	.0	.0	.0	-.1	.0	-.1
12.	NASA REVERSE SENSOR MV	.0	.0	.0	.0	.0	.0
13.	REVERSE POWER SIGNAL DBM	-.0	.0	.0	.0	.0	-.0
14.	VACUUM(VAUNS=LOG(W/M^3))	14.5	14.5	14.5	14.5	14.5	14.5
15.	BASEPLATE CALORIMETER W	.0	.0	.0	.0	.0	.0
16.	RF OUTPUT CALORIMETER W	124.3	111.6	98.9	90.5	98.9	98.9
17.	RF DRIVE DBM	15.7	15.7	15.7	15.7	15.7	15.7
18.	MW	37.4	37.3	37.2	37.5	37.6	37.5
19.	OUTPUT POWER DBM	51.3	51.0	50.5	50.2	50.5	50.5
20.	WATTS	134.7	126.4	112.9	105.1	112.0	113.1
21.	GAIN DB	35.6	35.3	34.8	34.5	34.7	34.8
22.	TOTAL COLLECTOR MA	74.9	75.2	75.0	75.0	75.1	74.7
	BODY LOSSES:						
23.	INTERCEPTION MA	2.0	1.9	1.8	1.8	1.8	1.9
24.	WATTS	13.4	12.7	12.3	12.1	12.2	12.5
25.	RF LOSS WATTS	47.1	44.2	39.5	36.8	39.2	39.6
26.	TOTAL WATTS	60.5	56.9	51.8	48.9	51.4	52.1
27.	RESIDUAL BEAM POWER AT COLLECTOR WATTS	655.4	667.2	685.8	697.9	687.1	685.3
*28.	TOTAL HV INPUT WATTS	333.7	324.2	308.6	304.3	308.7	308.1
29.	OUTPUT+INTCPT+LOSS W	195.2	183.3	164.7	154.0	163.5	165.2
30.	COLLECTOR DISSIP. W	138.5	140.9	143.9	150.3	145.3	142.8
31.	AVGE. IMPACT VOLTS	1850	1875	1919	2004	1935	1913
32.	COLLECTOR EFFICIENCY PCT	78.9	78.9	79.0	78.5	78.9	79.2
33.	OVERALL EFFIC INCL HTR	39.9	38.5	36.1	34.1	35.8	36.2
35.	ELECTRONIC EFFIC. PCT	21.4	20.1	17.9	16.7	17.8	18.0
36.	NASA DEF. PCT	15.6	14.9	13.3	12.3	13.2	13.3
37.	THERMISTOR NO. 1 DEG C	69.0	69.1	69.1	68.9	68.8	68.7
38.	THERMISTOR NO. 2 DEG C	220.4	220.4	220.4	220.4	220.4	223.3
39.	THERMISTOR NO. 3 DEG C	58.0	58.1	58.2	58.2	58.2	58.3
40.	THERMISTOR NO. 4 DEG C	60.3	60.7	60.6	60.3	60.2	60.1

LITTON 10 REV. A

COL. 1 TO 6 SAT POWER OUTPUT -3 dB = +15.4 dBm DRIVE

COL. 1 TO 6 55 DEGREE C BASE PLATE

III(m)

TUBE # L-5394 #2022R-1, TEST DATE 23APR75 (1), SHEET 14 NAS 3-15330

COLLECTOR VOLTAGES RELATIVE TO CATHODE:

NO.						
1	11206	11205	11185	11230	11207	11208
2	8947	8951	8945	8983	8961	8957
3	7812	7821	7836	7869	7840	7825
4	6753	6714	6734	6759	6735	6742
5	5614	5562	5579	5604	5584	5589
6	4513	4449	4459	4481	4467	4476
7	3345	3335	3347	3372	3355	3323
8	2203	2222	2240	2277	2215	2234
9	1121	1152	1152	1164	1085	1067
10	0	0	0	0	0	0

COLLECTOR CURRENTS, MA:

NO.						
1	2.4	2.2	2.0	1.9	2.0	2.0
2	2.5	2.2	2.0	1.8	1.9	2.0
3	5.9	5.0	3.9	3.5	4.2	4.7
4	10.1	9.5	8.7	8.5	9.1	9.2
5	4.1	4.3	4.0	4.0	4.2	4.0
6	5.9	6.2	6.5	6.6	6.5	6.2
7	10.4	11.8	12.7	12.9	12.8	12.2
8	22.8	22.9	22.2	20.9	18.7	16.7
9	11.7	11.7	13.6	15.3	16.2	18.1
10	-.9	-.7	-.6	-.5	-.5	-.6

COLLECTOR INPUT POWERS, WATTS:

NO.						
1	27.3	25.0	22.5	21.7	22.5	22.9
2	22.3	19.9	17.4	16.5	17.2	17.6
3	45.9	39.4	30.4	27.6	33.0	37.0
4	66.3	63.7	58.8	57.5	61.0	62.3
5	23.0	24.0	22.1	22.5	23.6	22.4
6	26.4	27.4	29.0	29.4	29.2	27.8
7	34.8	39.4	42.4	43.5	42.9	40.7
8	50.2	50.8	49.8	47.7	41.3	37.3
9	13.1	13.5	15.7	17.8	17.5	19.4
10	.0	.0	.0	.0	.0	.0

COLLECTOR DISSIPATIONS, WATTS:

NO.						
1	4.5	4.2	3.9	3.9	3.9	3.9
2	4.6	4.2	3.7	3.7	3.7	3.7
3	10.9	9.4	7.4	7.0	8.1	9.0
4	18.7	17.8	16.8	17.1	17.5	17.7
5	7.6	8.1	7.6	8.0	8.2	7.7
6	10.8	11.5	12.5	13.1	12.7	11.9
7	19.3	22.1	24.3	25.8	24.8	23.4
8	42.1	42.9	42.6	42.0	36.1	32.0
9	21.6	22.0	26.1	30.7	31.3	34.7
10	1.6	1.3	1.1	1.0	1.0	1.1

LITTON 10 REV. A

III(n)

TUBE # L-5394 #2022R-1, TEST DATE 23APR75 (1), SHEET 15 NAS 3-15830

COL. #:	1	2	3	4	5	6
1. FREQUENCY, GHZ	12.091	12.100	12.110	12.120	12.130	12.079
2. CATHODE VOLTS	11197	11197	11197	11197	11197	11197
3. MA	76.0	76.0	76.0	76.0	76.0	75.0
4. BEAM WATTS	850.6	850.6	850.4	850.4	850.6	850.4
5. MOD ANODE VOLTS	251	251	252	252	252	251
6. MA	-.0	-.0	-.0	-.0	-.0	-.0
7. WATTS	.0	.0	.0	.0	.0	.0
8. HEATER VOLTS	3.29	3.29	3.29	3.29	3.29	3.29
9. AMPS	1.29	1.29	1.29	1.29	1.29	1.29
10. WATTS	4.24	4.24	4.24	4.24	4.24	4.24
11. NASA OUTPUT SENSOR MV	-.1	-.1	-.1	-.1	-.1	-.1
12. NASA REVERSE SENSOR MV	-.1	.0	-.1	.0	.0	-.1
13. REVERSE POWER SIGNAL DBM	.0	-.0	-.0	.0	.0	.0
14. VACUUM(VAUNS=LOG(N/M^3))	14.5	14.5	14.4	14.5	14.4	14.5
15. BASEPLATE CALORIMETER W	.0	.0	.0	.0	.0	.0
16. RF OUTPUT CALORIMETER W	98.9	98.9	90.5	56.7	22.8	.0
17. RF DRIVE DBM	15.7	15.7	15.7	15.7	15.7	8.9
18. MW	37.4	37.4	36.9	36.9	36.9	7.7
19. OUTPUT POWER DBM	50.4	50.5	50.1	48.8	46.6	43.3
20. WATTS	110.7	113.3	103.3	75.5	45.5	21.2
21. GAIN DB	34.7	34.8	34.5	33.1	30.9	34.4
22. TOTAL COLLECTOR MA	74.9	74.7	75.4	75.2	75.0	75.5
BODY LOSSES:						
23. INTERCEPTION MA	1.9	1.9	1.9	1.8	1.7	1.5
24. WATTS	12.6	12.7	12.6	12.2	11.4	10.1
25. RF LOSS WATTS	38.7	39.7	36.1	26.4	15.9	7.4
26. TOTAL WATTS	51.4	52.4	48.8	38.6	27.3	17.5
27. RESIDUAL BEAM POWER AT COLLECTOR WATTS	686.5	684.9	698.4	736.3	777.8	811.8
28. TOTAL HV INPUT WATTS	305.6	307.8	305.8	267.8	224.7	189.2
29. OUTPUT+INTCPT+LOSS W	162.0	165.6	152.0	114.1	72.7	38.6
30. COLLECTOR DISSIP. W	143.5	142.1	153.8	153.7	151.9	150.5
31. AVGE. IMPACT VOLTS	1916	1902	2040	2045	2025	1993
32. COLLECTOR EFFICIENCY PCT	79.2	79.3	78.0	79.1	80.5	81.5
33. OVERALL EFFIC INCL HTR	35.7	36.3	33.3	27.8	19.9	10.9
35. ELECTRONIC EFFIC. PCT	17.6	18.0	16.4	12.0	7.2	3.4
36. NASA DEF. PCT	13.0	13.3	12.1	8.9	5.3	2.5
37. THERMISTOR NO. 1 DEG C	68.5	68.6	68.8	68.7	67.9	61.0
38. THERMISTOR NO. 2 DEG C	220.4	223.3	223.3	220.4	220.4	220.4
39. THERMISTOR NO. 3 DEG C	58.2	58.2	58.2	58.2	58.1	55.4
40. THERMISTOR NO. 4 DEG C	59.9	59.9	59.8	59.3	58.2	49.9

LITTON 18 REV. A

COL. 1 to 6 55 DEGREE C BASE PLATE
COL. 1 to 5 SAT DRIVE -3 dB = +15.4 dBm
COL. 6 REFERENCE ONLY

III(o)

TUBE # L-5394 #2022R-1, TEST DATE 23APR75 (1), SHEET 16 NAS 3-15[illegible]

COLLECTOR VOLTAGES RELATIVE TO CATHODE:

NO.						
1	11207	11207	11207	11211	11215	11217
2	8753	8754	8950	8957	8968	8932
3	7821	7813	7815	7950	7861	7886
4	6756	6737	6733	6750	6786	6840
5	5609	5585	5579	5589	5585	5630
6	4493	4473	4470	4467	4449	4505
7	3327	3331	3337	3331	3345	3404
8	2242	2230	2310	2296	2255	2230
9	1035	1007	1086	1068	1041	1054
10	0	0	0	0	0	0

COLLECTOR CURRENTS, MA:

NO.						
1	2.0	2.1	2.1	1.6	1.1	.6
2	2.0	2.0	2.0	1.5	.9	.5
3	4.9	5.4	5.0	2.5	1.4	.6
4	9.3	9.6	9.5	7.2	3.2	1.0
5	4.1	4.2	4.1	3.8	3.2	1.7
6	6.2	6.0	5.9	5.9	5.7	4.1
7	11.5	10.8	10.3	10.8	10.8	8.6
8	14.3	13.2	13.5	15.5	18.3	26.6
9	21.3	22.0	23.6	27.0	31.0	32.2
10	-.7	-.6	-.6	-.6	-.5	-.2

COLLECTOR INPUT POWERS, WATTS:

NO.						
1	22.6	23.4	23.4	18.2	11.9	6.5
2	17.5	18.3	18.1	13.3	8.1	4.0
3	38.2	42.5	38.9	19.5	11.4	4.9
4	62.8	64.6	63.6	48.8	21.8	6.6
5	23.2	23.3	23.1	21.2	18.0	9.3
6	27.9	26.8	26.4	26.1	25.5	18.6
7	38.3	36.0	34.3	35.9	36.0	29.1
8	32.0	29.5	31.2	35.7	41.2	59.1
9	22.1	22.1	25.7	28.9	32.2	34.0
10	.0	.0	.0	.0	.0	.0

COLLECTOR DISSIPATIONS, WATTS:

NO.						
1	3.9	4.0	4.3	3.3	2.1	1.2
2	3.7	3.9	4.1	3.0	1.8	.9
3	9.4	10.3	10.2	5.1	2.9	1.2
4	17.8	18.2	19.3	14.9	6.5	1.9
5	7.9	7.9	8.4	7.8	6.5	3.3
6	11.9	11.4	12.1	12.0	11.6	8.2
7	22.1	20.5	21.0	22.0	21.8	17.0
8	27.3	25.2	27.5	31.8	37.0	53.0
9	40.8	41.8	48.2	55.2	62.7	64.2
10	1.2	1.2	1.3	1.3	1.0	.5

LITTON 18 REV. A

III(p)

TUBE # L-5394 #2022R-1, TEST DATE 23APR75 (1), SHEET 17 NAS 3-15830

COL. #:	1	2	3	4	5	6
1. FREQUENCY, GHZ	12.030	12.040	12.050	12.060	12.070	12.080
2. CATHODE VOLTS	11197	11197	11197	11197	11197	11197
3. MA	76.0	76.0	76.0	76.0	76.0	76.0
4. BEAM WATTS	850.4	850.6	850.6	850.6	850.6	850.4
5. MOD ANODE VOLTS	251	252	251	251	251	251
6. MA	-.0	-.0	-.0	-.0	-.0	.0
7. WATTS	.0	.0	.0	.0	.0	.0
8. HEATER VOLTS	3.29	3.29	3.29	3.29	3.29	3.29
9. AMPS	1.29	1.29	1.29	1.29	1.29	1.29
10. WATTS	4.24	4.24	4.24	4.24	4.24	4.24
11. NASA OUTPUT SENSOR MV	.0	.0	-.1	-.1	.0	-.1
12. NASA REVERSE SENSOR MV	.0	-.1	.0	-.1	.0	-.1
13. REVERSE POWER SIGNAL DBM	-.0	.0	-.0	-.0	.0	.0
14. VACUUM(VAUNS=LOG(N/M^3))	14.5	14.5	14.5	14.5	14.5	14.5
15. BASEPLATE CALORIMETER W	.0	.0	.0	.0	.0	.0
16. RF OUTPUT CALORIMETER W	.0	.0	.0	.0	.0	.0
17. RF DRIVE DBM	8.9	8.9	8.9	8.9	8.9	8.9
18. MW	7.7	7.7	7.8	7.8	7.8	7.8
19. OUTPUT POWER DBM	44.1	43.9	43.1	42.3	42.5	43.2
20. WATTS	25.6	24.4	20.2	17.0	17.8	21.2
21. GAIN DB	35.2	35.0	34.2	33.4	33.6	34.4
22. TOTAL COLLECTOR MA	75.3	75.3	75.4	75.3	75.4	75.3
BODY LOSSES:						
23. INTERCEPTION MA	1.6	1.5	1.5	1.5	1.5	1.5
24. WATTS	10.4	10.3	10.1	10.0	9.9	9.9
25. RF LOSS WATTS	8.9	8.5	7.1	6.0	6.2	7.4
26. TOTAL WATTS	19.4	18.8	17.1	16.0	16.1	17.4
27. RESIDUAL BEAM POWER AT COLLECTOR WATTS	805.5	807.3	813.2	817.6	816.6	811.9
28. TOTAL HV INPUT WATTS	194.7	194.4	188.0	181.2	181.5	184.4
29. OUTPUT+INTCPT+LOSS W	44.9	43.2	37.3	33.0	33.9	38.6
30. COLLECTOR DISSIP. W	149.8	151.2	150.7	148.2	147.6	145.8
31. AVGE. IMPACT VOLTS	1989	2007	1998	1967	1956	1937
32. COLLECTOR EFFICIENCY PCT	81.4	81.3	81.5	81.9	81.9	82.0
33. OVERALL EFFIC INCL HTR	12.8	12.3	10.5	9.2	9.6	11.3
35. ELECTRONIC EFFIC. PCT	4.1	3.9	3.2	2.7	2.8	3.4
36. NASA EFF. PCT	3.0	2.9	2.4	2.0	2.1	2.5
37. THERMISTOR NO. 1 DEG C	60.4	60.6	60.5	60.3	60.2	60.1
38. THERMISTOR NO. 2 DEG C	220.4	223.3	220.4	220.4	220.4	217.7
39. THERMISTOR NO. 3 DEG C	54.7	54.6	54.5	54.4	54.4	54.3
40. THERMISTOR NO. 4 DEG C	48.8	48.8	48.6	48.4	48.3	48.2

REV. A

COL. 1 TO 6 SAT. OUTPUT POWER -10 dB = +8.82 dBm

COL. 1 TO 6 55 DEGREE C BASE PLATE

III(q)

TUBE # L-5394 #2022R-1, TEST DATE 23APR75 (1), SHEET 18 NAS 3-15837

COLLECTOR VOLTAGES RELATIVE TO CATHODE:

NO.						
1	11218	11218	11218	11218	11218	11218
2	8980	8970	8980	8981	8977	8976
3	7824	7805	7825	7826	7817	7817
4	6732	6721	6724	6728	6719	6728
5	5645	5627	5630	5640	5625	5636
6	4508	4481	4481	4501	4479	4499
7	3357	3350	3398	3363	3382	3352
8	2159	2209	2195	2193	2202	2208
9	1124	1188	1165	1134	1138	1120
10	0	0	0	0	0	0

COLLECTOR CURRENTS, MA:

NO.						
1	.6	.6	.5	.5	.5	.5
2	.5	.4	.4	.4	.4	.4
3	.6	.6	.6	.5	.5	.6
4	1.0	1.0	.9	.8	.9	.9
5	1.7	1.7	1.5	1.4	1.5	1.5
6	4.4	4.0	3.7	3.3	3.4	3.7
7	8.1	7.3	6.0	5.4	6.3	7.9
8	31.2	31.9	32.1	30.7	28.4	26.3
9	27.9	28.5	30.2	32.6	33.8	33.6
10	-.6	-.6	-.5	-.4	-.3	-.2

COLLECTOR INPUT POWERS, WATTS:

NO.						
1	6.5	6.2	6.1	5.8	5.7	6.1
2	4.0	3.9	3.6	3.5	3.5	3.7
3	4.9	4.7	4.4	4.1	4.1	4.4
4	6.7	6.5	5.9	5.7	5.7	6.1
5	9.8	9.3	8.6	8.0	8.2	8.6
6	19.6	18.1	16.5	14.9	15.3	16.7
7	27.0	24.4	20.5	18.1	21.4	26.5
8	67.4	70.6	70.5	67.3	62.5	58.1
9	31.3	33.8	35.2	37.0	38.5	37.6
10	.0	.0	.0	.0	.0	.0

COLLECTOR DISSIPATIONS, WATTS:

NO.						
1	1.2	1.1	1.1	1.0	1.0	1.0
2	.9	.9	.8	.8	.8	.8
3	1.2	1.2	1.1	1.0	1.0	1.1
4	2.0	1.9	1.8	1.7	1.7	1.7
5	3.5	3.3	3.0	2.8	2.9	3.0
6	8.7	8.1	7.4	6.5	6.7	7.2
7	16.0	14.6	12.1	10.6	12.4	15.3
8	62.1	64.1	54.2	60.4	55.5	51.0
9	55.5	57.1	60.3	64.2	66.1	65.1
10	1.2	1.1	1.0	.7	.5	.4

REV. A

III(r)

NAS 3-15830

TUBE # L-5394 #2022R-1. TEST DATE 23APR75 (1). SHEET 19

COL. #:		1	2	3	4
1. FREQUENCY, GHZ		12.090	12.101	12.120	12.130
2. CATHODE VOLTS		11197	11197	11197	11197
3.	MA	76.0	76.0	76.0	76.0
4. BEAM WATTS		850.4	850.4	850.6	850.4
5. MOD ANODE VOLTS		252	251	251	251
6.	MA	-.0	-.0	.0	-.0
7.	WATTS	.0	.0	.0	.0
8. HEATER VOLTS		3.29	3.29	3.29	3.29
9.	AMPS	1.29	1.29	1.29	1.29
10.	WATTS	4.24	4.24	4.24	4.24
11. NASA OUTPUT SENSOR	MV	.0	-.1	-.1	-.1
12. NASA REVERSE SENSOR	MV	-.1	.0	.0	-.1
13. REVERSE POWER SIGNAL DBM		.0	-.0	.0	-.0
14. VACUUM(VAUNS=LOG(N/M^3))		14.4	14.5	14.4	14.5
15. BASEPLATE CALORIMETER	W	.0	.0	.0	.0
16. RF OUTPUT CALORIMETER	W	.0	.0	.0	.0
17. RF DRIVE	DBM	8.9	8.9	8.8	8.8
18.	MW	7.7	7.7	7.6	7.6
19. OUTPUT POWER	DBM	43.2	42.8	40.7	38.3
20.	WATTS	20.8	19.3	11.9	6.7
21. GAIN DB		34.3	34.0	31.9	29.5
22. TOTAL COLLECTOR MA		75.5	75.4	75.6	75.4
BODY LOSSES:					
23. INTERCEPTION	MA	1.5	1.5	1.4	1.4
24.	WATTS	9.9	9.8	9.7	9.6
25. RF LOSS	WATTS	7.3	6.7	4.2	2.4
26. TOTAL	WATTS	17.2	16.5	13.8	12.0
27. RESIDUAL BEAM POWER AT COLLECTOR	WATTS	812.4	814.6	824.9	831.7
28. TOTAL HV INPUT	WATTS	163.6	181.7	172.4	162.9
29. OUTPUT+INTCPT+LOSS	W	38.1	35.8	25.7	18.7
30. COLLECTOR DISSIP.	W	145.5	145.9	146.7	144.2
31. AVG. IMPACT VOLTS		1927	1934	1940	1912
32. COLLECTOR EFFICIENCY PCT		82.1	82.1	82.2	82.7
33. OVERALL EFFIC INCL HTR		11.1	10.4	6.7	4.0
35. ELECTRONIC EFFIC.	PCT	3.3	3.1	1.9	1.1
36. NASA DEF.	PCT	2.5	2.3	1.4	.8
37. THERMISTOR NO. 1	DEG C	60.0	60.2	60.4	60.5
38. THERMISTOR NO. 2	DEG C	217.7	220.4	220.4	220.4
39. THERMISTOR NO. 3	DEG C	54.2	54.2	54.3	54.4
40. THERMISTOR NO. 4	DEG C	48.1	48.1	48.0	47.8

COL. 1-4 SATURATED OUTPUT POWER -10DB = +8.82 dBm

LITTON REV. A

COL. 1 TO 4 55 DEGREE C BASE PLATE

III(s)

NAS 3-15830

TUBE # L-5394 #2022R-1. TEST DATE 23APR75 (1). SHEET 20

COLLECTOR VOLTAGES RELATIVE TO CATHODE:

NO.				
1	11218	11218	11218	11219
2	8976	8976	8972	8980
3	7814	7815	7810	7820
4	6747	6731	6725	6733
5	5656	5643	5634	5644
6	4517	4487	4499	4511
7	3349	3347	3381	3425
8	2185	2226	2253	2225
9	1082	1113	1113	1088
10	0	0	0	0

COLLECTOR CURRENTS, MA:

NO.				
1	.6	.5	.5	.5
2	.4	.4	.4	.3
3	.6	.6	.5	.5
4	.9	.9	.8	.7
5	1.6	1.5	1.3	1.2
6	3.9	3.7	3.0	2.6
7	8.1	8.0	6.1	3.8
8	25.0	23.7	23.4	24.1
9	34.6	36.3	39.9	42.0
10	-.2	-.2	-.2	-.1

COLLECTOR INPUT POWERS, WATTS:

NO.				
1	6.3	6.1	5.3	5.0
2	3.9	3.7	3.3	3.0
3	4.7	4.4	3.9	3.5
4	6.3	6.1	5.4	4.8
5	9.1	8.7	7.5	6.7
6	17.6	16.7	13.3	11.5
7	27.2	26.6	20.5	13.0
8	54.6	52.7	52.7	53.7
9	37.4	40.4	44.4	45.7
10	.0	.0	.0	.0

COLLECTOR DISSIPATIONS, WATTS:

NO.				
1	1.1	1.0	.9	.9
2	.8	.8	.7	.6
3	1.2	1.1	1.0	.9
4	1.8	1.7	1.6	1.4
5	3.1	3.0	2.6	2.3
6	7.5	7.2	5.7	4.9
7	15.6	15.4	11.8	7.2
8	48.1	45.8	45.4	46.1
9	66.6	70.1	77.4	80.2
10	.4	.3	.3	.3

LITTON REV. A

III(t)

TUBE # L-5394 #2022R-1, TEST DATE 23APR75 (1), SHEET 21

NAS 3-15330

	COL. #:	1
1.	FREQUENCY, GHZ	12.079
2.	CATHODE VOLTS	11197
3.	MA	76.0
4.	BEAM WATTS	850.6
5.	MOD ANODE VOLTS	251
6.	MA	-.0
7.	WATTS	.0
8.	HEATER VOLTS	3.29
9.	AMPS	1.29
10.	WATTS	4.24
11.	NASA OUTPUT SENSOR MV	-.1
12.	NASA REVERSE SENSOR MV	.0
13.	REVERSE POWER SIGNAL DBM	.0
14.	VACUUM(VAUNS=LOG(N/M^3))	14.4
15.	BASEPLATE CALORIMETER W	.0
16.	RF OUTPUT CALORIMETER W	.0
17.	RF DRIVE DBM	-35.5
18.	MW	.0
19.	OUTPUT POWER DBM	-52.0
20.	WATTS	.0
21.	GAIN DB	.0
22.	TOTAL COLLECTOR MA	75.6
	BODY LOSSES:	
23.	INTERCEPTION MA	1.4
24.	WATTS	9.4
25.	RF LOSS WATTS	.0
26.	TOTAL WATTS	9.4
27.	RESIDUAL BEAM POWER AT COLLECTOR WATTS	841.1
28.	TOTAL HV INPUT WATTS	143.4
29.	OUTPUT+INTCPT+LOSS W	9.4
30.	COLLECTOR DISSIP. W	134.0
31.	AVGE. IMPACT VOLTS	1773
32.	COLLECTOR EFFICIENCY PCT	64.1
33.	OVERALL EFFIC INCL HTR	.0
35.	ELECTRONIC EFFIC. PCT	.0
36.	NASA DEF. PCT	.0
37.	THERMISTOR NO. 1 DEG C	61.1
38.	THERMISTOR NO. 2 DEG C	220.4
39.	THERMISTOR NO. 3 DEG C	54.5
40.	THERMISTOR NO. 4 DEG C	47.8

LITTON 18

REV. A

COL. 1 NO DRIVE

COL. 1 55°C BASE PLATE

III(u)

7.3 QF-3 TEST DATA (Flight Backup, Prime, S/N 2025)

10.0 Specifications Parameter			QF Design Specification		Actual Value
10.1	Saturation Characteristics				
10.1.1	Frequency	(GHz)	12.038-12.123		12.038-12.123
10.1.2	Gain	(dB)	30^{+2}_{-1}	A	29.1 (29.0) Min
10.1.3	Output Power, Pos, Min.	(W)	180	A	177 (160) Min.
10.1.4	Overall Efficiency, Min.	(%)	40	A	39.7 (34.6) Table IIe(IIIe)
10.1.5	DC Input Power, Max.	(W)	500		470 (484) Table IIe(IIIe)
10.1.6	Beam Transmission @ 50°C Baseplate, Min.	(%)	92	A	96 (92.7) Min.
10.1.7	AM/PM (pos to Pos -2dB)	(°/dB)	6	B	6.0
10.1.8	Second Order Phase Deviation Max.	($^{o}/MHz^{2}$)	0.3	B	Not computed
10.1.9	Harmonic Output Power, 2nd and 3rd, Max.	(dBm)	+23	B	+13
10.1.10	Thermal Input to Baseplate, Max.	(W)	150	A	91 (100) Table IIe(IIIe)
10.2	Small Signal Characteristics (Po = saturation Po -10 dB)				
10.2.1	Gain Variation, peak to peak	(dB)	5	A	2.1 (2.7)
10.2.2	Gain-Below 11.928 GHz, Max.	(dB)	20	B	5.6
10.3	Noise Figure, Max.	(dB)	40	B	30.5
10.4	Differential Gain (3 to 23 dB below Pos)	(dB)	0.7	A	1.0 (1.2)
10.5	Spurious Output Power (Pd = 0 and Pds, excluding harmonically related signals)				
	a. In any 4 kHz band between 14.0 and 14.3 GHz	(dBm)	-10	B	<10
	b. In any 100 MHz band between 10.0 and 18.0 GHz	(dBm)	-10	B	<10

10.0 Specifications (continued)

Parameter		QF Design Specification		Actual Value
10.6 Overdrive without OST damage, Continuous, Max.	(dBm)	+29	A	+29 (+28.5)
Short Term, ≤ 0.5 sec, Max.	(dBm)	+43.4	A	+43.4 (OST S/N 2032)
10.7 Power Processor Requirements (Set to OST decal values)				
10.7.1 Cathode Voltage with respect to ground.	(kV)	-11.3 ±0.3	A	-11.45
10.7.2 Anode Voltage with respect to ground.	(V)	350 ±200	A	150
10.7.3 Anode Current, Max.	(mA)	0.1	A	<0.1
10.7.4 Heater Current, (constant current supply).	(A)	1.3 ±0.1	A	1.29
10.7.5 Heater Voltage with respect to cathode.	(V)	4.2	A	3.42
10.7.6 Body Current Overload Trip	(mA)	10	A	10
10.7.7 Ion Pump Supply Voltage	(kV)	2.3 - 3.3	A	3.0
10.7.8 Ion Pump Current Overload Trip (Sum of two pumps)	(μA)	10	A	≤ 10
10.7.9 Collector Voltages, Electrode #1 - #10 (% of cathode voltage)		0, 20, 30, 40, 50, 60, 70, 80 90 and 100	A	OK
10.7.10 Baseplate Temperature				
Operating	(°C)	0 to +58	A	0 to +85
At Turn on	(°C)	-15 to +58	A	0 to +85
Non-Operating	(°C)	-20 to +65	A	0 to +85
10.8 Refocusing Magnetic Field		PM		PM
10.9 Weight OST	(lb)	26.02 Max.	C	26.4
10.10 Design Life	(yr)	2		2
10.11 Waveguide Type		WR-75		WR-75

FINAL TEST DATA SUMMARY

Baseplate Temperature = 0°C

(Table Ia)

Cathode Voltage	E_k	-11450	Volts
Cathode Current	I_k	74.4	mA
Anode Voltage	E_A	150	Volts
Heater Voltage	E_f	3.42	Volts
Heater Current	I_f	1.29	Amps
Cathode Temperature	T_k	1090	Deg. C

MDC Electrode No.	1	2	3	4	5
Electrode Voltage (kV)	0.00	2.29	3.43	4.58	5.72
(Relative to Gnd)	6	7	8	9	10
	6.87	8.01	9.16	10.30	11.45

Frequency (MHz)		12040	12080	12120
Sat. Output Power (W)		185	200	183
Sat. Drive Power (dBm)		23.0	23.1	23.0
(mW)		201	202	199
Sat. Gain (dB)		29.6	29.9	29.6
Body Current, Sat. (mA)		2.9	3.0	3.0
Transmission, Sat. (%)		96.1	96.0	96.0
Overall Eff., Sat. (%)		39.9	42.1	39.7
Total DC Power, Sat (W)		458	469	455
Second Harmonic, Sat. (dBm)	B	+13	+6	+7
Third Harmonic, Sat. (dBm)	B	<+15	<+15	<+15
Notch Filter IL (dB)	B	0.5	0.2	0.2
MCS Waveguide Coupler IL (dB)	B	.12	.13	0.12

NOTES

A. Baseplate temperature = 0°C with thermal shroud enclosing all of OST except MDC and top side of notch filter unless otherwise noted.

B. ATD of 4 March 1975 (prior to focus trim) with baseplate temperature = 53°C.

C. Thermistor R/T Calibration Figures 23 and 24.

D. RF System NASA #1 Certificate of Conformance Western Automatic Test Services on 4/8/75.

E. Total Filament Hours at Litton 1329.

F. Total Cathode Pulse Hours at Litton 275.

G. Total Cathode CW Hours at Litton 656.

FINAL TEST DATA SUMMARY

Baseplate Temperature = 85°C

(Table Ib)

Cathode Voltage	E_k	-11450	Volts
Cathode Current	I_k	74.4	mA
Anode Voltage	E_A	150	Volts
Heater Voltage	E_f	3.42	Volts
Heater Current	I_f	1.29	Amps
Cathode Temperature	T_k	1090	Deg. C

MDC Electrode No.	1	2	3	4	5
Electrode Voltage (KV)	0.00	2.29	3.43	4.58	5.72
(Relative to Gnd).	6	7	8	9	10
	6.87	8.01	9.16	10.30	11.45

Frequency (MHz)		12040	12080	12120
Sat. Output Power (W)		177	186	159
Sat. Drive Power (dBm)		23.0	23.1	23.0
(mW)		201	202	199
Sat. Gain (dB)		29.5	29.6	29.0
Body Current, Sat. (mA)		5.3	5.1	5.2
Transmission, Sat. (%)		92.9	93.1	93.0
Overall Eff., Sat. (%)		36.8	38.0	34.6
Total DC Power, Sat. (W)		477	484	456
Second Harmonic, Sat. (dBm)	B	+13	+6	+7
Third Harmonic, Sat. (dBm)	B	<+15	<+15	<+15
Notch Filter IL (dB)	B	0.5	0.2	0.2
MCS Waveguide Coupler IL (dB)	B	.12	.13	0.12

NOTES

A. Baseplate temperature = 85°C with thermal shroud enclosing all of OST except MDC and top side of notch filter unless otherwise noted.

B. ATD of 4 March 1975 (prior to focus trim) with baseplate temperature = 53°C.

/VAJ51021/ L-5394 DATA REDUCTION (VERSION 12/6/74); MOD. FOR ALEXOVICH CIRCUIT

TUBE # L-5394 #2025. TEST DATE 18AUG75 (1)

RUN # 1. OPERATOR LRB

COL. #:	1	2	3
1. FREQUENCY, GHZ	12.040	12.080	12.120
2. CATHODE VOLTS	11480	11480	11480
3. MA	74.4	74.4	74.3
4. BEAM WATTS	853.7	853.5	853.4
5. MOD ANODE VOLTS	159	160	159
6. MA	-.0	-.0	.0
7. WATTS	.0	.0	.0
8. HEATER VOLTS	3.42	3.42	3.42
9. AMPS	1.29	1.29	1.29
10. WATTS	4.41	4.41	4.41
11. NASA OUTPUT SENSOR MV	-.1	-.1	-.1
12. NASA REVERSE SENSOR MV	.0	.0	.0
13. REVERSE POWER SIGNAL DBM	.0	.0	.0
14. VACUUM(VAUNS=LOG(N/M^3))	13.0	13.0	13.0
15. BASEPLATE CALORIMETER W	.0	.0	.0
16. RF OUTPUT CALORIMETER W	68.7	43.8	25.0
17. RF DRIVE DBM	28.5	28.6	28.5
18. MW	712.9	716.1	706.3
19. OUTPUT POWER DBM	49.4	47.7	46.5
20. WATTS	86.9	59.5	44.5
21. GAIN DB	20.9	19.2	18.0
22. TOTAL COLLECTOR MA	70.0	69.5	69.3
BODY LOSSES:			
23. INTERCEPTION MA	4.4	4.8	5.0
24. WATTS	30.0	33.3	34.5
25. RF LOSS WATTS	30.4	20.8	15.6
26. TOTAL WATTS	60.4	54.1	50.1
27. RESIDUAL BEAM POWER AT COLLECTOR WATTS	706.4	739.9	758.9
28. TOTAL HV INPUT WATTS	356.9	339.9	330.2
29. OUTPUT+INTCPT+LOSS W	147.3	113.6	94.5
30. COLLECTOR DISSIP. W	209.6	226.3	235.7
31. AVGE. IMPACT VOLTS	2994	3255	3400
32. COLLECTOR EFFICIENCY PCT	70.3	69.4	68.9
33. OVERALL EFFIC INCL HTR	24.1	17.3	13.3
35. ELECTRONIC EFFIC. PCT	13.7	9.4	7.0
36. NASA DEF. PCT	10.2	7.0	5.2
37. THERMISTOR NO. 1 DEG C	28.6	27.8	27.4
38. THERMISTOR NO. 2 DEG C	168.9	168.9	168.2
39. THERMISTOR NO. 3 DEG C	28.6	29.5	28.2
40. THERMISTOR NO. 4 DEG C	37.1	37.8	36.3
41. TIME	1311	1313	1314

Table IIa Saturation Drive Power +5.5 dB (0°CBaseplate).

03/19 13:54

TUBE # L-5394 #2025. TEST DATE 18AUG75 (1). SHEET 2

COLLECTOR VOLTAGES RELATIVE TO CATHODE:			
NO. 1	11474	11478	11484
2	9181	9185	9174
3	8044	8036	8022
4	6868	6888	6904
5	5745	5749	5773
6	4568	4541	4566
7	3437	3387	3398
8	2270	2241	2225
9	1087	1128	1095
10	0	0	0
COLLECTOR CURRENTS, MA:			
NO. 1	2.0	1.7	1.4
2	1.8	1.4	1.2
3	3.1	2.2	1.9
4	7.5	4.3	3.6
5	8.6	7.1	6.3
6	12.0	13.3	13.2
7	12.3	16.8	17.7
8	13.4	16.4	17.2
9	13.4	8.9	9.5
10	-4.0	-2.6	-2.7
COLLECTOR INPUT POWERS, WATTS:			
NO. 1	23.1	18.9	16.0
2	16.1	13.0	11.1
3	25.1	17.8	15.2
4	51.5	29.9	24.6
5	49.4	41.0	36.6
6	54.7	60.2	60.4
7	42.1	57.0	60.3
8	30.5	36.7	38.2
9	14.5	10.1	10.4
10	.0	.0	.0
COLLECTOR DISSIPATIONS, WATTS:			
NO. 1	6.0	5.4	4.7
2	5.2	4.6	4.1
3	9.3	7.2	6.5
4	22.5	14.1	12.1
5	25.7	23.2	21.6
6	35.8	43.2	44.9
7	36.7	54.7	60.3
8	40.2	53.3	58.4
9	40.0	29.0	32.2
10	11.9	8.4	9.1

Table IIb - Saturation Drive Power +5.5 dB

TUBE # L-5394 #2025. TEST DATE 18AUG75 (1). SHEET 3

	COL. #:	1	2	3
1.	FREQUENCY, GHZ	12.040	12.080	12.119
2.	CATHODE VOLTS	11500	11480	11480
3.	MA	74.4	74.4	74.4
4.	BEAM WATTS	855.5	854.0	853.9
5.	MOD ANODE VOLTS	159	158	159
6.	MA	-.0	-.0	.0
7.	WATTS	.0	.0	.0
8.	HEATER VOLTS	3.42	3.42	3.42
9.	AMPS	1.29	1.29	1.29
10.	WATTS	4.41	4.41	4.41
11.	NASA OUTPUT SENSOR MV	-.1	-.1	-.1
12.	NASA REVERSE SENSOR MV	-.1	.0	.0
13.	REVERSE POWER SIGNAL DBM	.0	.0	.0
14.	VACUUM(VAUNS=LOG(N/M^3))	13.0	13.0	13.3
15.	BASEPLATE CALORIMETER W	.0	.0	.0
16.	RF OUTPUT CALORIMETER W	156.2	156.2	143.7
17.	RF DRIVE DBM	26.0	26.1	26.0
18.	MW	401.8	402.7	397.2
19.	OUTPUT POWER DBM	52.2	52.1	51.7
20.	WATTS	165.9	162.8	147.7
21.	GAIN DB	26.2	26.1	25.7
22.	TOTAL COLLECTOR MA	70.9	70.9	70.8
	BODY LOSSES:			
23.	INTERCEPTION MA	3.5	3.5	3.6
24.	WATTS	24.4	23.8	24.9
25.	RF LOSS WATTS	58.1	57.0	51.7
26.	TOTAL WATTS	82.5	80.7	76.6
27.	RESIDUAL BEAM POWER AT COLLECTOR WATTS	607.1	610.5	629.6
28.	TOTAL HV INPUT WATTS	439.0	434.9	428.8
29.	OUTPUT+INTCPT+LOSS W	248.4	243.5	224.3
30.	COLLECTOR DISSIP. W	190.6	191.4	204.5
31.	AVGE. IMPACT VOLTS	2690	2698	2890
32.	COLLECTOR EFFICIENCY PCT	68.6	68.7	67.5
33.	OVERALL EFFIC INCL HTR	37.4	37.1	34.1
35.	ELECTRONIC EFFIC. PCT	26.2	25.7	23.4
36.	NASA DEF. PCT	19.4	19.1	17.3
37.	THERMISTOR NO. 1 DEG C	31.4	30.2	30.5
38.	THERMISTOR NO. 2 DEG C	163.8	164.4	165.0
39.	THERMISTOR NO. 3 DEG C	31.2	31.0	30.7
40.	THERMISTOR NO. 4 DEG C	48.8	50.3	49.3
41.	TIME	1402	1403	1404

Table IIc - Saturation Drive Power +3 dB

TUBE # L-5394 #2025. TEST DATE 18AUG75 (1). SHEET 4

COLLECTOR VOLTAGES RELATIVE TO CATHODE:

NO.			
1	11489	11470	11469
2	9164	9137	9131
3	7997	7985	7980
4	6836	6856	6857
5	5629	5632	5625
6	4503	4484	4467
7	3225	3193	3178
8	2060	2050	1972
9	919	932	881
10	0	0	0

COLLECTOR CURRENTS, MA:

NO.			
1	3.5	3.5	3.6
2	5.1	6.2	6.6
3	12.9	12.8	12.4
4	12.1	9.1	8.0
5	6.8	6.6	6.0
6	7.3	9.5	9.0
7	7.7	9.9	9.6
8	8.2	7.3	10.9
9	13.2	8.8	6.9
10	-6.0	-2.7	-2.3

COLLECTOR INPUT POWERS, WATTS:

NO.			
1	40.3	40.0	41.4
2	46.8	56.6	60.2
3	103.5	101.9	98.8
4	82.6	62.6	55.1
5	38.3	36.9	33.5
6	33.0	42.6	40.2
7	24.7	31.7	30.4
8	16.8	14.9	21.6
9	12.1	8.2	6.1
10	.0	.0	.0

COLLECTOR DISSIPATIONS, WATTS:

NO.			
1	9.4	9.4	10.4
2	13.7	16.7	19.0
3	34.8	34.4	35.8
4	32.5	24.6	23.2
5	18.3	17.7	17.2
6	19.7	25.6	26.0
7	20.6	26.8	27.7
8	22.0	19.6	31.6
9	35.5	23.7	20.1
10	16.1	7.1	6.6

Table IId - Saturation Drive Power +3 dB

TUBE # L-5394 #2025, TEST DATE 18AUG75 (1), SHEET 5

		1	2	3
	COL. #:	1	2	3
1.	FREQUENCY, GHZ	12.040	12.080	12.120
2.	CATHODE VOLTS	11480	11480	11480
3.	MA	74.4	74.4	74.4
4.	BEAM WATTS	854.2	854.1	854.0
5.	MOD ANODE VOLTS	159	159	159
6.	MA	-.0	-.0	.0
7.	WATTS	.0	.0	.0
8.	HEATER VOLTS	3.42	3.42	3.42
9.	AMPS	1.29	1.29	1.29
10.	WATTS	4.41	4.41	4.41
11.	NASA OUTPUT SENSOR MV	-.1	-.1	.0
12.	NASA REVERSE SENSOR MV	-.1	.0	.0
13.	REVERSE POWER SIGNAL DBM	.0	.0	.0
14.	VACUUM(VAUNS=LOG(N/M^3))	13.0	13.3	13.3
15.	BASEPLATE CALORIMETER W	.0	.0	.0
16.	RF OUTPUT CALORIMETER W	175.0	193.7	181.2
17.	RF DRIVE DBM	23.0	23.1	23.0
18.	MW	200.8	202.1	199.0
19.	OUTPUT POWER DBM	52.7	53.0	52.6
20.	WATTS	184.7	199.5	182.6
21.	GAIN DB	29.6	29.9	29.6
22.	TOTAL COLLECTOR MA	71.5	71.4	71.4
	BODY LOSSES:			
23.	INTERCEPTION MA	2.9	3.0	3.0
24.	WATTS	20.2	20.9	20.9
25.	RF LOSS WATTS	64.6	69.8	63.9
26.	TOTAL WATTS	84.8	90.7	84.8
27.	RESIDUAL BEAM POWER AT COLLECTOR WATTS	584.7	563.9	586.7
28.	TOTAL HV INPUT WATTS	458.2	469.5	455.2
29.	OUTPUT+INTCPT+LOSS W	269.5	290.2	267.3
30.	COLLECTOR DISSIP. W	188.6	179.3	187.9
31.	AVGE. IMPACT VOLTS	2639	2513	2633
32.	COLLECTOR EFFICIENCY PCT	67.7	68.2	68.0
33.	OVERALL EFFIC INCL HTR	39.9	42.1	39.7
35.	ELECTRONIC EFFIC. PCT	29.2	31.5	28.9
36.	NASA DEF. PCT	21.6	23.4	21.4
37.	THERMISTOR NO. 1 DEG C	31.0	32.3	32.5
38.	THERMISTOR NO. 2 DEG C	163.2	161.0	161.0
39.	THERMISTOR NO. 3 DEG C	31.4	33.4	33.4
40.	THERMISTOR NO. 4 DEG C	51.7	53.4	53.4
41.	TIME	1423	1424	1425

Table IIe - Saturation Output Power

TUBE # L-5394 #2025, TEST DATE 18AUG75 (1), SHEET 6

COLLECTOR VOLTAGES RELATIVE TO CATHODE:

NO.			
1	11474	11484	11484
2	9210	9192	9197
3	8041	8045	8044
4	6897	6905	6902
5	5739	5729	5718
6	4602	4568	4537
7	3380	3431	3375
8	2252	2247	2222
9	1100	1106	1121
10	0	0	0

COLLECTOR CURRENTS, MA:

NO.			
1	4.1	4.3	4.4
2	6.5	8.5	8.8
3	15.1	16.7	15.8
4	13.2	10.6	8.5
5	5.3	4.6	4.3
6	5.0	5.9	6.1
7	5.8	5.3	5.8
8	7.7	7.1	9.9
9	13.7	11.0	9.7
10	-4.9	-2.6	-1.7

COLLECTOR INPUT POWERS, WATTS:

NO.			
1	47.3	49.8	50.0
2	60.1	78.4	80.7
3	121.0	133.9	126.8
4	90.7	73.1	58.4
5	30.6	26.1	24.8
6	22.9	27.1	27.6
7	19.5	18.2	19.5
8	17.3	15.9	21.9
9	15.1	12.2	10.9
10	.0	.0	.0

COLLECTOR DISSIPATIONS, WATTS:

NO.			
1	10.9	10.9	11.5
2	17.2	21.4	23.1
3	39.7	41.8	41.5
4	34.7	26.6	22.3
5	14.1	11.4	11.4
6	13.1	14.9	16.0
7	15.2	13.3	15.2
8	20.3	17.7	25.9
9	36.2	27.6	25.6
10	12.8	6.5	4.6

Table IIf - Saturation Drive Power

TUBE # L-5394 #2025, TEST DATE 18AUG75 (1), SHEET 7

	COL. #:	1	2	3
1.	FREQUENCY, GHZ	12.040	12.080	12.120
2.	CATHODE VOLTS	11480	11489	11480
3.	MA	74.4	74.4	74.4
4.	BEAM WATTS	853.9	854.0	854.1
5.	MOD ANODE VOLTS	159	159	159
6.	MA	.0	-.0	-.0
7.	WATTS	.0	.0	.0
8.	HEATER VOLTS	3.42	3.42	3.42
9.	AMPS	1.29	1.29	1.29
10.	WATTS	4.41	4.41	4.41
11.	NASA OUTPUT SENSOR MV	.0	-.1	-.1
12.	NASA REVERSE SENSOR MV	.0	.0	.0
13.	REVERSE POWER SIGNAL DBM	.0	.0	.0
14.	VACUUM(VAUNS=LOG(N/M^3))	13.0	13.3	13.3
15.	BASEPLATE CALORIMETER W	.0	.0	.0
16.	RF OUTPUT CALORIMETER W	75.0	100.0	75.0
17.	RF DRIVE DBM	16.2	16.2	16.1
18.	MW	41.3	41.5	40.8
19.	OUTPUT POWER DBM	49.7	50.5	49.2
20.	WATTS	92.9	111.1	83.0
21.	GAIN DB	33.5	34.3	33.1
22.	TOTAL COLLECTOR MA	72.0	72.1	72.2
	BODY LOSSES:			
23.	INTERCEPTION MA	2.3	2.3	2.2
24.	WATTS	16.1	15.8	15.4
25.	RF LOSS WATTS	32.5	38.9	29.0
26.	TOTAL WATTS	48.6	54.7	44.5
27.	RESIDUAL BEAM POWER AT COLLECTOR WATTS	712.3	688.2	726.7
28.	TOTAL HV INPUT WATTS	325.2	345.7	319.1
29.	OUTPUT+INTCPT+LOSS W	141.6	165.8	127.4
30.	COLLECTOR DISSIP. W	183.7	179.9	191.7
31.	AVGE. IMPACT VOLTS	2550	2495	2656
32.	COLLECTOR EFFICIENCY PCT	74.2	73.9	73.6
33.	OVERALL EFFIC INCL HTR	28.2	31.7	25.6
35.	ELECTRONIC EFFIC. PCT	14.7	17.6	13.1
36.	NASA DEF. PCT	10.9	13.0	9.7
37.	THERMISTOR NO. 1 DEG C	63.6	21.5	66.6
38.	THERMISTOR NO. 2 DEG C	168.9	168.2	170.3
39.	THERMISTOR NO. 3 DEG C	73.0	60.8	76.4
40.	THERMISTOR NO. 4 DEG C	40.0	40.3	39.3
41.	TIME	1627	1629	1630

Table IIg - Saturation Output Power -3 dB

TUBE # L-5394 #2025, TEST DATE 18AUG75 (1), SHEET 8

COLLECTOR VOLTAGES RELATIVE TO CATHODE:

NO.			
1	11473	11484	11486
2	9185	9195	9211
3	8061	8064	8088
4	6872	6864	6877
5	5731	5740	5741
6	4578	4589	4583
7	3403	3504	3451
8	2394	2273	2271
9	1130	1095	1107
10	0	0	0

COLLECTOR CURRENTS, MA:

NO.			
1	2.1	2.4	2.0
2	1.8	2.7	1.8
3	4.9	7.5	5.4
4	7.6	8.2	7.1
5	5.9	5.0	5.3
6	8.0	7.0	8.2
7	12.0	9.9	9.9
8	16.6	16.9	18.0
9	15.0	14.5	17.3
10	-1.8	-2.1	-2.7

COLLECTOR INPUT POWERS, WATTS:

NO.			
1	24.0	27.9	22.7
2	16.3	25.2	16.3
3	39.5	60.4	43.7
4	52.5	56.1	48.7
5	33.7	28.6	30.4
6	36.4	32.0	37.5
7	40.8	34.8	34.0
8	38.2	38.5	40.9
9	17.0	15.9	19.2
10	.0	.0	.0

COLLECTOR DISSIPATIONS, WATTS:

NO.			
1	5.3	5.1	5.3
2	4.5	5.8	4.7
3	12.5	18.7	14.3
4	19.5	20.4	18.8
5	15.0	12.4	14.1
6	20.3	17.4	21.7
7	30.6	24.9	26.2
8	42.3	42.3	47.8
9	38.3	36.2	46.0
10	4.6	5.2	7.3

Table IIh - Saturation Output Power -3 dB.

TUBE # L-5394 #2025. TEST DATE 18AUG75 (1). SHEET 9

	COL. #:	1	2	3	4
1.	FREQUENCY, GHZ	12.040	12.080	12.120	NONE
2.	CATHODE VOLTS	11480	11480	11480	11480
3.	MA	74.4	74.4	74.5	74.5
4.	BEAM WATTS	853.9	853.9	854.7	854.7
5.	MOD ANODE VOLTS	158	158	159	159
6.	MA	-.0	.0	-.0	-.0
7.	WATTS	.0	.0	.0	.0
8.	HEATER VOLTS	3.42	3.42	3.42	3.42
9.	AMPS	1.29	1.29	1.29	1.29
10.	WATTS	4.41	4.41	4.41	4.41
11.	NASA OUTPUT SENSOR MV	-.1	-.1	-.1	-.1
12.	NASA REVERSE SENSOR MV	-.1	-.1	.0	-.1
13.	REVERSE POWER SIGNAL DBM	.0	.0	.0	.0
14.	VACUUM(VAUNS=LOG(N/M^3))	13.0	13.0	13.0	13.3
15.	BASEPLATE CALORIMETER W	.0	.0	.0	.0
16.	RF OUTPUT CALORIMETER W	6.3	12.5	.0	6.3
17.	RF DRIVE DBM	10.2	10.2	10.1	
18.	MW	10.4	10.4	10.3	.0
19.	OUTPUT POWER DBM	43.8	44.0	41.9	5.2
20.	WATTS	23.8	25.3	15.5	.0
21.	GAIN DB	33.6	33.9	31.8	.0
22.	TOTAL COLLECTOR MA	72.4	72.4	72.6	72.6
	BODY LOSSES:				
23.	INTERCEPTION MA	2.0	2.0	1.9	1.9
24.	WATTS	13.7	13.6	13.1	12.7
25.	RF LOSS WATTS	8.3	8.9	5.4	.0
26.	TOTAL WATTS	22.0	22.4	18.5	12.7
27.	RESIDUAL BEAM POWER AT COLLECTOR WATTS	808.0	806.1	820.7	841.9
28.	TOTAL HV INPUT WATTS	243.4	250.1	237.3	208.3
29.	OUTPUT+INTCPT+LOSS W	45.9	47.8	34.0	12.7
30.	COLLECTOR DISSIP. W	197.6	202.4	203.3	195.6
31.	AVGE. IMPACT VOLTS	2729	2795	2802	2694
32.	COLLECTOR EFFICIENCY PCT	75.5	74.9	75.2	76.8
33.	OVERALL EFFIC INCL H.R	9.6	10.0	6.4	.0
35.	ELECTRONIC EFFIC. PCT	3.8	4.0	2.4	.0
36.	NASA DEF. PCT	2.8	3.0	1.8	.0
37.	THERMISTOR NO. 1 DEG C	54.3	83.4	68.3	93.7
38.	THERMISTOR NO. 2 DEG C	173.2	177.3	176.5	177.3
39.	THERMISTOR NO. 3 DEG C	62.6	95.1	74.1	101.4
40.	THERMISTOR NO. 4 DEG C	32.4	31.2	31.3	30.2
41.	TIME	1645	1646	1647	1648

Table III - Saturation Output Power -10 dB (Column 4 - Zero Drive Case).

TUBE # L-5394 #2025. TEST DATE 18AUG75 (1). SHEET 10

COLLECTOR VOLTAGES RELATIVE TO CATHODE:

NO.				
1	11484	11474	11474	11474
2	9156	9165	9154	9159
3	8014	8034	8009	8012
4	6961	6987	6957	6966
5	5799	5797	5800	5827
6	4591	4599	4602	4634
7	3421	3431	3426	3475
8	2281	2268	2259	2270
9	1148	1137	1132	1147
10	0	0	0	0

COLLECTOR CURRENTS, MA:

NO.				
1	.8	1.0	.9	.7
2	.7	.8	.7	.5
3	1.0	1.2	1.1	.8
4	1.4	1.7	1.6	1.1
5	2.8	3.5	3.0	1.8
6	9.1	9.7	8.0	5.1
7	14.4	12.8	12.4	8.5
8	26.4	27.1	27.2	30.6
9	17.5	16.1	18.6	24.2
10	-1.6	-1.3	-.9	-.6

COLLECTOR INPUT POWERS, WATTS:

NO.				
1	9.3	10.9	10.0	7.7
2	6.1	7.1	6.5	4.6
3	7.9	9.2	8.5	6.1
4	9.5	11.8	11.3	7.7
5	16.3	20.5	17.6	10.6
6	42.0	44.5	36.9	23.5
7	49.2	43.8	42.3	29.6
8	60.2	61.5	61.4	69.5
9	20.0	18.2	21.1	27.7
10	.0	.0	.0	.0

COLLECTOR DISSIPATIONS, WATTS:

NO.				
1	2.2	2.7	2.4	1.8
2	1.8	2.2	2.0	1.3
3	2.7	3.2	3.0	2.0
4	3.7	4.7	4.5	3.0
5	7.7	9.9	8.5	4.9
6	24.9	27.1	22.5	13.7
7	39.3	35.7	34.6	22.9
8	72.1	75.7	76.2	82.5
9	47.6	44.9	52.2	65.1
10	4.5	3.6	2.6	1.7

Table IIj - Saturation Output Power -10 dB (Column 4 - Zero Drive Case).

182

//AUG1021/ L-5394 DATA REDUCTION (VERSION 12/6/74): 08/18 11:19
MOD. FOR ALEXOVICH CIRCUIT
TUBE # L-5394#2025, TEST DATE 16AUG75 (1)
BENCH # 1, OPERATOR LR3

		1	2	3
	COL. #:	1	2	3
1.	FREQUENCY, GHZ	12.039	12.080	12.120
2.	CATHODE VOLTS	11500	11500	11500
3.	MA	74.1	74.1	74.1
4.	BEAM WATTS	852.0	852.0	852.0
5.	MOD ANODE VOLTS	165	164	164
6.	MA	.0	.0	-.0
7.	WATTS	.0	.0	.0
8.	HEATER VOLTS	3.42	3.42	3.42
9.	AMPS	1.29	1.29	1.29
10.	WATTS	4.41	4.41	4.41
11.	NASA OUTPUT SENSOR MV	.0	-.1	-.1
12.	NASA REVERSE SENSOR MV	.0	-.1	.0
13.	REVERSE POWER SIGNAL DBM	.0	.0	.0
14.	VACUUM(VAUNS=LOG(N/M^3))	13.0	13.3	13.0
15.	BASEPLATE CALORIMETER W	.0	.0	.0
16.	RF OUTPUT CALORIMETER W	31.3	25.0	6.3
17.	RF DRIVE DBM	28.5	28.5	28.5
18.	MW	714.5	719.4	706.3
19.	OUTPUT POWER DBM	47.5	46.8	44.4
20.	WATTS	56.4	48.0	27.4
21.	GAIN DB	19.0	18.2	15.9
22.	TOTAL COLLECTOR MA	65.4	65.6	65.1
	BODY LOSSES:			
23.	INTERCEPTION MA	9.6	9.4	9.8
24.	WATTS	66.3	64.9	67.4
25.	RF LOSS WATTS	19.7	16.8	9.6
26.	TOTAL WATTS	86.0	81.7	77.0
27.	RESIDUAL BEAM POWER AT COLLECTOR WATTS	709.6	722.3	747.6
28.	TOTAL HV INPUT WATTS	374.4	370.8	352.8
29.	OUTPUT+INTCP.+LOSS W	142.4	129.8	104.5
30.	COLLECTOR DISSIP. W	231.9	241.0	248.3
31.	AVGE. IMPACT VOLTS	3547	3673	3812
32.	COLLECTOR EFFICIENCY PCT	67.3	66.6	66.8
33.	OVERALL EFFIC INCL HTR	14.9	12.8	7.7
35.	ELECTRONIC EFFIC. PCT	8.9	7.6	4.3
36.	NASA D.F. PCT	6.6	5.6	3.2
37.	THERMISTOR NO. 1 DEG C	121.3	120.4	123.1
38.	THERMISTOR NO. 2 DEG C	140.3	142.0	141.7
39.	THERMISTOR NO. 3 DEG C	89.6	89.9	91.7
40.	THERMISTOR NO. 4 DEG C	84.0	85.2	82.7
41.	TIME	1404	1406	1407

Table IIIa – Saturation Drive Power +5.5 dB
(85°C Baseplate)

TUBE # L-5394#2025, TEST DATE 16AUG75 (1), SHEET 2

COLLECTOR VOLTAGES RELATIVE TO CATHODE:

NO.			
1	11493	11494	11497
2	9189	9191	9195
3	8061	8062	8072
4	6869	6878	6901
5	5755	5757	5788
6	4612	4613	4621
7	3443	3425	3417
8	2262	2255	2257
9	1132	1122	1122
10	0	0	0

COLLECTOR CURRENTS, MA:

NO.			
1	1.5	1.4	1.1
2	1.2	1.2	.9
3	1.8	1.8	1.3
4	4.0	3.4	2.2
5	7.1	6.8	4.7
6	12.7	12.9	12.7
7	14.4	16.3	17.7
8	15.4	15.3	16.1
9	9.0	8.0	10.3
10	-1.6	-1.4	-1.8

COLLECTOR INPUT POWERS, WATTS:

NO.			
1	17.0	16.4	12.2
2	11.1	10.8	8.2
3	14.8	14.3	10.6
4	27.3	23.4	14.9
5	40.7	39.0	27.4
6	58.4	59.5	58.9
7	49.5	55.7	60.5
8	34.8	34.5	36.3
9	10.2	9.0	11.5
10	.0	.0	.0

COLLECTOR DISSIPATIONS, WATTS:

NO.			
1	5.3	5.3	4.0
2	4.3	4.3	3.4
3	6.5	6.5	5.0
4	14.1	12.5	8.2
5	25.1	24.9	18.0
6	44.9	47.4	48.6
7	51.0	59.8	67.5
8	54.5	56.2	61.4
9	31.9	29.3	39.1
10	5.7	5.0	6.9

Table IIIb
Saturation Drive Power
+5.5 dB

TUBE # L-5394#2025, TEST DATE 16AUG75 (1), SHEET 3

	COL. #:	1	2	3
1.	FREQUENCY, GHZ	12.040	12.080	12.120
2.	CATHODE VOLTS	11500	11500	11500
3.	MA	74.0	74.0	74.0
4.	BEAM WATTS	851.1	851.2	851.1
5.	MOD ANODE VOLTS	156	155	155
6.	MA	-.0	-.0	.0
7.	WATTS	.0	.0	.0
8.	HEATER VOLTS	3.42	3.42	3.42
9.	AMPS	1.29	1.29	1.29
10.	WATTS	4.41	4.41	4.41
11.	NASA OUTPUT SENSOR MV	-.1	-.1	-.1
12.	NASA REVERSE SENSOR MV	.0	.0	-.1
13.	REVERSE POWER SIGNAL DBM	.0	.0	.0
14.	VACUUM(VAUNS=LOG(N/M^3))	13.0	13.3	13.0
15.	BASEPLATE CALORIMETER W	.0	.0	.0
16.	RF OUTPUT CALORIMETER W	131.2	137.5	118.7
17.	RF DRIVE DBM	26.0	26.1	26.0
18.	MW	401.8	405.5	396.3
19.	OUTPUT POWER DBM	51.6	51.8	51.1
20.	WATTS	146.0	150.6	127.7
21.	GAIN DB	25.6	25.7	25.1
22.	TOTAL COLLECTOR MA	68.7	69.1	69.1
	BODY LOSSES:			
23.	INTERCEPTION MA	6.2	6.0	5.9
24.	WATTS	42.8	41.1	41.0
25.	RF LOSS WATTS	51.1	52.7	44.7
26.	TOTAL WATTS	93.9	93.8	85.7
27.	RESIDUAL BEAM POWER AT COLLECTOR WATTS	611.2	606.8	637.8
28.	TOTAL HV INPUT WATTS	445.7	454.4	435.7
29.	OUTPUT+INTCPT+LOSS W	239.9	244.5	213.3
30.	COLLECTOR DISSIP. W	205.8	210.0	222.4
31.	AVGE. IMPACT VOLTS	2994	3038	3216
32.	COLLECTOR EFFICIENCY PCT	66.3	65.4	65.1
33.	OVERALL EFFIC INCL HTR	32.4	32.8	29.0
35.	ELECTRONIC EFFIC. PCT	23.2	23.9	20.3
36.	NASA DEF. PCT	17.2	17.7	15.0
37.	THERMISTOR NO. 1 DEG C	127.2	124.2	125.5
38.	THERMISTOR NO. 2 DEG C	160.0	162.1	161.0
39.	THERMISTOR NO. 3 DEG C	99.1	98.5	100.2
40.	THERMISTOR NO. 4 DEG C	96.4	98.9	96.4
41.	TIME	1457	1500	1502

Table IIIc – Saturation Drive Power +3 dB

TUBE # L-5394#2025, TEST DATE 16AUG75 (1), SHEET 4

COLLECTOR VOLTAGES RELATIVE TO CATHODE:

NO.			
1	11483	11482	11483
2	9208	9193	9201
3	8052	8041	[illegible]
4	6903	6921	6927
5	5778	5786	5800
6	4676	4671	4676
7	3474	3467	3474
8	2280	2272	2243
9	1132	1155	1159
10	0	0	0

COLLECTOR CURRENTS, MA:

NO.			
1	3.2	3.5	3.4
2	4.2	5.7	4.9
3	10.4	11.9	10.9
4	10.9	8.7	8.0
5	7.0	6.2	5.4
6	8.7	9.1	8.7
7	9.1	9.4	9.6
8	7.2	8.3	11.9
9	10.4	7.0	6.8
10	-2.2	-.6	-.4

COLLECTOR INPUT POWERS, WATTS:

NO.			
1	36.5	40.2	39.3
2	38.3	51.9	45.5
3	83.3	[illegible]	57.7
4	75.5	60.5	55.6
5	40.3	35.8	31.2
6	40.6	42.4	40.5
7	31.6	32.7	33.2
8	16.3	18.8	26.7
9	11.8	6.1	7.8
10	.0	.0	.0

COLLECTOR DISSIPATIONS, WATTS:

NO.			
1	9.5	10.6	11.0
2	12.5	17.2	15.9
3	31.0	36.1	35.0
4	32.7	26.6	25.8
5	20.9	18.8	17.3
6	26.0	27.6	27.9
7	27.3	28.6	30.7
8	21.4	25.2	38.2
9	31.1	21.2	21.7
10	6.6	1.9	1.2

Table IIId – Saturation Drive Power +3dB

TUBE # L-5394#2025, TEST DATE 16AUG75 (1), SHEET 5

COL. #:	1	2	3
1. FREQUENCY, GHZ	12.040	12.080	12.120
2. CATHODE VOLTS	11480	11500	11500
3. MA	74.0	74.0	74.0
4. BEAM WATTS	849.7	851.2	851.2
5. MOD ANODE VOLTS	156	155	156
6. MA	-.0	-.0	-.0
7. WATTS	.0	.0	.0
8. HEATER VOLTS	3.42	3.42	3.42
9. AMPS	1.29	1.29	1.29
10. WATTS	4.41	4.41	4.41
11. NASA OUTPUT SENSOR MV	-.1	-.1	-.1
12. NASA REVERSE SENSOR MV	.0	-.1	.0
13. REVERSE POWER SIGNAL DBM	.0	.0	.0
14. VACUUM(VAUNS=LOG(V/M^3))	13.3	13.0	13.3
15. BASEPLATE CALORIMETER W	.0	.0	.0
16. RF OUTPUT CALORIMETER W	162.5	175.0	156.2
17. RF DRIVE DBM	23.0	23.1	23.0
18. MW	200.7	202.1	199.0
19. OUTPUT POWER DBM	52.5	52.7	52.0
20. WATTS	177.1	185.9	159.1
21. GAIN DB	29.5	29.6	29.0
22. TOTAL COLLECTOR MA	69.5	69.8	69.8
BODY LOSSES:			
23. INTERCEPTION MA	5.3	5.1	5.2
24. WATTS	36.2	35.3	35.7
25. RF LOSS WATTS	62.0	65.1	55.7
26. TOTAL WATTS	98.1	100.4	91.4
27. RESIDUAL BEAM POWER AT COLLECTOR WATTS	574.6	565.0	600.8
28. TOTAL HV INPUT WATTS	477.2	484.4	455.5
29. OUTPUT+INTCPT+LOSS W	275.2	286.2	250.5
30. COLLECTOR DISSIP. W	202.0	198.2	205.0
31. AVGE. IMPACT VOLTS	2908	2841	2939
32. COLLECTOR EFFICIENCY PCT	64.8	64.9	65.9
33. OVERALL EFFIC INCL HTR	36.8	38.0	34.6
35. ELECTRONIC EFFIC. PCT	28.1	29.5	25.2
36. NASA DEF. PCT	20.8	21.8	18.7
37. THERMISTOR NO. 1 DEG C	124.7	123.9	123.1
38. THERMISTOR NO. 2 DEG C	158.9	159.4	160.5
39. THERMISTOR NO. 3 DEG C	101.3	102.0	100.1
40. THERMISTOR NO. 4 DEG C	100.5	100.8	101.1
41. TIME	1517	1519	1520

Table IIIe - Saturation Output Power

TUBE # L-5394#2025, TEST DATE 16AUG75 (1), SHEET 6

COLLECTOR VOLTAGES RELATIVE TO CATHODE:

NO.			
1	11465	11484	11487
2	9159	9167	9178
3	7988	8005	8016
4	6817	6856	6867
5	5610	5634	5632
6	4451	4474	4461
7	3236	3260	3253
8	2029	2040	2012
9	873	898	905
10	0	0	0

COLLECTOR CURRENTS, MA:

NO.			
1	4.3	4.5	4.1
2	7.1	6.8	7.6
3	16.2	17.2	15.2
4	11.5	9.3	7.8
5	5.0	4.7	4.7
6	5.8	6.1	7.0
7	5.6	4.6	5.6
8	5.7	6.6	9.4
9	12.7	10.5	9.9
10	-4.5	-2.5	-1.5

COLLECTOR INPUT POWERS, WATTS:

NO.			
1	48.7	51.6	47.3
2	65.3	69.9	69.6
3	129.3	137.5	121.8
4	76.7	63.8	53.4
5	28.2	25.5	25.6
6	25.9	27.4	31.2
7	18.1	15.0	18.1
8	11.6	13.4	19.9
9	11.1	9.4	8.9
10	.0	.0	.0

COLLECTOR DISSIPATIONS, WATTS:

NO.			
1	12.4	12.8	12.1
2	20.7	25.1	22.3
3	47.1	45.9	44.6
4	33.6	26.5	22.9
5	14.6	13.4	13.9
6	17.0	17.4	20.6
7	16.2	13.0	16.4
8	16.6	18.7	27.7
9	36.8	29.7	29.0
10	13.0	7.2	4.5

Table IIIf - Saturation Output Power

TUBE # L-5394#2025, TEST DATE 16AUG75 (1), SHEET 7

COL. #:	1	2	3
1. FREQUENCY, GHZ	12.040	12.080	12.120
2. CATHODE VOLTS	11500	11500	11500
3. MA	74.0	74.0	74.0
4. BEAM WATTS	851.5	851.5	851.5
5. MOD ANODE VOLTS	155	155	155
6. MA	.0	.0	.0
7. WATTS	.0	.0	.0
8. HEATER VOLTS	3.42	3.42	3.42
9. AMPS	1.29	1.29	1.29
10. WATTS	4.41	4.41	4.41
11. NASA OUTPUT SENSOR MV	-.1	-.1	-.1
12. NASA REVERSE SENSOR MV	-.1	.0	.0
13. REVERSE POWER SIGNAL DBM	.0	.0	.0
14. VACUUM(VAUNS=LOG(N/M^3))	13.3	13.3	13.0
15. BASEPLATE CALORIMETER W	.0	.0	.0
16. RF OUTPUT CALORIMETER W	75.0	75.0	50.0
17. RF DRIVE DBM	16.1	16.1	16.1
18. MW	41.2	41.1	40.9
19. OUTPUT POWER DBM	49.7	49.7	48.1
20. WATTS	93.8	92.4	64.2
21. GAIN DB	33.6	33.5	32.0
22. TOTAL COLLECTOR MA	72.1	72.1	72.2
BODY LOSSES:			
23. INTERCEPTION MA	2.9	2.9	2.8
24. WATTS	20.2	19.9	19.4
25. RF LOSS WATTS	32.8	32.3	22.5
26. TOTAL WATTS	53.0	52.2	41.9
27. RESIDUAL BEAM POWER AT COLLECTOR WATTS	704.7	705.8	745.4
28. TOTAL HV INPUT WATTS	344.8	347.9	314.0
29. OUTPUT+INTCPT+LOSS W	146.8	144.6	106.1
30. COLLECTOR DISSIP. W	198.0	203.2	207.9
31. AVGE. IMPACT VOLTS	2745	2817	2879
32. COLLECTOR EFFICIENCY PCT	71.9	71.2	72.1
33. OVERALL EFFIC INCL HTR	26.8	26.2	20.2
35. ELECTRONIC EFFIC. PCT	14.9	14.7	10.2
36. NASA DEF. PCT	11.0	10.9	7.5
37. THERMISTOR NO. 1 DEG C	115.5	114.5	115.8
38. THERMISTOR NO. 2 DEG C	168.9	172.5	169.6
39. THERMISTOR NO. 3 DEG C	97.8	96.9	98.3
40. THERMISTOR NO. 4 DEG C	89.7	89.2	89.4
41. TIME	1604	1605	1606

Table IIIg-Saturation Output Power -3 dB

TUBE # L-5394#2025, TEST DATE 16AUG75 (1), SHEET 8

COLLECTOR VOLTAGES RELATIVE TO CATHODE:

NO.			
1	11489	11488	11493
2	9185	9182	9193
3	8093	8084	8117
4	6929	6934	6950
5	5752	5757	5755
	4673	4669	4660
7	3416	3433	3425
8	2289	2292	2282
9	1166	1165	1150
10	0	0	0

COLLECTOR CURRENTS, MA:

NO.			
1	2.2	2.3	1.9
2	2.0	2.3	1.5
3	6.0	6.8	3.8
4	8.6	8.0	6.5
5	5.8	5.4	5.9
6	7.8	8.1	9.3
7	10.7	9.5	9.6
8	17.1	17.0	18.0
9	12.4	13.7	17.0
10	-.4	-1.0	-1.1

COLLECTOR INPUT POWERS, WATTS:

NO.			
1	25.3	26.4	21.3
2	18.3	21.5	13.9
3	48.2	54.8	30.8
4	59.5	55.3	45.4
5	33.4	31.1	33.7
6	36.2	36.0	43.4
7	36.7	32.5	32.8
8	39.1	39.0	41.0
9	14.4	16.0	19.5
10	.0	.0	.0

COLLECTOR DISSIPATIONS, WATTS:

NO.			
1	6.0	6.5	5.3
2	5.5	5.6	4.3
3	16.4	19.1	10.9
4	23.6	22.5	18.8
5	16.0	15.2	16.8
6	21.3	22.9	26.8
7	29.5	26.7	27.6
8	46.9	48.0	51.7
9	34.0	38.6	48.9
10	1.0	2.8	3.3

Table IIIh - Saturation Output Power -3 dB.

TUBE # L-5394#2025. TEST DATE 16AUG75 (1). SHEET 9

FREQUENCY OUT OF CALIBRATION RANGE

COL. #:		1	2	3	4
1.	FREQUENCY, GHZ	12.040	12.080	12.120	NONE
2.	CATHODE VOLTS	11480	11500	11500	11500
3.	MA	74.1	74.1	74.0	74.1
4.	BEAM WATTS	850.1	851.6	851.5	851.6
5.	MOD ANODE VOLTS	155	156	156	155
6.	MA	-.0	-.0	-.0	.0
7.	WATTS	.0	.0	.0	.0
8.	HEATER VOLTS	3.42	3.42	3.42	3.42
9.	AMPS	1.29	1.29	1.29	1.29
10.	WATTS	4.41	4.41	4.41	4.41
11.	NASA OUTPUT SENSOR MV	.0	.0	-.1	-.1
12.	NASA REVERSE SENSOR MV	-.1	-.1	.0	.0
13.	REVERSE POWER SIGNAL DBM	.0	.0	.0	.0
14.	VACUUM(VAUNS=LOG(N/M^3))	13.0	13.0	13.3	13.0
15.	BASEPLATE CALORIMETER W	.0	.0	.0	.0
16.	RF OUTPUT CALORIMETER W	.0	.0	6.3	6.3
17.	RF DRIVE DBM	10.2	10.2	10.1	
18.	MW	10.4	10.4	10.2	.0
19.	OUTPUT POWER DBM	43.4	42.8	40.9	-50.5
20.	WATTS	22.0	19.1	12.2	.0
21.	GAIN DB	33.3	32.6	30.8	.0
22.	TOTAL COLLECTOR MA	72.6	72.8	72.9	72.9
	BODY LOSSES:				
23.	INTERCEPTION MA	2.5	2.4	2.3	2.3
24.	WATTS	17.2	16.6	16.1	15.7
25.	RF LOSS WATTS	7.7	6.7	4.3	.0
26.	TOTAL WATTS	24.8	23.3	20.4	15.7
27.	RESIDUAL BEAM POWER AT COLLECTOR WATTS	803.3	809.1	818.8	835.9
28.	TOTAL HV INPUT WATTS	256.6	259.3	248.7	225.8
29.	OUTPUT+INTCPT+LOSS W	46.8	42.5	32.7	15.7
30.	COLLECTOR DISSIP. W	209.8	216.8	216.0	210.1
31.	AVGE. IMPACT VOLTS	2889	2979	2965	2883
32.	COLLECTOR EFFICIENCY PCT	73.9	73.2	73.6	74.9
33.	OVERALL EFFIC INCL HTR	8.4	7.3	4.8	.0
35.	ELECTRONIC EFFIC. PCT	3.5	3.0	1.9	.0
36.	NASA DEF. PCT	2.6	2.2	1.4	.0
37.	THERMISTOR NO. 1 DEG C	109.2	109.2	107.8	107.9
38.	THERMISTOR NO. 2 DEG C	178.2	179.1	163.0	179.1
39.	THERMISTOR NO. 3 DEG C	97.1	98.3	96.5	96.7
40.	THERMISTOR NO. 4 DEG C	82.9	83.5	82.3	82.3
41.	TIME.	1620	1621	1622	1623

Table IIIi - Saturation Output Power -10 dB (Column 4 - Zero Drive Case)

TUBE # L-5394#2025. TEST DATE 16AUG75 (1). SHEET 10

COLLECTOR VOLTAGES RELATIVE TO CATHODE:

NO.				
1	11478	11497	11497	11498
2	9181	9201	9203	9209
3	8028	8045	8046	8054
4	6808	6823	6829	6837
5	5652	5672	5678	5695
6	4459	4492	4502	4516
7	3216	3251	3248	3274
8	2024	2040	2040	2020
9	1152	1175	1170	1158
10	0	0	0	0

COLLECTOR CURRENTS, MA:

NO.				
1	1.1	1.2	1.1	.9
2	.9	1.0	.9	.7
3	1.3	1.5	1.4	1.1
4	2.1	2.5	2.2	1.5
5	4.4	4.4	4.0	3.1
6	11.2	11.0	9.7	7.8
7	13.7	12.1	11.9	9.8
8	23.2	24.3	24.8	27.8
9	15.2	14.9	16.5	19.8
10	-.3	.0	.3	.5

COLLECTOR INPUT POWERS, WATTS:

NO.				
1	12.1	13.2	12.4	10.3
2	8.0	5.7	8.0	6.4
3	10.5	12.1	10.9	8.5
4	14.2	16.7	15.2	10.5
5	24.9	25.0	22.7	17.4
6	50.0	49.5	43.9	35.3
7	43.9	39.3	35.8	32.0
8	45.9	49.5	50.6	56.2
9	17.5	17.5	19.3	22.9
10	.0	.0	.0	.0

COLLECTOR DISSIPATIONS, WATTS:

NO.				
1	3.0	3.4	3.2	2.6
2	2.5	2.8	2.6	2.0
3	3.8	4.5	4.0	3.0
4	6.0	7.3	6.6	4.4
5	12.7	13.1	11.8	8.8
6	32.3	32.9	28.9	22.5
7	39.5	35.0	35.4	28.1
8	67.0	72.4	73.5	80.3
9	43.9	44.4	48.9	57.0
10	.9	.1	1.3	1.3

Table IIIj - Saturation Output Power -10 dB (Column 4 - Zero Drive Case)

7.4 QF-5 TEST DATA (Flight backup, S/N 2030)

				QF Design Specification	Actual Value
10.0	Specifications	Parameter			
10.1	Saturation Characteristics				
10.1.1	Frequency		(GHz)	12.038-12.123	12.040-12.12 (for Table I data)
10.1.2	Gain, Min.		(dB)	30^{+2}_{-1}	30.3 Table IIk
10.1.3	Output Power, Pos, Min.		(W)	180 –	210 Table II(k)
10.1.4	Overall Efficiency, Min.		(%)	40	44.8 Table II(i)
10.1.5	DC Input Power, Max.		(W)	500	487 Table II(i)
10.1.6	Beam Transmission @ 50°C Baseplate, Min.		(%)	92	91.1
10.1.7	AM/PM (Pos to Pos -2dB), Max.		(°/dB)	6	7
10.1.8	Second Order Phase Deviation Max.		($^{o}/MHz^{2}$)	0.3	Not compute
10.1.9	Harmonic Output Power, 2nd and 3rd, Max.		(dBm)	+23	+22 Table I(a)
10.1.10	Thermal Input to Baseplate, Max.		(W)	150	115 Table II(k)
10.2	Small Signal Characteristics (Po = saturation Po -10 dB)				
10.2.1	Gain Variation, Max, pk to pk		(dB)	5	3
10.2.2	Gain-Below 11.928 GHz, Max.		(dB)	20	<20
10.3	Noise Figure, Max.		(dB)	40	36
10.8	Refocusing Magnetic Field			PM	PM
10.9	Weight OST		(lb)	26.02 Max.	26.5
10.10	Design Life		(yr)	2	2
10.11	Waveguide Type			WR-75	WR-75

C-3

10.0 Specifications (continued)

	Parameter		QF Design Specification	Actual Value
10.4	Differential Gain (3 to 23 dB below Pos)	(dB)	0.7	0.78
10.5	Spurious Output Power (Pd • 0 and Pds, excluding harmonically related signals)			
	a. In any 4 kHz band between 14.0 and 14.3 GHz	(dBm)	-10	<10
	b. In any 100 MHz band between 10.0 and 18.0 GHz	(dBm)	-10	<10
10.6	Overdrive without OST damage, Continuous, Max.	(dBm)	+29	No test
	Short Term, ≤ 0.5 sec, Max.	(dBm)	+43.4	No Test
10.7	Power Processor Requirements (Set to OST decal values)			
10.7.1	Cathode Voltage with respect to ground.	(kV)	-11.3 ±0.3	-11.3
10.7.2	Anode Voltage with respect to ground.	(V)	350 ±200	250
10.7.3	Anode Current, Max.	(mA)	0.1	<0.1
10.7.4	Heater Current, (constant current supply).	(A)	1.3 ±0.1	1.23
10.7.5	Heater Voltage with respect to cathode, Max.	(V)	4.2	3.3
10.7.6	Body Current Overload Trip	(mA)	10	10
10.7.7	Ion Pump Supply Voltage	(kV)	2.3 - 3.3	3.0
10.7.8	Ion Pump Current Overload Trip (Sum of two pumps)	(μA)	10	10
10.7.9	Collector Voltages, Electrode #1 - #10 (% of cathode voltage)		0, 20, 30, 40, 50, 60, 70, 80, 90 and 100	OK
10.7.10	Baseplate Temperature			
	Operating	(°C)	0 to +58	35 to 55
	At Turn on	(°C)	-15 to +58	No test
	Non-Operating	(°C)	-20 to +65	No Test

FINAL TEST DATA SUMMARY
(Table Ia)

Cathode Voltage	E_k	11,300		Volts		
Cathode Current	I_k	77.2		mA		
Anode Voltage	E_A	250		Volts		
Heater Voltage	E_f	3.30		Volts		
Heater Current	I_f	1.23		Amps		
Cathode Temperature	T_k	1050		Deg. C		
MDC Electrode No.	1	2	3	4	5	
Electrode Voltage (kV)	0.0	2.26	3.39	4.52	5.65	
(Relative to Gnd)	6	7	8	9	10	
	6.78	7.91	9.04	10.17	11.30	

Frequency (MHz)	12040	12080	12120
Sat. Output Power (dBm)	53.3	53.6	53.2
Sat. Output Power (W)	216.2	231	210
Sat. Drive Power (dBm)	23	23	23
(mW)	200	201	197
Sat. Gain (dB)	30.3	30.6	30.3
Body Current, Sat.(mA)	5.2	4.8	5.4
Transmission, Sat.(%)	93.2	93.7	92.9
Overall Eff., Sat. (%)	45	48	46
Total DC Power, Sat(W)	474	479	454
Second Harmonic, Sat (dBm)	@ F=24080 +22	@F=24160 +17	@F=24240 +15
Third Harmonic, Sat (dBm)	@ F=36120 <-15	@F=36240 <-15	@F=36360 <-15
Notch Filter IL (dB)	1.0	0.6	0.5
MCS Waveguide Coupler IL (dB)	0.2	0.15	0.20

NOTES

A. Thermistor R/T Calibration Figures 23 and 24.
B. RF System NASA #1 Certificate of Calibration Western Automatic Test Services on 4/18/75.
C. Total Filament Hours 730.5 on 5/19/75.
D. Total Cathode Pulse Hours 241.9 on 5/19/75.
E. Total Cathode CW Hours 303.8 on 5/19/75.
F. Baseplate Temperature is 39°C.

FINAL TEST DATA SUMMARY
(Table Ib)

Cathode Voltage	E_k	11,300		Volts		
Cathode Current	I_k	77.2		mA		
Anode Voltage	E_A	250		Volts		
Heater Voltage	E_f	3.30		Volts		
Heater Current	I_f	1.23		Amps		
Cathode Temperature	T_k	1050		Deg. C		
MDC Electrode No.	1	2	3	4	5	
Electrode Voltage (kV)	0.0	2.26	3.39	4.52	5.65	
(Relative to Gnd)	6	7	8	9	10	
	6.78	7.91	9.04	10.17	11.30	

Frequency (MHz)	12040	12080	12120
Sat. Output Power(dBm)	53.2	53.5	53.0
Sat. Output Power(W)	208	222	201
Sat. Drive Power (dBm)	23	23	23
(mW)	200	201	193
Sat. Gain (dB)	30.2	30.4	30.2
Body Current, Sat.(mA)	6.4	6.3	6.8
Transmission, Sat.(%)	91.6	91.8	91.1
Overall Eff., Sat.(%)	42.	45	43
Total DC Power, Sat. (W)	488	490	461

NOTE

A. Baseplate Temperature is 55°C.

8.0 CURRENT STATUS

During the completion of the two-phase contract, a total of thirty two OST's were fabricated. Approximately one-half of these units were delivered to LeRC for evaluation, test, and flight. The delivered units represent several configurations and contain various designed/selected subassemblies. Table 8-1 provides a summary of the units fabricated, the unit destination or location, the contractual designator if applicable, and any unusual design feature of characteristic and/or utilization associated with the unit. In the case where units did not complete the fabrication process or they were dismantled for subassembly reuse, or salvaged for some other purpose, it is noted.

OST S/N 2022 (QF-4) is presently in orbit via the CTS satellite, and appears to be functioning in accordance with specification requirements. The summary data and acceptance test data associated with this unit shows that the output power exceeds 200 watts, and the efficiency is approximately 50% with a gain of 30 dB. The values shown reveal that the unit meets or exceeds the specification values in all but three minor categories, including weight. The data shows an excess unit weight of approximately three ounces, or less than 0.1 kilogram. The out of specification readings were considered to have little or no impact on system operation, and the unit was accepted by NASA and designated for flight operation.

OST S/N 2020 (ETM-3) was selected for life test at LeRC, although the U-tab collector was not the flight design. A summary of the acceptance data for this unit is contained in section 7.0, herein. At present, the tube has experienced over 14,000 hours of continuous duty without changes in performance. It is scheduled for additional test until an accumulation of approximately 20,000 hours has been reached.

OST S/N 2025 (QF-3) was selected as the prime flight unit backup. A summary of the acceptance data, together with a limited amount of test data for this unit, is shown in section 7.0.

Other units are being subjected to a variety of functional optimization tests, subsystem verification investigations, and other related test projects.

PRECEDING PAGE BLANK NOT FILMED

Table 8-1. Status of Units

UNIT NO.	DESIGNATOR	STATUS/ LOCATION	COMMENT/UNIT UTILIZATION
1	E-1	Not Assembled	Incomplete unit
2	E-2	LeRC	Two stage collector, demo unit
3	P-1	LeRC	Phase I evaluation
4	-	Not fabricated	Incomplete unit
5	ETM-1	LeRC	Phase I evaluation, Preliminary integration tests
6	P-2	Litton	Moveable collector spike
7	ETM-2	LeRC	Phase I evaluation, MDC aperature experiment
8	-	Scrapped	PPS integration tests and vibration
9	-	Not fabricated	
10	-	Litton	Single step taper
11	-	Scrapped	Low power
12	-	Disassembled	Hard limiting, pulse breakup
13	-	Litton	Refocus design tests, pin-yoke, MDC vibration tests
14	Experimental	Litton	Circuit subassembly evaluation
15	Experimental	Litton	Kidney slot coupling evaluation
16	-	Litton	Short MDC spike, life test
17	-	LeRC	Temperature tests, rf test
18	-	Not fabricated	
19	QF-1	LeRC	Retrofit for ETM-1
20	ETM-3	LeRC	Life test, ongoing
21	QF-2	CRC	Integration tests, U tab MDC
22	QF-4	LeRC-CTS	Flight unit, in orbit via CTS
23	-	Litton	Transit mishap, vibration test
24	-	Disassembled	Marginal stability
25	QF-3	LeRC	Flight backup (Prime)
26	-	Litton	Low frequency
27	QF-6	LeRC	Flight backup
28	-	Disassembled	Cathode Auger analysis
29	-	Disassembled	Marginal stability

Table 8-1. Status of Units (Continued)

UNIT NO.	DESIGNATOR	STATUS/ LOCATION	COMMENT/UNIT UTILIZATION
30	QF-5	LeRC	Storage test-flight backup
31	-	LeRC	Display model-sectioned
32	-	Litton	Marginal stability
33	-	Litton	Marginal stability
34	QF-7	LeRC	Flight backup
35	-	Litton	Modified taper, improved stability
36	QF-8	LeRC	Display model, packaged

9.0 CONCLUSIONS

This section presents the conclusions, observations and the new technology results obtained during the overall CTS TWT program effort.

9.1 ATTAINMENT OF OBJECTIVES

The purpose of this program was to demonstrate the feasibility for the design, through analysis, limited production, and test, of a high efficiency 12 GHz traveling wave tube that produces 200 watts of cw output power for use in the Communications Technology Satellite. The principle features of the tube included a coupled cavity rf circuit, velocity taper, and a multistage depressed collector which provided an overall efficiency of approximately 50 percent from a circuit operating at 26 percent electronic efficiency. The objectives of the program were met with the end result being an operational satellite in orbit providing television transmissions using the L-5394 traveling wave tube.

The results of this program show that design and performance of a highly efficient 200 watt traveling wave tube for space communication are practical and attainable within the bounds of existing technology. The tube defined during this program uses periodic permanent magnet focusing. A two-step velocity taper is incorporated in the slow wave structure for velocity resynchronization with the modulated beam. The spent beam is reconditioned in a permanent magnet refocusing section before it is collected in the multistage depressed collector. The collector is radiation cooled to deep space, and is heat insulated from the tube body. At saturation, the tube provides a cw output power of 225 watts with a 30 dB gain and an overall efficiency of 48 percent. The weight of the tube is approximately 26 pounds (11.75 kilograms).

9.2 OBSERVATIONS

During the design, fabrication, and test of the tube, several problems were encountered. A summary of the problems has been presented in a previous section; however, resolutions to some of these problems resulted in providing observations relating to interrelated design goals, fabrication techniques, and test methods. Some of these observations are presented herein:

a. Variations in performance characteristics of a tube do not necessarily indicate a deficiency in the basic design, but probably the result of construction, focusing, and alignment operations.

PRECEDING PAGE BLANK NOT FILMED

b. A coupled cavity circuit can be designed and fabricated for greater than 30 percent basic efficiency over the 85 MHz band at 12 GHz using a two-step velocity taper.

c. The performance of a high efficiency coupled cavity traveling wave tube with a low perveance design can be predicted using computer analyses.

d. It is possible to experience frequency shifts when the circuit assemblies are exposed to a brazing process. This shift is usually downward and must be considered prior to final dimensioning or selection of the pole pieces, spacers, and axial dimension related piece parts.

e. The length and functional characteristics of the refocusing section have significant impact on the collector performance. The increased length of the refocusing section improves the overall efficiency of the tube.

f. The MDC with nine depressed stages designed by Dr. Kosmahl of LeRC improves the overall efficiency to greater than 50 percent with collector efficiencies of approximately 80 percent.

g. The collector for a 200 watt tube operates at acceptable temperatures within the vacuum envelope using radiation cooling to deep space.

h. The spike length affects the optimization and average energy sorting efficiency. If it is too long (greater than 1.6 cm), the result is excessive dispersion of the most energetic electrons. If it is too short, an insufficent number of the electons are dispersed, resulting in high power dissipation. The collector design is insensitive to variations in voltages, beam size and space charge as long as the beam is refocused and its entering dispersion angle is in the range of $1°$ to $6°$.

i. Utilizing an experimental tube circuit in a test environment, the following results were obtained: (1) Maximum electronic efficiency is shown when the taper starts several dB, 2.5 to 5 depending on frequency, below saturation, (2) simple cavity probes can be useful in determining forward and backward wave power, and can be included in experimental designs without a significant impact on tube reliability; (3) it is possible to separate the forward and backward waves with a probe, even though it is considered a non-directional device, and (4) the experimental design displayed a substantial margin of stability in both the input and center sections, as indicated by the absence of oscillations over a wide range of beam voltage and input source VSWR.

j. The L-5394, 200 watt tube with the cantileavered multistage depressed collector will withstand a launch environment and function successfully in a deep space environment.

k. The design and application of the high power traveling wave tube need not be limited to a singular space communication transmission system, but could be extended to many other applications where low cost ground terminals can be used. The frequencies reserved exclusively for satellite communications and used by the CTS are devoid of the interference problem associated with other terrestial communications systems. This could result in the expansion of numerous vital links to isolated communities or outposts and could include transmittal of intercommunity contact information, medical data for improved health care or remote diagnosis, wide coverage educational information or specialized instructional data, and emergency/disaster data.

9.3 NEW TECHNOLOGY

The phenomenon of minute ion oscillations called "ticking" was studied in conjunction with the test of two late model production tubes. The oscillations were minor and did not cause any operational degradation of the tubes. A possible technique for suppressing these ion oscillations in linear beam microwave amplifiers was presented to NASA via the new technology reporting method and a summary is repeated herein. This technique involves the use of the first collector electrode and the gun anode to provide a potential barrier at each end of a rf interaction circuit.

A. The Problem:

The ticks are small irregular variations of the body current, with a generally triangular waveform. The amplitude was 0 to 0.3 mA, superimposed on the dc 2 to 8 mA body current, frequency 0.5 to 10 Hz, duration .02 to .2 sec.

Occasionally the ticks change from a triangular to a square waveform. Small changes in the rf output are observed coincident with the ticks. Figure 9-1 is a simplified illustrative display of ticking records under changing test conditions. A previous figure; 2-6 is a diagram of the OST, sectioned along the axis, showing the location of the gun anode and first collector electrode.

B. Observations:

1. Ticking is only seen in hard, well-aged tubes.

2. Ticking occurs with or without rf drive, but the amplitude and frequency are modified by the drive.

3. Ticking occurs at all values of anode voltage from 0 to 550 volts, but is modified by the voltage; a generally optimum region at about 250 volts was seen on both tubes.

4. Ticking is independent of E_{c1} (potential on collector element No. 1 with respect to body) up to +80 volts and is suppressed by higher positive voltages. It is also suppressed by similar positive voltages on E_{c2} if E_{c1} is below the suppression range. The voltage range over which suppression occurs is only about 20 V.

5. Ticking is modified by collector temperature; but the observations are somewhat inconsistent. One tube showed a reduction of ticking rate with increasing T_c (one test only), while the other tube showed an increasing ticking rate and decreasing amplitude, with increasing T_c, in repeated tests.

6. Ticking rate increases and amplitude decreases (sometimes to zero) with application of heat to either the eight or one liter/second ion pump, whether the pump is operating or not. Application of heat to other parts of the tube produced only a slight increase of ticking rate except on the refocus section which produced a slight decrease.

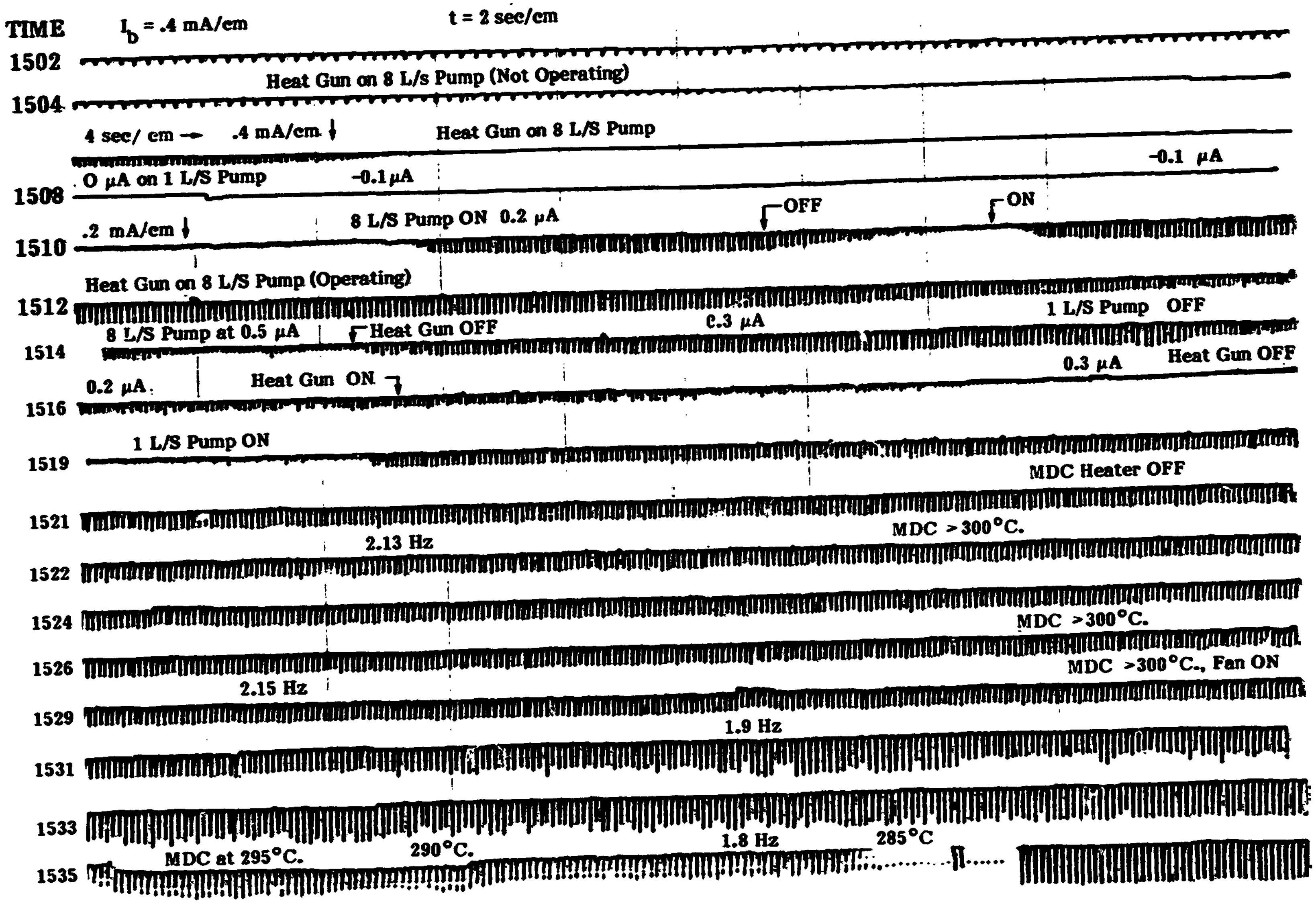

Figure 9-1. Ticking Observations, Body Current vs. Time

7. In the tests noted in 6.0, pressure readings of about 0.3 μA on the 8 liter/second pump and 0.2 μA on the one liter/second pump were observed when the heat was sufficient to reduce the tick amplitude to .05 mA or less. No pressure indication was seen under the other conditions. The 0.3 μA on the 8 liter pump corresponds to 3×10^{-9} Torr (14 vauns, or 10^{14} molecules/m^3).

8. No ticking was observed in cathode pulsed operation (collector voltages on dc), at any duty cycle (maximum at approximately 80%), or at any pulse length (maximum 18 msec, minimum 70 μsec). There was excessive hash when operating in pulse mode, and small ticks may have been present, but might not have been observed.

9. In dc operation with cathode voltages switched off and on again, ticking took about 2 seconds to restart on one unit, independent of the off period in the range 1.5 to 10 seconds; for longer (several minutes) off periods the ticking took longer to reappear. In the other unit, the ticking reappeared faster, but went through a quite complicated but fairly reproducible cycle of repetition rate changes - slowing for 2-3 seconds, then increasing rapidly, then decreasing slowly over an hour or so.

C. Theories:

Several causes for the ticking existence can be posited. These causes are listed and briefly discussed herein.:

1. Insulator breakdown and recharging.

2. Thermo-mechanical distortion of a part heated by the beam.

3. Gas discharges (i.e. arcs).

4. Ion discharges.

The last cause seems by far the most probable since: (1) can be ruled out by the great similarity in behavior of the two units with respect to collector voltages; and (2) can be ruled out by the range of ticking frequencies produced by, for example, heating the pumps. Thermo-mechanical oscillations would be expected to have a narrow frequency range controlled by the elastic and heat sink properties of the moving part, which would change very little. The gas breakdown, (3), is more difficult to rule out, but the observed pressures are low for this to occur, and it is difficult to see why it would not have been observed much earlier at higher pressure. The discharge of ions trapped in the beam potential well, (4), fits most of the observations except the variation with collector temperature on the first unit. It does agree with the more numerous observations on the second unit.

Briefly, the theory is that at a pressure of $<3 \times 10^{-9}$ [illegible], ions are formed in the beam at a rate of about 10^{16} per sec per [illegible], or 10^{9} per sec within the beam volume. At this rate, the beam will be neutralized in a few seconds, and the ions will be able to flow over the weak potential barrier formed by the beam expansion at the collector end. When about 10% of the ions have escaped, the potential barrier reasserts itself, and the accumulation continues. Thus the interval between ticks should be on the order of 10% of the time to the first tick, when the pressure is constant. After long off periods the pressure is lower, so the time to the first tick is larger.

The current represented by the escaping pulse of ions is only a few nanoamps, so this is not the observed current. The escaping ions change the potential in the beam, and thus cause a small change in beam diameter, on the order of 6×10^{-4} cm; when the beam is already scraping the tunnel wall (which it is, because we observe dc body current), then a 6×10^{-4} cm change of diameter is enough to cause the observed changes in body current. This change in beam size is consistent with a few volts change in beam potential, which in turn is consistent with the calculated 20 volts depression for the electron beam by itself.

On this theory, in a poor vacuum the ions are generated fast enough to pour over the potential barrier in a continuous stream, and the barrier cannot assert itself until the pressure is down to about 14 vauns. It is not clear why the amplitude of the ticks varies as it does. All the evidence so far is that as the vacuum improves beyond 14 vauns, the ticks get slower and larger. The limit on amplitude was not determined.

D. Technology Conclusions

If this theory is correct, then all hard tubes will eventually develop ticking, as the vacuum improves. The vacuum would have to be less than 12 vauns (approximately 10^{-11} Torr) to make ticking infrequent enough (less than 1 per minute) to ignore. This is probably unlikely in a closed or sealed tube.

Ion oscillations are suppressed when an insurmountable potential barrier is established at the collector end of the interaction circuit by raising E_{c1} to +150 volts. This worked, under all conditions tested, on both units. A potential barrier at the gun end of the interaction circuit was established by a positive potential of +150 to +550 volts applied to the anode.

A possible technique to suppress ion oscillations in linear beam tubes (such as the OST) would include the use of the first collector electrode and the gun anode to provide a potential barrier at each end of a rf interaction circuit. This technique could be utilized and demonstrated in future tube designs.

APPENDIX 1

ASSEMBLY DRAWINGS

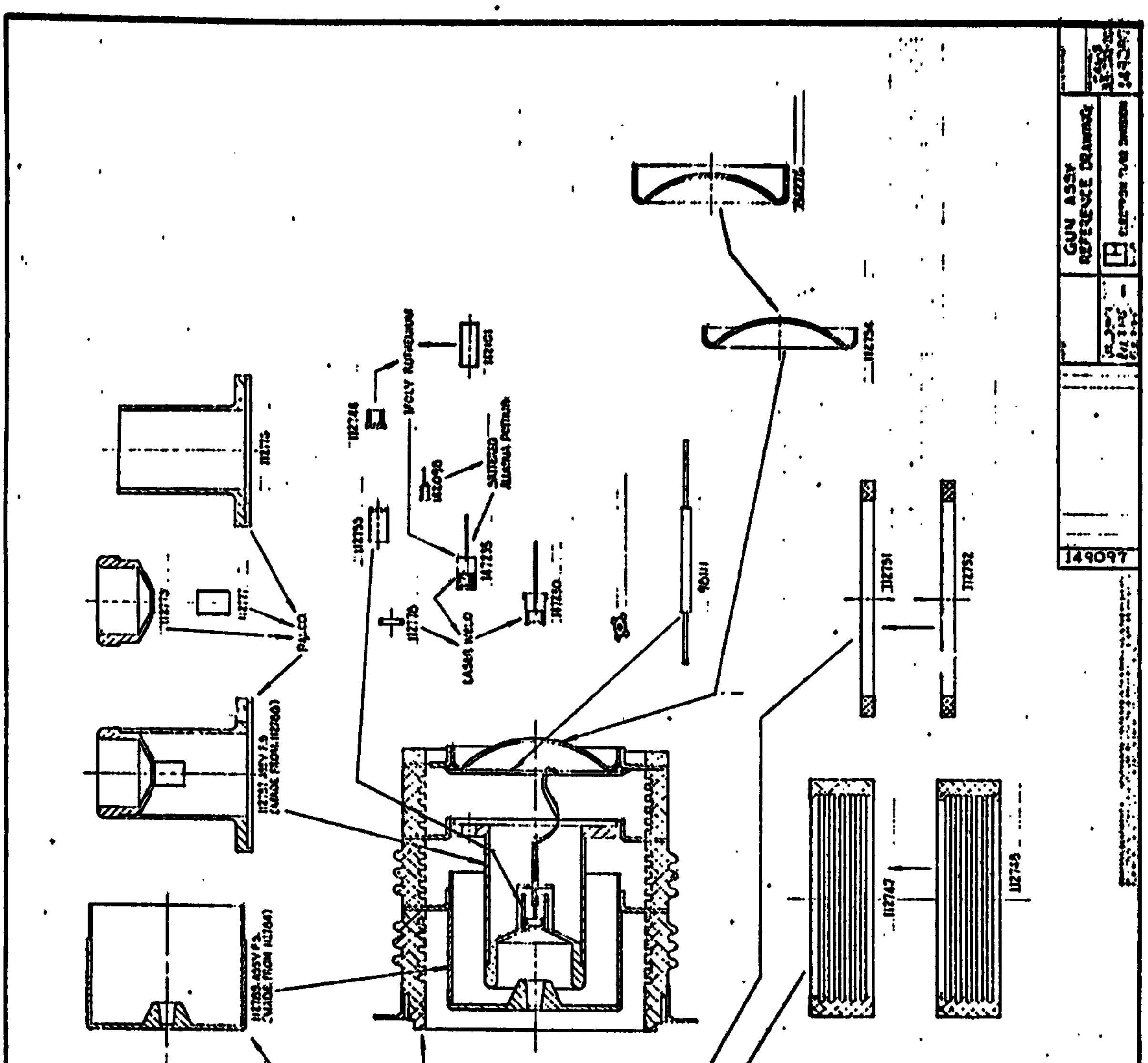

GUN ASSY
REFERENCE DRAWING
149097
LASER WELD

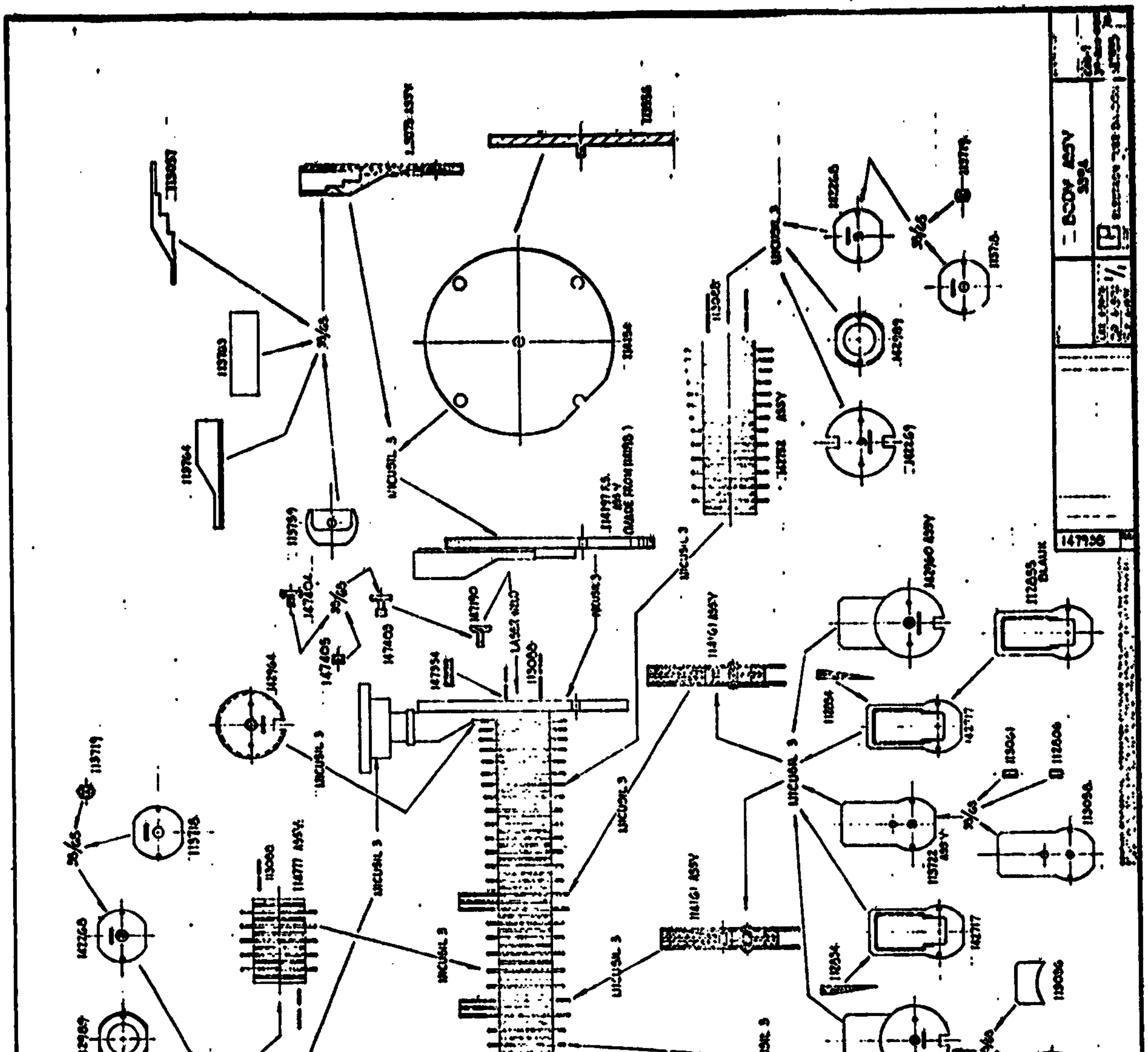

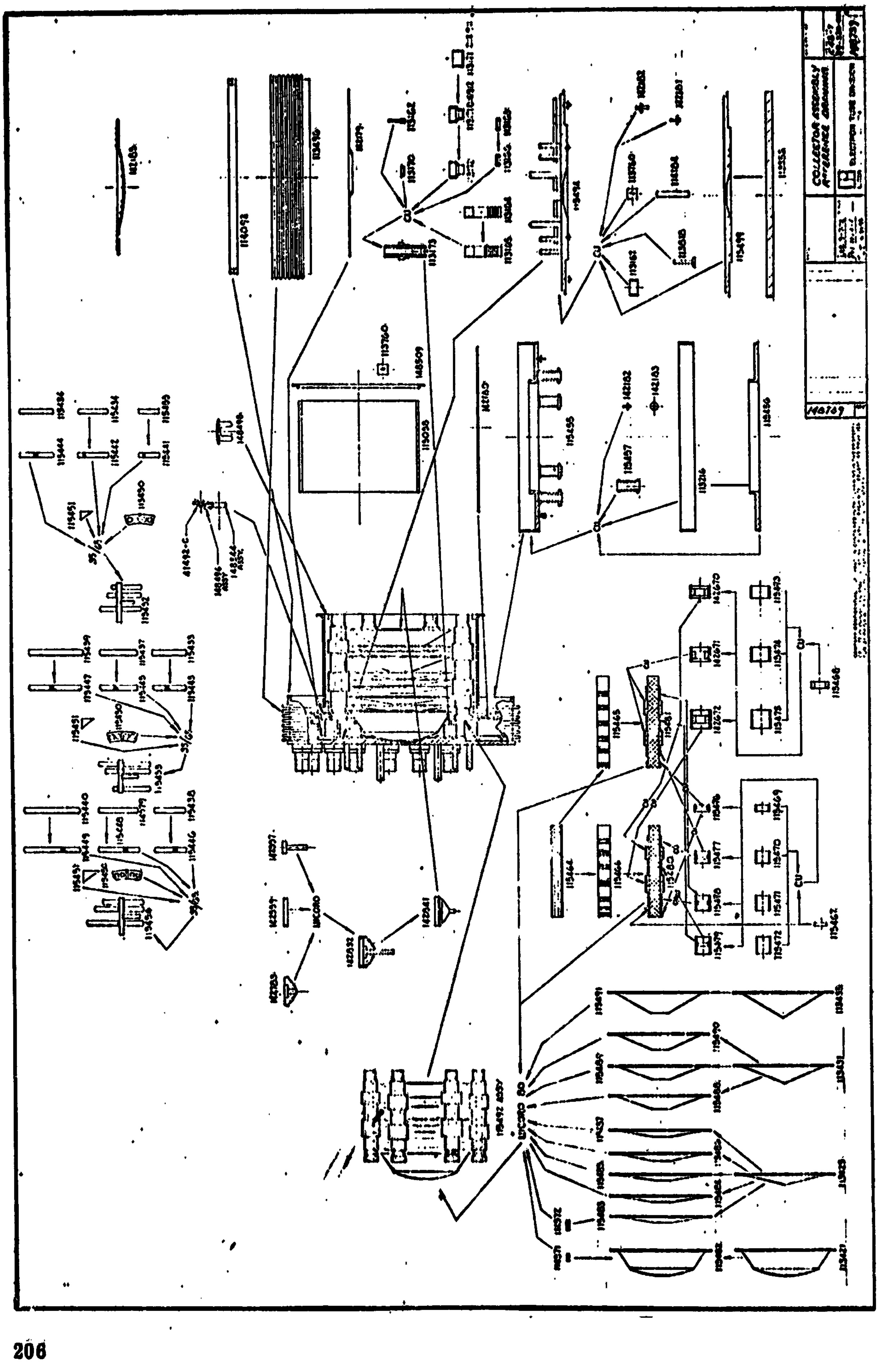

APPENDIX 2

DEFINITIONS AND SYMBOLS LIST

1.0 DEFINITIONS

CTS	Communications Technology Satellite
S/C	The CTS Spacecraft
TWT	Traveling Wave Tube
MDC	Multistage depressed collector
OST	Output stage tube; combination of the TWT and MDC
PPS	Power Processing Subsystem; converts solar cell power into usable power.
TEP	Transmitter Experiment Package; the combination of the OST, PPS, instrumentation, controls and structure.
LeRC	Lewis Research Center, Cleveland, Ohio
ETM	Engineering Test Model
QF	Qualification Flight Model OST
NF	The ratio of the total to available output noise power if the amplifier were noiseless (Noise Figure).
BW	Bandwidth
CG	Center of Gravity
CL	Center Line
SHF	Super High Frequency
CRC	Communications Research Centre (Canada)
PB	Passband (the three dB small signal bandwidth)

2.0 SYMBOLS

B	magnetic flux density
b	Pierce velocity parameter, or beam radius
C	Pierce gain parameter
d	Pierce attenuation parameter
E	Voltage

2.0 SYMBOLS (Continued)

e	electronic charge
f	frequency
h	cavity height
I_c	collector electrode current
I_o	dc current
K	interaction impedance
L	loss in circuit, dB
l_o	cavity period
m	particle mass
l_c	magnetic focusing period
nP	nonopers (Pervance)
P_o	rf output power
r_a	beam tunnel radius
r_b	beam radius
rf	radio frequency
t	time variable
μ_o	dc electron velocity
V	electric potential, Volts
V_o	cathode to body voltage
v_g	group velocity
v_p	phase velocity
γ	radial propagation constant
λ	wavelength
η	efficiency
λ_p	plasma wavelength
ϕ	phase shift angle per cavity, radians

3.0 SUBSCRIPTS

c	collector
ct	circuit
dis	dissipation
in	input
K	cathode
n	collector electrode number
o	standard section or initial value
p	plateau value
out	output
r	radial component
rec	recovered
z	axial component

APPENDIX 3

REFERENCES

1. Sauseng, O. G.; Basiulis, A.; and Tammaru, I.: Analytical Study Program to Develop the Theoretical Design of Traveling Wave Tubes, Hughes Aircraft Co. (NASA CR-72450), 1968.

2. Ayers, W. R.; and Harman, W. A.: Design, Construction and Evaluation of a 12.2 GHz, 4.0 KW-CW Coupled-Cavity Traveling Wave Tube, Varian Associates (NASA CR-120920), 1973.

3. Lewis, R.: Development of a High Power 12 GHz PPM Focused Traveling Wave Tube, Litton Industries (NASA CR-134856), 1975.

4. Christiansen, J. A., Tammaru, I.: Development of a 200 Watt CW High Efficiency Traveling Wave Tube at 12 GHz, (NASA CR-134734), 1974.

5. Kosmahl, Henry G.: Electrostatic Collector for Charged Particles, U.S. Patent No. 3, 702, 951, 1972.

6. Branch, G. M.; and Neugebauer, W.: Refocusing of the Spent Axisymmetric Beam in Klystron Tubes, General Electric Co. (NASA CR-121114), 1972.

7. Kosmahl, Henry G.: A Novel Axisymmetric, Electrostatic Collector for Linear Beam Microwave Tubes, (NASA TN D-6093), 1971.

9. Kosmahl, H. G., McNary, B. D. and Sauseng, O.: High Efficiency, 200 Watt, 12 GHz, Traveling Wave Tube, Litton Industries (NASA TN D-7709 and TN D-7910), 1974.

10. Kosmahl, Henry G.: An Electron Beam Controller, U.S. Patent No. 3, 764, 850, 1973.

11. Alexovich, R.: The 200 Watt SHF Transmitter Experiment Package, (NASA TMX-68106), 1972.

12. CTS Reference Manual, NASA LeRC (TM X-71824), 1975.

13. Pierce, J. R.: Theory and Design of Electron Beams, D. Van Nostrand Co., New York, 1954.

14. Cohn, S. B.: Optimum Design of Stepped Transmission Line Transformers, IRE Transactions on Microwave Theory and Techniques, April 1955.

15. Stankiewicz, N.: Evaluation of Magnetic Refocusing in Linear Beam Microwave Tubes (NASA TN D-7660), 1974.

PRECEDING PAGE BLANK NOT FILMED

APPENDIX 4

OST QUALIFICATION FLIGH' DESIGN DOCUMENT

1.0 Scope

This document describes the OST design configuration which will be produced for qualification and flight.

This document reflects the baseline status as of date of issue and will not be updated for each engineering change order.

2.0 Slow Wave Structure

The slow wave structure (or tube body) is composed of an input section, first sever (or termination), center section, second sever, and output section. The configuration of the various sections is set forth below:

2.1 Circuit Layout Drawing

The OST Circuit Layout Drawing is Litton Drawing #142753-XXX, where XXX will vary with each OST serial number to document dimensions defined in cold test. Cavity diameters and gaps specified below may be altered in cold test to obtain the desired match.

2.1.1 Input Section

No. cavities	10
Period	.125 inch (.318 cm)
Cavity diameter	.595 inch (1.511 cm)
Cavity height	.095 inch (.241 cm)
Gap	.0382 inch (.097 cm)

2.1.2 Center Section

No cavities	14
Period	.125 inch (.318 cm)
Cavity diameter	.595 inch (1.511 cm)
Cavity height	.095 inch (.241 cm)
Gap	.0382 inch (.097 cm)

2.1.3 Output Section

Cavities are listed in order from second termination to the output waveguide coupler.

PRECEDING PAGE BLANK NOT FILMED

	NO. OF CAVITIES	PERIOD (IN./CM)	DIAMETER (IN./CM)	HEIGHT (IN./CM)
STD 1	10	.1250/.318	.595/1.511	.0950/ .241
STD 2	3	.1197/.304	.608/1.544	.0897/.228
T - 1	1	.1175/.298	.608/1.544	.0875/.222
T - 2	1	.1150/.292	.608/1.544	.0850/.216
T - 3	1	.1100/.279	.608/1.544	.0800/.203
T - 4	1	.1050/.267	.608/1.544	.0750/.191
T - 5	5	.1000/.254	.608/1.544	.0700/.178
T - 6	1	.0950/.241	.607/1.542	.0650/.165
T - 7	1	.0900/.225	.607/1.542	.0600/.152
T - 8	4	.0850/.216	.607/1.542	.0550/.140

The gap-to-period ratio is nominally 0.3 but is subject to change in cold test to obtain the required match.

2.1.4 Cold Test Criteria

The following are goals of the cold test procedure:

1. Align the lower cutoff frequencies (Pi) points of each section to 12.010 GHz before braze. To the extent that some misalignment (±15 MHz) cannot be avoided the highest Pi points in the output section must be in T-5. The distribution of Pi points in the output section shall be verified by the methods given in Appendix A.

   Return loss curves shall have a clean sharp leading edge free from notches or other structure. As frequency increases above the onset of return loss, there shall be a rapid drop in power return ratio to at least -15 dB before any change in direction. Return loss shall remain below -10 dB until at least 175 MHz above the 10 dB return loss frequency.

   Before braze, characteristic frequencies as determined in cold test shall be as given below.

   Input Section

5 dB R.L.	12,025 ± 15 MHz
10 dB R.L.	12,050 ± 15 MHz
20 dB I.L.	11,965 ± 15 MHz

   Center Section

5 dB R.L.	12,015 ± 15 MHz
10 dB R.L.	12,030 ± 15 MHz
20 dB I.L.	11,985 ± 15 MHz

Output Section

5 dB R.L.	12,020 ± 15 MHz
10 dB R.L.	12,030 ± 15 MHz
20 dB I.L.	12,015 ± 15 MHz

In the output section, one of the three above characteristic frequencies taken in the forward direction shall exceed the same frequency taken in the reverse direction by more than 5 MHz. In any section, each of the three characteristic frequencies shall be the same in both directions within 15 MHz.

2. LeRC shall approve cold test results of output sections before braze.

2.1.5 Magnets

Manufacturer - Raytheon
Material - Samarium Cobalt
Peak Axial Field
Standard Section - 1500 Gauss (± 2 magnet rings)
Remainder of Section - 2200 Gauss
Focusing Scheme - Double period PPM (single period for each coupler)
Refocusing Field - 400-600 Gauss (determined in test)

3.0 Gun

The electron gun is comprised of a heater, cathode button, focusing electrode, anode, insulating ceramics and supporting structure. The purpose of the gun is to provide the electron beam for interaction.

3.1 The gun assembly shall be controlled by Litton Drawing #112783 and Litton Gun Assembly Procedure CFPA 154.

3.2 Description

Cathode type	Impregnated tungsten
Manufacturer	Litton Industries
Design Perveance	62 ±2 nanoperv
Operating temperature	<1100 degrees C
Beam minimum diameter	<.030 inch (.076 cm)

3.3 Cathode Processing

Cathode preglow and temperature calibration shall be controlled by Litton procedure CFPT 301. A normal sequence is as follows:

1. Assemble focus electrode into cathode support assembly.
2. Place cathode assembly into gun assembly (air exposure).
3. Preglow gun assembly and run temperature calibration.

4. Activate to run beam analyzer tests per Litton gun assembly testing procedure CFPT 300.

5. Install on OST (air exposure).

4.0 Collector

The collector is composed of ten (10) electrodes, an electrically insulated support structure and a vacuum enclosure. The purpose of the collector is to provide a means of recovering kinetic energy from the spent beam, thereby increasing efficiency and reducing heat loading of the baseplate.

1. Collector assembly shall be controlled by Litton Drawing #115493.

2. Description

Electrode material	Molybdenum
Aperture	4 degrees
Spike length	.316 inches (.803 cm)

5.0 Tube Processing

All OST's are baked out in a double vacuum retort prior to hot test. The inside of the OST is evacuated at high temperature to remove gas and volatile compounds and provide the vacuum necessary for successful cathode operation and life. The external vacuum that is provided on the tube, at the same time as the internal vacuum, prevents atmospheric oxygen from attacking the circuit braze material and causing leaks. It also prevents the exterior of the copper circuit from oxidizing.

5.1 Exhaust processing shall be controlled by Litton procedure CFPE307. Several salient features of this procedure are as follows:

1. Tube body baked at 450°C, collector at 600°C.

2. Cathode, hot flashed 10 minutes at 1200°C when internal pressure $<8 \times 10^{-7}$ Torr.

3. Cathode operated at 1100°C during remainder of exhaust processing run.

4. Tube processed twelve hours after low pressure level is achieved.

5.2 Subsequent to exhaust preliminary packaging is done, such as bonding of the bus bars, gun leads, gun shield, and, the magnets are installed, then the tube is focused. The tube operating duty cycle shall then be raised to continuous operation (cw) at all drive levels with the collector jacket externally heated to 300°C. This allows removal of gases released by impingement of the electron beam on various collector plates.

1. Bus bar epoxy - ECCOBOND 56C, Catalyst 9

2. Magnet epoxy - STYCAST 2850 FT., Catalyst 9

6.0 Final Packaging

After a NASA decision is made that a specific OST is a candidate for a deliverable item, final packaging is carried out. This includes the addition of structural support members, thermistors, and air bakeout to outgas the exterior of the tube.

6.1 The packaged OST shall conform to Litton Drawing #113420.

6.2 OST exterior bakeout - 12 hours at 125°C in air.

6.3 Notch filter shall be adjusted such that the small signal gain shall be 20 dB or less at frequencies below 11.928 GHz.

6.4 Refocusing field optimization shall be performed to maximize overall efficiency with saturated power output.

6.5 Collector paint - Sperex SP-101

7.0 Data Package

This paragraph describes the minimum data required by NASA to determine that an OST is suitable for final packaging. It also describes the minimum data NASA requires to determine whether a tube is acceptable for delivery as a qualification flight model.

7.1 Preliminary Data Package

1. Purpose

   To determine whether to package a tube as a QF tube candidate.

2. Contents

   All data shall be taken at the optimum cathode voltage unless otherwise specified. Frequencies and operating conditions of any oscillations or deviation from normal performance shall be specifically identified. Examples of such deviations are oscillations, spurious signals, limiting, "cathode slump", unstable focusing or unstable body current, leakage or shorts between elements, collector "buzz" or breakdown of collector voltages less than 1.5 times nominal operating voltage.

   a. List of deviations from controlling master list.

   b. List of non-conformances to this control document and request for waivers.

   c. Body current and P_o versus frequency at centerband drive levels adequate to produce saturation, saturation drive plus 6 dB, and saturation output minus 10 dB. Data shall be taken at the optimum cathode voltage and at two other voltages within the 11.0 to 11.6 kV range, each voltage different from the other two by 200 Volts.

   d. P_o versus P_{in} at frequencies of 12.040, 12.080 and 12.120 GHz. Data shall be taken at the optimum cathode voltage and at two other voltages as specified in 7.1.c.

e. Vidar data set - 11 frequencies, 12.030 GHz through 12.130 GHz in 10 MHz increments at centerband drive levels adequate to produce saturation, and saturation output minus 10 dB. Vidar data shall also be taken at three frequencies (12.040, 12.080 and 12.120 GHz) at centerband drive levels adequate to produce saturation and saturation output minus 10 dB for two other values of cathode voltage as specified in 7.1c.

7.2 Final Data Package

1. Purpose

To document final tube performance data in flight packaged condition and determine acceptability as QF tube.

2. Contents

a. Frequencies and operating conditions of any oscillations or deviation from normal performance shall be specifically identified. Examples of such deviations are oscillations, spurious signals, limiting, "cathode slump", unstable focusing or unstable body current, leakage or shorts between elements, collector "buzz" or breakdown of collector voltages less than 1.5 times nominal operating voltage.

b. List of deviations from controlling master list.

c. List of non-conformance to the requirements of this document and NASA approved waivers.

d. Body current versus frequency at centerband drive levels adequate to produce saturation, saturation drive plus 6 dB, and saturation output minus 10 dB.

e. P_o versus P_{in} at frequencies of 12.040, 12.080 and 12.120 GHz.

f. Vidar data set - zero drive case plus 11 frequencies 12.030 GHz through 12.130 GHz in 10 MHz increments at centerband drive levels adequate to produce saturation, saturation output minus 3 dB and saturation output minus 10 dB.

g. Coupler and equalizer/notch filter insertion loss and return loss characteristic.

h. Wideband pulse data to demonstrate that equalizer/notch filter criterion of section 6.3 is met (11.750-12.250 GHz).

i. An envelope of saturated power output versus frequency for the optimum cathode voltage shall be provided (12.030-12.130 GHz).

j. The radio frequency noise at the OST output, at zero rf drive, including in-band and out-of-band components when operating the OST from a dc power supply. The radio frequency noise shall be determined over the frequency band from 10 GHz to 18 GHz.

k. Calibration of the telemetry sensors.

l. The power and phase of the OST rf output as a function of frequency with five rf input levels recorded for the two temperatures listed.

Frequency range:	12.030 to 12.130 GHz
Baseplate Temp:	35°C 65°C
Rf input range:	saturation drive saturation drive +6 dB saturation drive +3 dB saturation output - 3 dB saturation output -10 dB

m. The test data shall include:

spurious outputs
second harmonic power
third harmonic power
noise figure

8.0 <u>Master List</u>

A Master (parts) List will be issued for each OST S/N to document the actual parts contained in each tube. The controlling master list for the OST baseline design will be the master list for OST 2024. Litton QA shall review, approve, and document for NASA any deviations from the baseline design on OST's subsequent to OST 2024.

9.0 <u>Configuration Control Changes</u>

9.1 Litton Engineering will maintain configuration control via the Litton Engineering Change Order (ECO) procedure. All Class I changes will require the approval of the LeRC Technical Contract Manager or the LeRC TEP Project Office Manager. Litton will suppy LeRC copies of all ECO's.

9.2 Class II Changes are defined as:

1. Errata Changes.
2. Changes to alleviate manufacture, assembly, and installation difficulties not affecting contract specifications or this configuration control requirements document.
3. Correcting drafting error.

All other changes are considered Class I and require the above noted approval.

9.3 Changes to the Configuration Control Description Document are to be handled as Class I changes.

10.0 Specifications

Qualification Flight specification requirements are as defined in table 1.

Table 1. Specifications

PARA. NO.	PARAMETER	VALUE
10.1	Saturation Characteristics	
10.1.1	Frequency, GHz	12.038-12.123
10.1.2	Gain, dB	30 +2, -1
10.1.3	Output Power, $P_o s$, Min., W	180
10.1.4	Overall Efficiency, Min., %	40
10.1.5	DC Input Power, Max., W	500
10.1.6	Beam Transmission at 50°C baseplate, Min., %	92
10.1.7	AM/PM ($P_o s$ to $P_o s$ -2 dB), °/dB	6
10.1.8	Second order phase deviation, Max., °/MHz^2	0.3
10.1.9	Harmonic Output Power 2nd and 3rd, Max., dBm	23
10.1.10	Thermal Input to Baseplate, Max., W	150
10.2	Small Signal Characteristics (Po = Saturation Po -10 dB)	
10.2.1	Gain Variation, peak to peak, dB	5
10.2.2	Gain below 11.928 GHz, Max., dB	20
10.3	Noise Figure, Max., dB	40
10.4	Differential Gain (3 to 23 dB below $P_o s$), dB	±0.7
10.5	Spurious Output Power (Pd = 0 and Pds, excluding harmonically related signals)	
	a. In any 4 kHz band between 14.0 and 14.3 GHz, dBm	-10
	b. In any 100 MHz band between 10.0 and 18.0 GHz, dBm	-10
10.6	Overdrive without OST damage,	
	a. Continuous, Max., dBm	+29
	b. Short Term, <0.5 sec, Max., dBm	+43.4

Table 1. Specifications (Continued)

PARA. NO.	PARAMETER	VALUE
10.7	<u>Power Processor Requirements (Set to OST decal values)</u>	
10.7.1	Cathode Voltage with respect to ground, kV	11.3 ± 0.3
10.7.2	Anode Voltage with respect to ground, V	350 ± 200
10.7.3	Anode Current, Max., mA	0.1
10.7.4	Heater Current, (constant current supply), A	1.3 ± 0.1
10.7.5	Heater Voltage with respect to cathode, Max, V	4.2 V
10.7.6	Body Current Overload Trip, mA	10
10.7.7	Ion Pump Supply Voltage, kV	2.3 - 3.3
10.7.8	Ion Pump Current Overload Trip (sum of two pumps), μA	10
10.7.9	Collector Voltages, Electrode #1 - #10. (% of cathode voltage)	0, 20, 30, 40, 50, 60, 70, 80 90 and 100.
10.7.10	Baseplate Temperature, operating, °C	0 to +58
	a. At turn-on, °C	-15 to +58
	b. Non-Operating, °C	-20 to +65
10.8	Refocusing Magnetic Field	PM
10.9	Weight OST, Max, lb	26.02 (11.8 Kg)
10.10	Design Life, yr	2
10.11	Waveguide Type	WR-75

APPENDIX 5

LITTON L-5394 TWT

FINAL DATA PACKAGE

I. Determine the Operating Parameters

A. From the preliminary data choose and record the optimum

1. Cathode voltage
2. Anode voltage
3. Heater current

B.. Measure and record the actual heater voltage and cathode current.

1. Measure the heater voltage at the socket with a DVM with cathode voltage off.

2. Measure the actual cathode current with a floating standard.

C. Determine the drive power to get the "best shape" over the NASA band, (+23 dBm is the maximum allowable drive power).

1. Change to single frequency at 12.080 GHz and record the drive power.

2. Calculate and record the drive power for saturation drive plus 3 dB and saturation drive plus 6 dB at 12.080 GHz.

3. At single frequency at 12.080 GHz measure and record the drive power necessary to achieve:

a. Saturation output -3 dBm.
b. Saturation output -10 dBm.

II. Plots of Output Power, Phase versus Frequency.

A. X-Y Recorder settings.

1. X-Axis

a. Frequency 12.030 to 12.130 GHz at 10 MHz/div. (100 mV/div.)

2. Y-Axis

a. Output Power at 1 dBm/div.

b. Phase at 10°/div.

B. Plots required at 35°C baseplate.

1. Output power, phase versus frequency at saturation drive +6 dB.
2. Output power, phase versus frequency at saturation drive +3 dB.
3. Output power, phase versus frequency at saturation drive .
4. Output power, phase versus frequency at saturation output -3 dB.
5. Output power, phase versus frequency at saturation output -10 dB.

C. Plots required at 65°C baseplate.

1. Output power, phase versus frequency at saturation drive +6 dB.
2. Output power, phase versus frequency at saturation drive +3 dB.
3. Output power, phase versus frequency at saturation drive.
4. Output power, phase versus frequency at saturation output -3 dB.
5. Output power, phase versus frequency at saturation output -10 dB.

III. Plot of Output Power, Forward Power Detector Voltage versus Frequency.

A. X-Y Recorder settings.

1. X-Axis
   a. Frequency 12.030 to 12.130 GHz at 10 MHz/div.
2. Y-Axis
   a. Output power at 1 dBm/div.
   b. Forward Power Detector Voltage at 20 mV/div.

B. Plots required at 35 to 65°C.

1. Output power, Forward Power Detector Voltage versus frequency.

IV. Plot of Saturated Output Power versus Frequency.

A. X-Y Recorder settings.

1. X-Axis
   a. Frequency 12.030 to 12.130 GHz 10 MHz/div.
2. Y-Axis
   a. Output power at 1 dBm/div.

B. Plot required at 35 to 65°C.

1. Saturated Output Power versus Frequency.
   a. On the plot saturate and mark the output power at 11 frequencies in 10 MHz increments.
   b. On the plot record the drive power necessary to achieve saturation.

V. Plot of Body Current versus Frequency.

A. X-Y Recorder setting.

1. Frequency 12.030 to 12.130 GHz at 10 MHz/div.
2. Body current at 2 mA/div.

B. Plot required at 35 to 65°C.

1. Body current versus frequency at Pd Sat. +6 dB, Pd Sat., and Po sat. -10 dB.

VI. Plots of Output Power, Phase versus Drive Power.

A. X-Y Recorder settings.

1. X-Axis

a. Drive Power at 5 dBm/div.

2. Y-Axis

a. Output Power at 5 dBm/div.

b. Phase at 10°/div.

B. Plots required at 35 to 65°C.

1. Output Power, Phase versus Drive Power at 12.040 GHz from Pd Sat. +3 dB to Po Sat. -30 dB.

2. Output Power, Phase versus Drive Power at 12.080 GHz from Pd Sat. +3 dB to Po Sat. -30 dB.

3. Output Power, Phase versus Drive Power at 12.120 GHz from Pd Sat. +3 dB to Po Sat. -30 dB.

VII. Plot of Forward Power Detector Voltage versus Output Power.

A. X-Y Recorder settings

1. X-Axis

a. Output Power at 5 dBm/div.

2. Y-Axis

a. Forward Power Detector Voltage at 50 mV/div.

B. Plot required at 35 to 65°C

1. Forward Power Detector Voltage versus Output Power at 12.040, 12.080 and 12.120 GHz from Pd Sat. +3 dB to Po Sat. -30 dB.

VIII. Plot of Reverse Power Detector Voltage versus Reverse Power.

A. X-Y Recorder settings.

1. X-Axis

a. Reverse Power at 5 dBm/div.

2. Y-Axis

a. Reverse Power Detector Voltage 100 mV/div.

B. Plot required at 35 to 65°C

1. Reverse Power Detector Voltage versus Reverse Power at 12.040, 12.080 and 12.120 GHz from +35 dBm to +10 dBm.

IX. Plot of Reverse Power Detector Voltage, Reverse Power versus Frequency.

A. X-Y Recorder settings.

1. X-Axis

a. Frequency 12.030 to 12.130 GHz at 10 MHz/div.

2. Y-Axis

a. Reverse Power Detector Voltage at 50 mV/div.

b. Reverse Power at 5 dBm/div.

B. Plot required at 35 to 65°C

1. Reverse Power Detector Power Voltage, Reverse Power versus frequency at Reverse Power equal to +30 dBm at 12.080 GHz.

X. Pulse Output Power versus Frequency.

A. X-Y Recorder settings.

1. X-Axis

a. Frequency 11.750 to 12.250 GHz at 50 MHz/div.

2. Y-Axis

a. Output Power at 5 dBm/div.

B. Peak Power Meter Settings.

1. Internal Trigger

2. Trigger delay 2.5 µsec.

3. Trigger Reset maximum

C. Plot required at 35 to 65°C

1. Output Power versus Frequency at Po Sat.-10 dB at 1% duty with a 50 µsec pulse.

XI. Vidar Data

A. Data at 35 and 65°C.

1. At 11 frequencies in 10 MHz increments from 12.030 to 12.130 GHz, take data at drive powers adequate to produce:

a. Saturated Output Power.

b. Saturated Output Power -3 dBm.

c. Saturated Output Power -10 dBM.

2. No drive.